60001769

Mining District File Summary Sheet

DISTRICT	Rosebud
DIST_NO	4010
COUNTY If different from written on document	Pershing
TITLE If not obvious	Petrography of Vein, Breccia, and Lithology Samples from the Rosebud Mine area, Nevada 23 December 1999
AUTHOR	Clark, I.; Allen K
DATE OF DOC(S)	1999
MULTI_DIST Y / N? Additional Dist_Nos:	
QUAD_NAME	Sulphur 7½'
P_M_C_NAME (mine, claim & company names)	Rosebud Mine; Rosebud Mining Co. LLC; Applied Petrographics
COMMODITY If not obvious	gold; silver
NOTES	Petrographic report; geology; photographs 171p.

Keep docs at about 250 pages if no oversized maps attached (for every 1 oversized page (>11x17) with text reduce the amount of pages by ~25)

SS: DP (Initials) 7/29/08 (Date)

DB: Initials Date

SCANNED: Initials Date

Revised: 1/22/08

60001769 4010

PETROGRAPHY OF VEIN, BRECCIA, AND LITHOLOGY SAMPLES FROM THE ROSEBUD MINE AREA, NEVADA

By

James G. Clark, Ph.D.

APPLIED PETROGRAPHICS
Tucson, Arizona

23 December 1999

Prepared for
Kurt D. Allen
The Rosebud Mining Company LLC
Winnemucca, Nevada

TABLE OF CONTENTS

TABLE OF CONTENTS (continued)

LIST OF TABLES

PROLOGUE

In reviewing the ensuing report, it is necessary to keep the following factors in mind:

1. Mineral identification in this study is based on optical petrographic techniques. In most cases this is sufficient for accurate identification. However, some phases, such as some silver sulfide and sulphosalt minerals, clay-fine sericite, and extremely fine-grained minor phases, may prove more difficult to identify and require analyses by SEM/EDAX, electron microprobe, or X-ray diffraction for positive identification.

2. Cathodoluminescence (CL) colors described in this report are based on visual observation and are thus somewhat subjective in nature and dependent upon the visual acuity of the observer. Quantification of CL colors requires spectral scans of the luminescence using a fiber optic probe and spectrometer apparatus. Applied Petrographics can arrange for this type of work to be done if required.

3. The colors in the CL photographs may differ from those described in the text owing to the long exposure times necessary for the photography and to changes induced by color balancing during the film processing.

4. Abbreviations used in the text for standard petrographic observations are:

TLX	-	transmitted light, crossed polars
TLP	-	transmitted light, plane polarized
RL	-	reflected light
RLX	-	reflected light, crossed polars
CL	-	cathodoluminmescence

INTRODUCTION

Applied Petrographics was requested to conduct a detailed petrographic study of thirty seven polished thin section samples of rocks from the Rosebud Mine area. The samples include mineralized veins and breccias, altered volcanic wall rocks, porphyries, volcaniclastic sedimentary rocks, and Triassic-Jurassic metasediments. The objectives of the study were:

1. Characterization of mineralized and barren vein and breccia mineralization, and attendant alteration.

2. Determination of ore minerals and parageneses.

3. Characterization of selected porphyries and volcanic stratigraphic units.

4. Identification of any key gangue or alteration minerals whose presence and distribution might help locate additional ore.

METHODOLOGY

Thirty-seven polished thin sections were prepared by Quality Thin Sections of Tucson, Arizona from samples selected by Kurt Allen, chief geologist for the Rosebud Mining company LLC. Sample numbers, locations, field descriptions, and available Au and Ag assay data are given in Table 1. Each section was examined subsequently in transmitted and reflected light using an Olympus BX60 polarizing microscope, and under cathodoluminescence using a Relion Industries Reliotron cathodoluminescence instrument mounted on an Olympus SZ60 stereo microscope with polarizing capability. Results are documented on photomicrographs taken with Nikon N2000 and Olympus OM-2 photographic systems. The photomicrographs accompany this report as Figures 1 -14 and 16-103. Results from the study are presented in two sections. Section I summarizes the results from the study and addresses the objectives ennumerated above, and Section II is a petrographic atlas of the individual polished thin section descriptions from each of the samples. Each description in Section II is accompanied by illustrative photomicrographs in TLX, TLP, and RL representative of the individual sample.

TABLE 1. LIST OF SAMPLES WITH LOCATION, DESCRIPTIVE, AND ASSAY DATA									
ID	Sample Prep	Level	Stope	Panel	Location	Description	Assay ID	Au (opt)	Ag (opt)
RB1	Polished Thin Section	4749	41	Acc	T41BS+69-72 LR	Silica Healed bxa w/marc 182, 72	56430	43.674	45.19
RB2	Polished Thin Section	4679	42	S3	S3BS+40 face	Silica Vein w/marc N55E, 54NW			
RB3	Polished Thin Section	4749	41	P4	P4BS+58 face	grn silica healed bxa w/marc in SRF			
RB4	Polished Thin Section	4749	41	Acc	T41BS+69-72 LR	Silica Healed bxa w/marc 182, 72	56430	43.674	45.19
RB5	Polished Thin Section	4679	42	S3	S3BS+15 face	Qtz vein in altered dozer			
RB6	Polished Thin Section	4679	42	S3	S3BS+40 face	Silica Healed bxa			
RB7	Polished Thin Section	4749	41	P6	P6BS+75.6 RR	Silica Healed bxa	58574	0.091	<0.05
RB8	Polished Thin Section	4763	41	P13	P13-1g+25 RR	BXA			
RB9	Polished Thin Section	4595	43	S4	S4-1g+80 face	Blk Silica w/ W.C. & Marc	58459	0.503	0.4
RB10	Polished Billet	4484	25	S3	S3-2G+28 f	Minz'ed pmbx	61980	60.499	64.27
RB11	Polished Billet	4616	23	P1	P1-2+38 RR	Minz'ed plam			
RB12	Polished Thin Section	4595	43	S4	S4-1g+80 face	Wht Silica vein w/ W.C.	58459	0.503	0.4
RB13	Polished Thin Section	4637	43	Acc	A43-4BS+18' RR	Barren Blk silica bxa	64775	0.009	<0.05
RB20	Thin Section	4595	43	S4	S4-1g+60	W.C. w/ X-Cutting Chlorite Fx			
RB41	Polished Thin Section	4749	41	RA	RABS+80 RR	Porph near Dozer Contact		0.03	
RB42	Polished Thin Section	4749	41	RA	RA/P10 LR	Porph on FW side of FW SRF			
RB43	Polished Thin Section	4749	41	RA	RA/P10 LR	Porph on HW side of FW SRF			
RB44a	Thin Section		Surf		95' N of 2088E, 4764N	Wht Alps porph			
RB44b	Thin Section		Surf		200' N20E of W. Alps outcrop	Wht alps porph/ choc bxa (or autobxa?)			
RB44c	Thin Section		Surf		N end of W. Alps outcrop	Bxa'ted and silicified Wht Alps Porph			
RB45	Thin Section		Surf		P.M.'s type location	Rosebud Qtz Latite / Bud Marker Porph			

TABLE 1 (continued)									
RB55	Thin Section	DH	RL-106		529'	Upper Bud			
RB56a									
RB56b	Thin Section		Surf		200' N20E of W. Alps outcrop	Auto bxa?			
RB57	Thin Section	DH	94-322		543.5'	Middle Bud Unit			
RB58	Thin Section	DH	94-317		505'	Bud Marker Porph			
RB59									
RB60a	Thin Section	4808	14	P0		Plat			
RB60b	Polished Thin Section	4772	21	Acc		Pl at start of Ore, WC+Pyrag+Sulfides			
RB60c	Thin Section	4808	14	P0	P0-2+01'	Plat/Vitrophyre			
RB61a	Thin Section	DH	RL-193		339-341'	LST		0.128	0.3
RB61b	Thin Section	4553	31	S4	P1BS+52.6	LST	58601		
RB61c	Thin Section	4736	21	S6		LST			
RB61d	Thin Section	4772	21	P1		LST - sampled 3/18/98			
RB62									
RB63a	Polished Thin Section	DH	RL-159		655-657'	PMBX w/sulfide veinlet		0.967	1.44
RB63b	Thin Section	2300	23	S1		PMBX			
RB64	Thin Section	4508	25	S1	S1-1g+20 LR	Lower Plam			
RB65a	Polished Thin Section	4472	25	P2		Lower PMBx			
RB65b									
RB66									
RB67									
RB68									
RB69a	Thin Section	DH	94-311		1096'	TOS			
RB69b	Thin Section	DH	94-317		1071'	TOS			
RB70a	Thin Section	4749	41	Acc	T41BS+71 LR				
RB70b	Thin Section	4749	41	Acc	T41BS+69 LR	Dozer			
RB71									
RB72	Thin Section	DH	D-91-94		890'	ALS			

SECTION I SUMMARY OF RESULTS

VEINS AND BRECCIAS

The veins and hydrothermal breccias are lumped together, because they appear similar on the scale of a standard polished thin section. They are represented primarily by samples RB-1 through RB-13 (see Table 1). The breccias and some of the veins contain abundant angular to sub-round fragments that range in size from <1mm to >3cm in diameter dispersed in a matrix of fine, polycrystalline xenomorphic-granular quartz, clay and a dominant composite pyrite-marcasite sulfide assemblage ± silver and gold-bearing phases. The fragments are poorly-sorted and mostly of altered tuffaceous volcanic origin. The altered tuffaceous volcanic fragments are a microcrystalline mosaic of quartz and clay ± alkali feldspar ± relict cloudy brown glass (?) ± disseminated pyrite, with patches of slightly coarser polycrystalline quartz. In some samples the fragments are rimmed with coarser polycrystalline quartz with the long axes of the crystals essentially perpendicular to the fragment margin. The matrix clay may be derived from the alteration of disaggregated volcanic material, but texturally, some of the clay may actually be derived during chemical corrosion of the quartz. Some of the fragments are completely altered to clay-fine sericite. Locally the breccias are invaded by veinlets of coarser polycrystalline quartz ± sulfides. Sample RB-5 is a crackle-brecciated devitrified volcanic lithology. The crackling veinlets are a stockwork of fine, polycrystalline, xenomorphic-granular quartz. The high-grade mineralized breccia represented by sample RB-10 consists of altered glassy volcanic wall rock fragments enveloped in a coarse, porous aggregate of skeletal composite pyrite-marcasite crystals, with significant accessory chalcopyrite, electrum, and a silver sulphosalt mineral. In the breccia/vein represented by sample RB-11, a silver sulphosalt is the dominant ore mineral, and chalcopyrite is absent. Veins and breccias with grades in excess of 0.5 opt Au generally carry gold-bearing minerals in the form of electrum and/or native gold. Examples of a mineralized breccia and vein are illustrated in Figures 1a-c and 2a-b, respectively.

High-grade vs Low Grade Mineralization

Primary gold-bearing minerals were not found in several samples carrying significant gold values (0.042 - 0.967 opt Au). These samples include:

RB-63a	(0.967 opt Au; 1.44 opt Ag)
RB-9	(0.503 opt Au; 0.4 opt Ag)
RB-5	(0.177 opt Au; 0.3 opt Ag)
RB-6	(0.11 opt Au; 1.85 opt Ag)
RB-42	(0.042 opt Au; <0.05 opt Ag)

Several explanations arise. The gold-bearing minerals might have been plucked from the slide during thin section preparation, despite the fact that the samples were all impregnated with epoxy prior to preparation. Secondly, the thin section sample may not be completely representative of the assay sample. The thin section billet depicts only a small part of the assay sample, which was probably in excess of several kilograms. The ore minerals may not have been uniformly distributed throughout the sample. At least part of the discrepancy in the lower grade samples (≤ 0.50 opt Au) may be that significant gold is present substitutionally in the lattice of the composite pyrite-marcasite crystals. This hypothesis is supported by electron microprobe

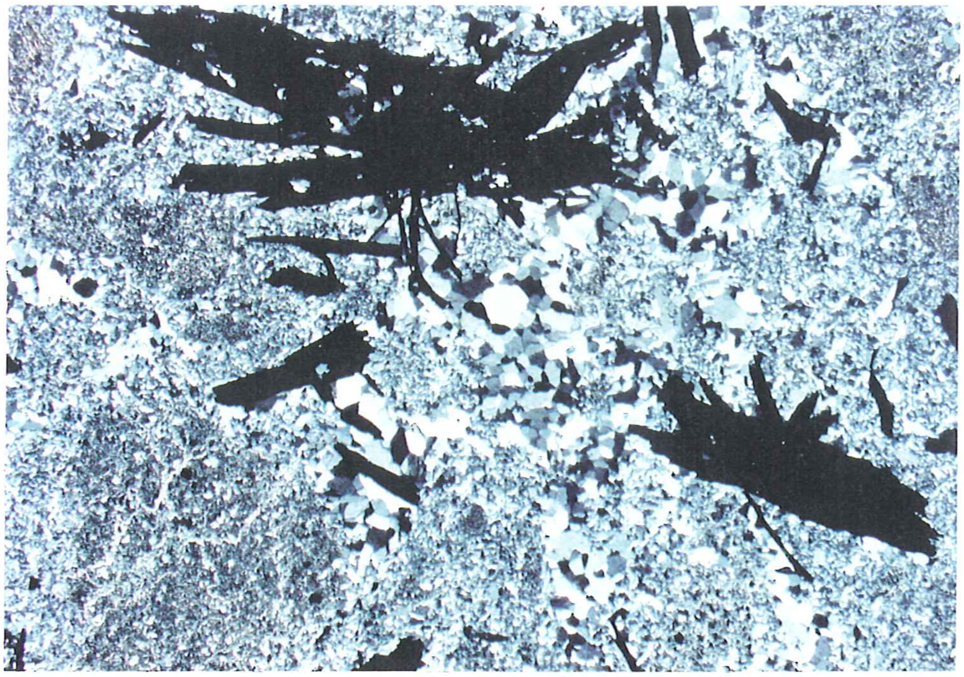

Figure 1a. RB-1/hydrothermal breccia. Tuffaceous volcanic fragments dispersed in a quart-sulfide matrix. TLX; 1cm on the photo= 0.532mm.

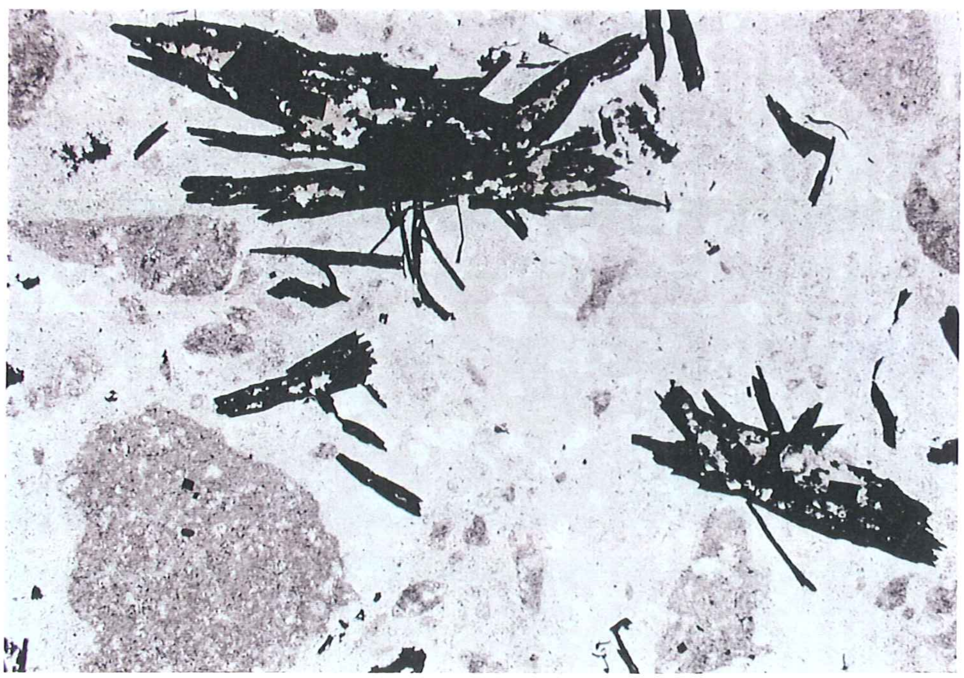

Figure 1b. RB-1/hydrothermal breccia. Same view and scale as figure 1a. TLP; 1cm on the photo= 0.532mm.

Figure 1c. RB-1/hydrothermal breccia. Quartz matrix breccia with clusters of skeletal composite pyrite-marcasite crystals. An electrum crystal occupies intercrystalline void space near the top edge center of the photo (white; high R). Same view and scale as figure 1a-b. RL; 1cm on the photo= 0.532mm.

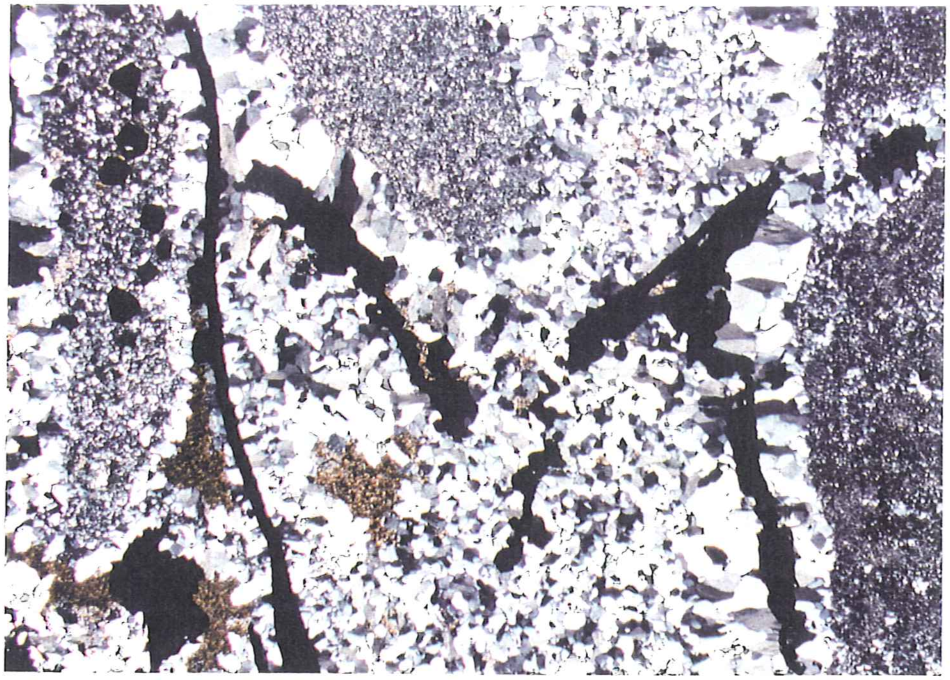

Figure 2a. RB-5/Quartz-sulfide vein. Quartz vein with skeletal composite pyrite-marcasite crystals. Disseminated pyrite in a wall rock fragment engulfed by the vein. TLX; 1cm on the photo= 0.532mm.

Figure 2b. RB-5/Quartz-sulfide vein. Same view and scale as figure 2a. RL; 1cm on the photo= 0.532mm.

analyses of pyrites and composite pyrite-marcasite crystals in sample RS-475-99. The microprobe analyses study were done by microprobe consultant Michael N. Spilde at the University of New Mexico Institute of Meteoritics with the objective of confirming the presence of extremely fine-grained native gold (< 0.004mm) identified by optical means in a vein sample intersected in an exploration drill hole. While the grain in question turned out to be chalcopyrite, anomalous gold abundances (470-670ppm Au) were identified in "Pyrite 2's", which appear to be similar to the skeletal composite pyrite-marcasite crystals that occur in 34 of 42 samples examined for this study. It is likely that the anomalous gold in at least some of the samples that lack primary gold-bearing mineral phases is carried substitutionally in the lattices of the skeletal composite pyrite-marcasite crystals.

ORE MINERALS

Ore minerals identified during this study from all samples include pyrite, composite pyrite-marcasite intergrowths, chalcopyrite, digenite, electrum, native gold, acanthite, silver sulphosalt minerals identified tentatively as pearceite series minerals and pyrargyrite, pyrrhotite, sphalerite, galena, arsenopyrite, goethite, and hematite. The distribution of the ore minerals in the samples examined for this study is summarized in Table 2. The characteristics and occurrence of the major ore minerals are described in the following sections.

Pyrite and composite pyrite-marcasite intergrowths

Pyrite is the most widespread of the sulfide mineral phases in the samples. Pyrite abundances range to several percent in some samples. It occurs as disseminations in all samples but two porphyries (40 of 42 samples). The pyrite is nearly ubiquitous as fine disseminations in volcanic or porphyry host rock and is present also as a component of vein and breccia assemblages. The pyrite commonly has finer crystal size than the composite pyrite-marcasite intergrowths. Pyrite generally forms euhedral to subhedral crystals with cubic, pyritohedron, or trapezoidal morphology. Rarely, these simple pyrites contain minor marcasite intergrowth. Fine-grained, cubic pyrites are commonly found as aggregates filling the interstices of the skeletal composite pyrite-marcasite crystals.

Euhedral to subhedral, prismatic, and generally elongate crystals of intergrown pyrite and marcasite are the next most widespread sulfide phase in the samples (Figures 3 and 4). They occur in 34 of 42 samples, and abundances range to more than five percent in some well-mineralized vein and breccia samples. Many of these crystals have a skeletal form characterized by narrow margins and patchy to elongate interior zones of marcasite, with much of the interior void space filled by aggregates of fine-grained (0.0Xmm diameter) euhedral pyrite crystals. The long dimension of the crystals reaches nearly 10mm in some samples. Maximum aspect ratios range to nearly 90:1, but are more commonly in the range of from 16:1 to 20:1. The skeletal crystals occur both individually and in aggregates. In some vein and breccia samples aggregates of skeletal composite pyrite-marcasite crystals occur in matted clusters with a moderate to strong preferred orientation, or as partly radiating clusters. Locally, significant intracrystalline void space (between the fine-grained pyrite crystals) is filled with a variable assemblage that can include one or more of the phases chalcopyrite, electrum, native gold, acanthite, silver sulphosalt mineral, and, rarely, pyrrhotite. When present, these phases also tend to occupy intercrystalline voids in aggregates of skeletal composite pyrite-marcasite crystals, as well as crystallize in edge contact with the pyrite-marcasite crystals.

TABLE 2. ORE MINERAL DISTRIBUTION IN ROSEBUD MINE AREA SAMPLES

Sample No.	Type	Au (opt)	Ag (opt)	py	py/mc	cp	digenite	electrum	native gold	acanthite	Ag sulphosalt	po-pn	aspy	sphalerite	galena	FeOx hm/goe
RB-1	minzd bx	43.67	45.19	X	X	X	X	X	X	X			X			
RB-2	vein	0.201	0.27	X	X			X		X				X		
RB-3	bx	0.14	0.31	X	X	X			X							
RB-4	minzd bx	43.674	45.19	X	X	X		X	X	X						
RB-5	vein	0.177	0.3	X	X									X		
RB-6	bx	0.11	1.85	X	X	X				X				X		
RB-7	bx	0.091	<0.05	X	X	X				X		X				
RB-8	bx			X	X	X		X								
RB-9	bx	0.503	0.4	X	X	X					X			X		
RB-10	minzd bx	60.499	64.27	X	X	X	X	X			X					
RB-11	vein/bx			X	X			X	X	X	X					
RB-12	vein/bx	0.503	0.4	X	X	X		X	X					X		
RB-13	bx	0.009	<0.05	X	X											
RB-20	lapilli tuff			X	X	X		X		X				X		
RB-41	porphyry	0.023	0.14	X	X			X								
RB-42	porphyry	0.042	<0.05	X	X	X								X		
RB-43	porphyry	0.026	0.06	X	X									X		
RB-44a	porphyry															X
RB-44b	porphyry															X
RB-44c	porphyry			X												X
RB-45	porphyry			X												X
RB-55	lapilli tuff			X	X							X		X		
RB56b	porphyry			X												X
RB-57	lapilli tuff	<0.001	<0.02	X		X						X		X		
RB-58	porphyry	0.006	0.08	X	X									X		
RB60a	tuff			X	X									X		
RB-60b	tuff			X	X						X					
RB-60c	lapilli tuff			X	X											
RB-61a	tuff	0.128	0.3	X	X				X					X		
RB-61b	tuff	0.014	1.06	X	X						X			X		
RB-61c	tuff			X	X				X							
RB-61d	tuff			X	X										X	
RB-63a	volcanic bx	0.967	1.44	X	X	X				X		X				
RB-63b	stkwk bx			X	X											
RB-64	tuff			X	X											
RB-65a	bx			X	X	X		X		X	X			X		
RB-69A	epiclastic bx	<0.001	<0.02	X	X									X		
RB-69b	epiclastic bx	0.006	<0.02	X										X		
RB-70a	tuff			X	X											
RB-70b	tuff			X	X									X		
RB-71	tuff. sandstone			X										X		
RB-72	carb. shale	<0.001	<0.02	X	X											

Figure 3. RB-9/hydrothermal breccia. Chalcopyrite (mustard yellow; moderate R) and acanthite (gray; low to moderate R) in simple intergrowth in edge contact with composite pyrite-marcasite crystals and as intercrystalline void fill. Note marcasite (grayish white; moderately high R) enveloping small, euhedral pyrites (creamy yellow; moderately high R) within the skeletal crystal. RL; 1cm on the photo= 0.021mm.

Figure 4. Aggregate of skeletal composite pyrite-marcasite crystals with chalcopyrite and a silver sulphosalt mineral partly filling an intercrystalline void. Note the linear intergrowths of marcasite (grayish white) with pyrite (creamy yellow) in the skeletal crystal. RL; 1cm on the photo= 0.532mm.

Samples RB-71 and RB-72 both contain disseminated pyrite, some of which is framboidal. Both samples are sedimentary lithologies. Sample RB-71 is a carbonaceous crystal-lithic tuffaceous sandstone related to the Tertiary volcanic section, while sample RB-72 is a carbonaceous shale member of the Jurassic-Triassic Auld Lang Syne group.

Chalcopyrite

Chalcopyrite is third most common and volumetrically significant sulfide phase in the sample population, although abundances are much subordinate to those of pyrite and pyrite-marcasite, and do not exceed about 0.3 percent. Chalcopyrite is present in 14 of 42 samples, and it has a strong tendency to occur with or proximal to breccia and veins well-mineralized with respect to gold and silver. The chalcopyrite is characterized by a mustard yellow color under reflected light against pyrite and marcasite, and its reflectance is slightly less than that of pyrite and marcasite. Chalcopyrite is generally present as fine, anhedral to subhedral crystals less than 0.4mm diameter. Occurrence modes include:

- crystallized in edge contact with pyrite or composite pyrite-marcasite crystals (Figure5).
- occupying intracrystalline void space within composite pyrite-marcasite crystals and/or intercrystalline void space in aggregates of composite pyrite-marcasite crystals.
- in edge contact or simple intergrowth with silver minerals or electrum as a variant of the above occurrence mode.
- discrete crystals intergranular to polycrystalline vein quartz (Figure6).
- rarely in edge contact or partial overgrowth on euhedral pyrite

In sample RB-10 chalcopyrite was noted with a partial rim of digenite. In this sample digenite occurs also as a linear intergrowth parallel to the long axis of the host skeletal composite pyrite-marcasite crystal. RB-2 and RB-11 are the only samples that contain significant gold-silver mineralization, but apparently lack chalcopyrite.

Gold-bearing phases

The primary gold-bearing phases are electrum and native gold. Except for sample RB-11, native gold is much subordinate to electrum in gold-mineralized samples. Electrum is probably the most important ore mineral for both gold and silver. Electrum was identified in 10 of 42 samples, including several samples that were not assayed for gold and silver (RB-8, RB-11, RB-20, and RB-65a). Electrum occurs as fine-grained, anhedral to subhedral crystals to 0.26mm in length/diameter, and in the following occurrence modes:

- partially to completely filling intercrystalline void spaces in skeletal composite pyrite-marcasite or pyrite crystal aggregates (Figures 5 and 7).

Figure 5. RB-8/hydrothermal breccia. Aggregate of pyrite crystals with later crystallizing electrum (pale whitish yellow; high R) in intercrystalline voids. Chalcopyrite is in edge contact with the pyrite aggregate in the lower right quadrant of the photo. RL; 1cm on the photo= 0.106mm.

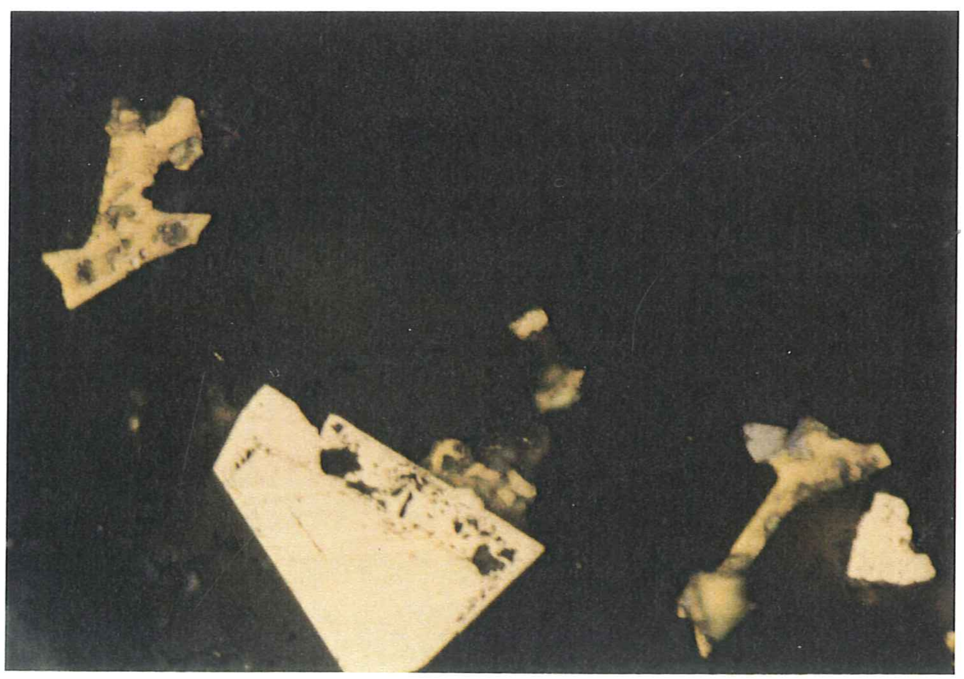

Figure 6. RB-20/lapilli tuff. Chalcopyrite (mustard yellow) and minor acanthite (gray) intergranular to polycrystalline quartz. Note euhedral pyrite crystal with porous margin. RL; 1cm on the photo= 0.021mm.

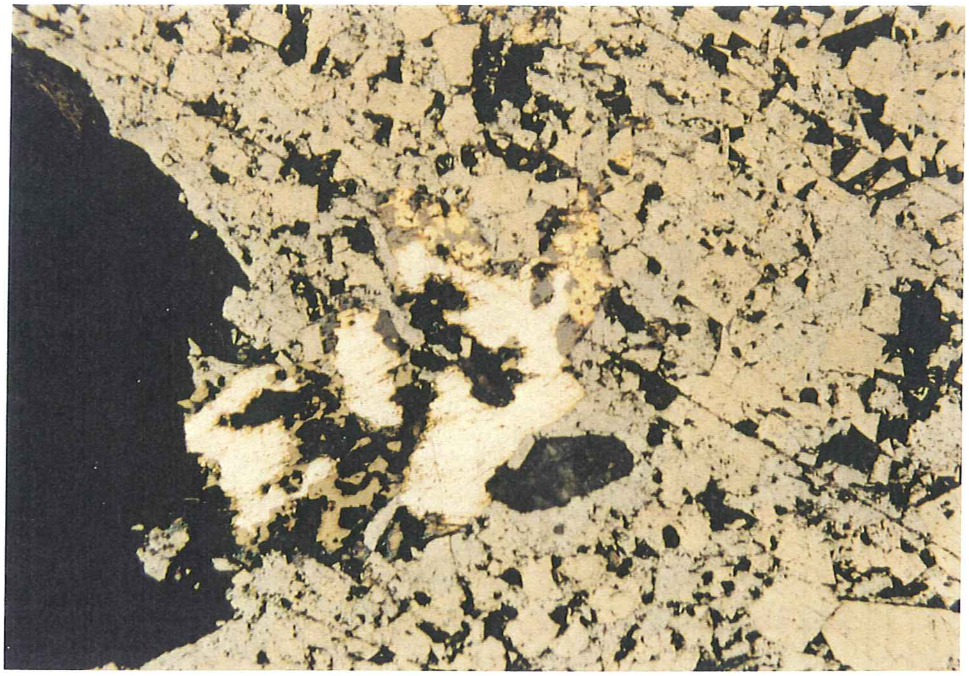

Figure 7. RB-4/hydrothermal breccia. Electrum (yellowish white; high R), native gold (pale yellow; high R), chalcopyrite (mustard yellow-brown), and acanthite (gray, low R)in void spaces within skeletal composite pyrite-marcasite crystals. RL; 1cm on the photo= 0.0532mm.

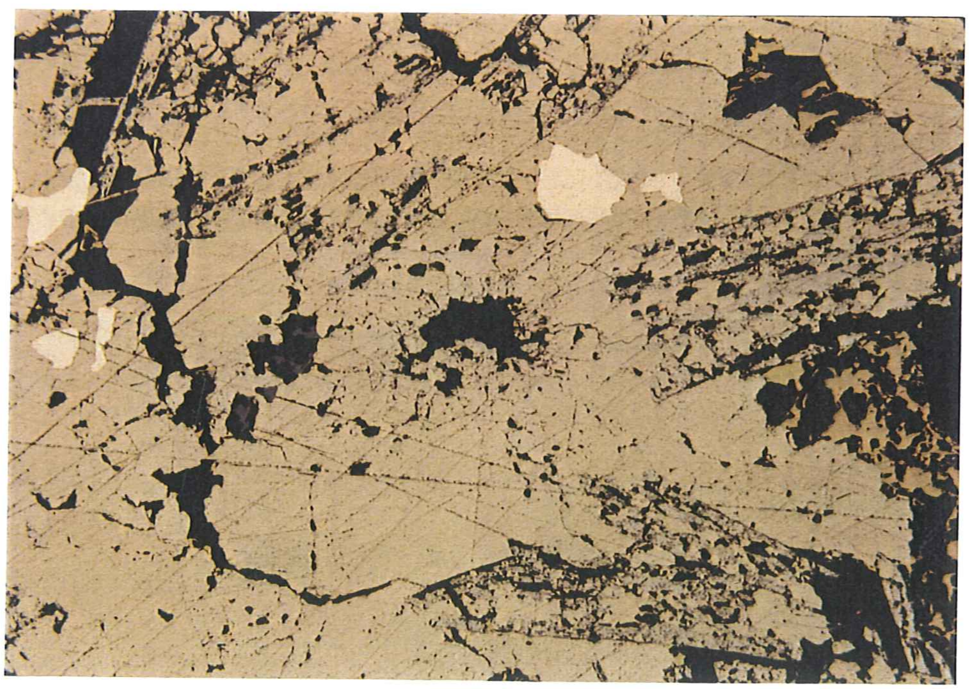

Figure 8. RB-65a/PMBX. Composite pyrite-marcasite crystals with electrum (yellowish white; high R) in intracrystalline voids. Chalcopyrite in edge contact with py-mc near right edge center of the photo. RL; 1cm on the photo= 0.106mm.

- occupying intracrystalline void spaces within individual composite pyrite-marcasite crystals (Figure 8).

- as discrete irregular grains intergranular to polycrystalline quartz or quartz-calcite in veins or breccia matrix.

- in edge contact with composite pyrite-marcasite crystals and/or chalcopyrite or silver sulphosalt minerals.

- as a component of small crystal aggregates with composite pyrite-marcasite ± chalcopyrite.

The electrum is characterized by very high reflectance and a bright white to yellowish white color in RL (reflected light). It tarnishes easily, sometimes within several hours after light polishing has removed the tarnish.

Native gold was identified in 7 of 42 samples. It occurs as very fine-grained, anhedral crystals to 0.26mm in diameter, though most are less than 0.1mm diameter. Occurrence modes include:

- discrete crystals or intergrown with acanthite or silver sulphosalt minerals in intracrystalline voids within skeletal composite pyrite-marcasite crystals. More rarely as blebby inclusions within the same crystal type.

- intergranular to polycrystalline quartz within veins or breccia matrix.

- discontinuous margins on electrum and aurostibite(?) crystals (Figure 9).

- fine blebs or discontinuous threads in a silver sulphosalt mineral (pearceite series?) in sample RB-11. The threads invade the silver phase and migrate along the margin of drusy quartz crystals encompassed by the silver mineral (Figure 10).

- rare partial overgrowths and fracture fill in disseminated pyrite or composite pyrite-marcasite.

- rare very fine disseminations in volcanic wall rock.

A third gold-bearing phase was identified tentatively in sample RB-11. The phase is characterized by white to creamy white color, high reflectance intermediate between pyrite and gold, and incomplete extinction under crossed polars (RLX). This phase is thought to be aurostibite. It was noted in edge contact with composite pyrite-marcasite crystals and a silver sulphosalt phase (pearceite series?). Locally, discontinuous margins of native gold intervene between the aurostibite and pearceite.

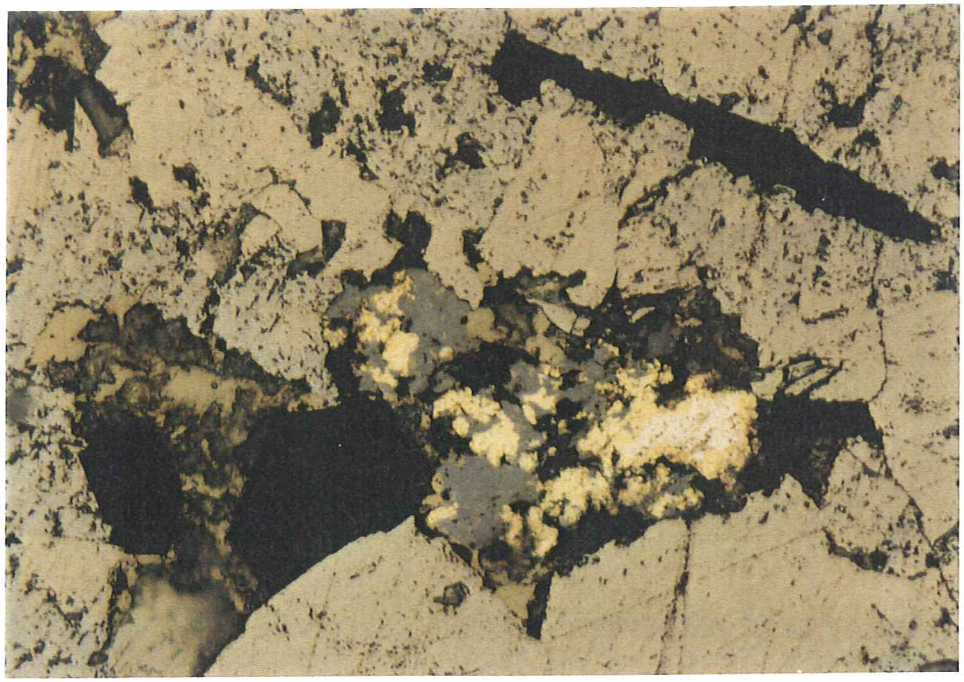

Figure 9. RB-4/hydrothermal breccia. Intergrown electrum-native gold-acanthite-chalcopyrite in intercrystalline void in composite pyrite-marcasite crystal aggregate. Note rims of pale yellow native gold on electrum. RL; 1cm on the photo= 0.021mm.

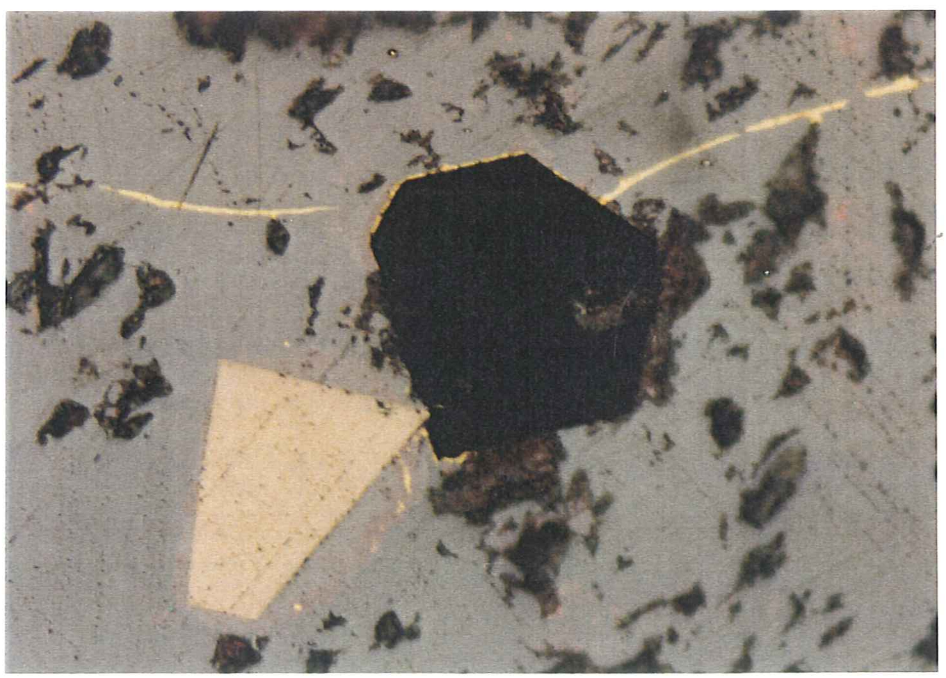

Figure 10. RB-11/breccia vein. Ag sulphosalt (pearceite?) encloses crystals of pyrite and quartz. A thread of pale yellow native gold cuts the silver mineral and migrates along the upper edge of the hexagonal quartz crystal. RL; 1cm on the photo= 0.021mm.

Silver-bearing phases

Primary silver minerals identified during this study are acanthite and at least two silver sulphosalt minerals (pyrargyrite and pearceite-antimonpearceite series). Acanthite was identified in 9 of 42 samples. It is characterized by a gray color, low to moderate reflectance ($R \approx 30$ - 31), and a low polishing hardness. Silver sulphosalt minerals were identified from 6 of 42 samples, two of which also contain acanthite. The pyrargyrite is characterized by a bluish gray color, low to moderate reflectance (R=28 - 31), and deep red internal reflections. The pearceite-antimonpearceite series minerals are characterized by gray color, low to moderate reflectance ($R \approx 30$), and deep red internal reflections much less pronounced than those from pyrargyrite (antimonpearceite has no internal reflections). The similarities in reflected light optical properties makes discrimination between the silver phases difficult at times.

Acanthite occurs as disseminations intergranular to polycrystalline quartz in veins or breccia matrix and as intra- and intercrystalline void fill in composite pyrite-marcasite crystals and crystal aggregates, where it is sometimes intergrown with chalcopyrite and/or native gold (Figure 11). It occurs also in edge contact with composite pyrite-marcasite crystals, either alone, or in association with electrum, chalcopyrite, or sphalerite. Maximum acanthite crystal size is on the order of 0.02mm diameter.

In sample RB-11 a pearceite series silver sulphosalt mineral is the dominant ore mineral. The pearceite occurs as large, porous, irregular crystal aggregates to > 10mm in length/diameter that encompass earlier crystallizing pyrite, composite pyrite-marcasite, and drusy quartz. The aggregates host blebby inclusions and discontinuous threads of native gold that is interpreted to be later than the pearceite. In the mineralized vein and breccia samples the silver sulphosalt minerals occur primarily as intra- and intercrystalline void fill in composite pyrite-marcasite crystals and crystal aggregates, where they reside alone or in association with chalcopyrite, native gold, or, rarely, pyrrhotite or aurostibite(?; Figure 12). They are observed also in edge contact with composite pyrite-marcasite crystals, where they may be intergrown with chalcopyrite, and as sparse inclusions in pyrite.

Pyrrhotite

Pyrrhotite is not common in the samples examined for this study. It was identified in 4 of 42 samples, and it is the most abundant sulfide component in sample RB-57 (though still less than 0.5 percent). Pyrrhotite occurs generally as euhedral to subhedral bladed crystals to 1.6mm length. One pyrrhotite blade encompasses a euhedral cubic pyrite crystal that appears to have crystallized within intracrystalline void space. Local aggregates of pyrrhotite crystals reach 7mm in length/diameter. The pyrrhotite can form sparse disseminations or bladed aggregates. It is abundant in a lithic lapillus in sample RB-57, where the crystals form a radiating bladed aggregate. Some of the bladed pyrrhotites contain linear intergrowths of pentlandite (white; isotropic; reflectance slightly higher than pyrrhotite; Figure 13). Rarely pyrite and pyrrhotite are present in the same crystal, where pyrite forms partial rims on the pyrrhotite. In some of the disseminations the pyrrhotite is in edge contact with traces of fine, anhedral sphalerite.

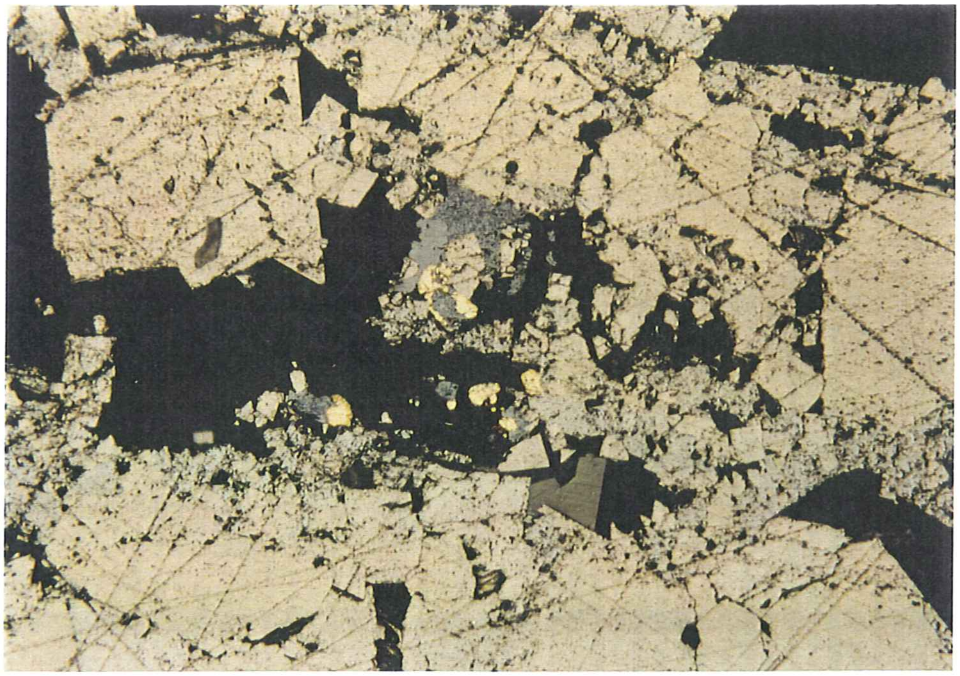

Figure 11. RB-1/hydrothermal breccia. Acanthite (gray; low to moderate R), electrum, and native gold in intercrystalline voids within aggregate of skeletal composite pyrite-marcasite crystals. RL; 1cm on the photo= 0.053mm.

Figure 12. RB-11/breccia vein. Skeletal composite py-mc crystal along right edge of photo. Tarnished creamy white phase with higher R than py-mc may be aurostibite (?). Ag sulphosalt mineral (gray moderate R; pearceite?) with minor intergrown electrum. Second gray phase with lower R may be tennantite. RL; 1cm on the photo= 0.053mm.

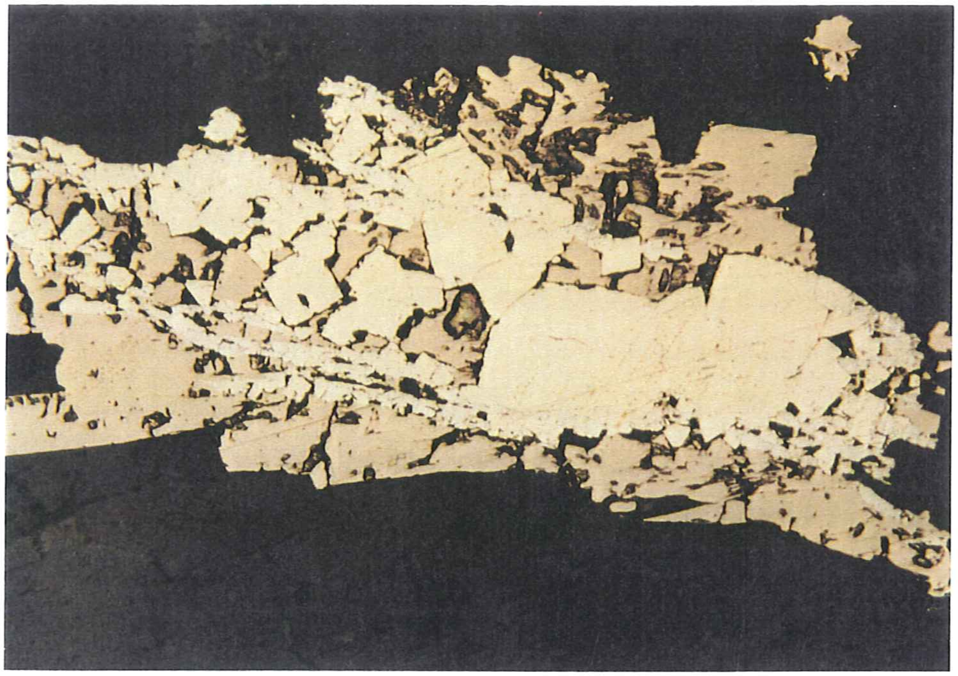

Figure 13. RB-57/lapilli tuff. Pyrrhotite (pinkish brown; lower R than py)in eu- to subhedral crystals grown in and around aggregates of pyrite crystals. Note linear intergrowths of pentlandite (creamy white; moderately high R). RL; 1cm on the photo= 0.053mm.

Figure 14. RB-20/lapilli tuff. Sphalerite gray; low R) partly rimming pyrite in tuffaceous wall rock. RL; 1cm on the photo= 0.021mm.

Sphalerite and galena

Sphalerite is widespread, although not abundant, in the samples examined for this study. It is present in 19 of 42 samples. Sphalerite forms anhedral crystals less than 0.1mm diameter and has the following occurrence modes:

- sparse disseminations in wall rock and in polycrystalline quartz in veins and breccia matrix.
- in edge contact with disseminations of pyrite, pyrrhotite, chalcopyrite, or composite pyrite-marcasite crystals (Figure 14).
- as partial inter- and intracrystalline void fill in composite pyrite-marcasite crystals.
- accompanying polycrystalline quartz and composite pyrite-marcasite ± chalcopyriteas pseudomorphs of feldspar phenocrysts in porphyry.

Galena was identified in only one sample (RB-61d), where it forms a fine (0.02mm diameter), anhedral crystal in a quartz-pyrite-marcasite stringer.

Other Opaque Minerals

In unmineralized porphyries the iron oxide minerals goethite and hematite were noted partly replacing primary mafic phenocrysts (biotite?) and probably primary Fe-Ti oxide phases, as well. Hematite pseudomorphs pyrite at the contact between quartz latite porphyry and breccia in sample RB-56b. Disseminated magnetite was observed in porphyry in one sample (RB-45), and a trace of rutile was noted in sample RB-7.

Parageneses

In most of the samples that contain pyrrhotite, the pyrrhotite appears to have crystallized earlier than pyrite. Disseminated pyrrhotite crystals were observed with pyrite rims, and pyrite is found also in voids intracrystalline to bladed pyrrhotite. One sample (RB-7) pyrrhotite is present in intracrystalline void space in a composite pyrite-marcasite crystal. In the remaining samples where they are present pyrite and composite pyrite-marcasite crystals were the first opaque minerals to crystallize. The skeletal composite pyrite-marcasite crystals may have precipitated earlier than the disseminated euhedral pyrites. Most of these crystals have skeletal morphology that may be indicative of rapid crystallization with growth accelerated along the c-axis. These crystals are filled commonly by aggregates of euhedral cubic pyrites similar to those disseminated in veins, breccia matrix, and wall rock. These pyrites are interpreted to crystallize shortly after formation of the skeletal crystals.

The intracrystalline voids in the skeletal composite pyrite-marcasite crystals and intercrystalline voids in aggregates of those crystals can contain a late-crystallizing group of minerals that includes one or more phases of an assemblage that includes chalcopyrite-digenite-acanthite-Ag sulphosalt minerals-native gold-electrum-sphalerite-pyrrhotite. Chalcopyrite, the silver minerals, and, more rarely, sphalerite are commonly in edge contact or simple intergrowth, and it is likely that they are co-crystalline. Electrum locally has rims of native gold and is interpreted to have crystallized slightly earlier than the gold. Native gold is the last significant ore mineral tpo precipitate in the depositional sequence.

VOLCANIC HOST ROCKS

The Rosebud mine area stratigraphic section provided by Kurt Allen is reproduced here as Figure 15. Based on this section and Kurt Allen's assessment of where the samples in this study fit into the stratigraphy, the study samples are grouped as follows:

Bud tuff	RB-55	(Upper Bud)
	RB-57	(Middle Bud)
LST	RB-61a	
	RB-61b	
	RB-61c	
	RB-61d	
Unnamed ash flow unit	RB-60a	(planar laminar flow zone)
	RB-60b	(planar laminar flow zone)
	RB-60c	(planar laminar flow zone)
	RB-63a	(Upper Pink Matrix Breccia)
	RB-63b	(Upper Pink Matrix Breccia)
	RB-64	(tuff/planar laminar flow zone)
	RB-65	(Lower Pink Matrix Breccia)
TOS (Oscar sediments?)	RB-69a	
	RB-69b	
Dozer tuff	RB-70a	
	RB-70b	
Volcaniclastic sediments	RB-71	

Bud Tuff

Samples from the middle and upper Bud tuff were examined for this study. Both appear to be lithic lapilli ash flow tuffs with abundant sub-round lithic fragments of tuffaceous volcanic origin dispersed in a very fine-grained, devitrified tuffaceous matrix of quartz, alkali feldspar, clay, and calcite (Figure . Pyrogenic crystals and crystal fragments of altered plagioclase, biotite, and hornblende are sporadically present in both lithic fragments and matrix. Sample RB-57 has well developed undulatory compaction bedding. Both samples contain disseminated sulfides that can include pyrite, pyrrhotite, and composite pyrite-marcasite. Pyrrhotite is a significant component of the sulfide assemblage in both samples. Of potential significance is the observation that both samples have tuffaceous lithic fragments that host veins carrying quartz-calcite ± sulfides (pyrite-marcasite or pyrrhotite; Figure 16a-b). It would appear that at least

ROSEBUD MINE STRATIGRAPHY

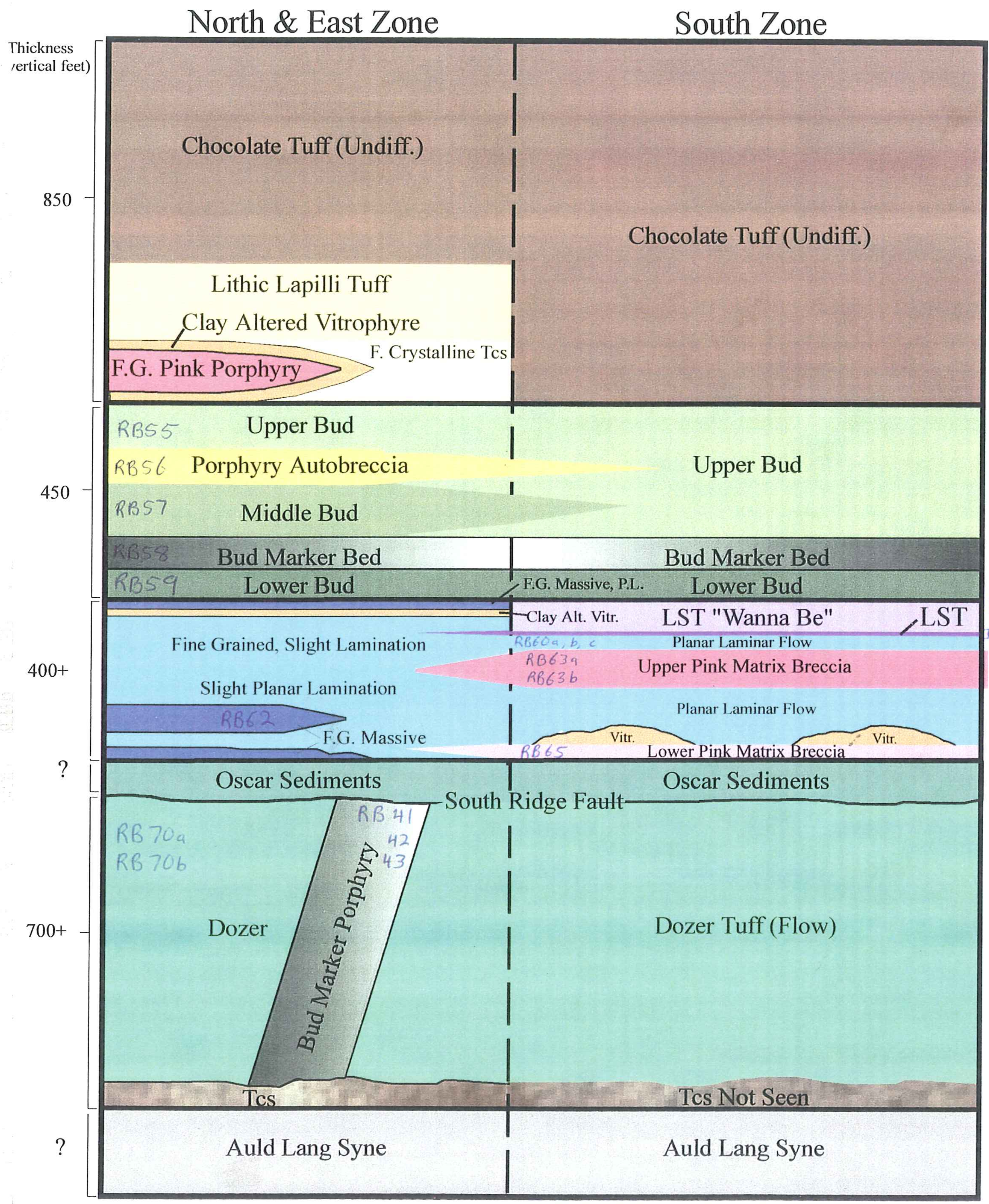

Figure 15

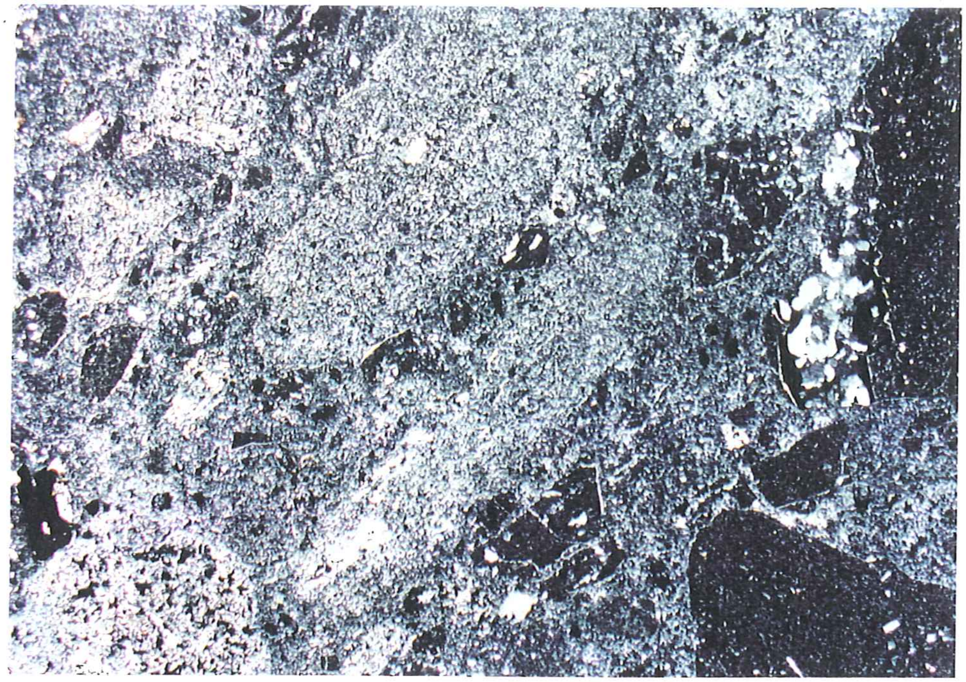

Figure 16a. RB-55/Bud tuff. Fragment in lapilli tuff contains part of a quartz-sulfide vein near right edge center of photo. TLX; 1cm on the photo= 0.532mm.

Figure 16b. RB-55/Bud tuff. Same view and scale as Figure 16a. TLP; 1cm on the photo= 0.532mm.

some of the vein mineralization in the Rosebud hydrothermal system preceded eruption and deposition of the Bud tuff.

LST

Samples RB-61a through RB-61d appear to be from a well-compacted ash flow tuff unit. They are essentially devoid of lithic fragments, but carry several percent pyrogenic crystals and crystal fragments of altered plagioclase, sanidine, and mafics (hornblende and/or biotite), all dispersed in a devitrified tuffaceous groundmass of extremely fine crystallites of quartz and alkali feldspar ± relict glass and clay. RB-61, b-d show well-developed compaction bedding and irregular, lensoid fiamme replaced variably by quartz, chlorite, clay, and sulfides, or some combination of these phases (Figure 17a-b). One of the replaced fiamme is cored by a composite pyrite-marcasite crystal with native gold filling microfractures. Locally partial or complete spherulites composed of radiating quartz crystals extend into the replaced fiamme. The presence of the spherulitic devitrification and undulatory compaction bedding may indicate that the tuffs were strongly welded and may have flowed rheomorphically.

Unnamed tuff unit

Seven samples were examined from a pyroclastic unit stratigraphically between the Bud and Dozer tuffs. Samples RB-60a-c and RB-64 are from zones in the tuff interpreted to be deposited in a planar laminar flow regime, according to Figure 1. Samples RB-60, a and b, and sample RB-64 are composed of sparse pyrogenic crystals and crystal fragments of altered feldspar and biotite dispersed in a devitrified tuffaceous groundmass of quartz and alkali feldspar (Figure 18a-c). The feldspars show minor to moderate clay alteration, and there is weak to moderate pervasive calcite flooding of the groundmass. The samples all show a crude compaction bedding and are cut by veins and stringers of quartz, clay, sulfide, and perhaps adularia (?). Sample RB-60c is described in the field as a vitrophyre. In thin section it is a densely welded lapilli tuff choked with lithic lapilli of tuffaceous volcanic origin. Both fragments and lapilli are devitrified to a microcrystalline mosaic of quartz and alkali feldspar. The sample contains abundant, narrow, discontinuous stringers of quartz and chlorite ± pyrite.

Samples RB-63a and 63 b, and RB-65a are from the Upper and Lower Pink Matrix Breccia units, respectively. The Upper Pink Matrix Breccia probably represents a pyroclastic breccia protolith. It contains abundant, poorly-sorted subangular to subround monolithic fragments of tuffaceous volcanic origin in a microcrystalline groundmass of quartz and alkali feldspar. Both lithic fragments and matrix are devitrified tuffaceous material. The breccia is cut by a stockwork of quartz-clay-calcite-sulfide veinlets. Calcite forms discontinuous stringers and replaces some of the lithtic fragments. Sample RB-63a carries about 10% sulfides and assays significant gold and silver. Sample RB-65a represents the Lower Pink Matrix Breccia (Figure 19a-b). Part of the sample appears to be a crackle breccia of devitrified tuff in a microcrystalline matrix of quartz and fine sericite or clay. Fragments and matrix are invaded by anastamosing veinlets of quartz and sericite ± calcite. The crackle breccia contains 2-3% sulfides as pyrite and composite pyrite-marcasite crystals. The crackle breccia is in contact with a densely welded tuff that is invaded by a coarse, irregular mass of radiating skeletal composite pyrite-marcasite crystals, quart, and calcite. Although no assay was provided for this sample significant gold and silver mineralization was noted associated with the coarse, radiating sulfides in the form of electrum, acanthite, and a silver sulphosalt mineral.

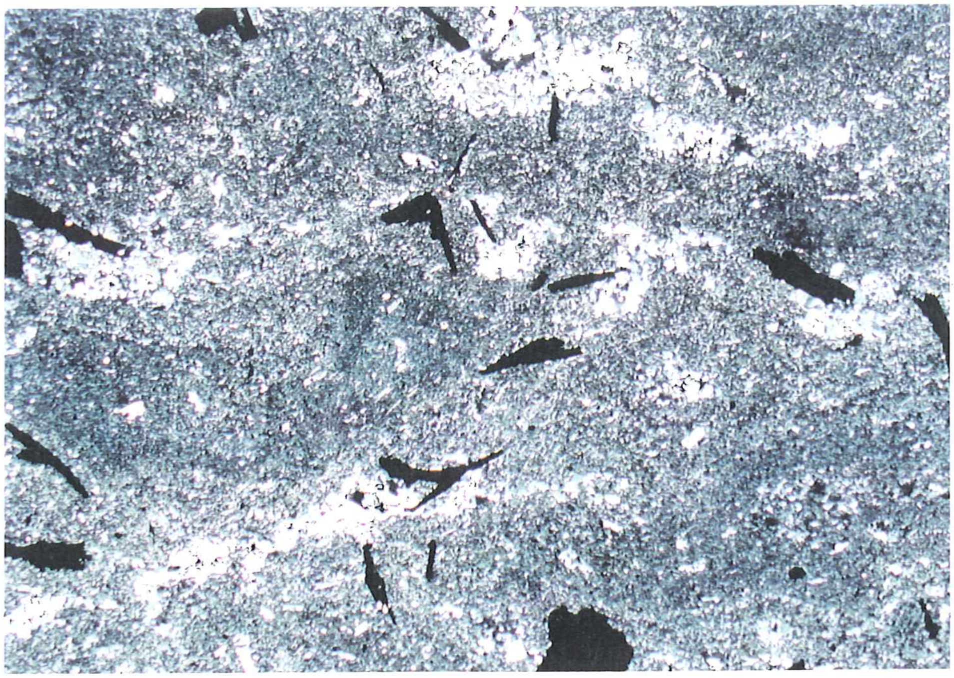

Figure 17a. RB-61c/LST bedded tuff. Bedded tuff with disseminated sulfides and fiamme replaced by quartz-clay ± sulfides. TLX; 1cm on the photo= 0.532mm.

Figure 17b. RB-61c/LST bedded tuff. Same view and scale as figure 17a. TLP; 1cm on the photo= 0.532mm.

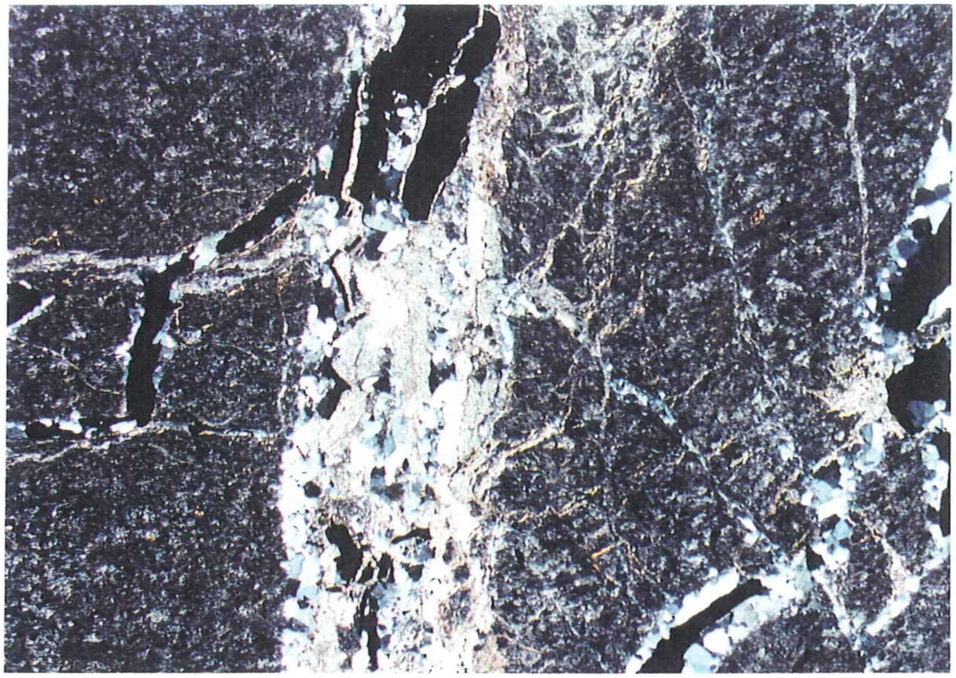

Figure 18a. RB-64/Lower Plam. Planar bedded tuff with quartz-clay-calcite-pyrite-marcasite veins. TLX; 1cm on the photo= 0.532mm.

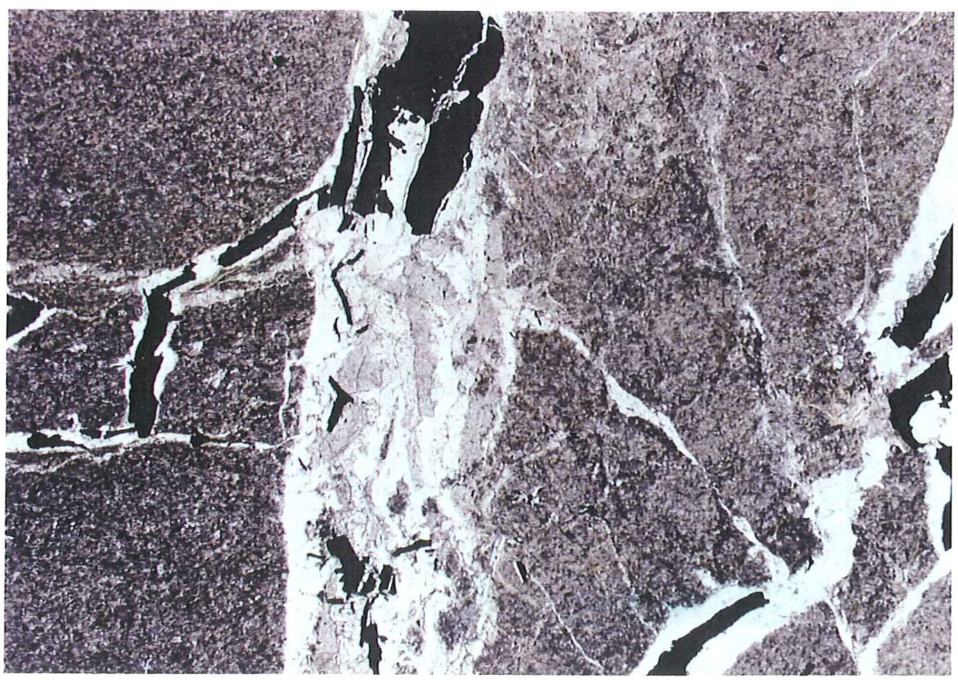

Figure 18b. RB-64/Lower Plam. Same view and scale as figure 18a. TLP; 1cm on the photo= 0.532mm.

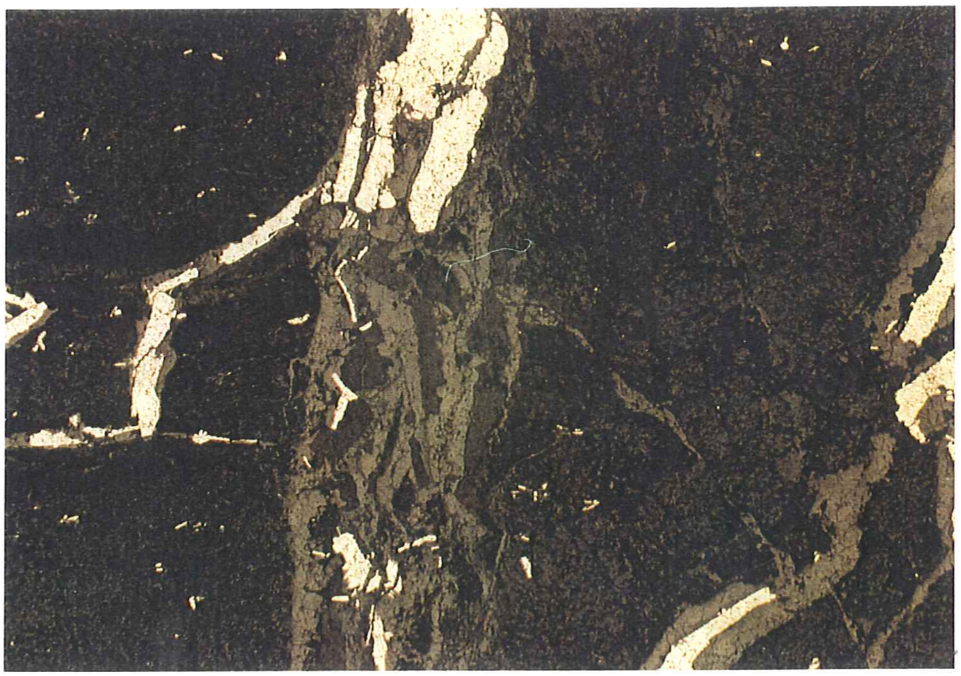

Figure 18c. RB-64/Lower Plam. Skeletal composite pyrite-marcasite crystals in quartz veins invading bedded tuff. Same view and scale as Figures 18a-b. RL; 1cm on the photo= 0.532mm.

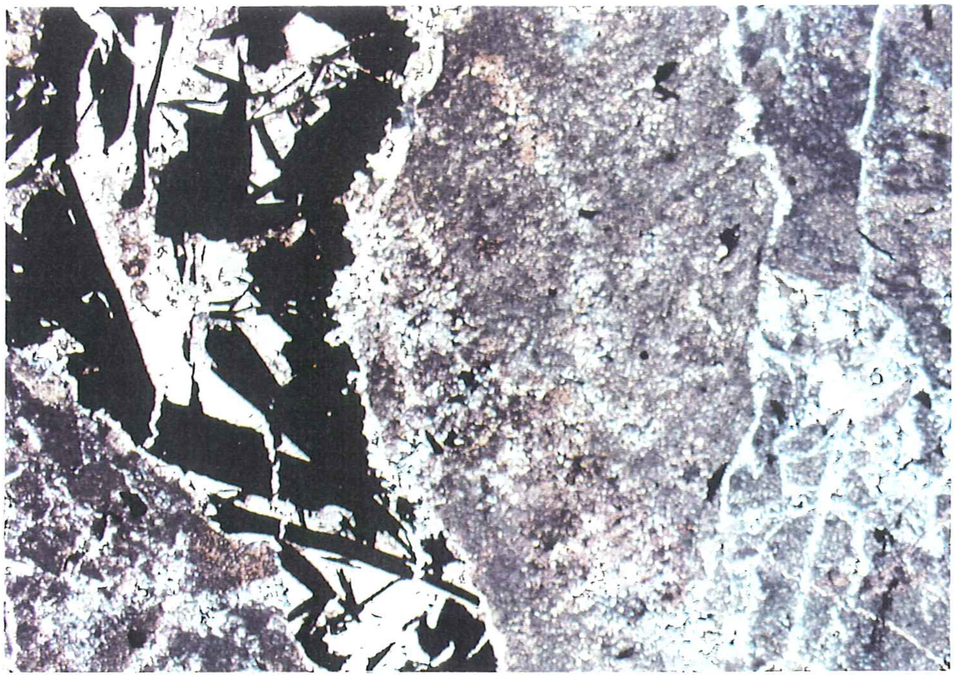

Figure 19a. RB-65a/Lower PMBX. Contact zone between two glassy tuff lithologies separated by a quartz-calcite-sulfide (py/mc) vein. Note the samll quartz matrix microbreccia zone at right photo edge. TLX; 1cm on the photo= 0.532mm.

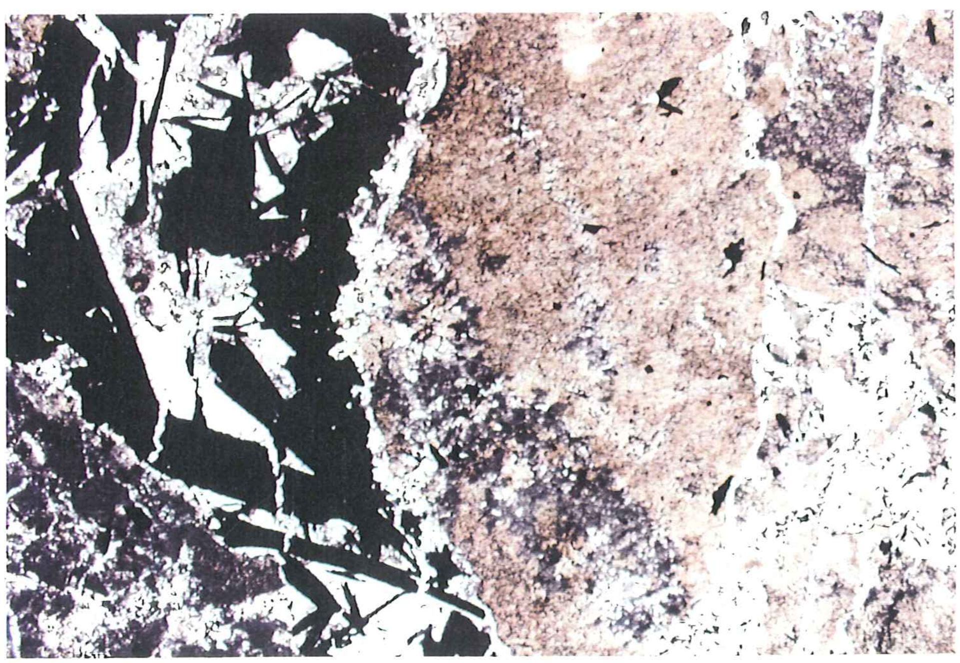

Figure 19b. RB-65a/Lower PMBX. Same view and scale as figure 19a. TLP; 1cm on the photo= 0.532mm.

TOS (Oscar sediments?)

Samples RB-69a and RB-69b appear to be volcaniclastic lithic breccia. They range from fragment-supported to matrix-supported, and are choked with angular to subround, lapilli-sized lithic fragments. The lithic fragments all appear to be of pyroclastic origin in sample RB-69b, but sample RB-69a contains fragments of quartz veins and epiclastic volcanic siltstone, as well (Figure 20a-b). Some of the pyroclastic volcanic fragments have traces of pyrogenic biotite and feldspar altered to chlorite and clay, respectively, but the lithic fragments commonly lack pyrogenic crystal phases. The devitrified fragments contain relict brown glass and very fine crystallites of quartz and alkali feldspar, some of which has altered to clay. The fragments are locally flooded by calcite. There is a crude stratification of the fragments in the very fine-grained devitrified ash matrix in sample RB-69b, but sample RB-69a does not show noticeable stratification on the scale of the thin section. The matrix is composed of a microcrystalline mosaic of quartz, alkali feldspar, clay, and late disseminated calcite. Both samples are laced by discontinuous, wispy veinlets of quartz, clay, and calcite, and both contained disseminated pyrite.

Dozer tuff

Samples from the Dozer tuff unit are both fine-grained, devitrified tuff with faint ± cm-scale bedding. Pyrogenic crystals and crystal fragments are sparse to absent. The devitrified groundmass is a microcrystalline mosaic of quartz, alkali feldspar, and clay, plus remnants of cloudy, grayish-brown glass. The tuffs are traversed by veinlets of quartz ± clay ± pyrite ± pyrite-marcasite (Figure 21a-b). Locally the veinlets disrupt the host tuff and form small zones of microbreccia. In places the tuff is partially silicified by irregular patches of fine, polycrystalline quartz.

Volcaniclastic sediments

A single sample of the volcaniclastic sediment unit was examined for this study. Sample RB-71 is a finely laminated, bedded crystal-lithic tuffaceous sandstone with significant organic material content. The sandstone is very fine-grained and moderately well-sorted. It contains abundant crystal fragments of quartz, biotite, and feldspar, plus microcrystalline lithic fragments, most of which are of probable volcanic origin, in a very fine-grained, microcrystalline groundmass of quartz, alkali feldspar, and clay that probably represents devitrified fine, ashy material. Fine, crenulated wisps of organic material impart a finely-laminated texture to the tuffaceous sediment (Figure 22a-b). There are a few concordant, very narrow, discontinuous quartz veinlets that appear to occlude bits of organic matter. The laminations show millimeter-scale offsets in several places along very narrow, discordant clay or clay-quartz (± py) veinlets. A trace of framboidal pyrite was noted in the sample.

PORPHYRIES

Nine porphyry samples were examined during the course of this study. The sample numbers and field designations as provided to the author are listed below:

RB-41	Bud Marker porphyry (near Dozer contact)
RB-42	Bud Marker porphyry (FW side of SRF)

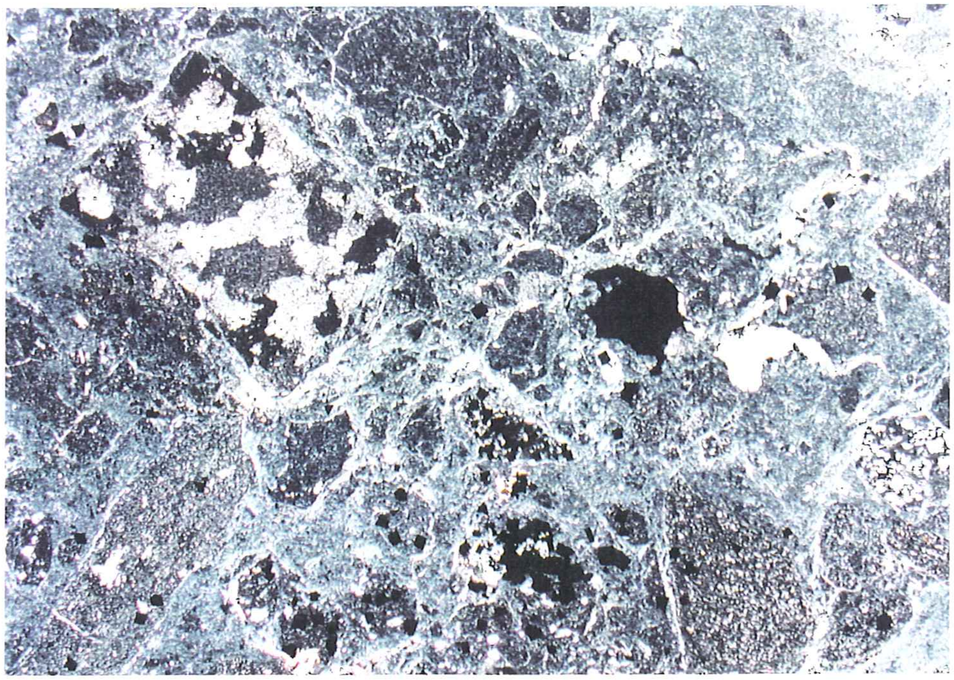

Figure 20a. RB-69a/TOS. Volcaniclastic lithic breccia. Note rectangular fragment of polycrystalline quartz (metamorphic quartz vein?). TLX; 1cm on the photo= 0.532mm.

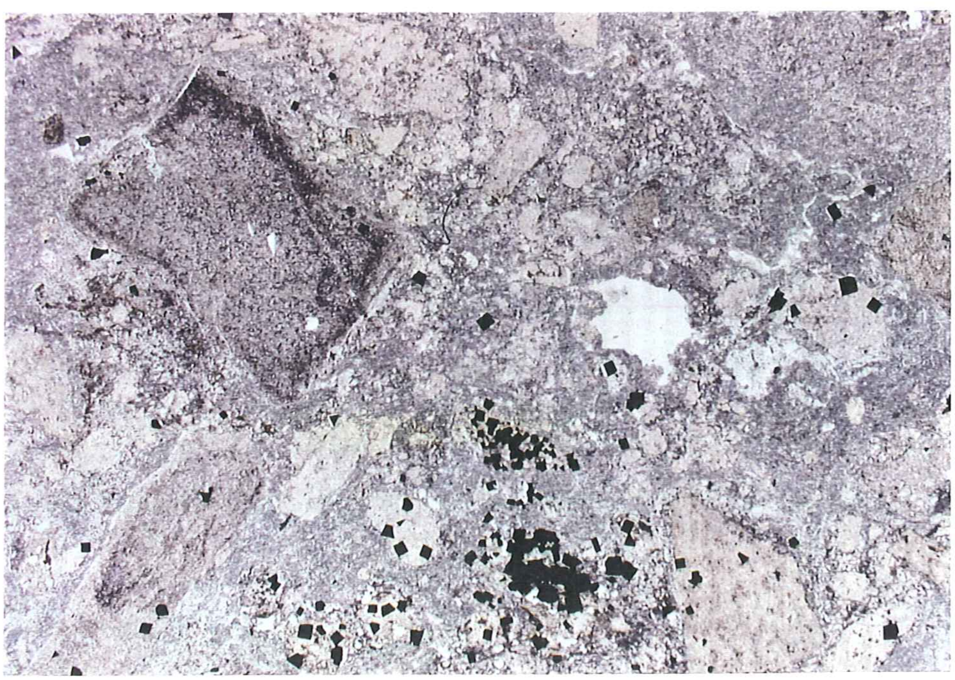

Figure 20b. RB-69a/TOS. Volcaniclastic lithic breccia. Same view and scale as figure 20a. TLP; 1cm on the photo= 0.532mm.

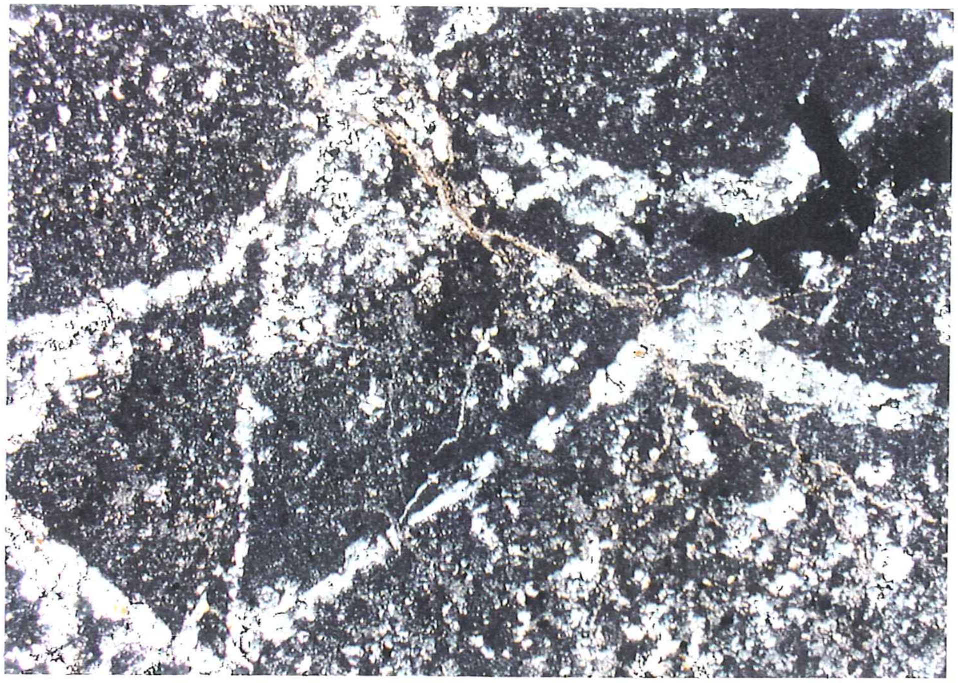

Figure 21a. RB-70a/Dozer tuff. Devitrified bedded tuff with stockwork quartz, clay, and quartz-clay veinlets. TLX; 1cm on the photo= 0.532mm.

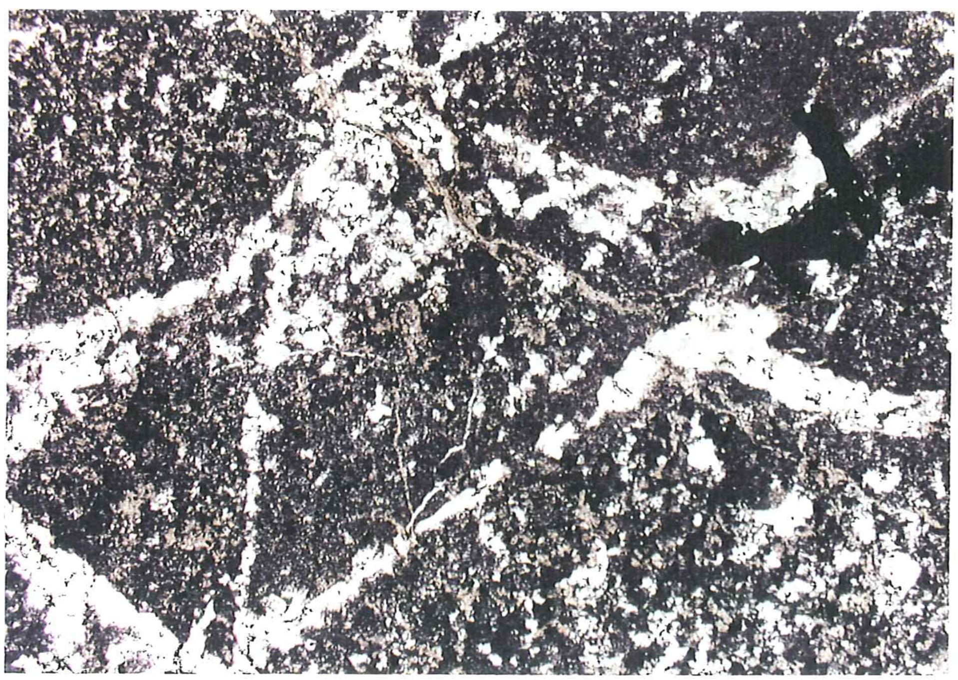

Figure 21b. RB-70a/Dozer tuff. Same view and scale as Figure 21a. TLP; 1cm on the photo= 0.532mm.

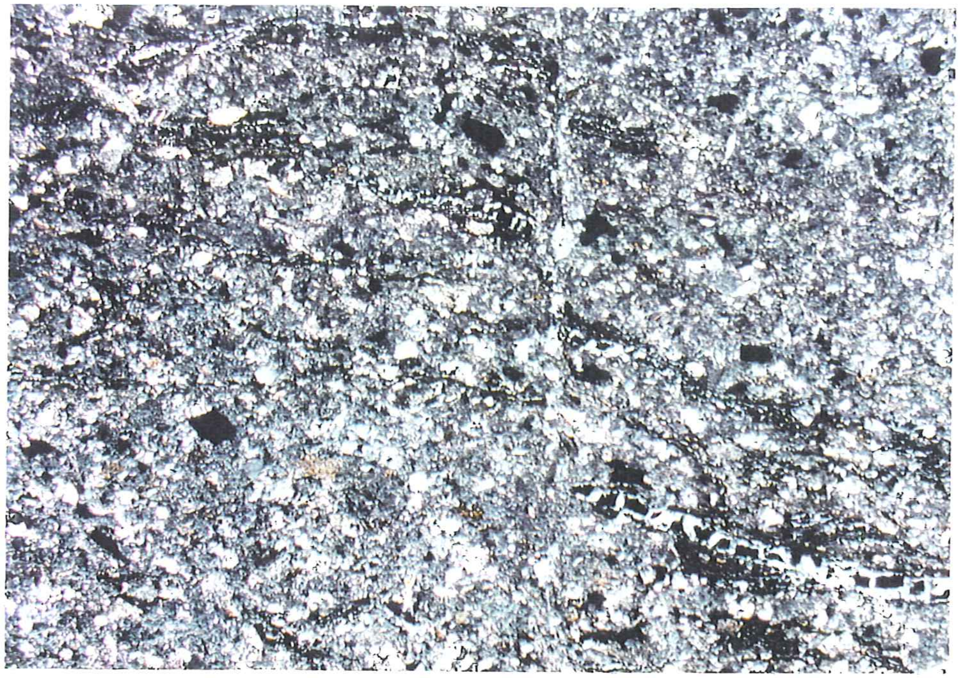

Figure 22a. RB-71/tuffaceous sandstone. Laminated, carbonaceous, crystal-lithic tuffaceous sandstone. Black streaks are organic debris that impart the laminated texture. The bedding has a minor offset along a narrow quartz vein. TLX; 1cm on the photo= 0.532mm.

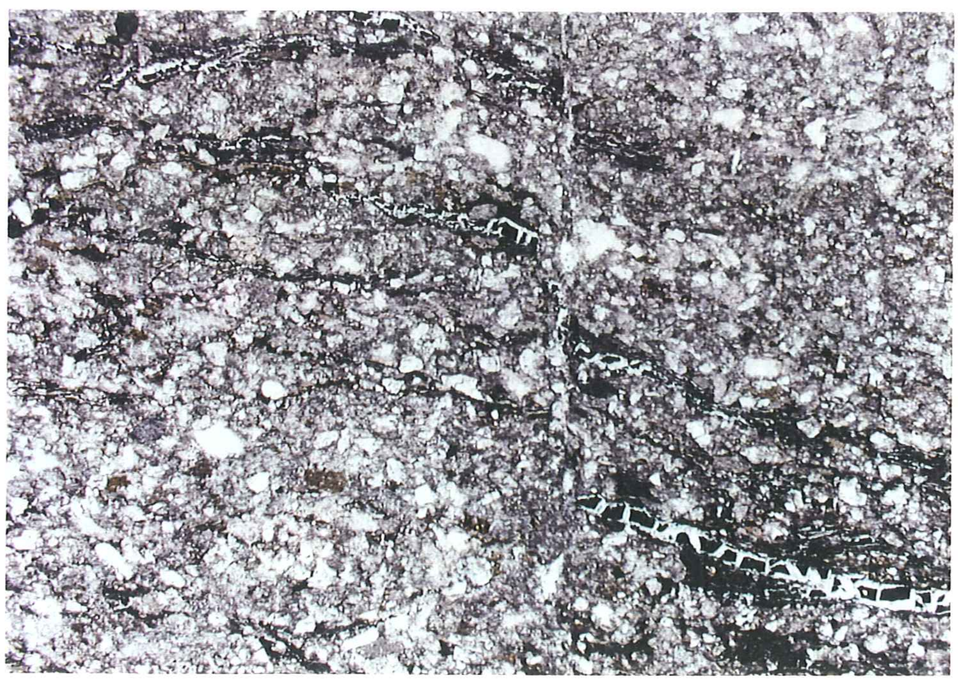

Figure 22b. RB-71/tuffaceous sandstone. Same view and scale as Figure 22a. TLP; 1cm on the photo= 0.532mm.

RB-43	Bud Marker porphyry (HW side of SRF)
RB-44a	White Alps porphyry
RB-44b	White Alps porphyry/choc bxa-or autobx?)
RB-44c	White Alps porphyry (brecciated and silicified)
RB-45	Rosebud Qlatite/Bud Marker porphyry
RB-56b	(porphyry autobreccia)
RB-58	Bud Marker porphyry

Bud Marker porphyry

The Bud Marker porphyry, as represented by samples RB-41, RB-42, and RB-43, are generally similar, sparsely porphyritic shallow intrusive rocks of dacitic to quartz latitic composition. They contain several percent partly altered and pseudomorphed phenocrysts of plagioclase, K feldspar, and mafics (biotite or hornblende) dispersed in a fine-grained, xenomorphic-granular groundmass of quartz, feldspar, and clay. Plagioclase appears to make up a considerable proportion of the groundmass feldspar, although much of the feldspar is altered to clay. K feldspar phenocrysts are partly to completely pseudomorphed by polycrystalline quartz, pyrite, and composite pyrite-marcasite (Figure 23a-b). Plagioclase is altered to microcrystalline quartz, sericite, and clay. Relict plagioclase indicates that original composition was in the sodic andesine range. The former mafic phenocrysts are completely altered to calcite and fine sericite, and they are usually associated with clusters of fine-grained apatite. All three of the samples contain weak gold mineralization. The gold is probably substitutional in composite pyrite-marcasite crystals in veins or disseminatioins.

Sample RB-58 has similar petrographic characteristics and can be reliably correlated with the Bud Marker porphyry.

White Alps porphyry

The White Alps porphyry as represented by samples RB-44a and RB-44b is a sparsely to moderately porphyritic shallow intrusive or, perhaps, extrusive rock of quartz latitic composition. It consists of from 3-12% phenocrysts of sanidine, plagioclase, mafics (biotite?), and quartz dispersed in in a fine groundmass composed of xenomorphic quartz, K feldspar, plagioclase, and significant partly devitrified grayish brown glass (Figure 24a-b). Observation under CL shows that the groundmass is partly replaced by calcite and has Kspar in excess of plagioclase. The plagioclase shows partial to complete alteration to microcrystalline quartz. Sanidine shows Carlsbad twinning and more equant morphology than the plagioclase. It occurs in local glomerocrystic aggregates with quartz. Quartz microphenocrysts are anhedral and exhibit edge corrosion. Quartz is present also in small round miarolytic cavities, where individual crystals grow inward from the cavity margin and show a pronounced growth zonation. Mafics are completely altered to an assemblage of goethite, hematite, and quartz. Goethite also replaces former Fe-Ti oxide phases. Disseminated apatite is not present.

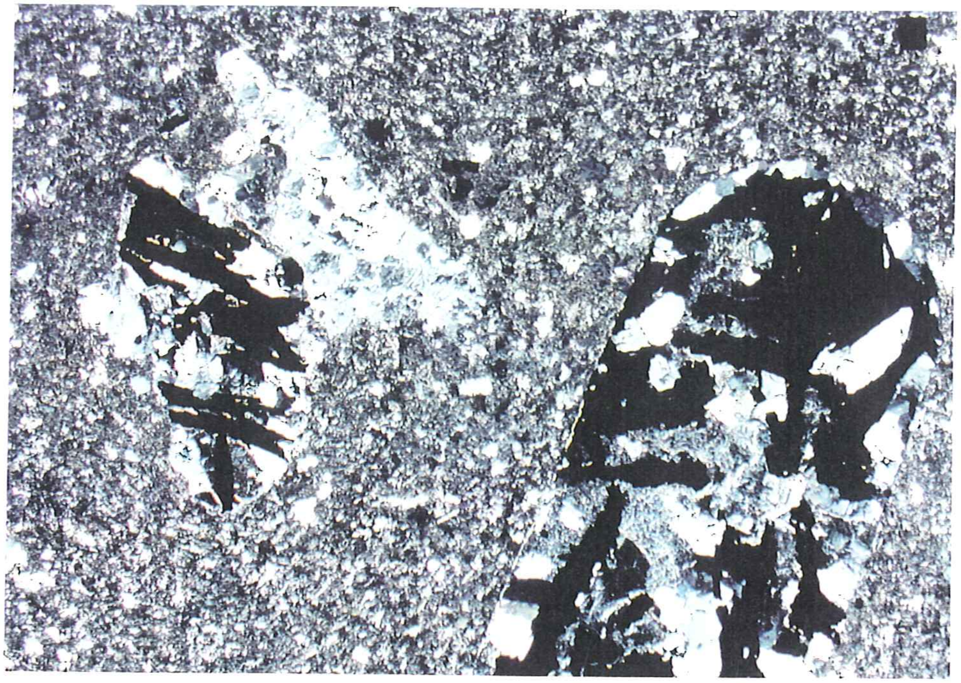

Figure 23a. RB-42/Bud Marker porphyry. Kspar phenocrysts are pseudomorphed by polycrystalline quartz and composite pyrite-marcasite crystals. The fine, xenomorphic-granualr groundmass is composed of quartz, plagioclase, Kspar, and clay. TLX; 1cm on the photo= 0.532mm.

Figure 23b. RB-42/Bud Marker porphyry. Same view and scsale as figure 23a. TLP; 1cm on the photo= 0.532mm.

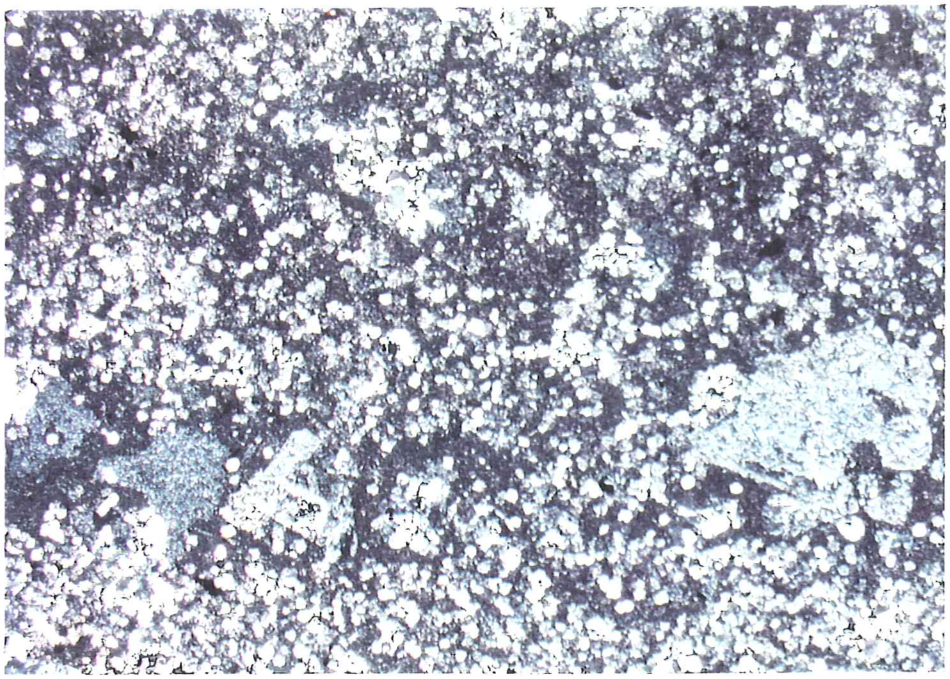

Figure 24a. RB-44b/White Alps porphyry. Quartz latite porphyry with faint flow-banding. Phenocrysts of plagioclase and sanidine are dispersed in a fine groundmass of quartz, Kspar, plagioclase, and glass. TLX; 1cm on the photo= 0.532mm.

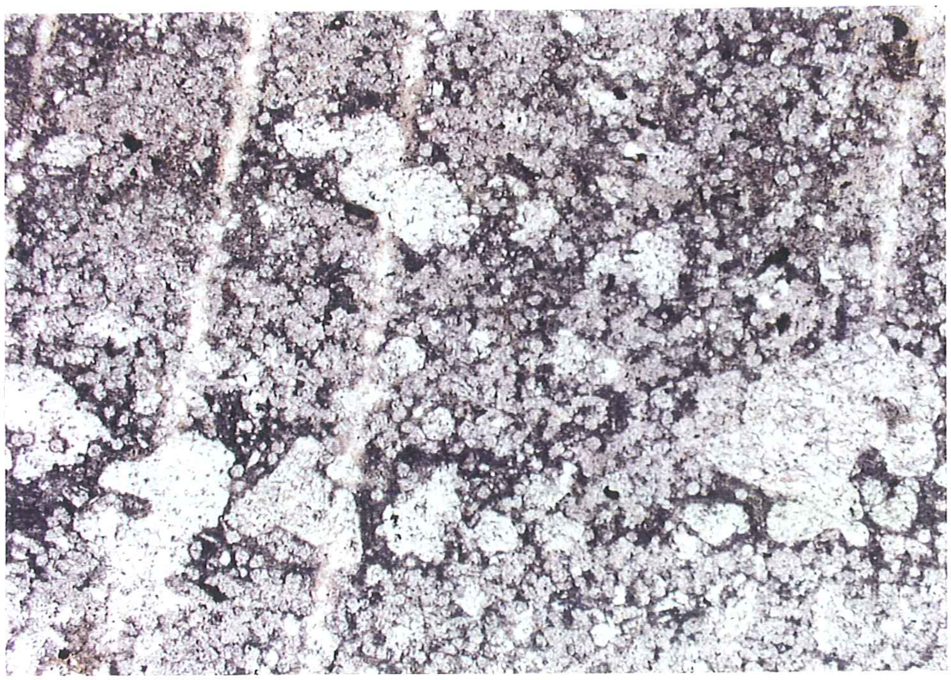

Figure 24b. RB-44b/White Alps porphyry. Same view and scale as figure 24a. TLP; 1cm on the photo= 0.532mm.

Other Porphyries

Sample RB-44c has petrographic characteristics distinct from samples RB-44a and RB-44b. It has an aplitic groundmass with no relict glass, and plagioclase and biotite were the only phenocryst phases noted. The porphyry is dacitic to quartz latitic in composition. In the sample the porphyry is in contact with a breccia lithology (lithic lapilli tuff or intrusion breccia?) that contains fragments of porphyry in a finer-grained matrix of microcrystalline quartz, alkali feldspar, and calcite (Figure 25a-b).

Sample RB-45 was designated as Rosebud quartz latite or Bud Marker porphyry. It appears to be a glassy, flow-banded dacite or latite porphyry and is interpreted to be an extrusive rock. It contains 3-5% plagioclase phenocrysts pseduomorphed by microcrystalline quartz, and less than one percent mafic phenocrysts pseudomorphed to an assemblage of epidote-calcite-chlorite-quartz. The flow-banded groundmass consists of dark brown glass partly devitrified to patchy microcrystalline quartz and alkali feldspar (Figure 26a-b).

TRIASSIC-JURASSIC METASEDIMENTS (Auld Lang Syne formation)

A single sample of Auld Lang Syne formation was examined for this study (sample RB-72). The sample is a carbonaceous shale with a finely-laminated structure imparted by fine streaks and lenticles of black to very dark green organic material. The spaces between the organic lenticles consist dominantly of microcrystalline quartz, white mica, and, locally, lensoid zones of slightly coarser (± 0 0.05mm diameter) polycrystalline quartz. The shale contains a thin quartzose silty bed with abundant disseminated pyrite. The bedding laminations are offset approximately 2mm along a quartz-pyrite-marcasite vein (Figure 27a-c). The shale contains disseminated pyrite, some of which is framboidal, as well as abundant finely disseminated hydrothermal(?) apatite.

ALTERATION

Alteration in the volcanic host rocks is predominantly silicification and argillization, with minor to locally significant calcite flooding. Significant calcite flooding affects mainly the groundmass of some porphyries. In a few samples minor chlorite replaces primary mafic phases, sometimes in conjunction with epidote, calcite, clay, quartz, or sericite. The alteration affects primarily tuffaceous pyroclastic volcanic rocks and glassy flow rocks, and is superimposed on devitrification of the glassy component in those lithologies.

Silicification

Silicification affects to some degree all wall rock proximal to veins and hydrothermal breccias. It is manifested as:

- patchy areas and wispy, discontinuous lenses of recrystallized polycrystalline, xenomorphic-granular quartz in devitrified tuffaceous groundmass. Locally some wall rock fragments are silicified to the point where they nearly disappear into the quartz matrix (Figure 1a-b).

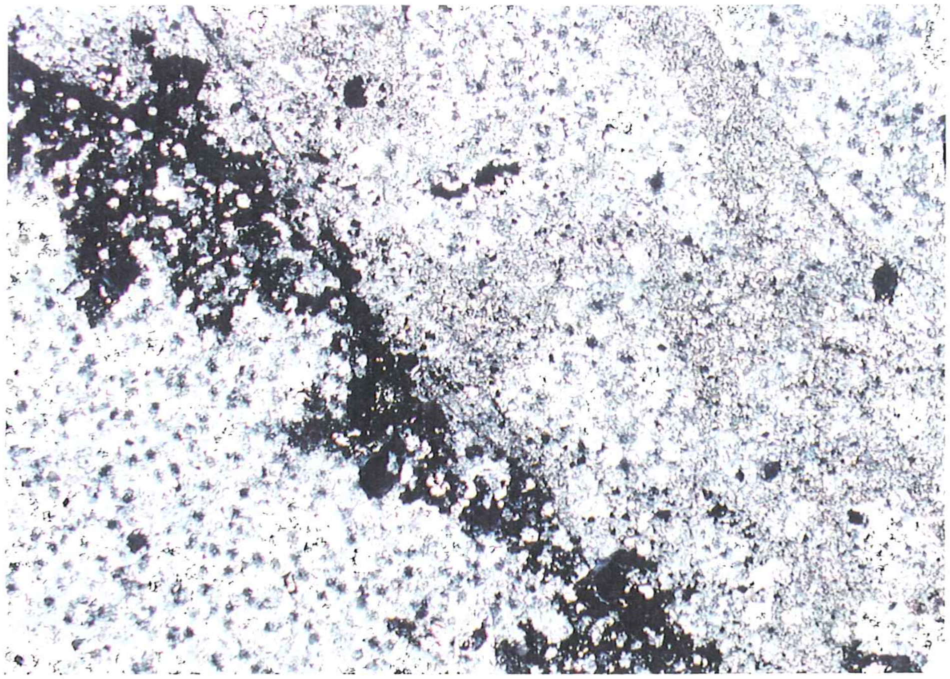

Figure 25a. RB-44c/porphyry. Contact zone between aplitic porphyry and a breccia of indeterminate origin (intrusion or volcanic breccia?). TLX; 1cm on the photo= 0.532mm.

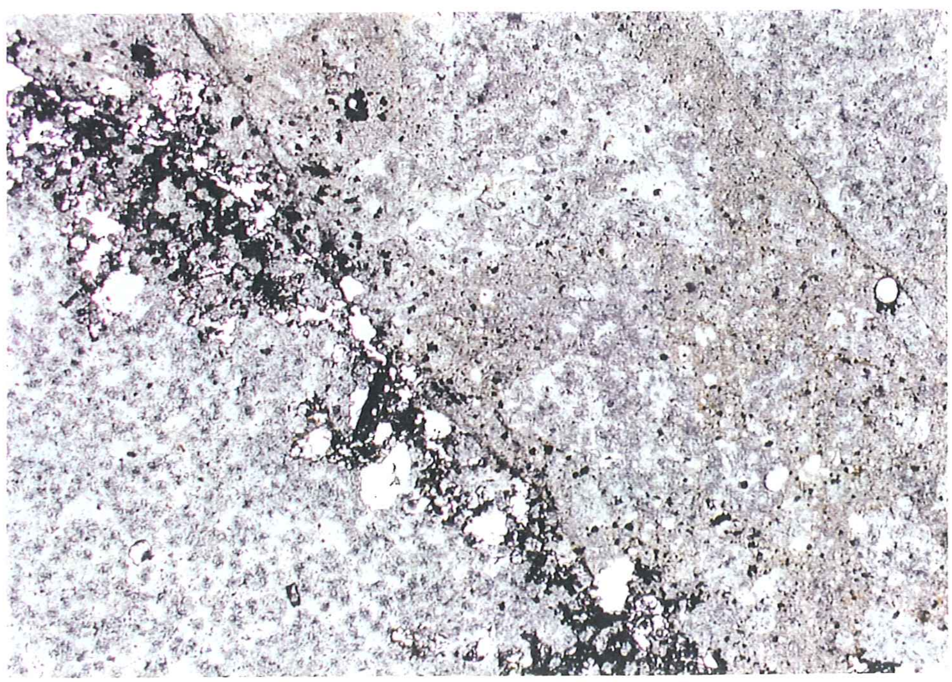

Figure 25b. RB-44c/porphyry. Same view and scale as figure 25a. TLP; 1cm on the photo= 0.532mm.

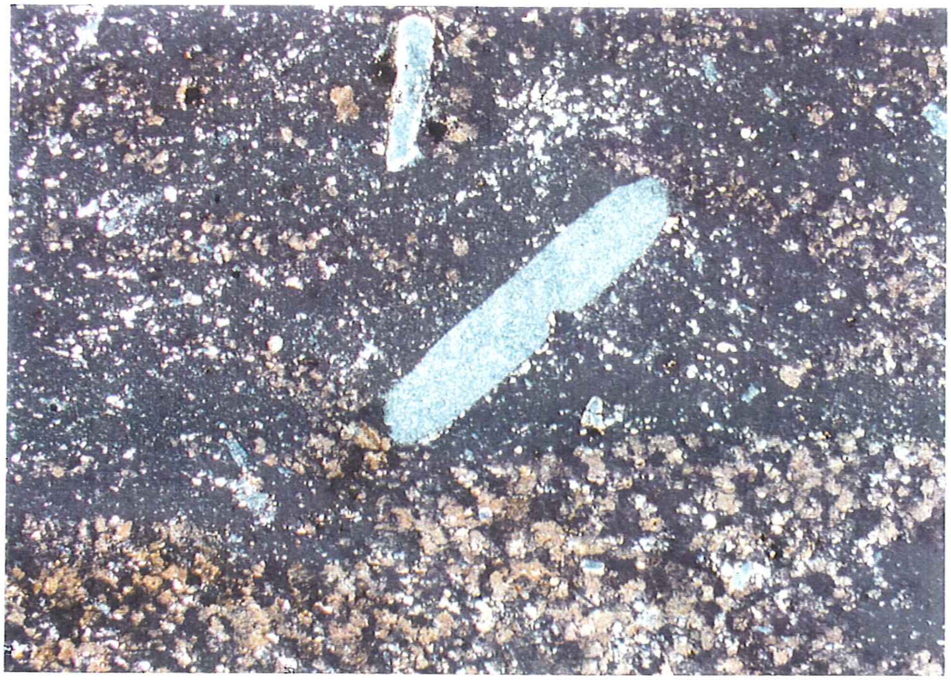

Figure 26a. RB-45/Rosebud quartz latite-Bud Marker porphyry (?). Glassy, flow-banded extrusive dacite or latite with feldspar phenocrysts pseudomorphed by microcrystalline quartz. TLX; 1cm on the photo= 0.532mm.

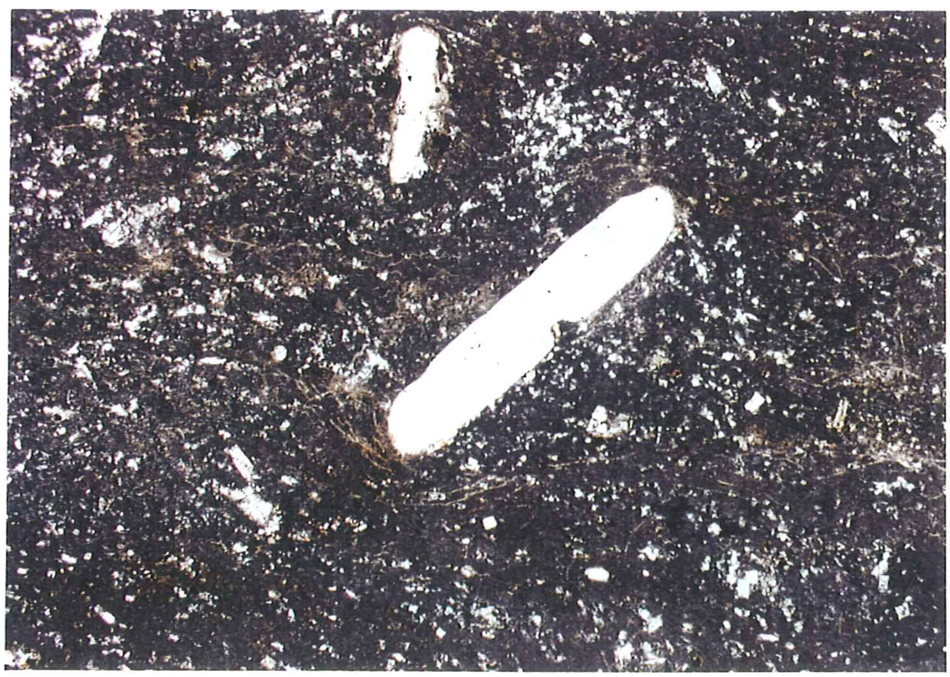

Figure 26b. RB-45/Rosebud quartz latite-Bud Marker porphyry (?). Same view and scale as figure 26a. TLP; 1cm on the photo= 0.532mm.

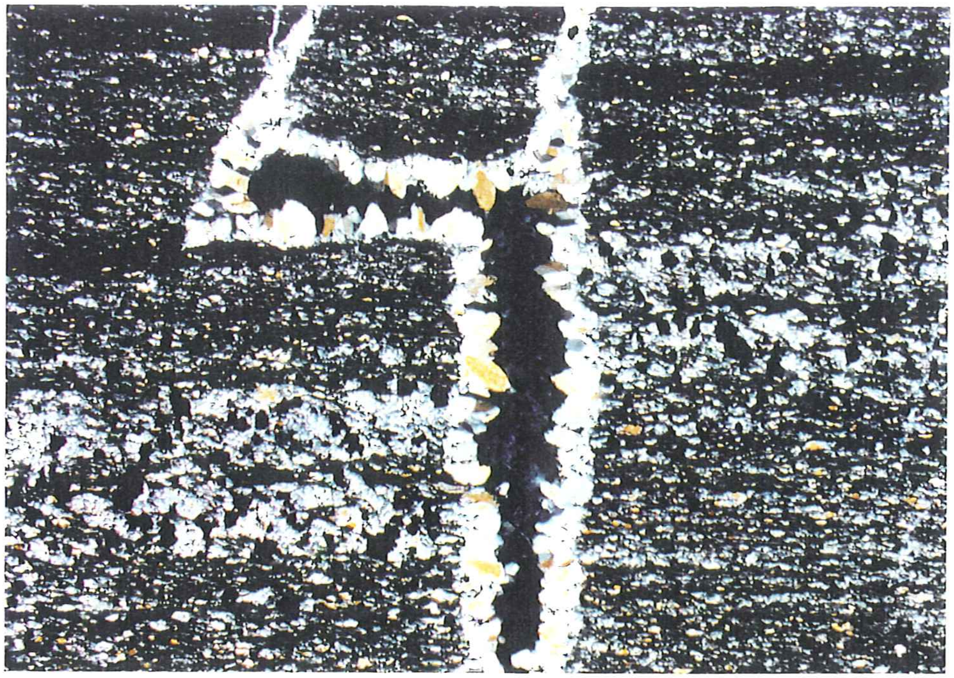

Figure 27a. RB-72/ALS. Carbonaceous shale of the Auld Lang Syne formation. The bedding is offset along a quartz vein. A silty layer carries abundant disseminated pyrite. TLX; 1cm on the photo= 0.532mm.

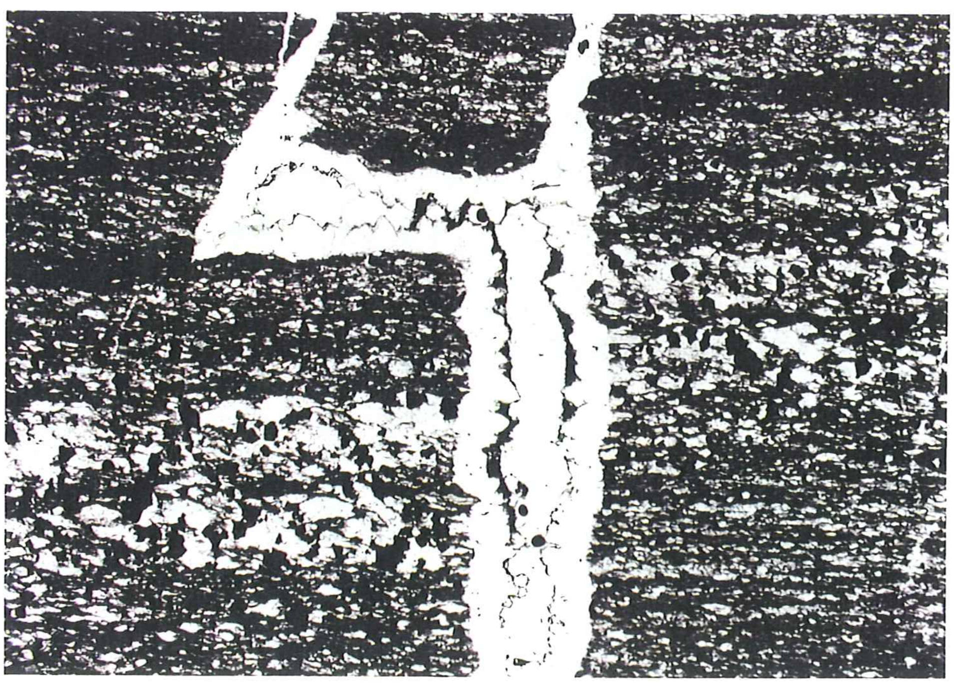

Figure 27b. RB-72/ALS. Carbonaceous shale of the Auld Lang Syne formation. Same view and scale as Figure 27a. TLP; 1cm on the photo= 0.532mm.

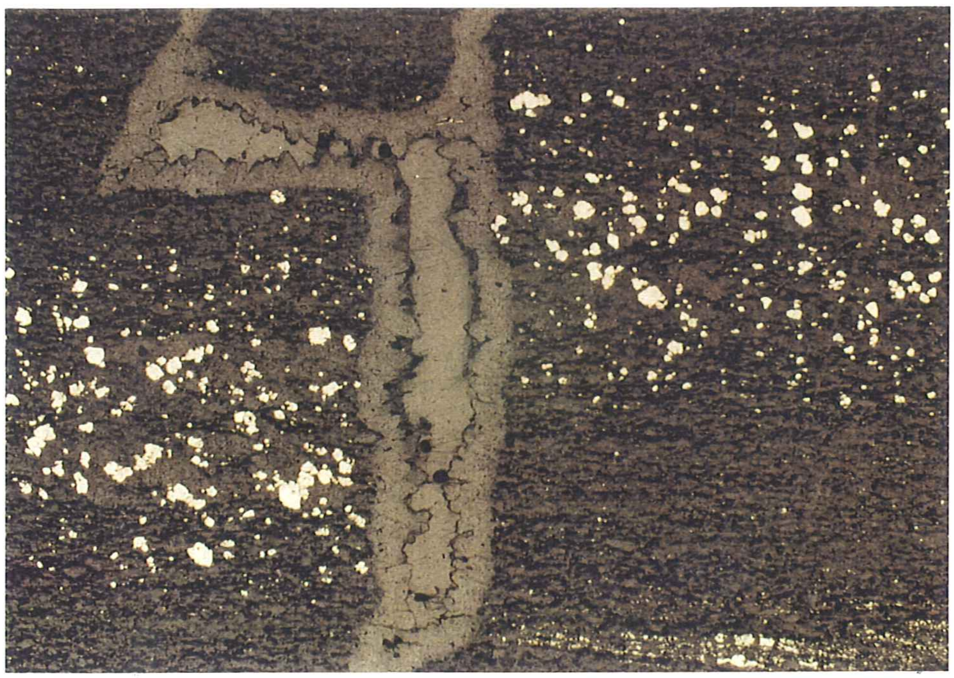

Figure 27c. RB-72/ALS. Carbonaceous shale of the Auld Lang Syne formation. Disseminated pyrite in a quartzose silty layer shows small, but prominent offset along the quartz vein. RL; 1cm on the photo= 0.532mm.

- crackled, discontinuous quartz veinlet stockworks in devitrified tuffaceous groundmass. In some samples the quartz microveinlets are thread-like (RB-11). Locally the crackle zones expand into areas of fine quartz matrix microbreccia (Figure 19a-b).

Clay-sericite

Likewise, clay-fine sericite alteration is ubiquitous in wall rock fragments in veins and breccias, and in wall rocks proximal to veins and breccias. The clay-fine sericite alteration is present as:

- small clay patches in polycrystalline quartz breccia matrix (Figure 28a-b). At least some of this clay may be derived from the alteration of disaggregated volcanic fragments dispersed in the veins or breccia matrix.

- discontinuous sericite-clay microveinlets locally transgress fragments and/or wall rock in some samples.

- sericite-clay rims some wall rock fragments carried in veins or breccia matrix (Figure 28a-b).

- clay insinuates along quartz crystal boundaries in vein and breccia matrix quartz (Figure 29).

- Locally clay appears to pit vein and breccia matrix quartz crystal surfaces and perhaps corrode the crystal margins (Figure 29). It is texturally permissible that some of this clay may have developed at the expense of the quartz.

APATITE AND CALCITE

Calcite is a locally significant component of some veins and breccia matrix, and occurs as minor disseminations to strong replacement in some volcanic wall rocks and porphyries. Calcite was noted as a component of veins or breccia matrix in twelve of the samples examined for this study (Figure 30a-b). Calcite was noted as disseminations or partial replacement of groundmass and phenocryst phases in wall rocks in 26 samples (Figure 31a-b). It is most prevalent as partial replacement of the groundmass in some porphyries (Figure 32a-b).

Apatite occurs as fine-grained, primary disseminations in 19 samples. The primary apatite is characterized by strong grayish yellow to lemon yellow luminescence under CL observation. Locally clusters of primary apatite mark former mafic phenocryst sites, now altered to sericite ± clay ± chlorite ± calcite (Figure 33a-b). Hydrothermal apatite was identified in 8 samples. It is characterized by salmon pink or straw yellow luminescence under CL observation (Figure 34a-b).

The distribution of apatite and calcite in the samples examined for this study is summarized in Table 3.

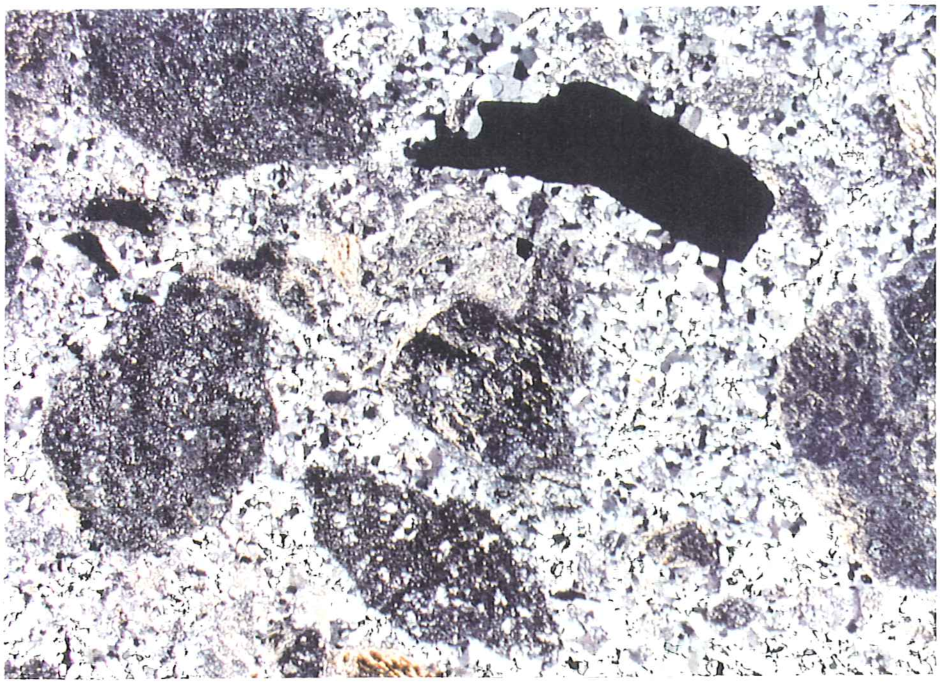

Figure 28a. RB-7/silicified breccia. Tuffaceous volcanic fragments have partial clay-altered margins and are set in a matrix of polycrystalline quartz, patchy clay, and pyrite. TLX; 1cm on the photo= 0.532mm.

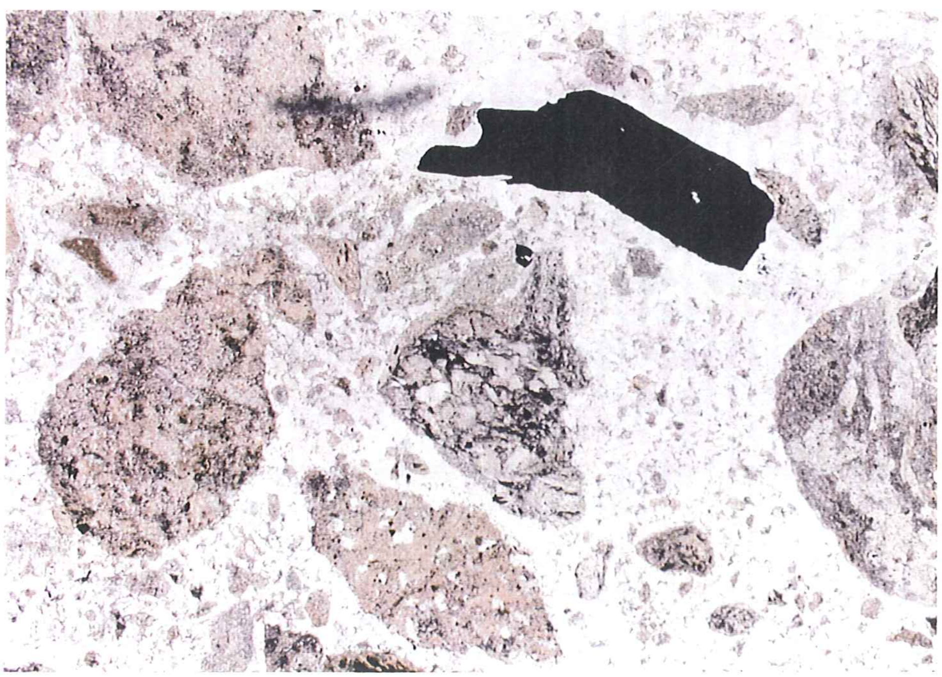

Figure 28b. RB-7/silicified breccia. Same view and scale as Figure 28a. TLP; 1cm on the photo= 0.532mm.

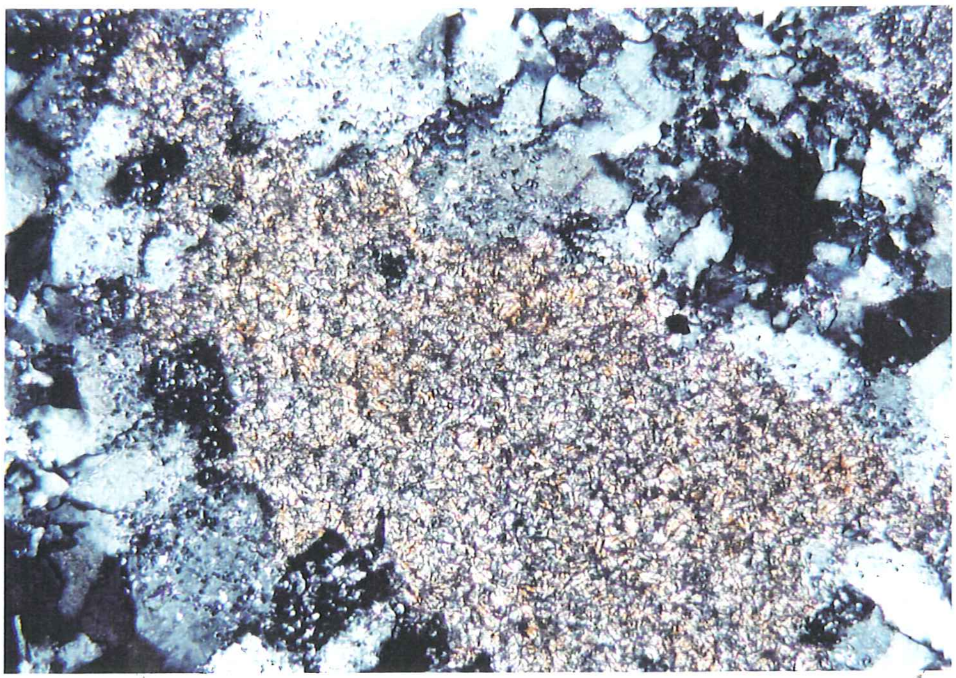

Figure 29. RB-13/hydrothermal breccia. Clay aggregate in polycrystalline quartz matrix. Clay insinuates locally along quartz crystal margins and appears to pit and corrode the quartz. TLX; 1cm on the photo= 0.053mm.

TABLE 3. CALCITE AND APATITE IN WALL ROCKS, VEINS, AND BRECCIAS FROM THE ROSEBUD MINE AREA

Sample No.	Type	Au (opt)	Ag (opt)	Calcite in veins/bx matrix	Hydrothermal Apatite	Disseminated primary apatite	Calcite in Wall Rocks
RB-1	minzd bx	43.67	45.19	X	X		
RB-2	vein	0.201	0.27			X	X
RB-3	bx	0.14	0.31			X	X
RB-4	minzd bx	43.674	45.19				
RB-5	vein	0.177	0.3	X			
RB-6	bx	0.11	1.85	X	X		
RB-7	bx	0.091	<0.05	X			X
RB-8	bx						X
RB-9	bx	0.503	0.4	X			
RB-10	minzd bx	60.499	64.27	X		X	X
RB-11	vein/bx				X		X
RB-12	vein/bx	0.503	0.4	X		X	
RB-13	bx	0.009	<0.05			X	
RB-20	lapilli tuff						
RB-41	porphyry	0.023	0.14			X	
RB-42	porphyry	0.042	<0.05			X	
RB-43	porphyry	0.026	0.06			X	
RB-44a	porphyry						X
RB-44b	porphyry						X
RB-44c	porphyry						X
RB-45	porphyry					X	X
RB-55	lapilli tuff			X	X	X	X
RB56b	porphyry						X
RB-57	lapilli tuff	<0.001	<0.02	X			X
RB-58	porphyry	0.006	0.08		X		
RB60a	tuff				X	X	X
RB-60b	tuff					X	X
RB-60c	lapilli tuff					X	
RB-61a	tuff	0.128	0.3			X	
RB-61b	tuff	0.014	1.06			X	X
RB-61c	tuff					X	X
RB-61d	tuff					X	X
RB-63a	volcanic bx	0.967	1.44	X		X	X
RB-63b	stkwk bx				X		
RB-64	tuff			X			X
RB-65a	bx			X			X
RB-69A	epiclastic bx	<0.001	<0.02				X
RB-69b	epiclastic bx	0.006	<0.02				X
RB-70a	tuff						
RB-70b	tuff					X	X
RB-71	tuff. sandstone						X
RB-72	carb. shale	<0.001	<0.02		X		X

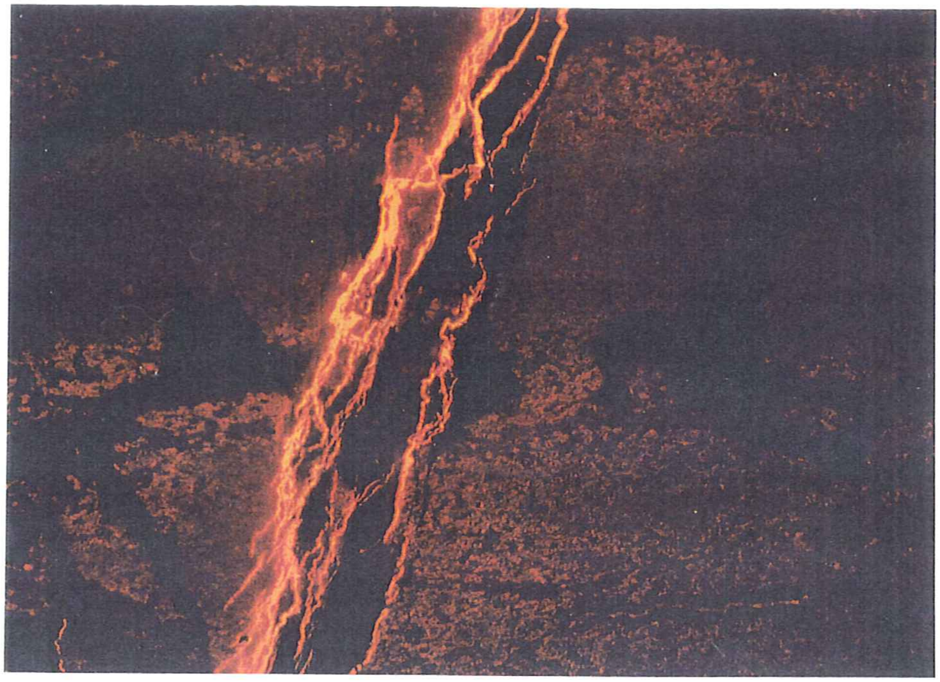

Figure 30a. RB-64/Lower Plam. A quartz-calcite vein cuts the tuff, which show significant replacement by calcite. The vein calcite has bright orange CL ($Mn2+$ activation), while the groundmass has a faded orange CL cast from the replacement calcite. CL; 1cm on the photo= 1.016mm.

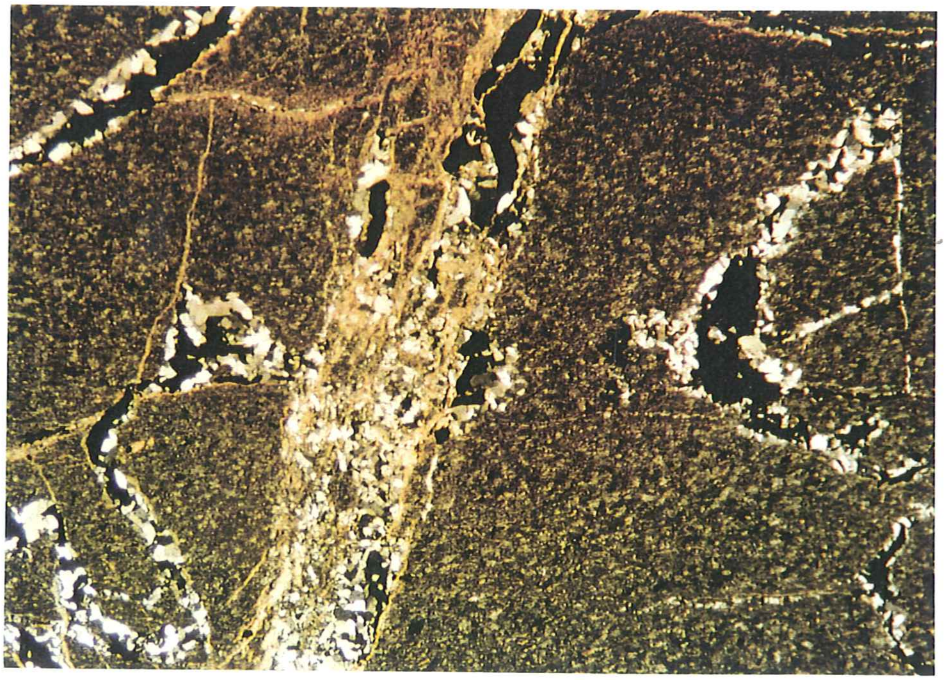

Figure 30b. RB-64/Lower Plam. Same view and scale as figure 30a. TLX; 1cm on the photo= 1.016mm.

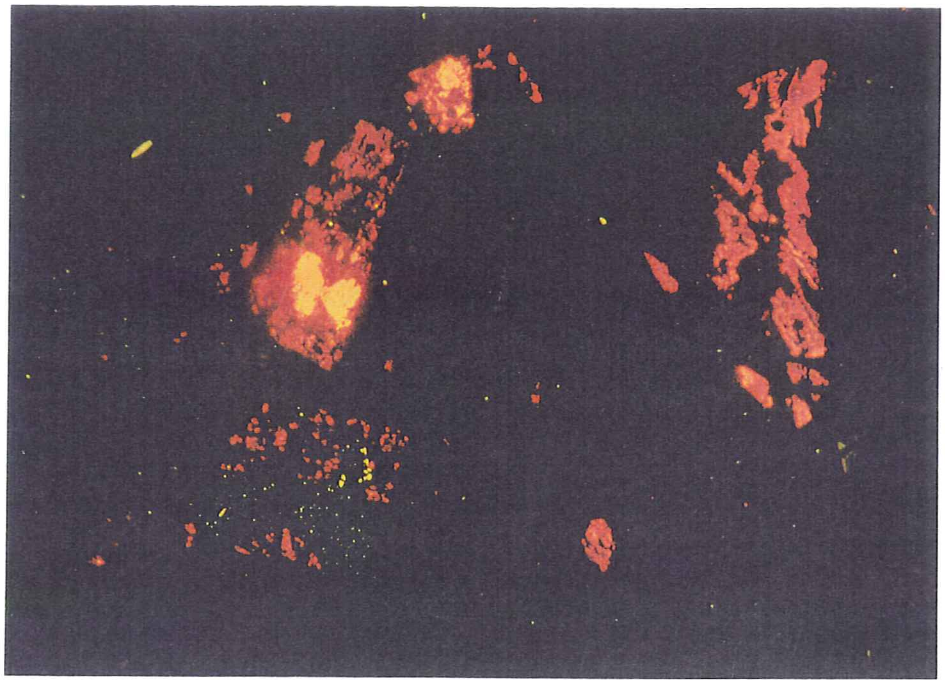

Figure 31a. RB-55/Upper Bud tuff. Partial replacement of plagioclase and lapilli fragments by calcite (bright yellow and orange CL; Mn2+ activation). There is a trace of fine-grained, disseminated apatite with lemon yellow CL (Mn2+ activation). CL; 1cm on the photo= 0.508mm.

Figure 31b. RB-55/Upper Bud tuff. Same view and scale as Figure 31a. TLX; 1cm on the photo= 0.508mm.

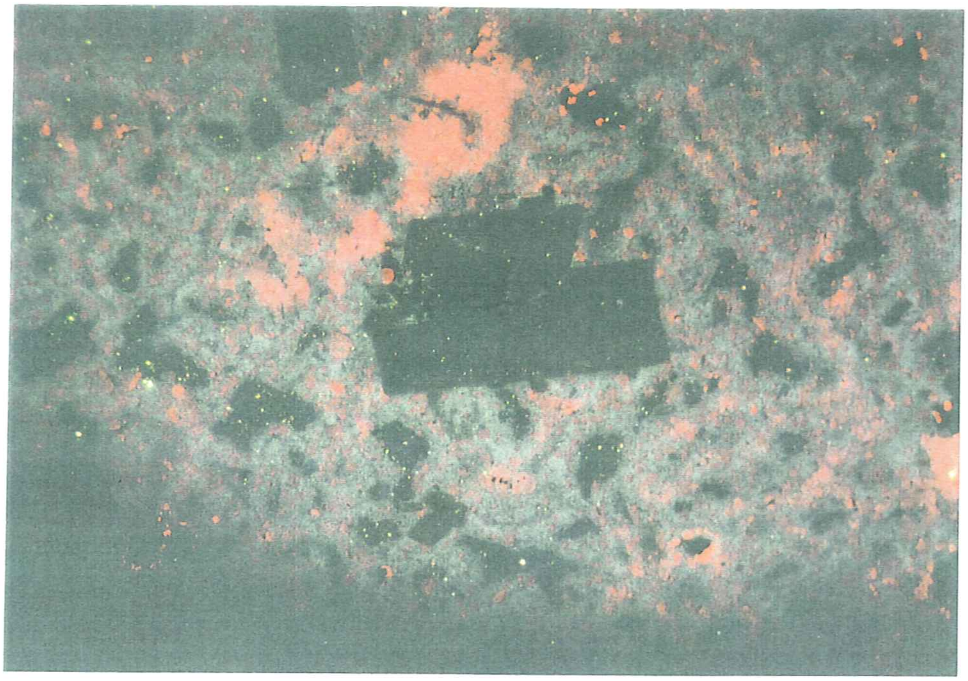

Figure 32a. RB-44a/White Alps porphyry. The porphyry shows partial flooding of the groundmass by calcite (reddish orange CL; Mn^{2+} activation). The light blue CL is from fine-grained Kspar in the groundmass (Ti^{4+} activation). CL; 1cm on the photo= 0.604mm.

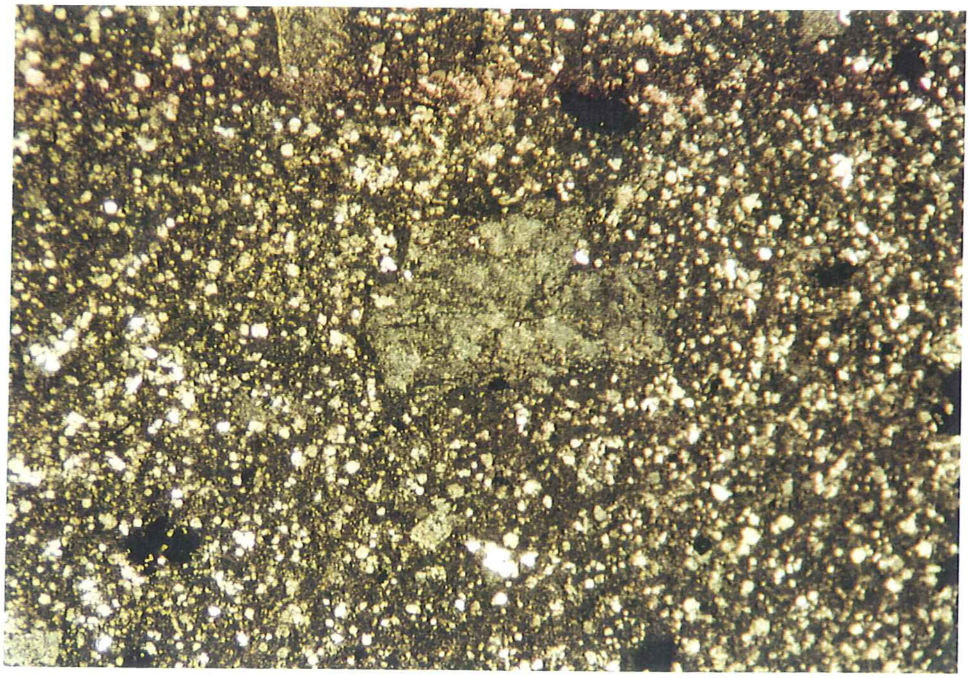

Figure 32b. RB-44a/White Alps porphyry. The calcite replacement in the groundmass is not apparent under TLX. Same view and scale as figure 32a. TLX; 1cm on the photo= 0.604mm.

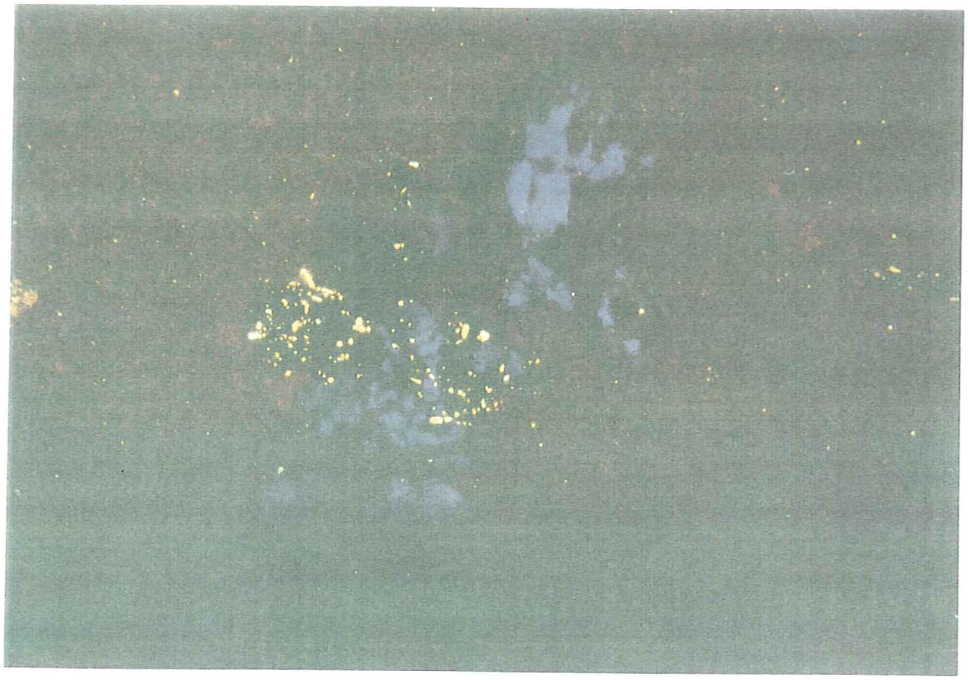

Figure 33a. RB-43/Bud Marker porphyry. Fine-grained apatite (greenish yellow CL) and kaolinite (royal blue CL) mark the site of a former aggregate of mafic and feldspar phenocrysts. The apatite probably marks a former biotite site. CL; 1cm on the photo= 0.604mm.

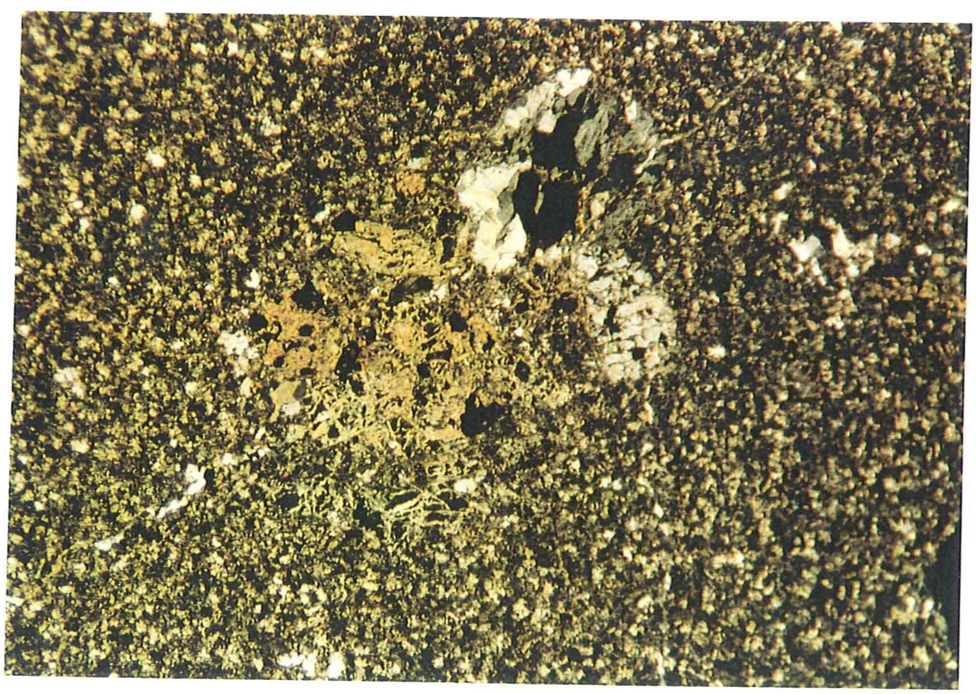

Figure 33b. RB-43/Bud Marker porphyry. Same view and scale as Figure 33a. TLX; 1cm on the photo= 0.604mm.

Figure 34a. RB-7/hydrothermal breccia. Apatite (salmon pink CL) occluded within a skeletal pyrite-marcasite crystal. Everything else is essentially non-luminescent. CL; 1cm on the photo= 0.680mm.

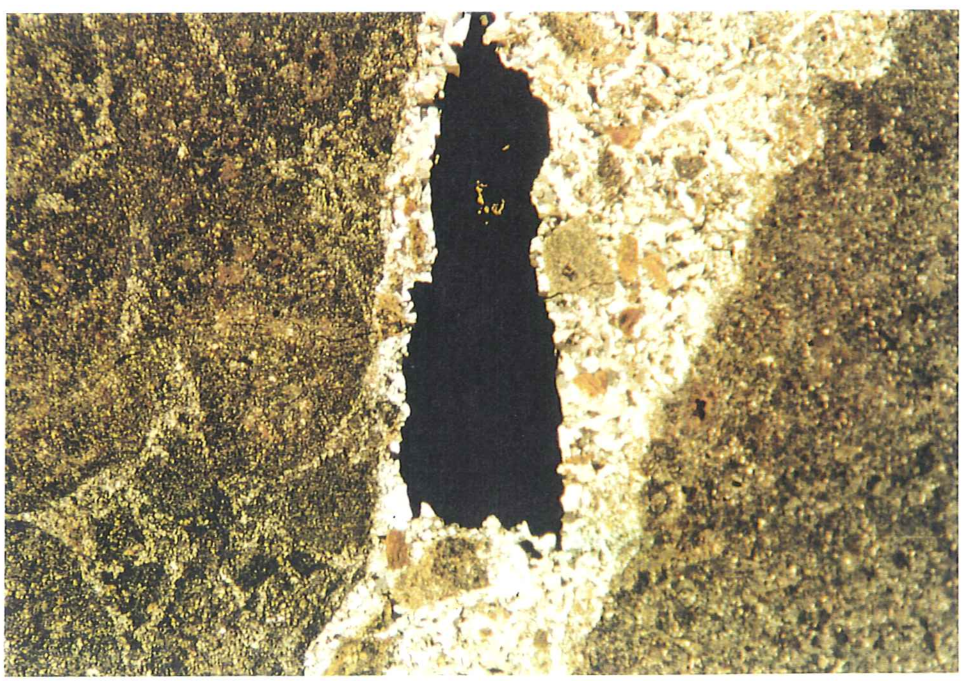

Figure 34b. RB-7/hydrothermal breccia. Skeletal pyrite-marcasite crystal in quartz vein cutting crackle-brecciated tuff. The occluded apatite is not visible in this view. TLX; 1cm on the photo= 0.680mm.

SECTION II

PETROGRAPHIC ATLAS OF SAMPLES FROM THE ROSEBUD MINE AREA

Sample RB-1 (silica-healed breccia with marcasite; assays 43.674opt Au and 45.19opt Ag)

Sample RB-1 is a hydrothermal breccia. Poorly-sorted, sub-angular to sub-round host rock fragments range in size from a few mm to approximately 1.4cm in length/diameter. The fragments are microcrystalline mosaics of quartz, clay, and alkali feldspar (?) with patches of slightly coarser recrystallized quartz. No relict phenocryst phases are observed, although small tabular patches of polycrystalline quartz may be pseudomorphs after primary feldspar phenocrysts. The fragments are of probable volcanic origin and are engulfed in a fine-grained, polycrystalline quartz-clay matrix. Patches of clay occur within the matrix and may be derived from fine, disaggregated host rock. Elsewhere in the polycrystalline quartz matrix, the clay insinuates along quartz crystal boundaries. Locally the clay may actually replace quartz, but this appearance may be illusory and due to the geometry of the billet cut. Some of the fragments are veined and/or rimmed by the coarser, polycrystalline quartz. Several fragments have abundant disseminated opaque minerals. Clots of elongate, skeletal pyrite-marcasite crystals are found throughout, generally within the quartzose breccia matrix, but locally growing into the breccia fragments. Coarser polycrystalline quartz is associated with these composite pyrite-marcasite clusters commonly.

CL: The breccia matrix quartz has a very dull red to red-brown CL. A trace of orange-luminescent calcite and moderate yellow-gray luminescent apatite were noted, occuring both in the breccia matrix, and in some breccia fragments. On occasion a weak royal blue CL phase was noted within some skeletal marcasite crystals. This phase may be kaolinite.

RL: Opaque minerals constitute approximately 10-15% of the sample. Skeletal composite pyrite-marcasite crystals are the dominant opaque phases. Pyrite abundances greatly exceed marcasite in the composite crystals. Native gold occurs sporadically intergranular to polycrystalline quartz and forms anhedral grains that range up to 0.26mm diameter, but are generally < 0.1mm length/diameter. Locally chalcopyrite is found crystallized in voids intracrystalline to the skeletal py-mc crystals. The chalcopyrite is sometimes tarnished. Silver mineralization is not abundant in this section. It is present as extremely fine-grained electrum (Au+Ag) and acanthite. Acanthite is noted to be extremely fine-grained and occur primarily in skeletal py-mc crystals. There is a trace of extremely fine-grained arsenopyrite (<0.022mm length). An electrum-native gold-acanthite assemblage occurs intergrown locally in intracrystalline voids of composite pyrite-marcasite crystals. An intergrowth of chalcopyrite-digenite-electrum-native gold-acanthite was observed in edge contact with a composite pyrite-marcasite occurs also intergrown with acanthite within the skeletal marcasite crystals. Native gold occurs locally as discontinuous margins on electrum crystals. Several breccia fragments contain abundant disseminated pyrite.

Representative photomicrographs of sample RB-1 are illustrated in Figures 1,11, and 35.

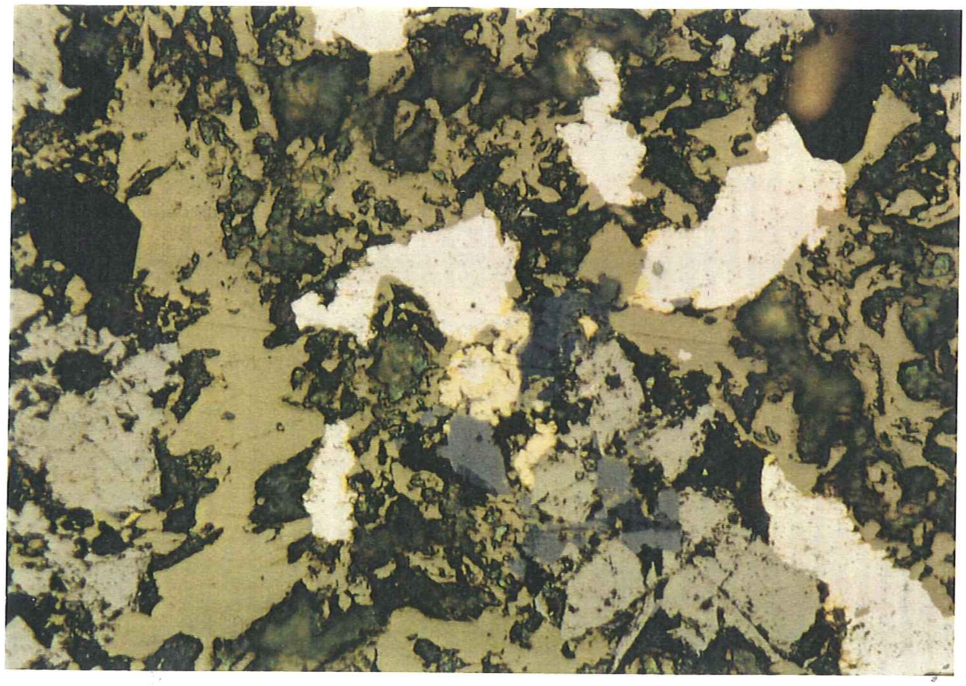

Figure 35. RB-1/silicified hydrothermal breccia. Intergrown chalcopyrite-digenite-electrum-native-gold-acanthite at the margin of a composite pyrite-marcasite crystal. RL; 1cm on the photo= 0.021mm.

Sample RB-2 (quartz vein with marcasite; N55E, 54NW; 0.201optAu, 0.27optAg)

The vein is dominated by fine-grained saccharoidal quartz and elongate, skeletal marcasite crystals. The quartz is coarser at the vein margin, where the individual quartz crystals are somewhate elongate and grow essentially perpendicular to the vein contact with wall rock in cockscomb fashion. Fragments of wall rock are incorporated into the vein and rimmed also by coarser quartz growing nearly perpendicular to the fragment margin, outward into the vein. The wallrock host outside the vein is crackled by discontinous quartz veinlets and contains recrystallized quartz. The wall rock fragments are a microcrystalline mosaic of quartz, clay, and possibly relict alkali feldspar. No relict phenocrysts were noted, although nearly tabular pods of polycrystalline quartz significantly coarser than the groundmass may be pseudomorphs after primary feldspar phenocrysts. The saccharoidal vein quartz has an average grains size of < 0.2mm diameter. The vein also contains irregular to subround clay aggregates to > several mm in length/diameter, some with included islands of saccharoidal quartz. Clay also insinuates locally along quartz crystal boundaries. There is a possibility that some of the clay may be derived from alteration of the quartz. Skeletal marcasite crystals locally exceed 5mm in length, with widths ranging from <0.1mm to >0.6mm.

CL: The vein quartz has dominantly a dull red or red-brown CL. In parts of the vein the dull red-brown CL quartz is seen to replace an earlier, dull blue CL quartz. Calcite (bright orange CL; Mn2+) and apatite (moderate yellow-gray CL; Mn2+) were noted disseminated in some of the wall rock fragments interior to the vein.

RL: Opaque minerals make up approximately 15% of the sample. The dominant sulfides are pyrite and marcasite, both as components of the skeletal marcasite crystals. These crystals tend to have narrow margins and elongate interior zones of marcasite, with generally cubic pyrite incompletely filling the remaining interior space. Noted also is a very fine-grained gray (brownish tint), isotropic phase with low reflectance and yellow-brown internal reflections in some of the interior voids of the skeletal crystals and as sparse disseminations in the vein quartz. This phase is probably sphalerite. Fine-grained pyrite cubes and pyritohedrons are disseminated in wall rock and wall rock xenoliths in the vein. Gold and silver mineralization in this sample are hosted in fine-grained electrum and acanthite (?). Electrum occurs in voids intracrystalline to composite pyrite-marcasite crystals and as subhedral crystals intergranular to clusters of skeletal pyrite-marcasite crystals. Maximum crystal size is approximately 0.12mm diameter. Electrum occurs more rarely as fine disseminations in the wall rock. Very fine-grained, anhedral acanthite was noted in contact with electrum and skeletal pyrite-marcasite crystals. Crystal size is on the order of 0.02mm length.

Representative photomicrographs from sample RB-2 are shown in Figures 36 and 37.

Figure 36a. RB-2/quartz-clay-pyrite-marcasite vein. Elongate skeletal composite pyrite-marcasite crystals in a quartz-clay vein. A small crystal of electrum (white; high reflectance) occurs in an angular fragment of volcanic wall rock bordered coarser polycrystalline quartz. RL; 1cm on the photo= 0.532mm.

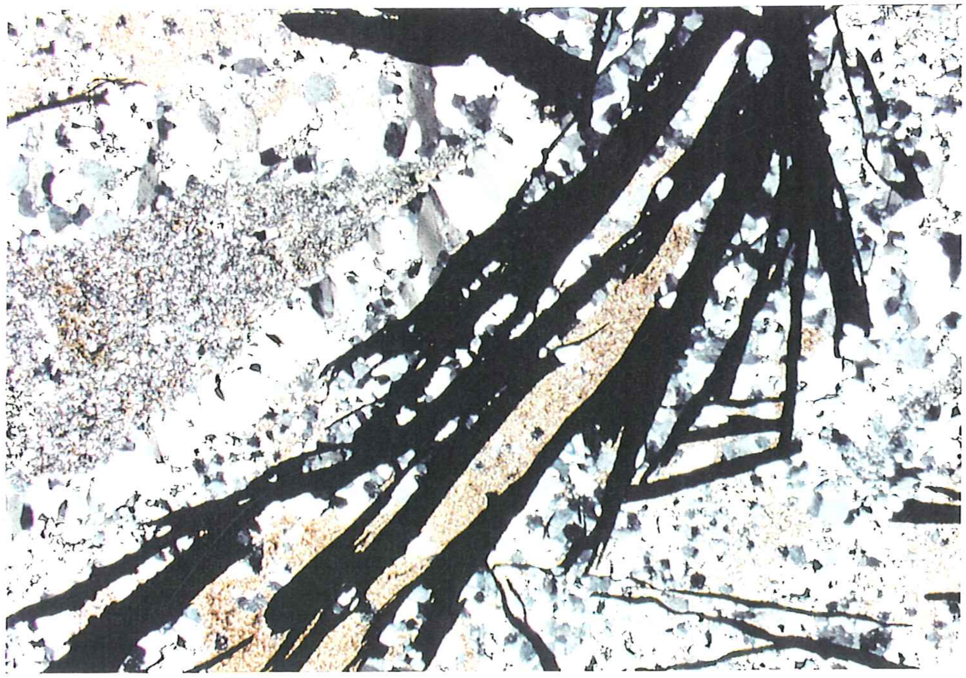

Figure 36b. RB-2/quartz-clay-pyrite-marcasite vein. Same view and scale as Figure 36a. Note coarser quartz bordering the volcanic wall rock fragment and the distribution of clay within the vein. TLX; 1cm on the photo= 0.532mm

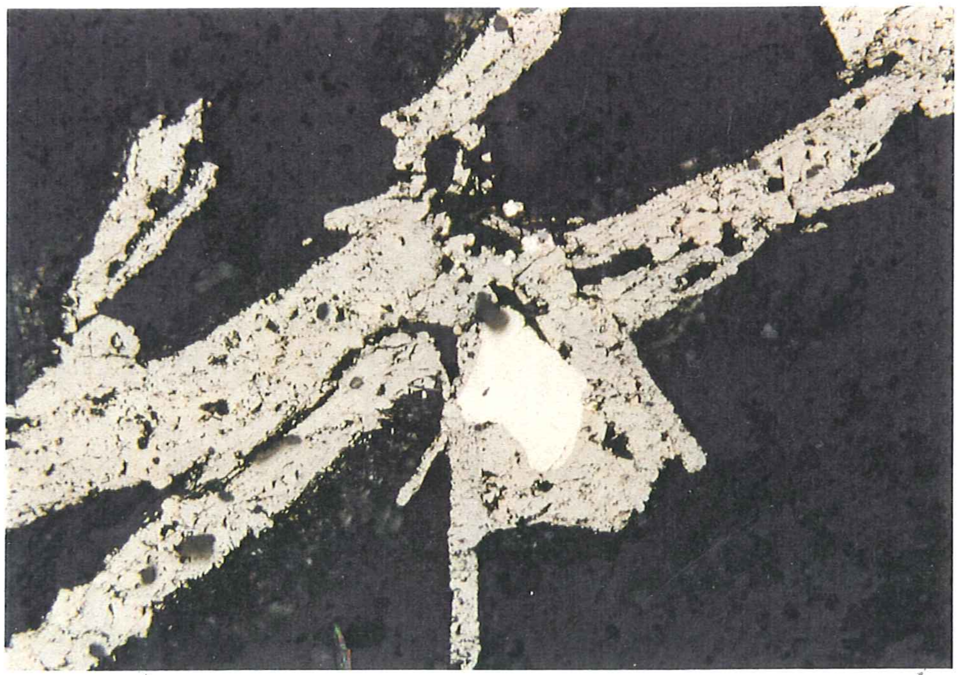

Figure 37. RB-2/quartz-clay-pyrite-marcasite vein. Skeletal composite pyrite-marcasite with electrum occupying an intracrystalline void. RL; 1cm on the photo= 0.053mm.

Sample RB-3 (green silica-healed breccia with marcasite in SRF; 0.14optAu, 0.31opt Ag)

Sample RB-3 is a poorly-sorted hydrothermal breccia. It contains sub-round to sub-angular fragments that range in size from <<1mm to nearly 3 cm dispersed in very fine-grained, polycrystalline quartz-clay matrix. The fragments are a very fine-grained to microcrystalline mosaic of quartz, clay, alkali feldspar (?), and bits of relict, partly devitrified cloudy brown glass. Faint stratification or layering is visible locally. Some fragments appear to be themselves fragmental in nature (lapilli tuff?). The matrix also includes pulverized "rock flour" from wall rock recrystallized to a very fine-grained quartz-clay aggregate. Average matrix quartz graine size is <0.1mm in length/diameter. Disseminated opaque minerals are present in both quartzose matrix and lithic fragments. The breccia is invaded by veinlets of coarser polycrystalline quartz that has a tendency toward crystal elongation perpendicular to the vein walls. The coarser vein quartz ranges to about 0.6mm in length. Also present are finer, discontinous quartz veinlets within some breccia fragments.

CL: The breccia matrix quartz has a very dull red or red-brown CL. Traces of calcite (orange CL) and apatite (yellow CL) are present in some fragments. The apatite is probably primary.

RL: Opaque phases constitute about one percent of the slide. The dominant opaque phases are disseminated pyrite and intergrown pyrite-marcasite as euhedral to subhedral crystals to 0.22mm diameter. The crystals are commonly cubic or pyritohedron in form. Some of the composite py-mc crystals are skeletal. These crystals commonly thin, discontinuous rims of marcasite and irregular cores of patchy marcasite-pyrite intergrowths. Also present are traces of fine-grained (<0.1mm diameter) chalcopyrite in limited intergrowth with pyrite at the margins of some pyrite crystals. A single grain of extremely fine-grained native gold was noted (<0.002mm diameter) in a bx fragment.

Reprentative photomicrographs from sample RB-3 appear in Figure 38.

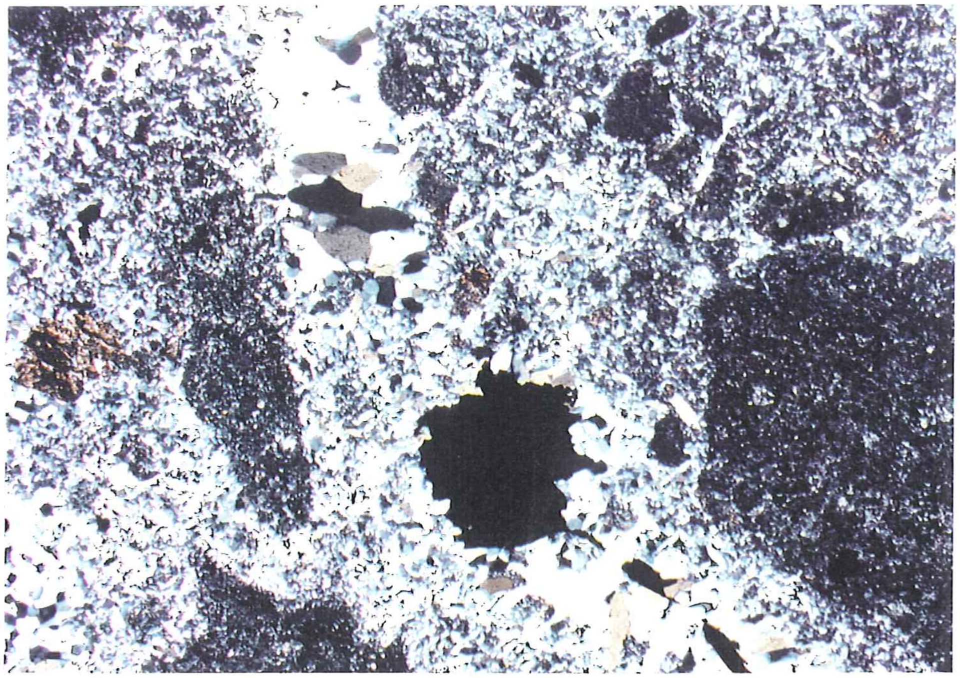

Figure 38a. RB-3/silicified hydrothermal breccia. Disaggregated fragments of volcanic wall rock dispersed in a quartz-sulfide matrix. The breccia is invaded by veinlets of coarser polycrystalline quartz and sulfides. TLX; 1cm on the photo= 0.532mm.

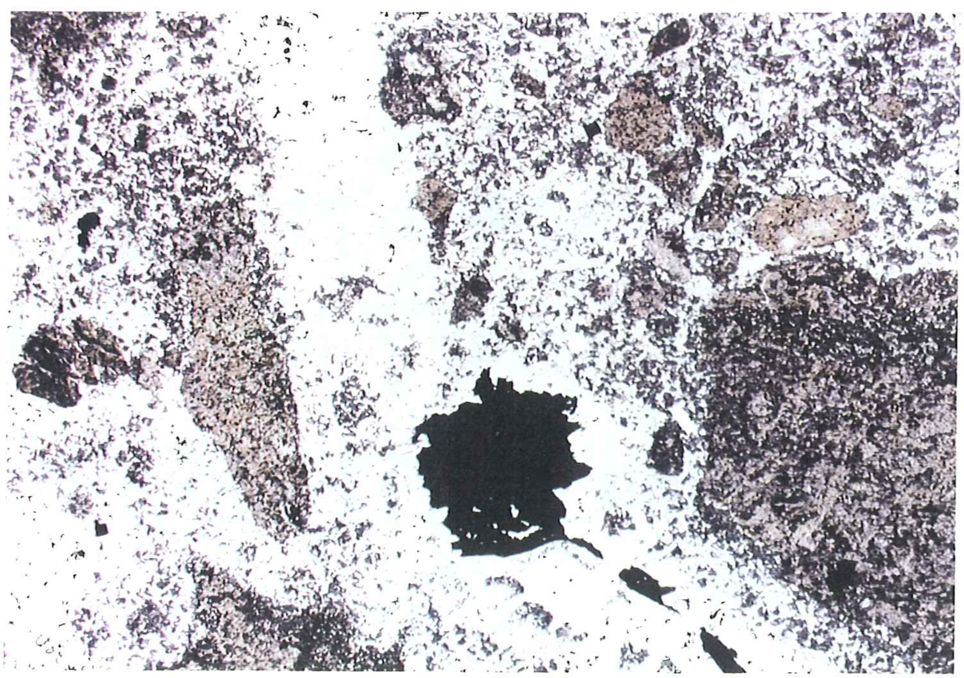

Figure 38b. RB-3/silicified hydrothermal breccia. The sulfides include both pyrite and composite pyrite-marcasite crystals. Same view and scale as Figure 38a. TLP; 1cm on the photo= 0.532mm.

Sample RB-4 (Silica-healed breccia with marcasite 182, 72; assays 43.674 opt Au, 45.19opt Ag)

Sample RB-4 is a mineralized hydrothermal breccia that contains closely packed, sub-angular to round wall rock fragments to appx. 3 cm in length set in a matrix of fine, polycrystalline quartz and aggregates of skeletal, elongate marcasite crystals. The wall rock is altered and recrystallized to a microcrystalline aggregate of quartz and clay and silicified with patches of slightly coarser polycrystalline quartz (±0.05mm diameter). It is probable that the lithic fragments are volcanic in origin. The breccia matrix has considerable variability in quartz grain size and incorporates pulverized wall rock material now recrystallized to a very fine-grained quartz-clay aggregate. Pockets of coarser matrix quartz have xenomorphic-granular texture with maximum grain size roughly 0.6mm in length. Finer polycrystalline xenomorphic-granular quartz in the matrix and wall rock fragments has a minimum grain size <0.015mm diameter. The breccia matrix has small zones where opaque phases (ore minerals) invade along quartz grain boundaries in a fine anastamosing network.

CL: The breccia matrix quartz has a very dull red or red-brown CL. No apatite or carbonate were noted.

RL: Sample RB-4 contains approximately 10-15% opaque minerals overall. Ore minerals identified include pyrite, marcasite, chalcopyrite, electrum, native gold, and acanthite (vfg, intergrown with py-mc-cp).The dominant opaque phases are pyrite and marcasite, mostly as skeletal composite crystals. In order of abundance -- py>mc>cp>electrum>acanthite>>native gold. Both gold and silver are dominantly held in the electrum.

Individual skeletal pyrite-marcasite crystals reach nearly 6mm in length. Maximum aspect ratio is about 20:1. These crystals generally have narrow rims and quasi-linear interior zones of marcasite and dense to porous interiors of pyrite or aggregates of small, cubic pyrite crystals. The skeletal py-mc crystals locally contain inclusions of electrum, as well as electrum, native gold, and acanthite (?) intergrown in intracrystalline void spaces. Chalcopyrite can be present also in intracrystalline void space, but is only locally intergrown with the Au-Ag mineralization. Some skeletal py-mc crystals contain relatively abundant electrum and native gold ± acanthite grown in intracrystalline void space.

Electrum occurs as generally irregularly-shaped grains <0.2mm length. The electrum grains were noted dispersed in vein quartz, in intracrystalline voids in skeletal py-mc crystals, and crystallized at the edge of some skeletal py-mc crystals, locally in contact with anhedral chalcopyrite. The electrum is commonly tarnished. Native gold locally forms partial, irregular rims on electrum.

There aere scattered areas with an extremely fine-grained (± 0.002mm diameter), light gray Ag (?) phase. This phase is isotropic and forms sub- to anhedral blebs, sometimes with a pseudo-graphic patterning. These zones are accompanied also by subordinate electrum of generally similar grain size.

Traces of very fine-grained native gold occur intercrystalline to polycrystalline quartz. Native gold occurs also as the aforementioned partial iregular rims on electrum crystals and filling small intracrystalline voids in skeletal composite pyrite-marcasite crystals.

Representative photomicrographs are illustrated in Figures 7, 9, 39, and 40.

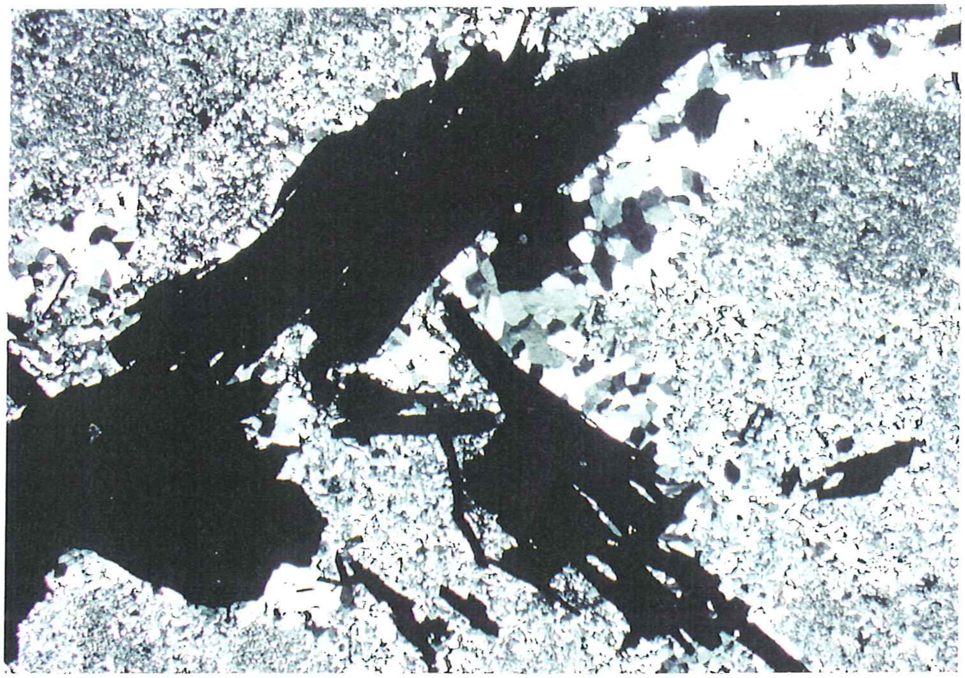

Figure 39a. RB-4/silicified hydrothermal breccia. Volcanic wall rock fragments are dispersed in a quartz-sulfide matrix. The opaque phases are dominantly skeletal composite pyrite-marcasite crystals. TLX; 1cm on the photo= 0.532mm.

Figure 39b. RB-4/silicified hydrothermal breccia. Same view and scale as Figure 39a. TLP; 1cm on the photo= 0.532mm.

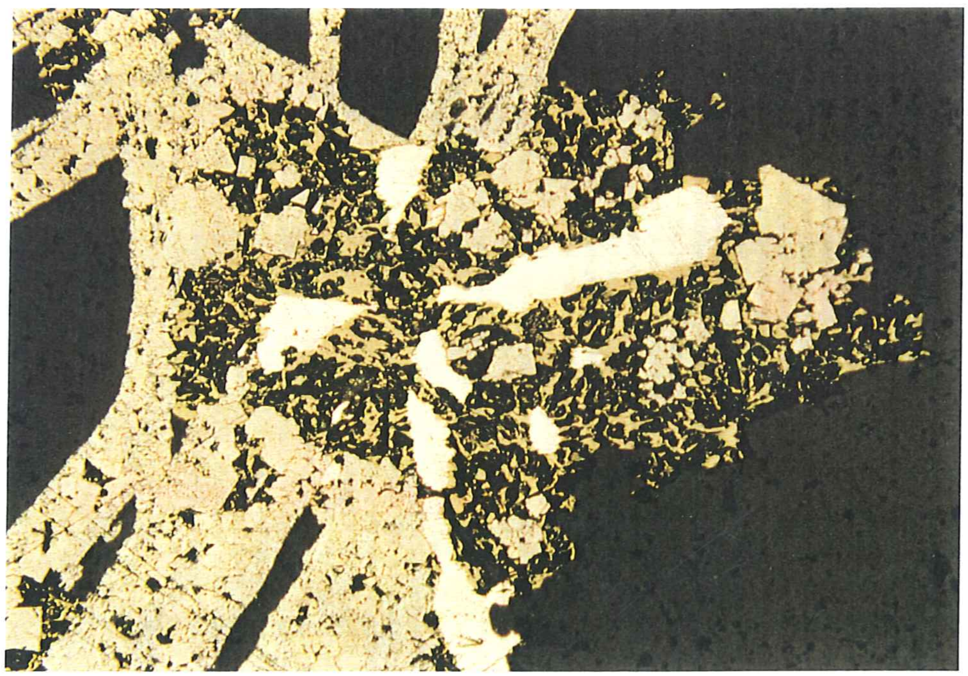

Figure 40. RB-4/silicified hydrothermal breccia. Skeletal composite pyrite-marcasite crystals with intergrown electrum (white; high R) and chalcopyrite (mustard yellow against py-mc and electrum). RL; 1cm on the photo= 0.106mm.

Sample RB-5 (Quartz vein in altered Dozer fm; 0.177optAu, 0.30 optAg)

The wall rock in sample RB-5 appears to be a crackle-brecciated volcanic lithology. In hand specimen the wall rock is a crackled, porcellanous white felsite. In thin section the groundmass is a microcrystalline mosaic of quartz, clay, and possibly alkali feldspar. It contains scattered , fine (± 0.1mm length), equant to tabular areas of polycrystalline quartz ± cubic to elongate pyrite that may pseudomorph feldspar microphenocrysts or pyrogenic feldspar. Minor disseminated opaque phases are present, as well. The wall-rock is crackled by a fine stockwork of polycrystalline quartz veinlets. The main quartz vein cutting the host rock is approximately 1.3 cm in width and incorporates lithic fragments similar to the wall rock. A narrow band of coarser quartz (to 0.6mm length) along vein margin has a tendency to crystallize with an elongation perpendicular to the vein margin. The bulk of the vein quartz is very fine-grained (±0.06mm diameter) and has a saccharoidal texture. Also present in the vein are irregular patches of clay to 3mm diameter. At one edge of the vein there is an unusual quartz variety. The quartz is anhedral, monocrystalline, and may have been inherited from an intrusive protolith. Skeletal marcasite is abundant in the part of the vein that incorporates the wall rock fragments.

CL: Microbreccia texture of wall rock outside vein shows up well under CL. Vein quartz is nearly non-luminescent. Trace of yellow-gray luminescent apatite in vein.

RL: The total sulfide abundance is approximately three percent, of which less than one percent occurs as disseminated pyrite and composite pyrite/marcasite outside vein margins in both wall rock and quartz crackle matrix. The pyrite is generally euhedral to subhedral, cubic to rectangular crystals to 0.6mm in length/diameter. Some pyrites have cores with tiny inclusions of a silver phase, probably acanthite, and rims filled with abundant matrix inclusions. Smaller pyrite crystals(<0.1mm length/diameter) can be anhedral. Skeletal, composite pyrite/marcasite crystals are dominantly pyrite. They tend to be elongate, euhedral, and up to 0.85mm length. Noted also in wall rock are traces of sphalerite (anhedral, 0.1mm diameter). Some sphalerite crystals have tiny inclusions of pyrite.

The vein itself contains dominantly skeletal, composite pyrite-marcasite crystals and eu- to subhedral pyrite crystals. The skeletal pyrite/marcasite crystals are elongate and up to 10mm in length, with aspect ratios to nearly 90:1. The pyrite crystals range to 0.7mm diameter. The proportion of sulfides in the main vein in this sample is approximately 6-8%. No acanthite inclusions were noted in pyrite or skeletal pyrite/marcasite crystals from within the vein, although such inclusions could have been plucked during the sample preparation process. Insufficient gold and silver-bearing phases were found in the polished thin section sample to explain the assay value for the sample of 0.177 optAu.

Figures 2 and 41 illustrate representative features of sample RB-5.

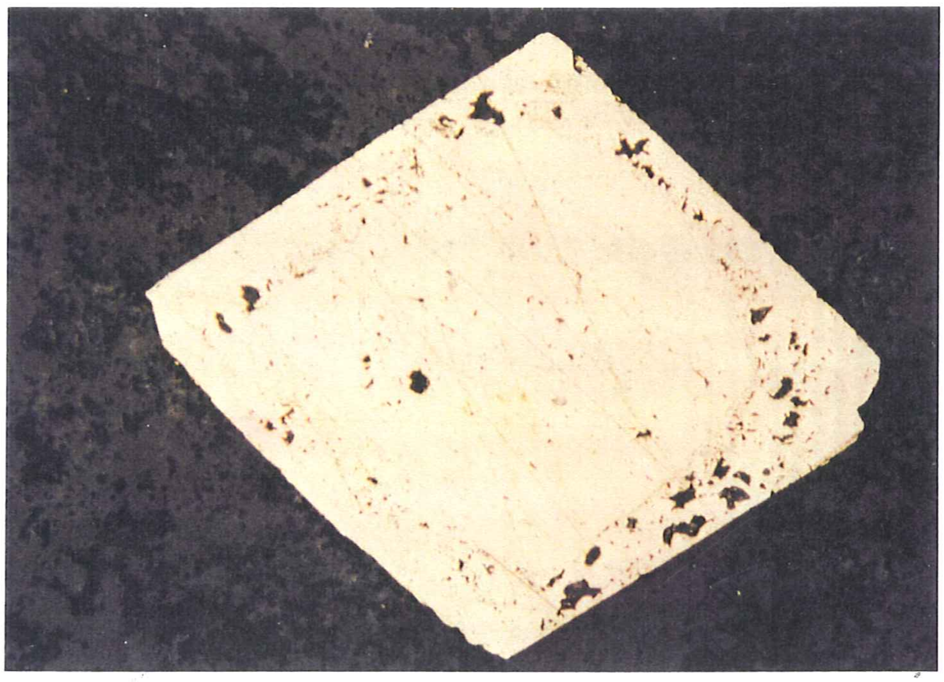

Figure 41. RB-5/quartz-sulfide vein in altered Dozer formation. Euhedral pyrite dissemination showing porous rim and solid core. RL; 1cm on the photo= 0.053mm.

Sample RB-6 (Silica-healed breccia; 0.110 opt Au, 1.85 opt Ag)

Sample RB-6 is a quartz matrix hydrothermal breccia. In hand specimen it consists of white to light green angular to sub-round fragments of porcellaneous felsite dispersed in a fine, gray to dark gray quartz-sulfide matrix. In the polished thin section the fragments range to more than 2cm in length/diameter. The larger fragments are crackled by discontinuous quartz microveinlets. The breccia fragments are altered to a microcrystalline aggregate of quartz and clay. Some fragments are partly rimmed by clay and/or sericite, while others have developed a net veining of clay-sericite. Some smaller fragments are replaced completely by very fine-grained sericite or illite. While it is difficult to determine the fragment protoliths owing to alteration, it appears that they may have been very fine-grained sediments or tuffaceous material, sedimentary or otherwise. Some fragments or parts of fragments have abundant disseminated opaque phases (pyrite and marcasite?). Some fragments contain abundant sericite-clay microveinlets. The altered wall rock fragments are distributed in a very fine- to fine-grained polycrystalline quartz matrix. The xenomorphic-granular quartz matrix is locally saccharoidal, but commonly has developed some random elongation to individual quartz crystals in the quartz mosaic. Maximum matrix quartz grain size is about 0.2mm diameter, but average quartz crystal size in the matrix is on the order of 0.02mm diameter. Minor clay-sericite is also dispersed in the matrix and is probably derived from the altered wall rock fragments.

CL: Quartz is nearly non-luminescent to very dull red-brown CL; traces of calcite and apatite in breccia matrix.

RL: Ore minerals constitute 5-7% of the sample and include pyrite, marcasite, and chalcopyrite. The dominant opaque phase is pyrite. The pyrite occurs as dominantly euhedral to subhedral crystals with cubic, rectangular, and pyritohedron form that reach approximately 1.4mm in length/diameter. Many of the crystals have solid cores in sharp contact with porous margins. Minor fine blebs of acanthite were noted as sparse inclusions in some pyrites. Some of the wall rock fragments are choked with fine-grained disseminated pyrite. Fine pyrite occurs also concentrated in matrix quartz.

Also common are elongate, high aspect ratio, skeletal composite pyrite/marcasite crystals similar to the skeletal composite pyrite-marcasite crystals noted commonly in many of the Rosebud ore samples examined for this study. The skeletal pyrite/marcasite crystals reach 2.8mm in length with aspect ratios to 20. Marcasite is not abundant in these crystals and occurs primarily along the rims. The interiors of these crystals appear to contain aggregates of fine, generally cubic pyrite crystals. The skeletal crystals are also present as fine, curvilinear wisps.

Chalcopyrite occurs as generally fine, anhedral crystals growing in contact with pyrite at the margins of the pyrite crystals, or within voids created in packed aggregates of pyrite crystals. Sometimes the chalcopyrite is intergrown with acanthite. Rarely chalcopyrite occurs as isolated anhedral crystals in the matrix quartz. Maximum dimension of the chalcopyrite crystals is approximately 0.1mm.

Sphalerite (gray; low reflectance; orange-red internal reflections) was identified in contact with an aggregate of pyrite crystals with chalcopyrite void fill. This phase has a single tiny inclusion of chalcopyrite and a partial irregular rim of acanthite along the edge not in contact with the pyrite

Representative photomicrographs from sample RB-6 are given in Figures 42 and 43.

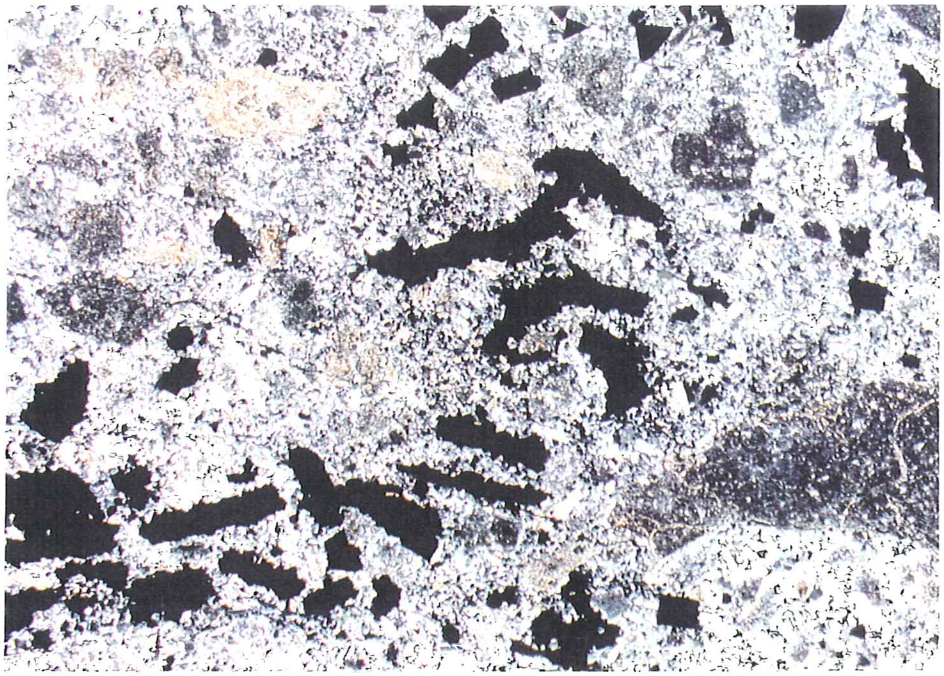

Figure 42a. RB-6/quartz matrix hydrothermal breccia. Fragments of altered volcanic wall rock dispersed in matrix of fine, polycrystalline quartz and sulfides, dominantly pyrite. TLX; 1cm on the photo= 0.532mm.

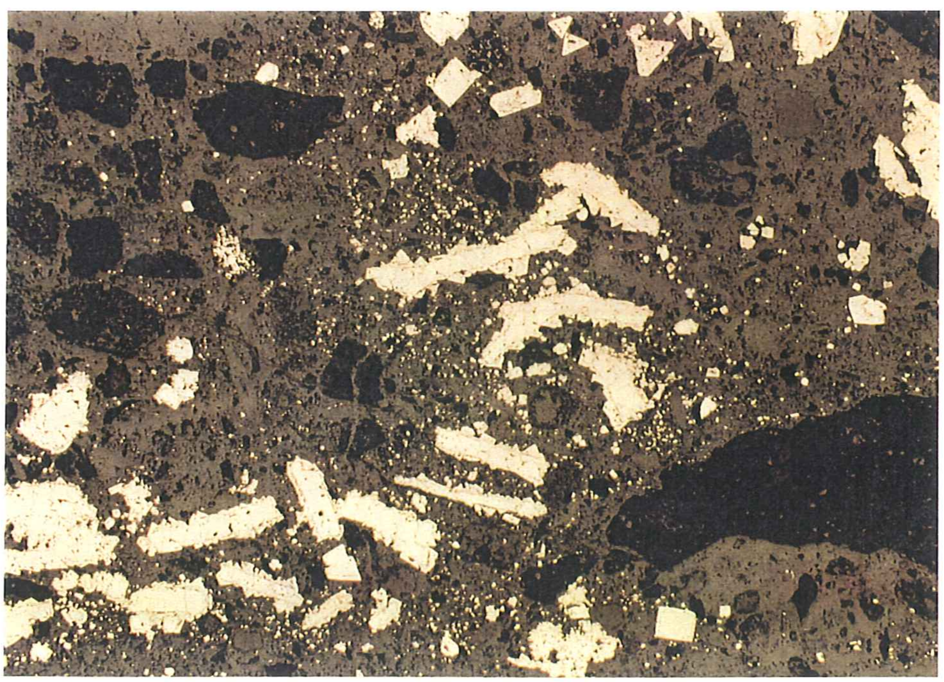

Figure 42b. RB-6/quartz matrix hydrothermal breccia. Same view and scale as Figure 42a. Matrix sulfides are dominantly pyrite with subordinate composite pyrite-marcasite. Many of the pyrites have porous rims and solid cores. RL; 1cm on the photo= 0.532mm.

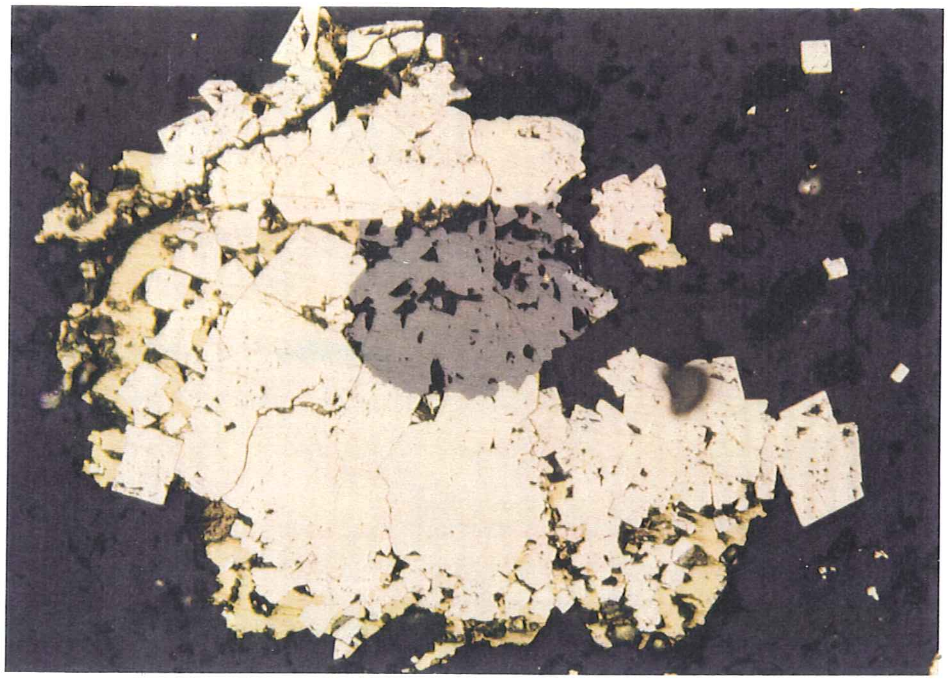

Figure 43. RB-6/quartz matrix hydrothermal breccia. Dense aggregate of pyrite crystals with chalcopyrite (mustard yellow; R < pyrite) in edge contact and in intercrystalline voids. The pyrites partially encompass sphalerite, and there is minor acanthite (?) along the right edge of the sphalerite crystal. RL; 1cm on the photo= 0.053mm.

Sample RB-7 (Silica-healed breccia; 0.091opt Au, <0.05opt Ag)

Sample RB-7 is a silicified hydrothermal breccia. In hand specimen the breccia contains large, angular fragments of flesh-colored , crackle-brecciated felsite in a light gray, vein-like, fine quartz-minor sulfide matrix. The quartz matrix has abundant smaller lithic fragments. In the polished thin section sample the largest angular fragment covers about 2/3 of the slide and may be a partly devitrified tuff. It is a microcrystalline aggregate of quartz, clay, and alkali feldspar, plus dispersed fine, cloudy gray-brown material that is probably devitrified glass. The fragment is crackled by fine, somewhat discontinuous, microcrystalline quartz veinlets. Outside of the larger fragments angular to sub-round fragments of altered (microcrystalline quartz-clay) wall rock are dispersed in a fine- to very fine-grained xenomorphic matrix of quartz and minor sericite-clay. These fragments range to >10mm in length/diameter. Some appear to be derived from welded ash flow tuff protoliths. A few of the fragments in the quartz-minor sericite-clay matrix are completely altered to sericite-clay. Fine-grained opaques are sparsely disseminated in some fragments. Scattered fine to coarse opaques are present in quartz-minor sericite-clay matrix. The opaques are eu- to subhedral and reach nearly 6mm in length..

CL: Quartz has very dull red-brown to reddish blue CL (nearly non-luminescent). Minor calcite with bright orange CL is present in altered wall rock fragments. Apatite (yellowish gray CL) was noted as inclusion within one skeletal pyrite-marcasite crystal.

RL: Opaque phases account for no more than 1-2% of the sample. The coarse opaques are essentially rectangular in shape and composed of marcasite-pyrite aggregates. They probably crystallized initially as marcasite in skeletal or spinifex fashion (growth response to supercooling?), as the rims are dominantly marcasite. The hollow interiors were then filled with an aggregate of fine, euhedral and generally cubic pyrite crystals. Marcasite is found also in the crystal interior, sometimes as a core with a porous texture resembling a "cornrow" hairdo. In one large crystal there is a rim and core of dominantly marcasite, with an essentially circumferential intermediate zone of aggregate pyrite crystals. Disseminated individual crystals of both pyrite and marcasite were noted in the quartz matrix.

Inclusions of a tan to pale brown or pinkish brown phase (moderate reflectance < pyrite; anisotropic blue-gray to brown) was noted in a coarse composite pyrite/marcasite. This phase is identified tentatively as pyrrhotite.

A trace of very fine-grained (appx 0.02mm length), anhedral chalcopyrite was noted in contact with a very fine-grained pyrite crystal disseminated in a breccia fragment.

A single crystal of acanthite (gray; moderate to low reflectance; anisotropic; low polishing hardness; cubic morphology retained from high temperature argentite) was noted dispersed in the quartz matrix.

Noted also were traces of a very fine-grained (<0.04mm diameter) gray phase (anhedral; somewhat porous; low to moderate reflectance; whitish yellow internal reflections). One crystal had scattered inclusions of extremely fine chalcopyrite. The phase is transluscent and may be rutile.

Despite the assay of 0.091 opt Au no primary gold-bearing phases (gold, electrum) were identified in this sample. The gold may be substitutional in pyrite and marcasite, or one of the lesser abundant phases.

Representative photomicrographs from sample RB-7 are illustrated in Figures 28, 34, and 44.

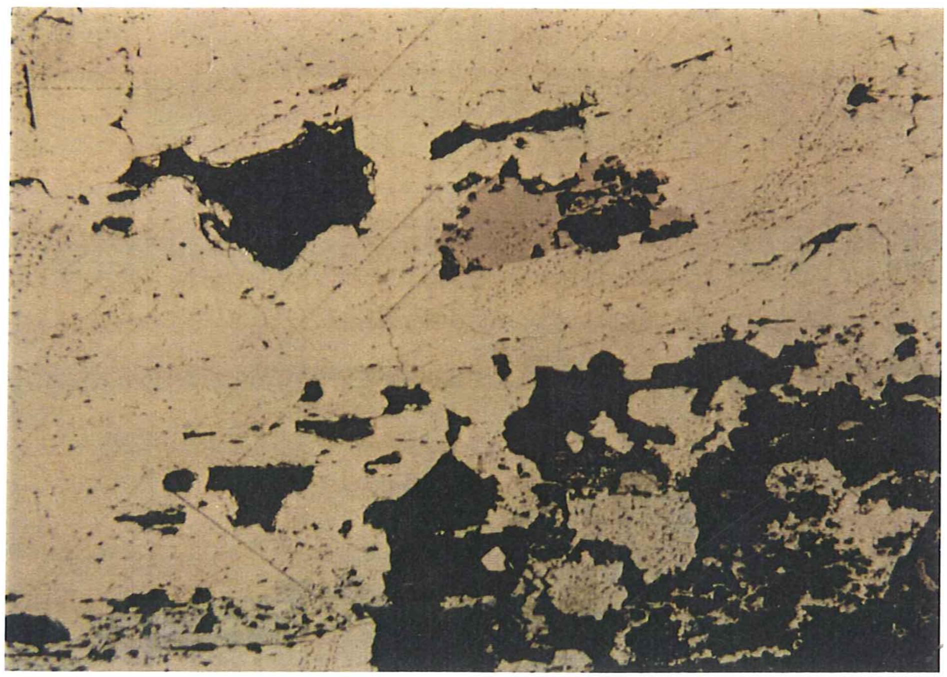

Figure 44. RB-7/silicified hydrothermal breccia. Pyrrhotite (pale brown; moderate reflectance) in an intracrystalline void within a composite pyrite-marcasite crystal. RL; 1cm on the photo= 0.053mm.

Sample RB-8 (Breccia)

Sample RB-8 is a hydrothermal breccia in which fragments of altered wall rock(clay-microcrystalline quartz) are encompassed by fine to very fine xenomorphic-granular quartz matrix with abundant coarse opaques and stringers of very fine-grained opaques. Scattered fine disseminated opaques occur also in the wall rock fragments. The altered wall rock fragments are very fine-grained, devoid of phenocryst phases, and appear relatively featureless. They may be a tuffaceous lithology, perhaps tuffaceous sediment or ash fall tuff. The larger fragments are crackled by an anastomosing net work of fine quartz veinlets. The coarser quartz at the margins of large fragments has a tendency to crystallize elongate perpendicular to the fragment margin and into the quartz matrix. Locally a honeycomb network of very fine-grained opaques crystallized along the boundaries between fine-grained quartz crystals.

CL: Quartz is essentially non-luminescent. Minor to trace disseminated calcite with bright orange CL is present in altered wall rock fragments.

RL: Opaque phases constitute 15-20% of the slide. The dominant opaque phases are composite pyrite-marcasite crystals. These are present as euhedral to subhedral crystals to 9mm in length/diameter. Many of the composite pyrite-marcasite crystals are skeletal with a high aspect ratio (to 16:1). The composite crystals are characterized by a narrow, discontinuous margin of marcasite, and an interior composed of a tightly-packed aggregate of very fine-grained, euhedral to subhedral, individual crystals of pyrite and marcasite (py > mc). Pyrite is also observed to form local fine, anastomosing, thread-like networks along quartz grain margins in the quartz mosaic matrix. Fine pyrite or pyrite threads or crystal aggregates rim and invade some breccia fragments.

Chalcopyrite is fairly common in sample RB-8, although subordinate to both pyrite and marcasite. It occurs as subhedral to anhedral crystals overgrown on fine, euhedral pyrites and as subhedral to anhedral crystals in edge contact and intergrown with pyrite-marcasite crystal aggregates. Maximum dimension for chalcopyrite crystals can exceed 0.6mm length/diameter. Chalcopyrite is present also as sparse, subhedral to anhedral disseminations in the fine, xenomorphic quartz matrix.

Significant electrum occurs locally in intra- and intercrystalline voids within composite pyrite-marcasite crystals and crystal aggregates.

Representative photomicrographs from sample RB-8 appear in Figures 5, 45, and 46.

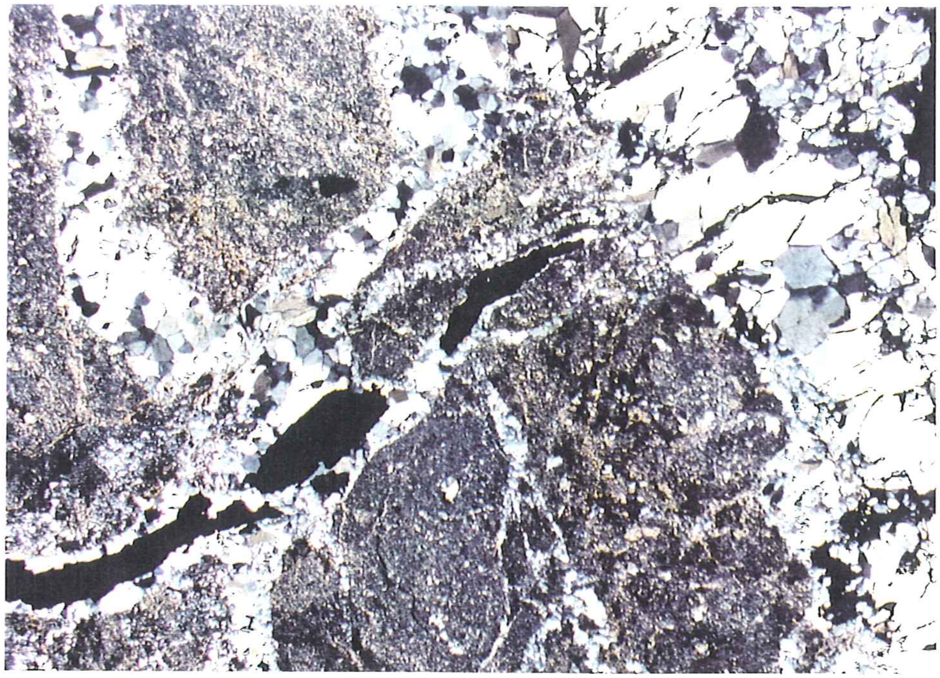

Figure 45a. RB-8/silicified hydrothermal breccia. Fragments of tuffaceous volcanic wall rock have patchy clay alteration and are laced with quartz microveinlets. The breccia matrix consists of quartz, pyrite, and composite pyrite-marcasite crystals. TLX; 1cm on the photo= 0.532mm.

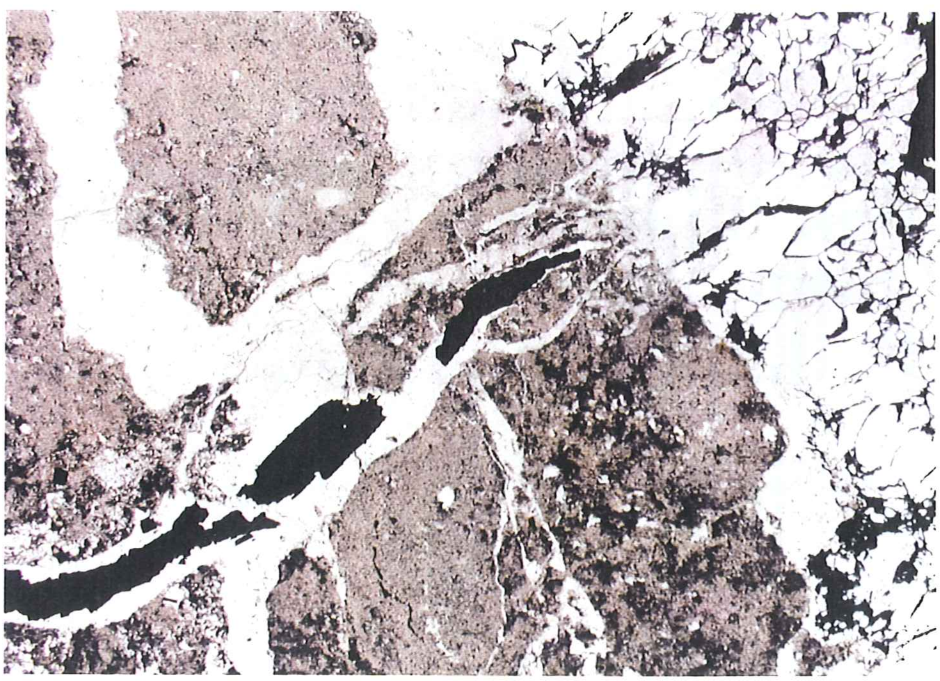

Figure 45b. RB-8/silicified hydrothermal breccia. Same view and scale as Figure 45a. TLP; 1cm on the photo= 0.532mm.

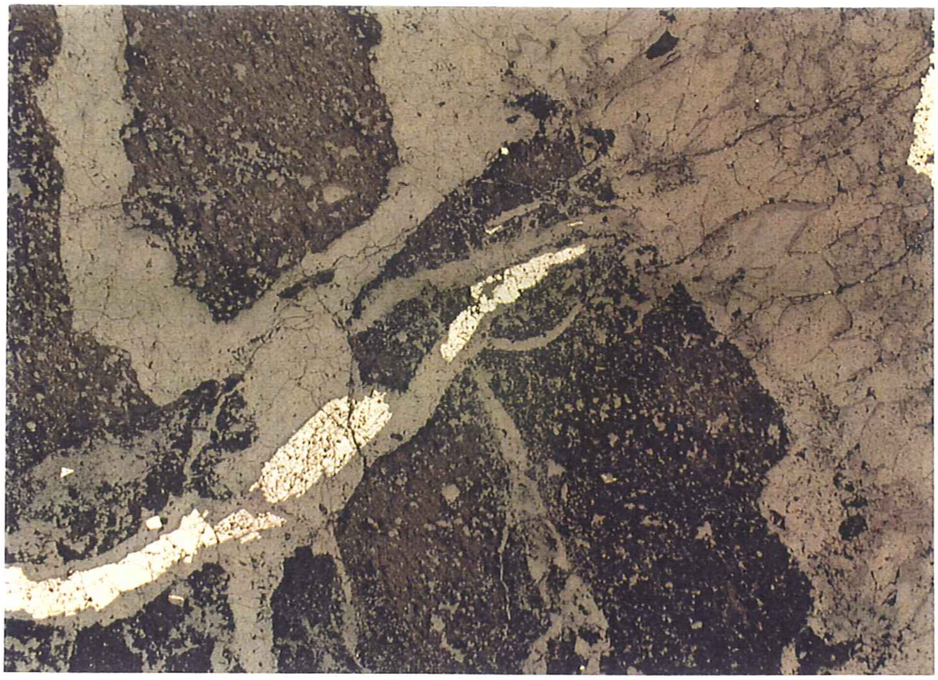

Figure 45c. RB-8/silicified hydrothermal breccia. Stringer of pyrite and composite pyrite-marcasite in quartz breccia matrix. Same view and scale as Figures 45a and 45b. RL; 1cm on the photo= 0.532mm.

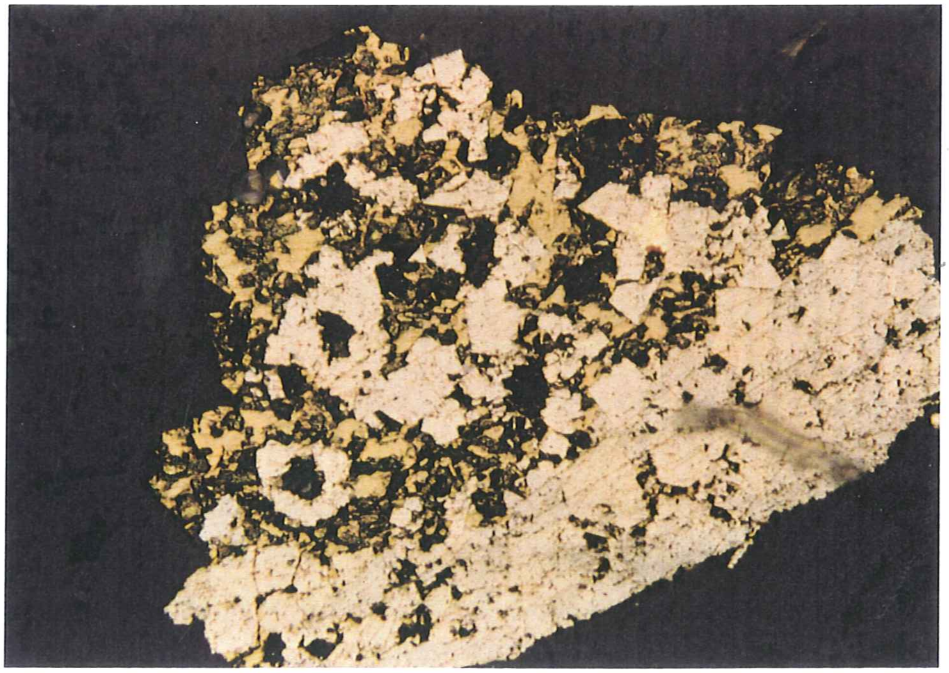

Figure 46. RB-8/silicified hydrothermal breccia. Aggregate of pyrite and composite pyrite-marcasite crystals. Chalcopyrite (mustard yellow) grows marginal to the aggregate and in intercrystalline voids. Electrum (pale yellowish white; high R) is present in the upper right quadrant of the photo intercrystalline to an aggregate of pyrite crystals. RL; 1cm on the photo=0.053mm.

Sample RB-9 (Black silica with W.C. and marcasite; 0.503opt Au, 0.4opt Ag)

Sample RB-9 is a hydrothermal breccia. It is matrix-supported and contains angular to rounded fragments of altered wall rock dispersed in a matrix of very fine-grained, light to dark-gray quartz. A band (vein?) of white quartz approximately 1cm in width is curvilinear and runs through the center of the slide. In thin section the fragments are composed of very fine-grained xenomorphic-granular quartz, clay, and minor sericite. Locally sparse former phenocrysts (feldspar?) are replaced by polycrystalline quartz. The protolith appears to be volcanic in origin. Locally some fragments are silicified to the point where they nearly disappear into the matrix. Larger fragments (to >12mm in this sample) are crackled with fine quartz veinlets. Locally fragments are partly rimmed with slightly coarser grained polycrystalline quartz. The breccia matrix consists of very fine-grained, xenomorphic-granular to saccharoidal quartz. Average matrix quartz crystal size is on the order of 0.04mm in length/diameter, and there are zones of slightly coarser polycrystalline quartz (to 0.2mm length). The white quartz vein is bounded irregularly by quartz with long axes perpendicular to the vein-breccia contact. Maximum crystal size of the bounding quartz is approximately 0.25mm length. The body of the vein contains finer quartz, with an average crystal size of about 0.06mm in length/diameter. There are minor disseminated opaque phases in fragments, breccia matrix, and vein. Euhedral to subhedral, dominantly cubic opaque phases (pyrite) are mostly confined to the fragments, whereas elongate, rectangular to needle-like opaques (skeletal composite pyrite-marcasite) occur in the gray quartz breccia matrix and white quartz vein .

CL: Quartz is nearly non-luminescent. One fragment noted with dull royal blue CL, possibly from kaolin. Trace calcite (bright orange CL; $Mn2+$) in matrix.

RL: Opaque phases constitute about 1-2% of the sample, mostly as fine-grained to very fine-grained, euhedral to subhedral pyrite crystals, less common marcasite, and scattered skeletal, high aspect ratio, composite pyrite-marcasite crystals. The pyrite crystals are mostly cubic and have a maximum diameter of about 0.35mm; most are much smaller. The skeletal composite py-mc crystals reach 2.2mm in length with aspect ratios to more than 20:1. The pyrites, marcasites, and composite pyrite-marcasites are disseminated in the quartzose matrix, while pyrite and marcasite are sparsely disseminated in the lithic breccia fragments.

Chalcopyrite is present as fine-grained (to 0.11mm diameter), anhedral to subhedral crystals generally associated with pyrite or marcasite. It is usually crystallized in edge contact with individual crystals or aggregates of pyrite or marcasite. Less commonly it is found in voids within close-packed pyrite aggregates, either alone or in simple intergrowth with a silver mineral. Chalcopyrite is present also as very fine-grained (0.2mm diameter) individual subhedral crystals disseminated in the quartz matrix, where it is sometimes intergrown with pyrite.

A light gray phase (low to moderate reflectance; weak anisotropy) is present locally crystallized in intercrystalline voids within skeletal py-mc crystals, either alone or with chalcopyrite. This phase is identified tentatively as acanthite. Traces of a second light gray phase were noted disseminated in the quartz breccia matrix. The phase is very fine-grained (0.04mm diameter) and is characterized by low to moderate reflectance and intense carmine red internal reflections). This phase is identified tentatively as pyrargyrite. It occurs also as sparse inclusions in pyrite.

A trace of very fine-grained sphalerite was noted disseminated in the quartz matrix. The sphalerite is characterized by low reflectance and yellow-brown internal reflections.

Opaque phases noted in the white vein quartz are skeletal composite pyrite-marcasite crystals and a trace of fine chalcopyrite (anhedral; to 0.03mm length)

Although the assay for this sample is 0.503opt Au and 0.4opt Ag, no primary gold-bearing phases were identified.

Representative photomicrographs from sample RB-9 are shown in Figures 3 and 47.

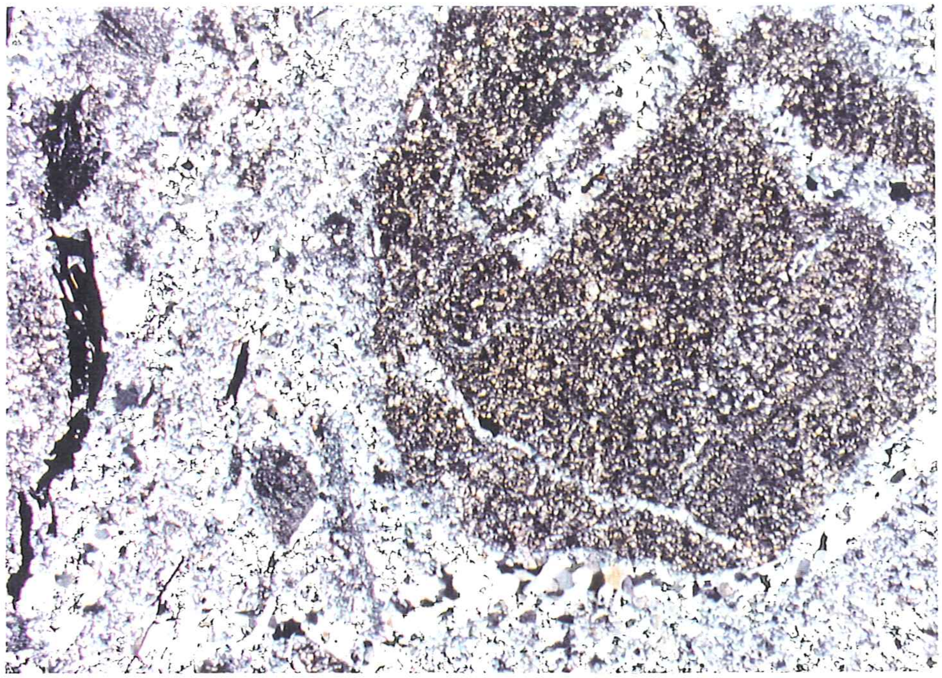

Figure 47a. RB-9/silicified hydrothermal breccia. Fragments of volcanic wall rock dispersed in a quartz-sulfide (pyrite-marcasite, pyrite) matrix. TLX; 1cm on the photo= 0.532mm.

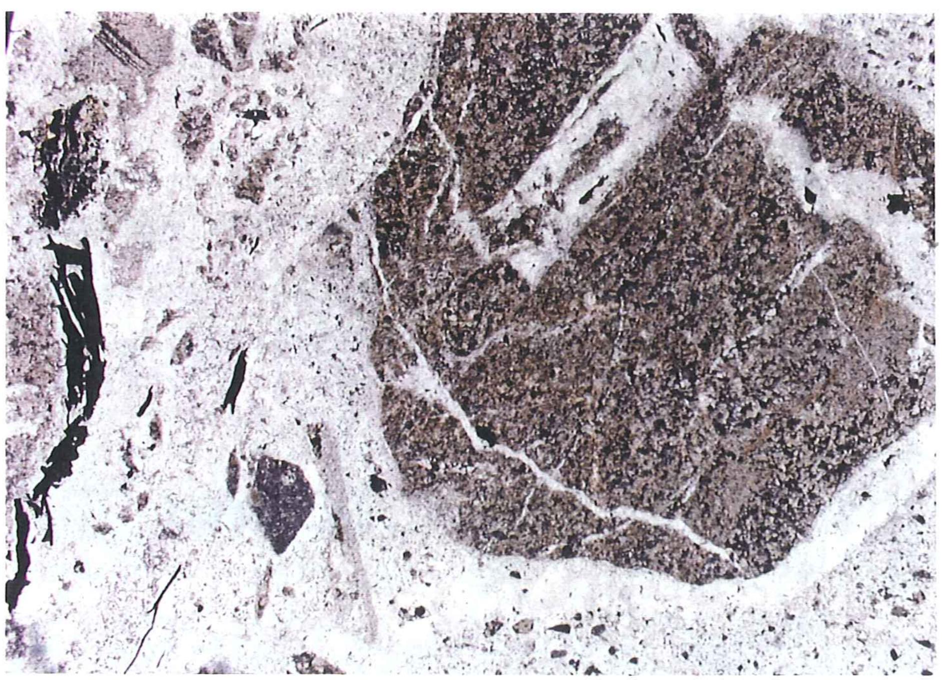

Figure 47b. RB-9/silicified hydrothermal breccia. Same view and scale as Figure 47a. TLP; 1cm on the photo= 0.532mm.

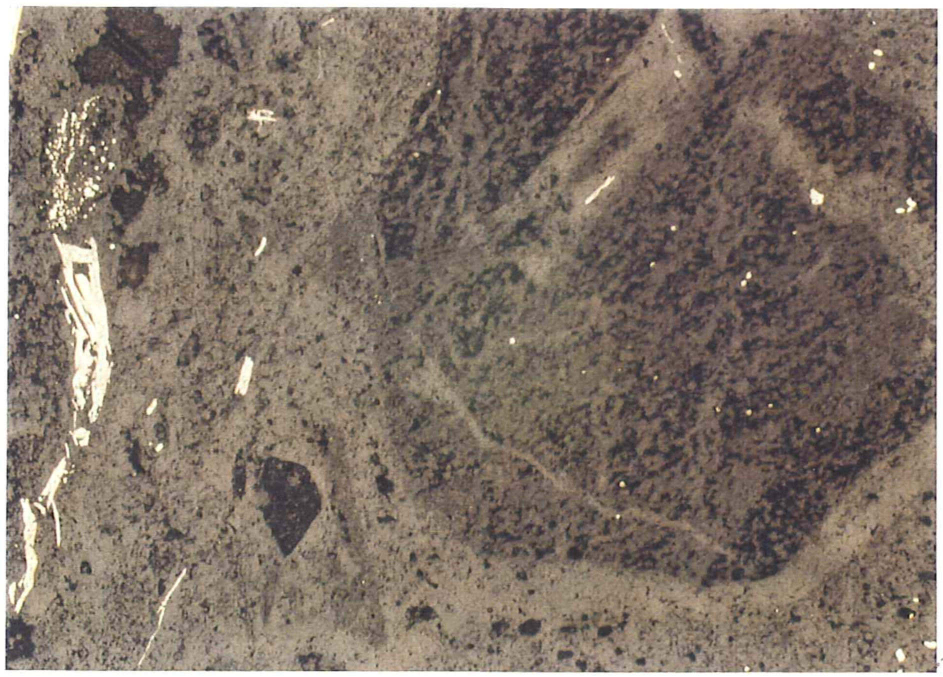

Figure 47c. RB-9/silicified hydrothermal breccia. Composite pyrite-marcasite crystals (high aspect ratio) and pyrite (finer-grained and more equant) in quartz breccia matrix. Same view and scale as Figures 47a and 47b. RL; 1cm on the photo= 0.532mm.

Sample RB-10 (Mineralized pmbx; 60.499opt Au, 64.27opt Ag)

Sample RB-10 consists of altered wallrock fragments encompassed by a coarse, porous aggegrate of skeletal composite pyrite-marcasite crystals. The nearly massive aggregate of composite pyrite-marcasite crystals spans the dimension of the slide. The crystals are generally euhedral to subhedral, and skeletal to rectangular, with maximum long dimension of nearly 6mm. Aspect ratios reach about 18:1. The wall rock fragments appear to be a tuffaceous volcanic lithology. They are composed of a fine-grained mass of predominantly recrystallized quartz and a cloudy, gray-brown, nearly isotropic material that may be relict glass. The quartz is xenomorphic and up to 0.22mm in diameter. Quartz also partly fills intercrystalline voids between pyrite-marcasite crystals. This quartz is subhedral to anhedral and up to 0.6mm in length.

CL: Altered wall rock may be fragmental volcanic. Minor calcite (orange CL; $Mn2+$) is present in the wall rock fragments. Fine-grained, euhedral apatite in the wall rock is probably primary (bright lemon yellow CL). Minor orange-luminescent calcite occurs in the sulfide matrix. Some dull royal blue CL material resides in interstices between sulfide crystals and may be kaolinite. Locally parts of the sulfide matrix have a strange dull tan CL (?).

RL: A closely-packed aggregate of composite pyrite/marcasite crystals makes up approximately 70-75 volume percent of the slide. The composite crystals are characterized generally by narrow, irregular and discontinuous margins of marcasite and interiors of pyrite with elongate narrow marcasite zones parallel to the long axis of the crystal. Some of the crystals are elongate with high aspect ratios and skeletal form. The skeletal crystals have narrow, irregular marcasite rims and interiors composed of closely packed fine pyrite crystals with irregular zones of marcasite. Maximum length of individual crystals is approximately 5mm in this sample, although crystal lengths in the vein may be longer. Some large pyrite-marcasite crystals have a square cross section with diameters to 2mm. These crystals may be cut perpendicular to the c-axis and have true lengths well in excess of 5mm. Aspect ratios of the elongate crystals reach 18:1. The interiors of some larger crystals or crystal aggregates sometimes have an oriented corroded internal structure similar in appearance to a "cornrow" hairdo.

Pyrite crystals are commonly disseminated in the minor amount of wall rock visible in this slide. The pyrites are euhedral to subhedral with dominantly pyritohedron crystal form.

Chalcopyrite is the next most common sulfide phase. It occurs primarily as anhedral to subhedral, somewhat motheaten crystals to 0.4mm in length/diameter. The chalcopyrite is found most commonly in edge contact along parts of some composite pyrite-marcasite crystals. It is present also as inclusions within the composite pyrite-marcasite crystals and, less commonly, as individual disseminations. Locally the chalcopyrite is rimmed or replaced by digenite. Digenite was noted also in linear intergrowths in voids parallel to the long axis of the rectangular pyrite-marcasite crystals. Rarely, the chalcopyrite associated with pyrite-marcasite crystals is accompanied by a fine-grained silver sulphosalt phase, possibly antimonpearceite.

Most of the silver in sample RB-10 and virtually all of the gold are contained in electrum. Electrum occurs most commonly as irregular to anhedral crystals up to 0.25mm in diameter in inter- and intracrystalline voids within composite pyrite-marcasite crystals. Less commonly the electrum forms smaller crystal aggregates with pyrite-marcasite ± chalcopyrite. The electrum tarnishes rapidly in air.

Representative photomicrographs from sample RB-10 are given in Figures 4, 48, 49, and 50.

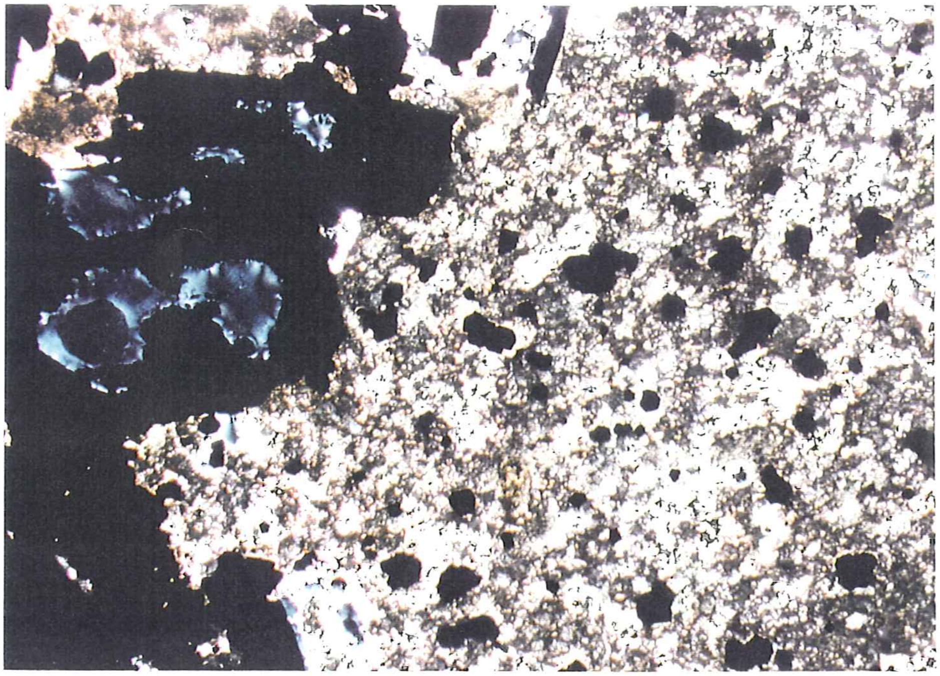

Figure 48a. RB-10/mineralized breccia vein. A porous vein composed predominantly of composite pyrite-marcasite crystals encompasses wall rock fragments of probable volcanic origin. This wall rock fragment contains abundant disseminated pyrite. TLX; 1cm on the photo= 0.532mm.

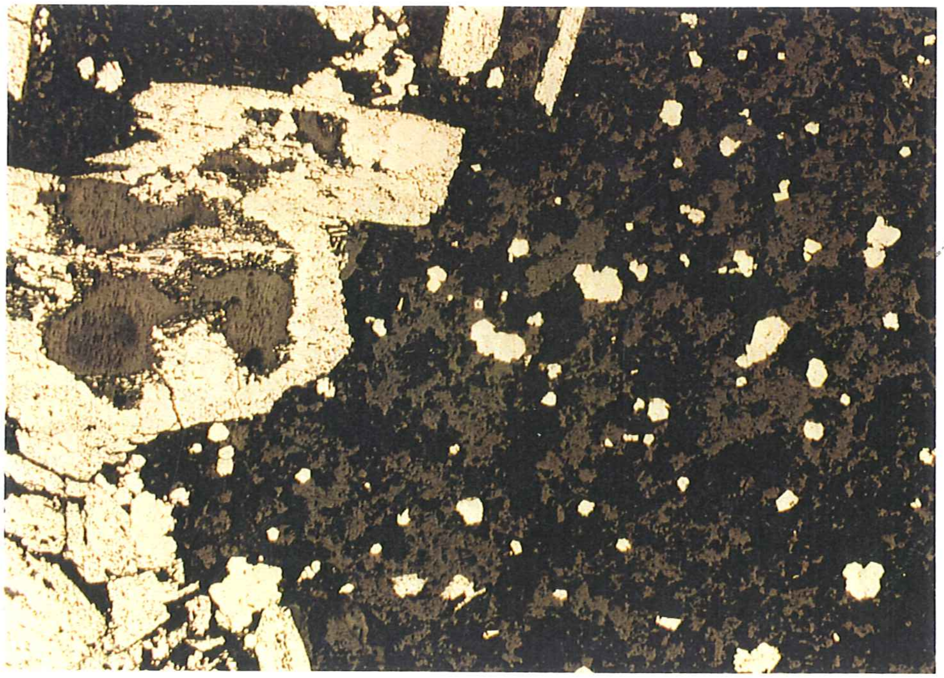

Figure 48b. RB-10/mineralized breccia vein. Coarser sulfides are composite pyrite-marcasite crystals, while finer disseminations are pyrite. Same view and scale as Figure 48a. RL; 1cm on the photo= 0.532mm.

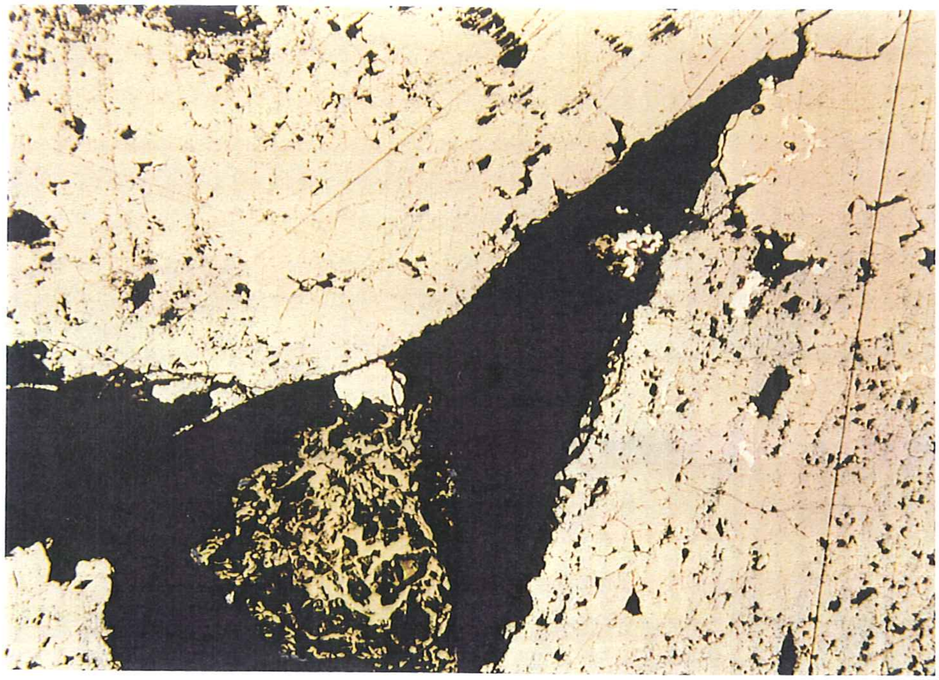

Figure 49. RB-10/mineralized breccia vein. Skeletal composite pyrite-marcasite crystals with minor inclusions of electrum (white; high R). Chalcopyrite (mustard yellow) and electrum partly fill intercrystalline void space. RL; 1cm on the photo= 0.106mm.

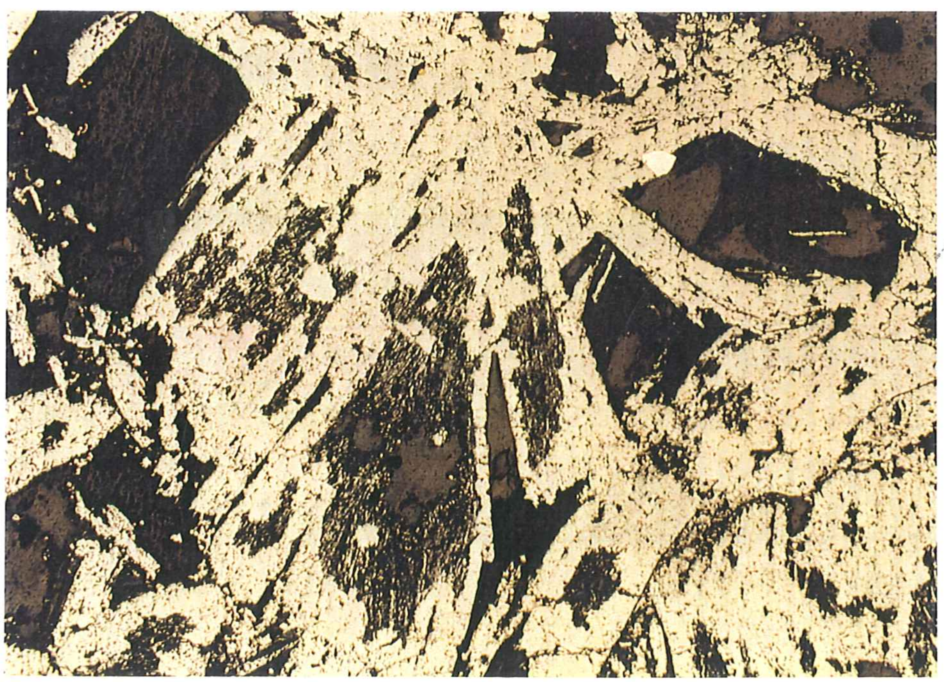

Figure 50. RB-10/mineralized breccia vein. Aggregate of composite pyrite-marcasite crystals. There is minor intercrystalline electrum (white; high R) in the upper right quadrant of the photo. Note porous "cornrow" texture in some py-mc crystals. RL; 1cm on the photo= 0.532mm.

Sample RB-11 (Mineralized plam)

Sample RB-11 is a piece of breccia or vein with fragments of altered white felsitic wall rock in a matrix of fine, gray quartz. In thin section the wall rock fragments are composed of partly devitrified amorphous brown glass and microcrystalline quartz. The brown "glass" is locally weakly anisotropic from devitrification. Some fragments contain sparse small phenocrysts or pyrogenic crystals that are tabular in form and reach 0.44mm in length. These crystal pseudomorphs contain relict alkali feldspar and polycrystalline quartz. Pale green chlorite replaces former biotite crystals. The fragments may be partly devitrified welded tuff. They are invaded by discontinuous, thread-like, fine quartz veinlets. Fragment margins are silicified locally by extremely fine, microcrystalline quartz. An elongate (7mm X 0.6mm) fragment or mineral phase is green in color and weakly pleochroic. This may be a fragment of glauconitic sediment (?). This phase has a green color in TLP and there is little change under TLX (glauconite?). Disseminated opaque phases are common in some fragments. The vein or breccia matrix consists of polycrystalline, saccharoidal quartz and abundant coarse opaque phases (py, mc, Ag minerals). Locally, coarser drusy quartz crystallized into the quartz matrix from wall rock fragments, with long axes perpendicular to the fragment margins. Maximum quartz grain size is approximately 0.4mm in length.

CL: Reddish orange luminescent calcite is distributed throughout most fragments of altered wall rock. A trace of apatite (yellow CL) is associated with sulfides in the breccia matrix.

RL: Opaque mineral phases constitute approximately 40-45% of the slide. They consist primarily of subequal amounts of pyrite or composite pyrite-marcasite crystals and a silver sulphosalt phase, possibly a pearceite-antimonpearceite series mineral. Less abundant phases include native gold and electrum.

Pyrite occurs as fine-grained disseminations in wall rock and as coarser individual crystals or aggregates dispersed in matrix quartz. The disseminated pyrite crystals are euhedral to subhedral pyritohedrons in form and reach 0.4mm diameter. The pyrites dispersed in the matrix quartz have both cubic and pyritohedron form and are up to 1.8mm in length/diameter.

The vein or breccia matrix mineralization consists of composite pyrite-marcasite crystals, most of which have skeletal form, pyrite, a silver sulphosalt mineral, and minor native gold and electrum.

The gangue sulfides are dominantly composite pyrite-marcasite crystals, most of which have an elongate, skeletal form. The skeletal crystals reach nearly 6mm in length and have aspect ratios as high as 40:1. They occur in crudely radiating to sheaf-like aggregates dispersed in the quartz matrix. The silver sulphosalt phase has crystallized in some of the intracrystalline void spaces within the skeletal pyrite-marcasite crystals, as well as in intercrystalline voids in pyrite-marcasite crystal aggregates. Extremely fine blebs of native gold are sometimes included within the silver mineral.

A silver sulphosalt mineral is the most common ore mineral. Reflected light properties suggest that the mineral belongs to the pearceite-antimonpearceite series. It is characterized by gray color, low to moderate reflectance (R=30-35), weak to moderate anisotropy, and deep red internal reflections along crystal boundaries. The pearceite has crystallized as irregular anhedral crystal aggregates to >10mm in overall length. The aggregates partly to completely encompass earlier crystallizing pyrite-marcasite, cubic tp pyritohedron pyrite, and drusy quartz. Under reflected light the crystal aggregates give the impression of large, porous crystals. Scattered fine blebs and discontinuous threads of native gold are present locally. Smaller irregular crystals of pearceite are observed in localized growth adjacent to some pyrite-marcasite crystals. A second silver-bearing phase may also be present, but in much lower abundance. Its reflectance is slightly lower than that for the mineral here identified as pearceite, and it displays distinct anisotropy with no internal reflections. This phase is identified tentatively as acanthite. It is found as irregular crystals both within and adjacent to composite pyrite-marcasite crystals.

Native gold occurs primarily as very fine blebs (to 0.03mm diameter) or discontinuous threads within pearceite. The threads locally invade pearceite and migrate along the margins of encompassed hexagonal drusy quartz crystals. Rarely very fine native gold occurs as inclusions within composite pyrite-marcasite crystals.

Electrum is much less common than native gold. It occurs as fine, anhedral crystals to 0.13mm diameter dispersed in matrix quartz, as fine, irregular crystals along the contact between much larger pearceite and pyrite-marcasite crystals, and, rarely, as inclusions along the margin of some composite pyrite-marcasite crystals.

In one portion of the slide an ore phase was noted with a white to creamy white color and a high reflectance intermediate between that of pyrite and gold. The phase appears isotropic, but has incomplete extinction under crossed polars. It is identified tentatively as aurostibite ($AuSb_2$). The phase is noted crystallized in contact with composite pyrite-marcasite crystals and pearceite. Locally, discontinuous margins of native gold separate the aurostibite from pearceite.

Representative photomicrographs from sample RB-11 are shown in Figures 10, 12, 51, and 52.

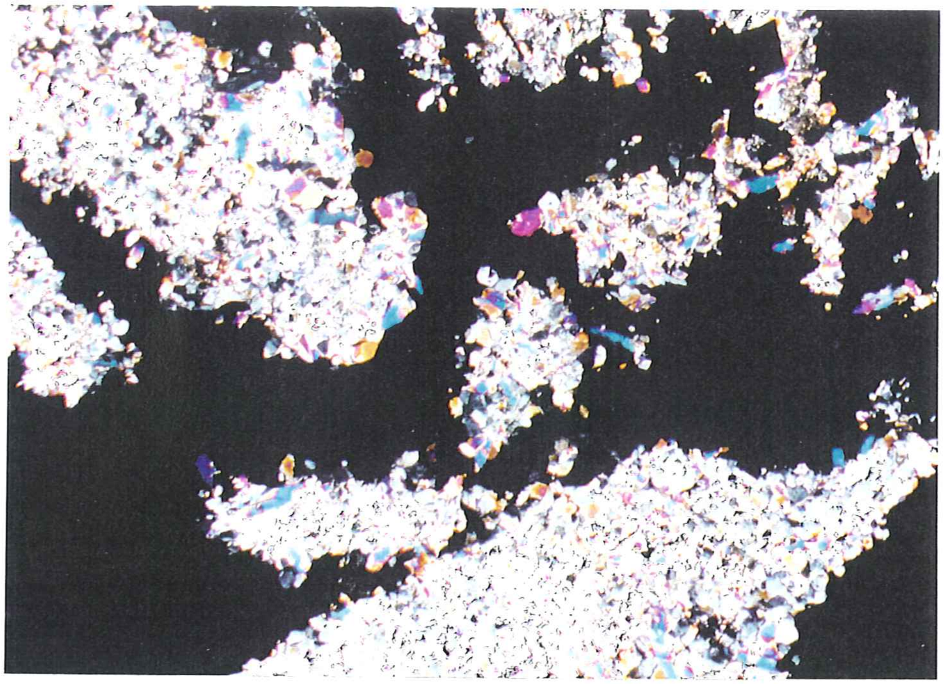

Figure 51a. RB-11/mineralized breccia vein (plam). Sulfides (py and py-mc) and silver sulphosalt minerals in a polycrystalline quartz matrix. The section is thick, and the quartz has commensurately higher birefringence. TLX; 1cm on the photo= 0.532mm.

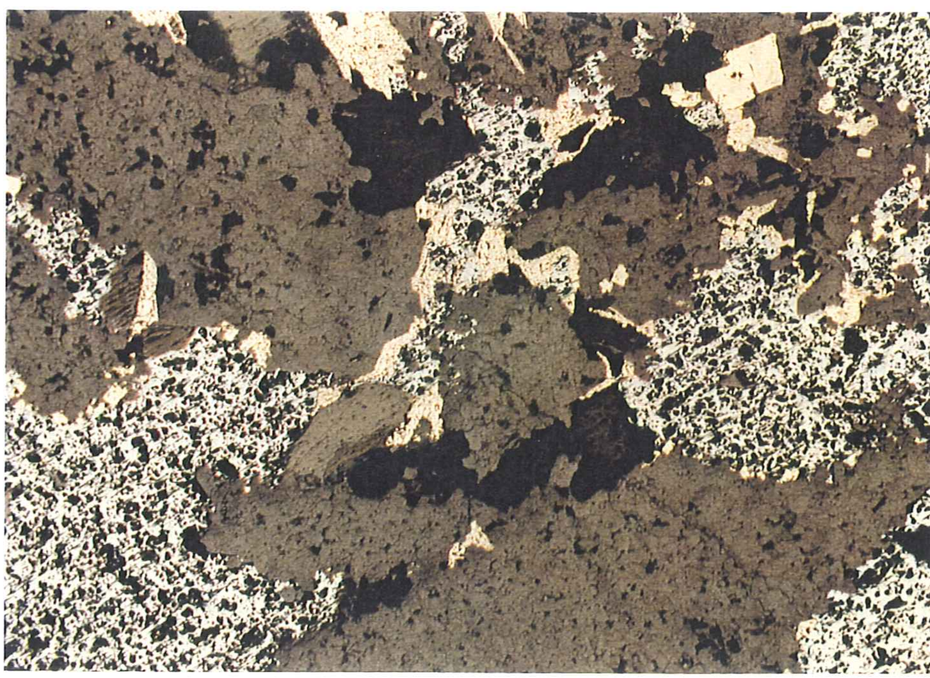

Figure 51b. RB-11/mineralized breccia vein (plam). Euhedral to subhedral pyrite and composite pyrite-marcasite crystals (creamy yellow in this view), and porous, anhedral masses of a silver sulphosalt phase (gray; pearceite series?) in a quartz matrix. Same view and scale as Figure 51a. RL; 1cm on the photo= 0.532mm.

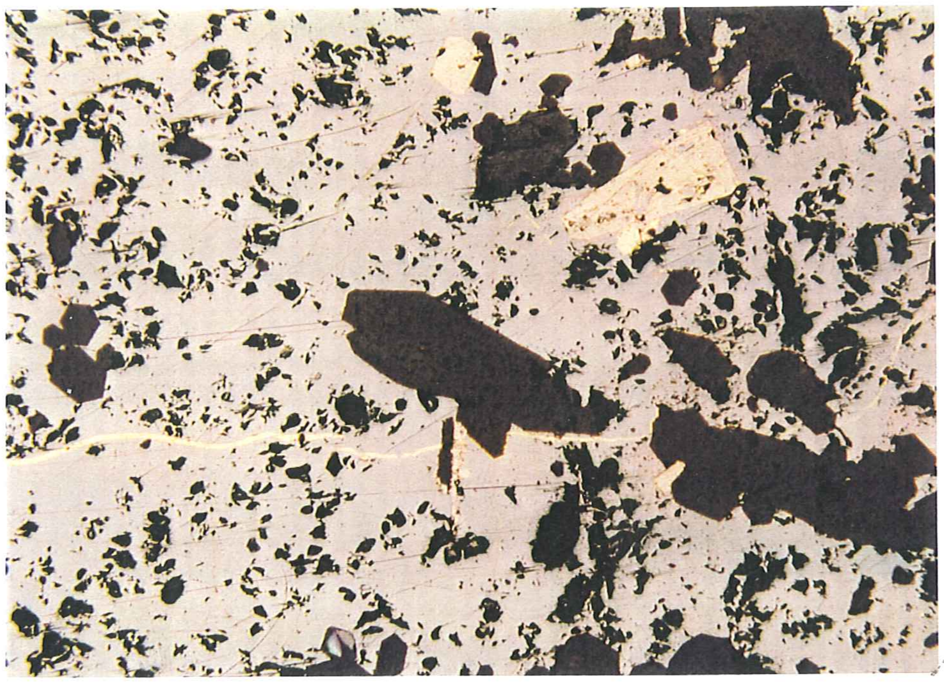

Figure 52. RB-11/mineralized breccia vein (plam). Silver sulphosalt phase grows around drusy quartz (dark, hexagonal crystals), pyrite and composite pyrite-marcasite crystals. The silver mineral is invaded by a thread of bright pale yellow native gold that migrates along the quartz crystal boundaries. RL; 1cm on the photo= 0.106mm.

Sample RB-12 (White silica vein with W.C.; 0.503opt Au and 0.4opt Ag)

Sample RB-12 is described as a white silica vein. The vein contains abundant angular to subround, white, felsitic lithic fragments dispersed in a very fine-grained white quartz matrix. The fragment/matrix mass is cut by anastomosing gray quartz-sulfide veinlets. Wall rock fragments are a microcrystalline mass of quartz and clay. They are silicified by fine quartz and strongly crackled by quartz veinlets and microveinlets. Wispy, discontinuous clay veinlets are common in some areas. The wall rock appears to have been somewhat fragmental, as angular, lapilli-size ghost fragments to 3mm in diameter can be seen through the alteration. Minor fine-grained disseminated opaques are present in the wall rock fragments. The white quartz matrix is xenomorphic-granular and has an average crystal size less than 0.05mm diameter. Locally the fragment/matrix boundaries are obscure. Irregular to elliptical pockets of clay and quartz are scattered throughout the matrix and may be derived from disaggregated wall rock. Clay also occurs finely dispersed through the matrix, generally along crystal boundaries in the saccharoidal quartz mosaic. Some of this clay may have developed at the expense of the quartz.

The gray vein quartz is very fine-grained, saccharoidal and polycrystalline. Maximum grain size is approximately 0.25mm in length/diameter. Its anastomosing veinlets encompass fragments of altered wall rock. Coarser cockscomb quartz borders the wall rock fragments. Maximum grain size of the cockscomb quartz is about 0.5mm length.

Opaque phases constitute approximately 2% of the slide, and most are concentrated in the vein quartz.

CL: All of the quartz, both vein and matrix is essentially non-luminescent. Fine, orange-luminescent calcite is commonly distributed throughout the quartz-opaques vein material. Traces of yellow-luminescent apatite were noted in altered wall rock. Discontinuous "veins" and pockets of dull royal blue CL material may be kaolinite.

RL: The dominant opaque phases in the vein are skeletal, composite pyrite-marcasite and pyrite. Also identified in subordinate amounts are sphalerite, chalcopyrite, and trace acanthite. The skeletal pyrite-marcasite crystals are euhedral to subhedral, and up to 3.5mm in length. They are distributed as individual crystals or crude, fan-like aggregates in the quartz-clay mosaic. Aspect ratios reach 18:1. In some of the veins a narrow zone of extremely fine-grained, granulated pyrite occurs immediately adjacent to the contact with the wall rock. Traces of chalcopyrite occur either dispersed in the vein or crystallized in contact with skeletal pyrite-marcasite. The chalcopyrite forms subhedral to anhedral crystals to 0.15mm in length. Rarely the chalcopyrite fills elongate intracrystalline voids within skeletal pyrite-marcasite crystals.

The wall rock contains less than 0.5% disseminated pyrite. The pyrite is dominantly subhedral to euhedral cubic in form and reaches 0.3mm in diameter. A trace of sphalerite was noted growing in association with disseminated pyrite in the wall rock. The sphalerite forms anhedral crystals to 0.15mm diameter and is in direct contact with the pyrite. It has characteristic gray color, low reflectance, and yellow-brown internal reflections. A trace of very fine-grained

(0.02mm diameter) native gold was observed in contact with a fine pyrite crystal disseminated in a wall rock fragment.

Gold and silver minerals are not abundant in this sample. Fine-grained electrum (<0.025mm diameter) occurs crystallized in edge contact with two composite pyrite-marcasite crystals in the vein quartz, and as tiny blebs in intracrystalline voids within one of the py-mc crystals. Chalcopyrite is also associated with this crystal cluster. The only other gold mineralization observed was the trace of very fine native gold crystallized with fine pyrite in the groundmass disseminations in a wall rock fragment.. Based on examination of the sample, I would not guess that it would assay 0.503 opt Au. Minor acanthite was noted in association with skeletal pyrite-marcasite and chalcopyrite, consistent with the silver assay of 0.4 opt Ag.

Photomicrographs depicting features from sample RB-12 are given in Figure 53.

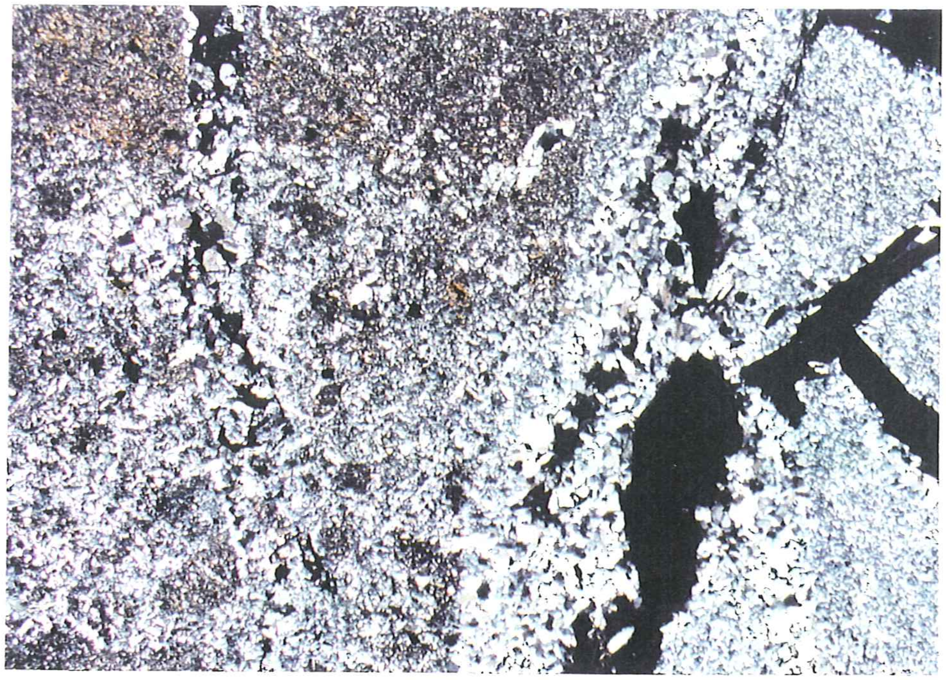

Figure 53a. RB-12/breccia vein. Quartz veins with skeletal pyrite-marcasite crystals cut the silicified breccia. The volcanic wall rocks and fragments are partly silicified and have patchy clay-sericite alteration. TLX; 1cm on the photo=0.532mm.

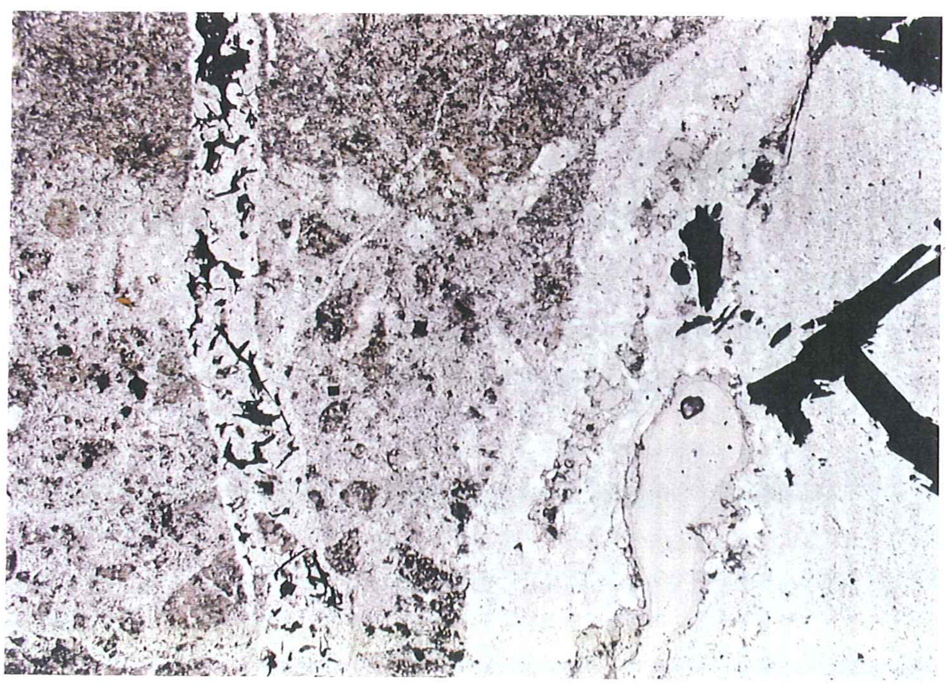

Figure 53b. RB-12/breccia vein. The microbreccia texture is more clearly visible under plane-polarized light. Same view and scale as Figure 53a. TLP; 1cm on the photo= 0.532mm.

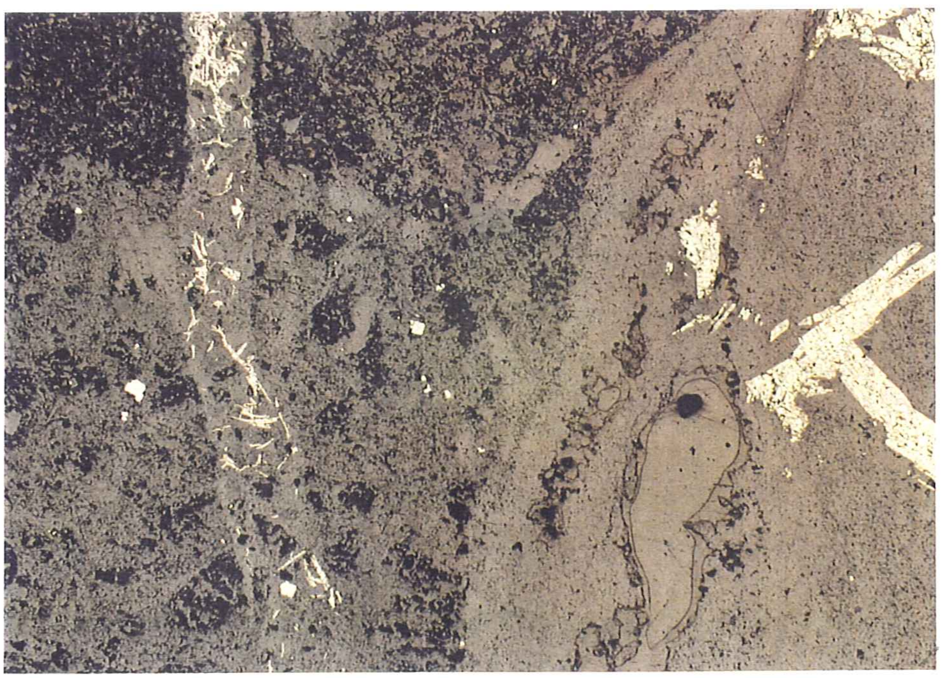

Figure 53c. RB-12/breccia vein. The sulfide minerals are dominantly composite pyrite-marcasite crystals (elongate morphology) and pyrite (smaller cubic crystals). Same view and scale as Figures 53a and 53b. RL; 1cm on the photo= 0.532mm.

Sample RB-13 (Barren black silica breccia; 0.009opt Au, <0.05opt Ag)

Sample RB-13 is a quartz matrix hydrothermal breccia. It is poorly-sorted and contains abundant angular to sub-round fragments of white, felsitic wall rock to 7mm in length/diameter dispersed in a very fine, dark gray quartz matrix. The breccia is generally matrix-supported, but fragments are commonly in point or edge contact, as well. The wall rock fragments appear to be a very fine-grained, non-descript tuffaceous volcanic lithology altered and recrystallized to a microcrystalline aggregate of quartz, clay, and sometimes a trace of sericite. A few fragments are partially rimmed by very fine sericite. The gray quartz matrix is a very fine-grained xenomorphic-granular quartz-clay mosaic. Average grain size of the xenomorphic-granular quartz mosaic is less than 0.1mm. Within the matrix are patches and discontinuous veinlets of slightly coarser polycrystalline quartz. A few small vugs have cockscomb-textured quartz with a maximum length of 0.2mm. Fine clay is dispersed throughout the dominantly quartz matrix. Clay also forms irregular aggregates to 1.5mm diameter. Some of the clay aggregates are partly or completely rimmed by slightly coarser polycrystalline quartz (>0.1mm length) and may be filling vugs in the breccia. Other clay aggregates appear to form within the quartz matrix and may have, in part, formed at the expense of matrix quartz. The sample contains less than one percent disseminated opaques in both matrix and fragments.

CL: Quartz has dull reddish brown CL. Several fragments have a trace of fine-grained apatite with yellow CL (probably primary).

RL: Total sulfide abundance is less than one percent. Wall rock fragments in the breccia have trace to significant disseminated pyrite. The pyrite is generally subhedral to anhedral and very fine-grained (<0.08mm diameter). The quartz-clay matrix has dispersed fine-grained pyrite and skeletal composite pyrite-marcasite crystals. The pyrites are subhedral to anhedral, cubic to rectangular crystals to 1.3mm in length. Average pyrite size is <0.4mm in length/diameter. The skeletal pyrite marcasite crystals are elongate prismatic in form. They reach a length of 2.5mm with aspect ratios to 20:1. Pyrite and skeletal composite pyrite-marcasite crystals were the only opaque minerals identified from this sample.

Representative photomicrographs are given in Figures 29 and 54.

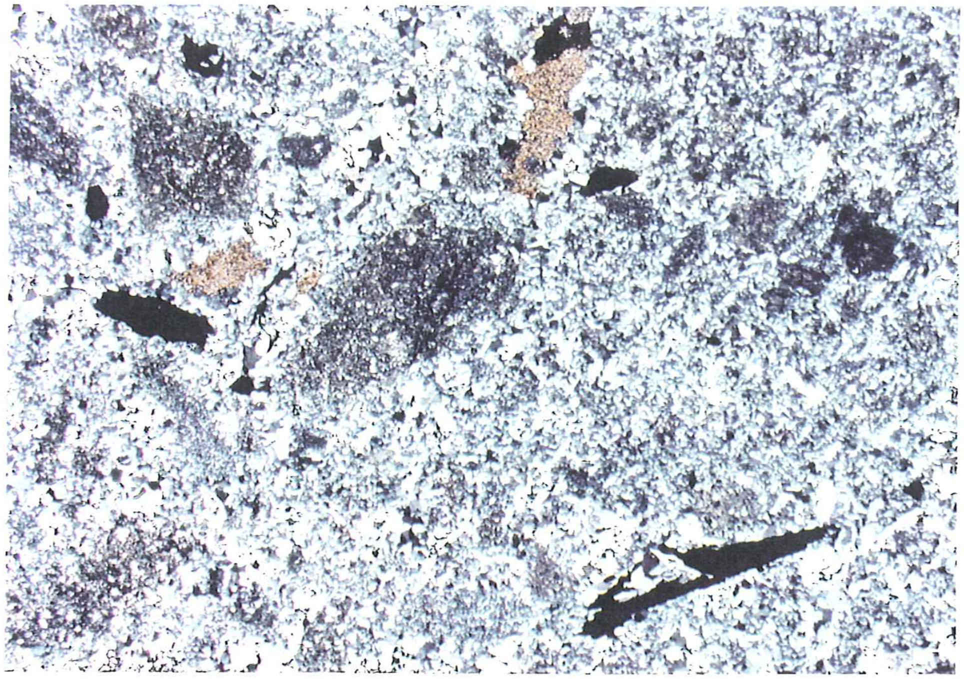

Figure 54a. RB-13/silicified hydrothermal breccia. Angular volcanic lithic fragments, clay aggregates, and skeletal composite pyrite-marcasite crystals dispersed in a fine-grained polycrystalline quartz matrix. TLX; 1cm on the photo= 0.532mm.

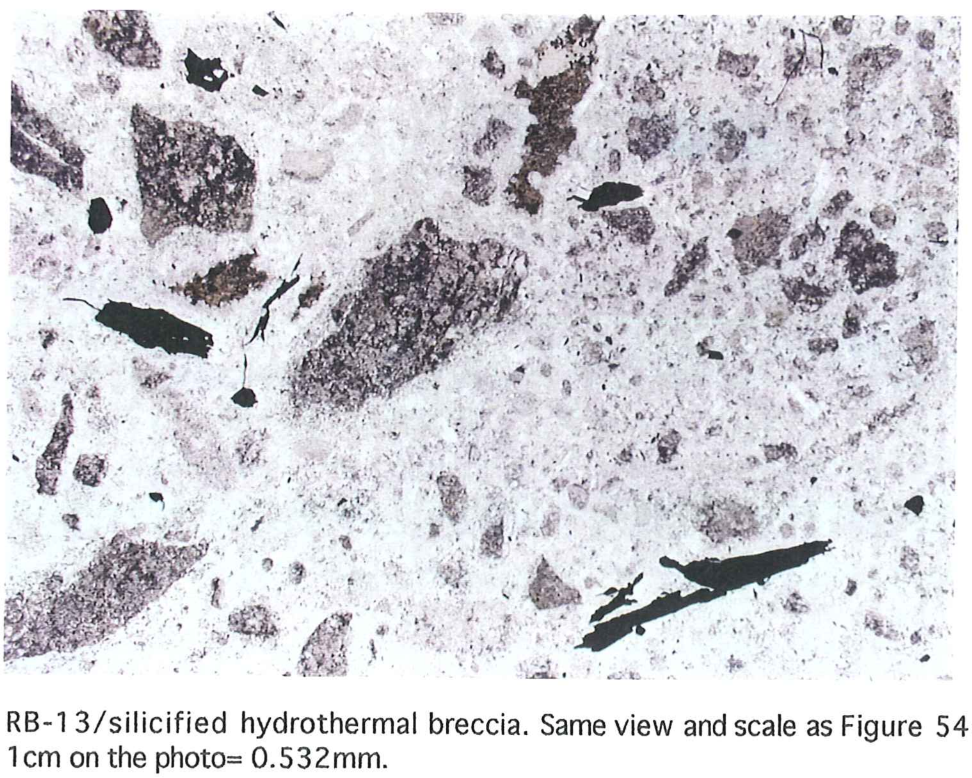

Figure 54b. RB-13/silicified hydrothermal breccia. Same view and scale as Figure 54a. TLP; 1cm on the photo= 0.532mm.

Sample RB-20 (W.C. with x-cutting chloritic fx)

Sample RB-20 appears to be a fragmental volcanic rock, perhaps a lapilli tuff, crackled by thin, very fine-grained polycrystalline quartz veinlets and discontinuous stringers. The lapilli tuff consists of poorly-sorted, angular to sub-round fragments to 6mm in length/diameter dispersed in a microcrystalline groundmass of quartz, scattered coarser quartz (<0.05mm diameter), possibly alkali feldspar, and minor clay and cloudy brown relict glass (?). The lithic lapilli fragments are similar, but for a much higher proportion of the cloudy brown amorphous material that may be relict glass. The crackling quartz veinlets are fine-grained. Individual quartz crystals have an average size of approximately 0.1mm length and tend to crystallize nearly perpendicular to the vein walls. A breccia vein has host rock fragments dispersed in a brown clay (illite?)-fine quartz matrix. The vein is irregular and about one centimeter in width. Individual fragments are rimmed by narrow bands of slightly coarser polycrystalline quartz. The vein walls are lined with similar quartz with an average crystal size of about 0.15mm length. Disseminated opaques are present in both matrix and fragments. They include skeletal marcasite and fine cubic pyrite. Chlorite was not identified.

CL: Quartz is essentially non-luminescent.

RL: Opaque minerals constitute 1-2% of the slide. The dominant disseminated sulfide is fine pyrite. The pyrite forms euhedral to subhedral cubic and, less commonly, pyritohedron crystals to 0.25mm diameter. It is dispersed both in host rock and quartz matrix. The skeletal pyrite-marcasite crystals are confined to the quartz matrix. They occur as elongate, euhedral to subhedral prisms to nearly 6mm in length. Aspect ratios are as high as 20:1. Some of the coarser skeletal py-mc crystals have interiors corroded to a porous, linear "cornrow" texture. Acanthite/argentite was noted in elongate intergrowth within one coarser skeletal py-mc crystal. A trace of sphalerite (gray, low reflectance, yellow-brown internal reflections) was noted in contact with disseminated pyrite in tuffaceous wall rock. The sphalerite forms irregular crystals to 0.15mm in diameter and is partly intergrown with the pyrite. The two phases may be co-crystalline.

A trace of chalcopyrite was noted crystallized in association with pyrite and acanthite intergranular to the matrix quartz. The chalcopyrite fills intergranular spaces between quartz crystals and reaches 0.05mm in length. Acanthite is crystallized locally in edge contact with the chalcopyrite.

A single crystal of electrum was noted in contact with a small aggregate of skeletal pyrite-marcasite crystals. The crystal has rectangular form and is 0.22mm in diameter.

Representative photomicrographs appear in Figures 14 and 55.

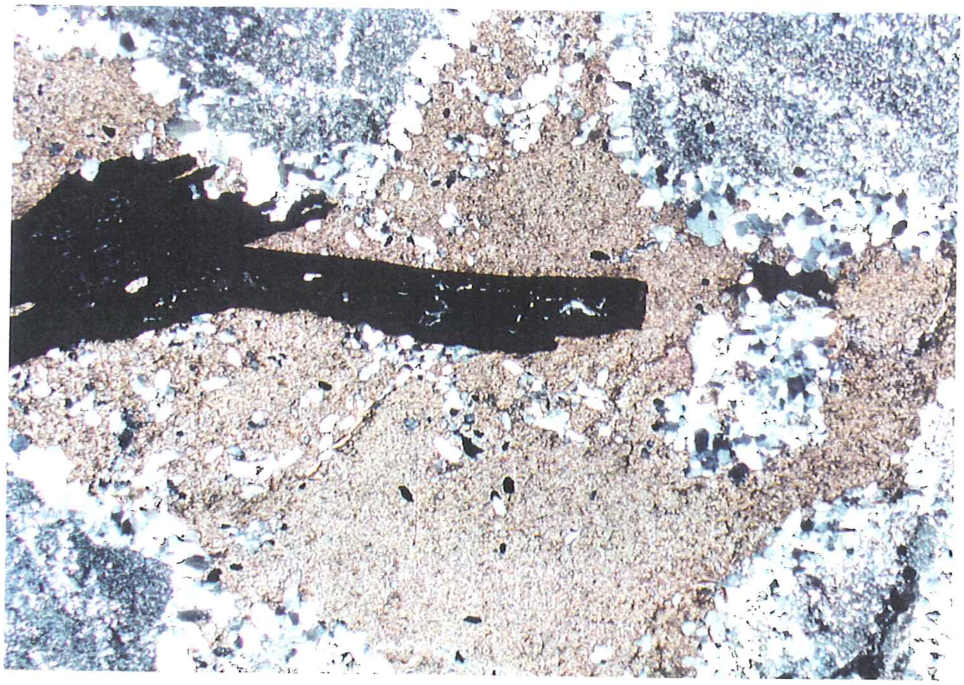

Figure 55a. RB-20/breccia vein. Skeletal pyrite-marcasite crystals in clay-quartz matrix flilling space between silicified volcanic fragments. Coarser quartz rims the fragments. TLX; 1cm on the photo= 0.532mm.

Figure 55b. RB-20/breccia vein. Skeletal composite pyrite-marcasite crystals in clay-quartz breccia matrix. A small crystal of electrum (white; high R) is crystallized with a py-mc aggregate near the right edge center of the photo. Same view and scale as Figure 55a. RL; 1cm on the photo= 0.532mm.

Sample RB-41 (porphyry near dozer contact; 0.023 opt Au, 0.14opt Ag)

Sample SB-41 is a very fine-grained, sparsely porphyritic shallow intrusive rock of dacitic or quartz latitic composition. Former feldspar phenocryst sites (?) appear to be pseudomorphed by polycrystalline quartz and served as nucleation sites for pyrite and skeletal composite pyrite-marcasite crystals. The primary feldspar phenocrysts appear to have been mostly euhedral and up to 4.5mm in length. Former mafic phenocryst sites are marked by carbonate, fine sericite, and clusters of fine-grained apatite (observable under the Luminoscope). The mafic pseudomorphs are up to 3mm in length/diameter. The mafic phenocrysts may have been hornblende or biotite. The groundmass of the porphyry is a very fine-grained, xenomorphic-granular aggregate of quartz and feldspar in which most of the feldspar is altered to clay. Average groundmass grain size is about 0.1mm diameter. Some vestiges of polysynthetic twinning can be observed, and it is likely that at least part of the feldspar was plagioclase. The porphyry is cut by narrow quartz or quartz-marcasite veinlets. The largest veinlet is 3-4mm in width. Cockscomb quartz lines the vein walls. Maximum grain size of the cockscomb quartz is about 0.8mm in length. Very fine-grained xenomorphic-granular quartz occupies most of the center of the vein, along with skeletal pyrite-marcasite. Coarse barite (?; 4.4mm in length) occupies a part of the vein center.

CL: Vein quartz and quartz replacing plagioclase phenocrysts is non-luminescent. Porphyry groundmass has dull red CL. There is minor disseminated apatite with orange yellow CL. Scattered clusters of apatite with similar CL are interpreted to be former mafic phenocryst sites. Local patches of material with dull royal blue CL that may be kaolinite replacing primary feldspar.

RL: Opaque phases constitute 2-3% of the slide. Most are concentrated in the veins or nucleated on former feldspar phenocryst sites. Minor fine-grained cubic to pyritohedron pyrite is disseminated in the porphyry groundmass. The pyrite is less tha 0.25mm in diameter.

The dominant opaque mineral in the veins is skeletal composite pyrite-marcasite. The crystals are elongate-prismatic in form and up to 6.6mm in length. Aspect ratios reach nearly 25:1. Pyrite abundance greatly exceeds that of marcasite in the composite crystals.

A tiny grain of electrum was observed in one of the smaller veinlets. The electrum is irregularly-shaped and approximately 0.2mm in length.

Representative photomicrographs from sample RB-41 are given in Figures 56, 57, and 58.

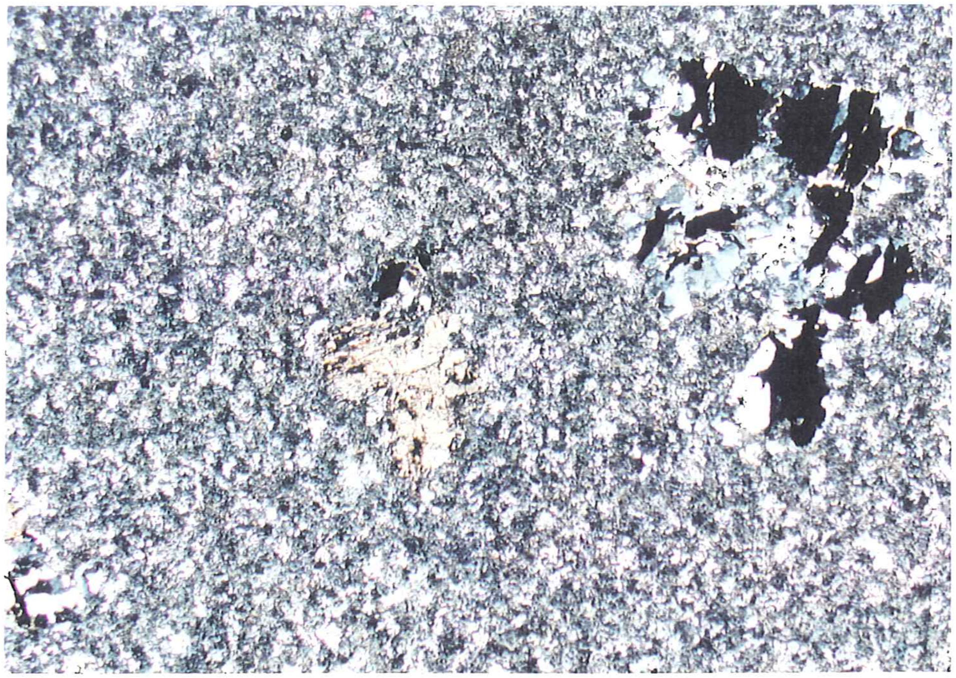

Figure 56a. RB-41/porphyry. Glomerocrystic aggregate of former feldspar phenocrysts pseudomorphed by quartz-pyrite-marcasite in a fine-grained, granular groundmass of quartz and clay-altered feldspar. Former mafic phenocrysts are pseudomorphed by carbonate and clay (photo center). TLX; 1cm on the photo= 0.532mm.

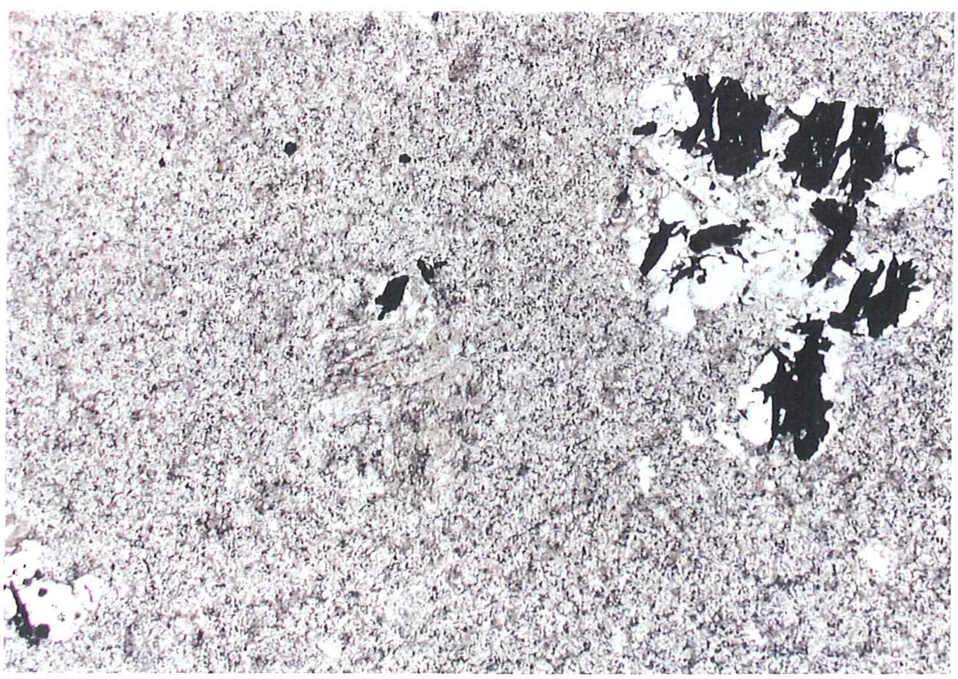

Figure 56b. RB-41/porphyry. Same view and scale as Figure 56a. TLP; 1cm on the photo= 0.532mm.

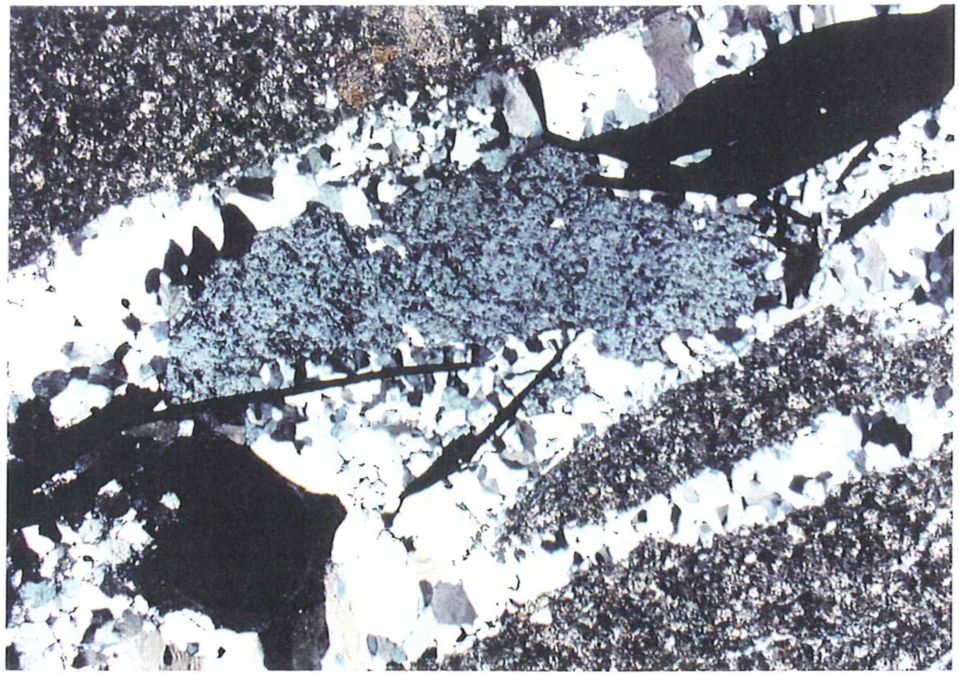

Figure 57a. RB-41/porphyry. The porphyry is cut by a quartz-barite(?)-composite pyrite-marcasite vein. TLX; 1cm on the photo= 0.532mm.

Figure 57b. RB-41/porphyry. Same view and scale as Figure 57a. TLP; 1cm on the photo= 0.532mm.

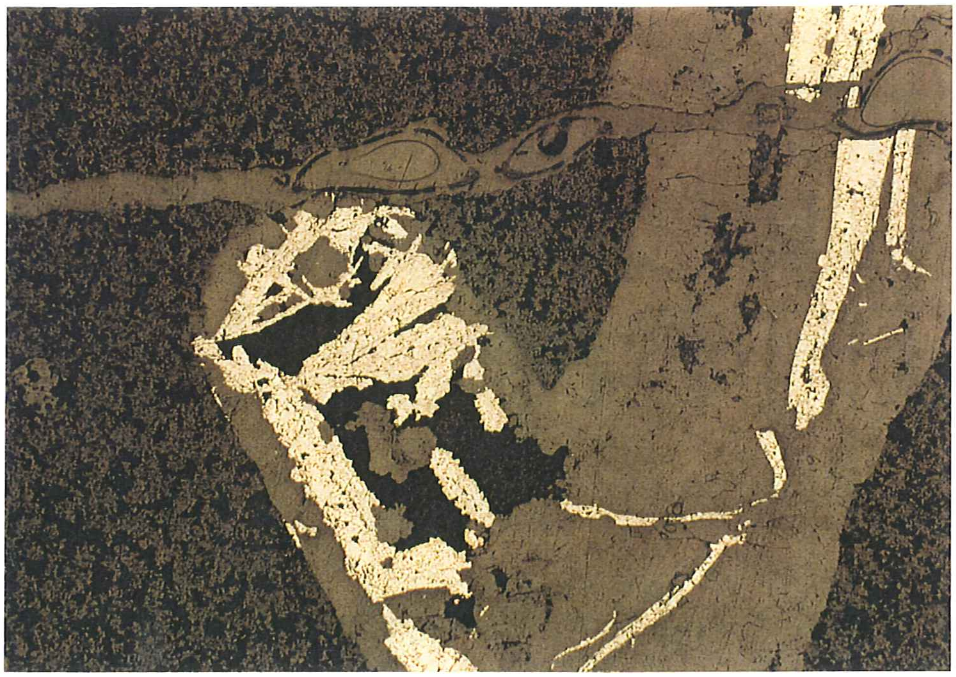

Figure 58. RB-41/porphyry. Quartz vein with skeletal py-mc truncates feldspar phenocryst pseudomorphed by polycrystalline quartz and skeletal py-mc. RL; 1cm on the photo- 0.532mm.

Sample RB-42 (porphyry on FW side of FW SRF; 0.042 opt Au, <0.05 opt Ag)

Sample RB-42 is a very fine-grained, porphyritic, dacitic intrusive rock. The groundmass consists of quartz and feldspar partly to completely altered to a clay-sericite assemblage. Plagioclase phenocrysts are partly to completely altered to sericite-clay. Kspar (orthoclase) phenocrysts serve locally as nucleation sites for skeletal marcasite and polycrystalline hydrothermal quartz (plus relict Kspar). Primary plagioclase phenocrysts were euhedral prisms to 9mm in length. Composition is in the sodic andesine range (Michel-Levy extinction angle is appx. 18°). The phenocrysts occur as isolated crystals and in glomerocrystic aggregates. Total phenocryst abundance is less than two percent. Evenly disseminated, fine-grained anhedral quartz to 0.3mm diameter may be related to initiation of silicification and quartz veining. The porphyritic dacite is cut by quartz veinlets ± sulfides (py, mc). The quartz veinlets are up to 2.5mm in width and are characterized by cockscomb texture at the margins. The cockscomb quartz has maximum length perpendicular to the vein margin of about 0.8mm. The interior of the vein is filled by fine-grained, xenomorphic-granular quartz, clay, and sulfide. The larger vein cuts several smaller veinlets. Pyrite is sparsely disseminated through most of the slide, but is very abundant in one small area. The pyrite is generally eu- to subhedral, cubic, and up to 0.5mm in diameter.

CL: Vein quartz and quartz replacing plagioclase phenocrysts is non-luminescent. The groundmass has dull reddish CL with scattered fine-grained areas that exhibit a weak decaying yellow CL. There is minor disseminated apatite with orange yellow CL. Scattered clusters of apatite with similar CL are interpreted to be former mafic phenocryst sites. A few pockets of kaolin (?) with dull royal blue CL are observed within the replaced plagioclase phenocrysts (Q-mc). Relict K feldspar in phenocrysts has a weak blue CL (Ti^{4+} activation; alteration degradation).

RL: Sample RB-42 contains 3-5% total opaque minerals. The dominant opaque minerals are skeletal composite pyrite-marcasite crystals. They occur as components of the quartz veins, and in conjunction with polycrystalline quartz as apparent pseudomorphs after Kspar phenocrysts. The skeletal py-mc crystals are euhedral to subhedral and range up to 7mm in length. Traces of very fine-grained, anhedral chalcopyrite and sphalerite were observed locally in intercrystalline voids in the skeletal py/mc. Minor very fine-grained chalcopyrite and sphalerite were noted also accompanying the Q-py/mc assemblage pseudomorphing former Kspar phenocrysts. Former sites for primary ilmenite are altered to leucoxene (gray, low reflectance, white internal reflections). Pyrite is disseminated throughout, very sparsely in some areas of the slide and very concentrated in one area of the slide. The pyrites occur as euhedral to anhedral, somewhat porous crystals to 0.6mm in length/diameter, and with generally cubic to rectangular morphology.

Representative photomicrographs are shown in Figures 23, 59, and 60.

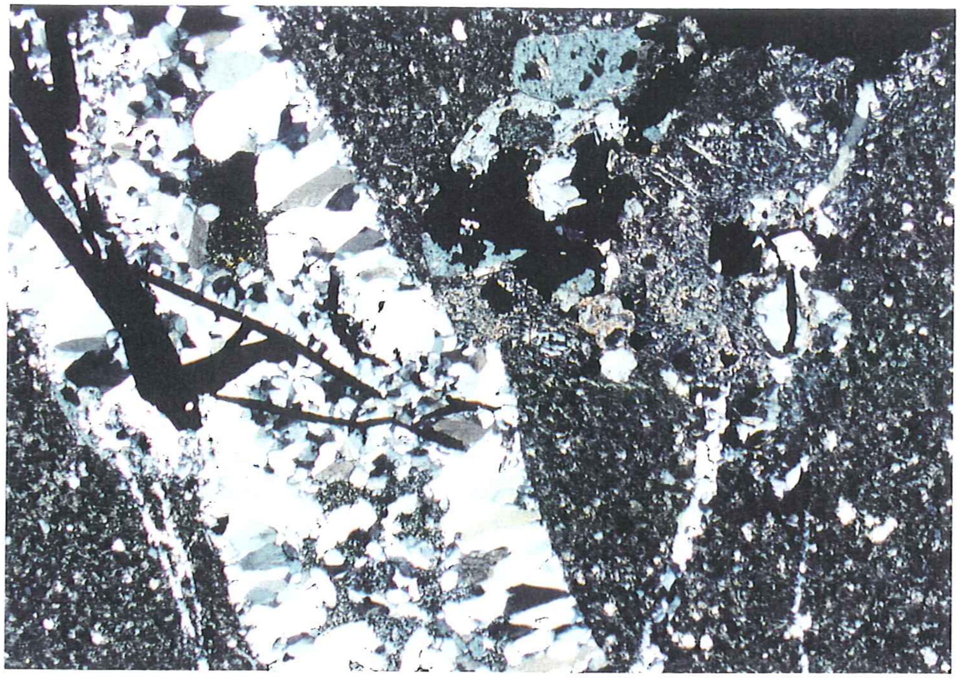

Figure 59a. RB-42/dacite porphyry. Kspar phenocryst adjacent to quartz-pyrite-marcasite vein is partly pseudomorphed by quartz and pyrite. TLX; 1cm on the photo= 0.532mm.

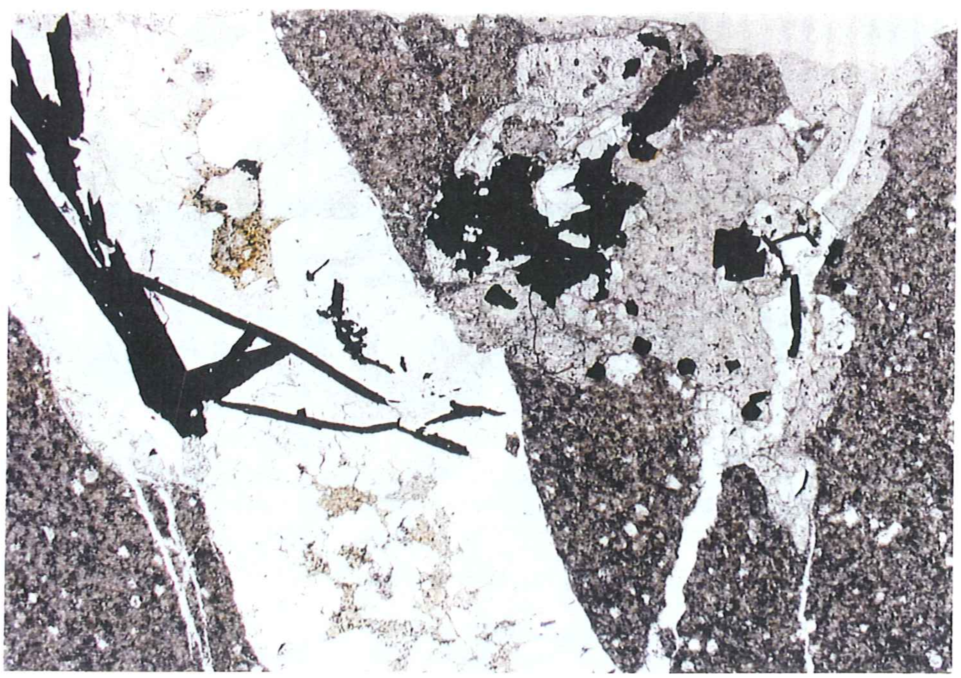

Figure 59b. RB-42/dacite porphyry. Same view and scale as Figure 59a. TLP; 1cm on the photo= 0.532mm.

Figure 60. RB-42/dacite porphyry. Quartz vein in dacite porphyry contains composite py-mc, and traces of sphalerite (gray; low R; upper right quadrant) and chalcopyrite (mustard yellow; R < py-mc; lower edge center of photo. RL; 1cm on the photo= 0.106mm.

Sample RB-43 (Porphyry on HW side of FW SRF; 0.026 opt Au, 0.06 opt Ag)

Sample RB-43 is a porphyritic quartz latitic to dacitic intrusive rock that contains 2-3% total phenocrysts. The primary phenocryst assemblage includes plagioclase, K feldspar, a mafic phase (biotite and/or hornblende?), and sparse quartz. The phenocrysts are dispersed in a very fine-grained granular groundmass of quartz, plagioclase, and K feldspar in which the feldspars are partly altered to clay and sericite. Plagioclase phenocrysts are euhedral to subhedral and up to 3mm in length. Most show nearly complete alteration to microcrystalline quartz and patchy to crudely net-veined fine clay and minor coarser sericite. Primary K feldspar phenocrysts are partly pseudomorphed by coarser xenomorphic-granular quartz with an average crystal size <0.3mm diameter. Former mafic phenocrysts are pseudomorphed by very fine-grained polycrystalline chlorite and are found commonly in association with apatite and, less commonly, zircon and opaque phases. The former mafic phenocrysts are subhedral to anhedral and less than 2mm in length/diameter. Plagioclase and mafic pseudomorphs are found locally in glomerophyric clusters. Sparse quartz phenocrysts are anhedral and less than 0.7mm in diameter. The rock is cut by an irregular quartz-sericite-chlorite-sulfide vein that bifurcates several times at one end of the slide The vein has a maximum width of about 5mm. The vein quartz has a xenomorphic-granular texture with a maximum quartz crystal size of 0.7mm length. Associated sulfides are euhedral to subhedral and reach 1.2mm in length. The vein has a narrow, discontinuous, fine-grained chloritic selvage that migrates interior to the vein at one edge of the slide. Patches of sericite and chlorite occur locally in the vein interior.The major quartz vein transects several very thin (<0.6mm) sericite-quartz veinlets. The quartz veins contain coarse pyrite as cubic, pyritohedron, or rectangular crystals. Minor disseminated pyrite occurs also outside the veins.

CL: Vein quartz is non-luminescent. The porphyry groundmass has dull red CL. Disseminated primary apatite has strong orange yellow CL. Clusters of apatite mark sites of former mafic phenocrysts. Clay alteration in former feldspar phenocrysts has weak royal blue CL (kaolinite?).

RL: The slide contains 2-3% total sulfides/opaque phases, more than half of which are contained within the quartz veins. Fine-grained pyrite is disseminated throughout, but appears to be more abundant proximal to the main quartz-sulfide vein. The disseminated pyrite occurs generally as euhedral cubic crystals up to 0.16mm diameter. Some of the disseminated pyrites appear to have nucleated adjacent to former primary ilmenite sites. The former ilmenites are altered to leucoxene. The dominant opaque mineral in the vein is pyrite with very minor marcasite patches. The pyrites occur as individual crystals or aggregates. They are euhedral to subhedral with cubic to rectangular morphology and reach 1.2mm in length. A trace of sphalerite was observed also in the vein.

Representative photomicrographs from sample RB-43 appear in Figures 33, 61, and 62.

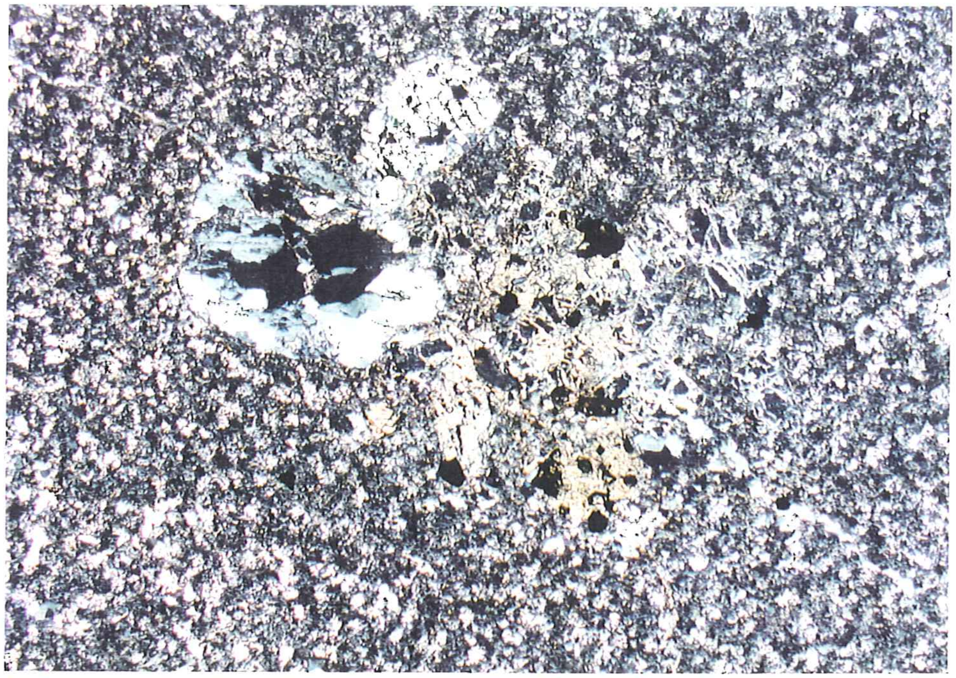

Figure 61a. RB-43/porphyry. Glomerocrystic aggregate of Kspar and biotite pseudomorphs in a fine, granular groundmass of altered feldspar and quartz. The Kspar is partly pseudomorphed by polycrystalline quartz, while biotite is pseudomorphed by chlorite and pyrite. TLX; 1cm on the photo= 0.532mm.

Figure 61b. RB-43/porphyry. Same view and scale as Figure 61a. Note the quartz microveinlet passing through the pseudomorphed phenocrysts. This veinlet may have been the passageway for the fluids that altered the phenocrysts. TLP; 1cm on the photo= 0.532mm.

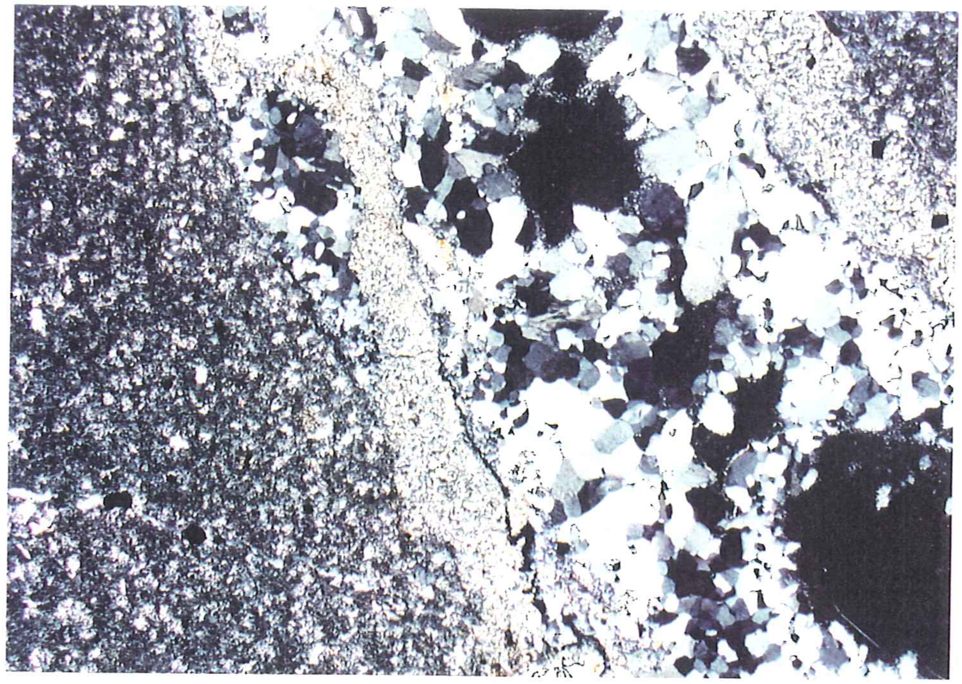

Figure 62a. RB-43/porphyry. Quartz vein with irregular chlorite selvage cuts the porphyry. TLX; 1cm on the photo= 0.532mm.

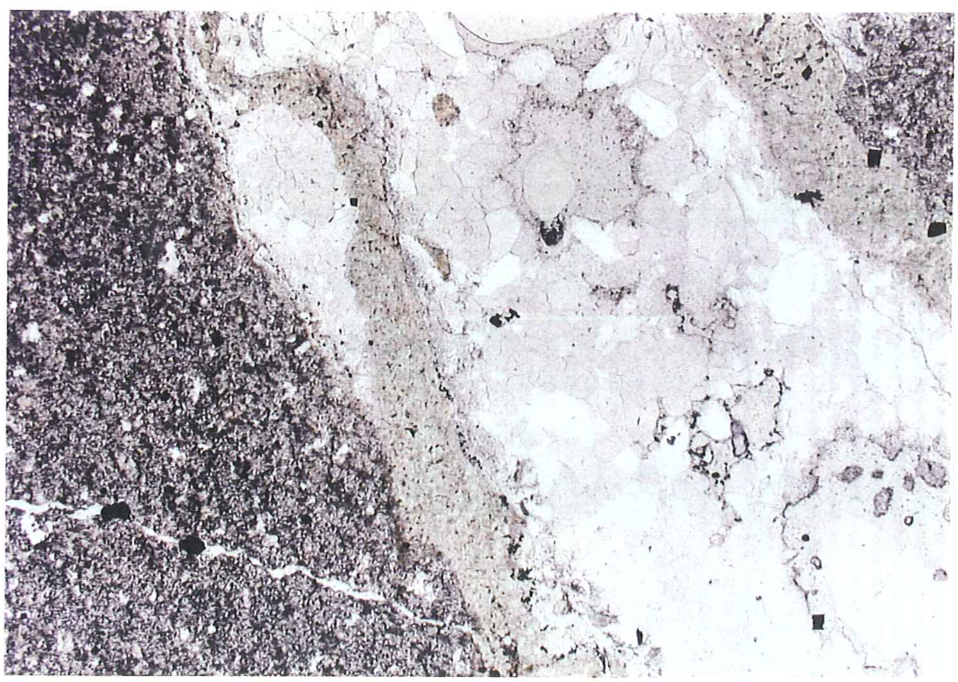

Figure 62b. RB-43/porphyry. Same view and scale as Figure 62a. TLP; 1cm on the photo= 0.532mm.

Sample RB-44a (White Alps porphyry)

Sample RB-44a is a quartz latite porphyry. The porphyry contains approximately 5-7% plagioclase phenocrysts partly to completely altered to very fine-grained cryptocrystalline quartz, 1-3% microphenocrysts of Kspar (sanidine), 1-2% corroded quartz microphenocrysts, and 2-3% mafic phenocrysts (probably biotite) mostly altered to hematite (?) dispersed in a cloudy, very fine-grained granular groundmass of quartz, K feldspar, plagioclase, and cloudy brown, partly devitrified glass(?).

Plagioclase phenocrysts are euhedral to subhedral prismatic crystals that reach 2.4mm in length. Most are completely altered to cryptocrystalline quartz, although relict plagioclase remains in a few phenocrysts. Albite twinning is indistinct in the relict plagioclase, and the plagioclase composition was not obtainable via optical methods.

Sanidine forms small (<1mm) euhedral to subhedral crystals that tend to be more equant than the plagioclase. Twinning on the Carlsbad law is visible occasionally and extinction under crossed polars is nearly parallel. The sanidines occur locally in glomerocrystic aggregates with quartz.

Quartz forms anhedral crystals to <1mm in diameter and exhibits considerable edge corrosion. Quartz occurs also as polycrystalline aggregates with a peculiar growth zoning. The polycrystalline quartz aggregates may be miarolytic cavity fill or, alternatively, xenolithic inclusions.

Mafic phenocrysts are completely altered to an assemblage of goethite, hematite, and quartz. Rare partly hexagonal crystal outlines and the goethite replacement texture suggest that the mafic phases were biotite. The mafic pseudomorphs are subhedral to anhedral and up to 1.5mm in length. Fine-grained disseminated opaques, probably primary ilmenite or titanomagnetite, are also altered to goethite (<0.3%; <0.3mm diameter).

The groundmass is a fine-grained, granular aggregate of K feldspar, quartz, plagioclase, and cloudy brown, partly devitrified glass. Average groundmass grain size is about 0.07mm diameter. CL observations suggest that Kspar is present in excess of plagioclase and that there is partial replacement of the groundmass by calcite.

CL: The groundmass has dull bluish gray CL with patchy replacement by reddish orange luminescent calcite. No apatite was noted. Altered feldspar phenocrysts have a very dull brown CL.

RL: Goethite and lesser hematite replace biotite. Disseminated goethite not related to biotite alteration is derived from alteration of primary disseminated Fe-Ti oxide minerals.

Representative photomicrographs from Sample RB-44a appear in Figures 32, 63, and 64.

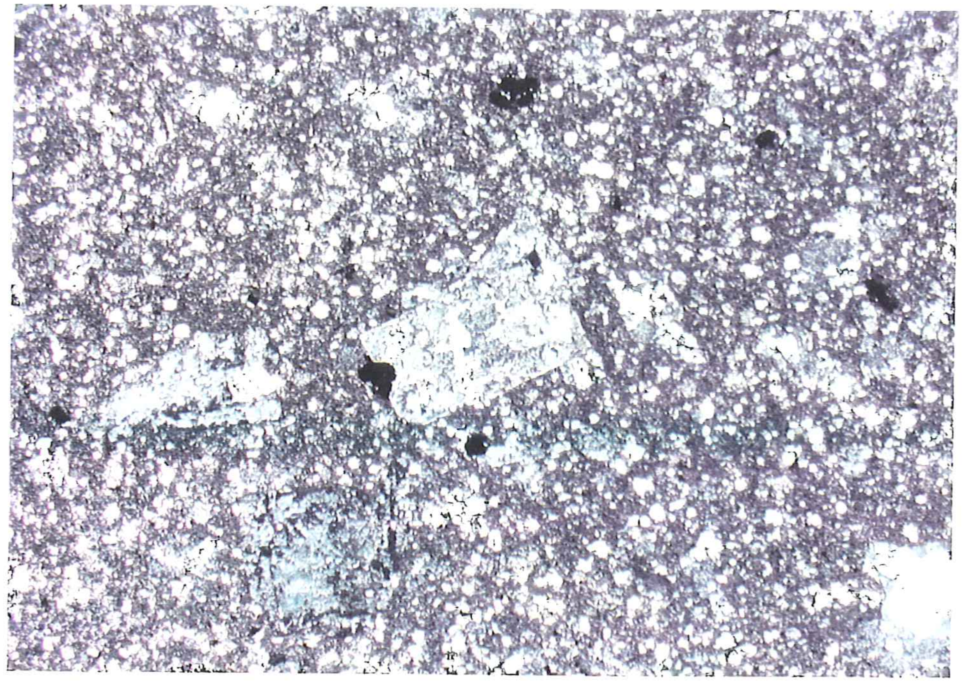

Figure 63a. RB-44a/quartz latite porphyry. Phenocrysts of plagioclase, sanidine, biotite, and quartz are dispersed in a fine, granular groundmass of Kspar, plagioclase, and quartz. TLX; 1cm on the photo= 0.532mm.

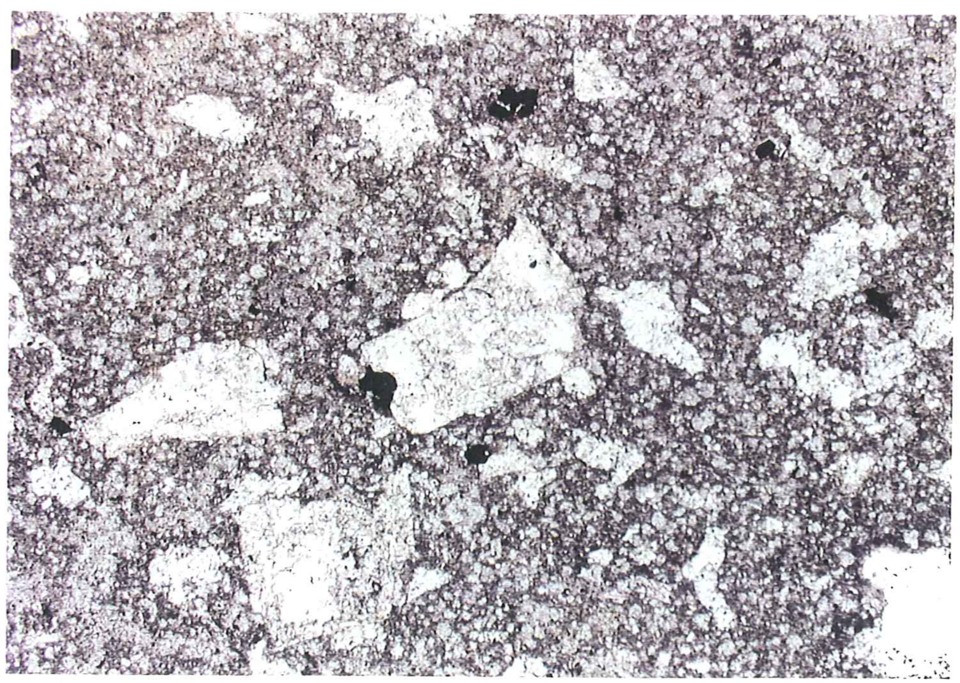

Figure 63b. RB-44a/quartz latite porphyry. Same view and scale as Figure 63a. TLP; 1cm on the photo= 0.532mm.

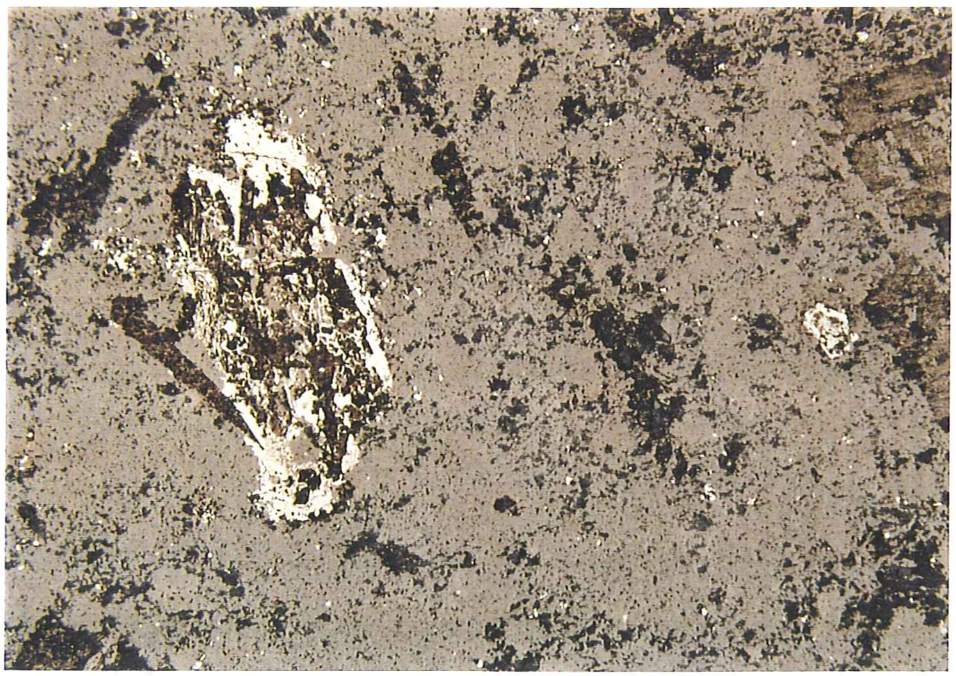

Figure 64. RB-44a/quartz latite porphyry. Goethite (bright gray; low R) partly replaces biotite. RL; 1cm on the photo= 0.106mm.

Sample RB-44b (White Alps porphyhry/choc bxa-or autobreccia?)

Sample RB-44b is also a quartz latite porphyry of probable intrusive origin. Phenocrysts of plagioclase, sanidine, quartz, and minor biotite are dispersed in a very fine-grained, granular, crudely flow-banded groundmass of sanidine, quartz, plagioclase, cloudy, partly devitrified glass, and sparsely disseminated opaque minerals. Scattered rounded clots (to 0.7mm diameter) of multiple quartz crystals with visible growth zoning and minor FeOx probably fill miarolytic cavities. No evidence of breccia texture was observed. Also present are minor disseminated opaque phases.

Plagioclase phenocrysts ($\pm$ 2%) occur as euhedral to subhedral prismatic crystals to 4.2mm in length. The plagioclase is partly to completely altered to cryptocrystalline quartz, especially in the core. Less altered plagioclase is usually present along the crystal rim. Less-altered and finer-grained plagioclase (to 0.25mm) is present in crystalline aggregates. It is possible that these aggregates are late albite and may also represent miarolytic cavity fill (as do the polycrystalline quartz aggregates).

Sanidine phenocrysts (actually microphenocrysts) form small euhedral to subhedral crystals to 0.4mm in length. Carlsbad twinning is common. The sanidines are characterized by near parallel extinction and small $2V\alpha$. Abundance is $\pm$ one percent.

Quartz ($\pm$ 0.5%) forms euhedral to subhedral microphenocrysts to 0.35mm. Some quartz phenocrysts have corroded edges, but others show euhedral hexagonal outline. Most of the quartz observed in the sample occurs as polycrystalline aggregates in which many individual crystals show growth zonation toward the center of the aggregate. The aggregates reach 0.7mm in diameter and are interpreted to be miarolytic cavity fill.

"Biotite" occurs also as a microphenocryst phase. All of the biotites are pseudomorphed by goethite and hematite (goethite >> hematite). The pseudomorphs are subhedral to anhedral and up to 0.5mm in length. Abundance is <0.5%.

The groundmass is a very fine-grained granular mosaic of sanidine, quartz, plagioclase, and cloudy, grayish brown, partly devitrified glass, and it shows crude flow-banding and has a cloudy appearance. CL observations suggest that sanidine abundance exceeds that of plagioclase and that the groundmass is partly replaced by carbonate. The groundmass contains <0.2% disseminated opaques as goethite and hematite after primary Fe-Ti oxide minerals.

CL: The groundmass has bluish gray CL with patchy calcite alteration (reddish orange CL). There is no evidence of breccia texture. No apatite was noted.

RL: Fine-grained disseminated opaques are goethite and hematite (goethite >> hematite). Goethite locally forms spherical to hemispherical botryoidal crystals and aggregates to 0.1mm diameter. In most cases the goethite and hematite are probably replacing primary Fe-Ti oxide phases in the porphyry.

Representative photomicrographs appear in Figures 24 and 65.

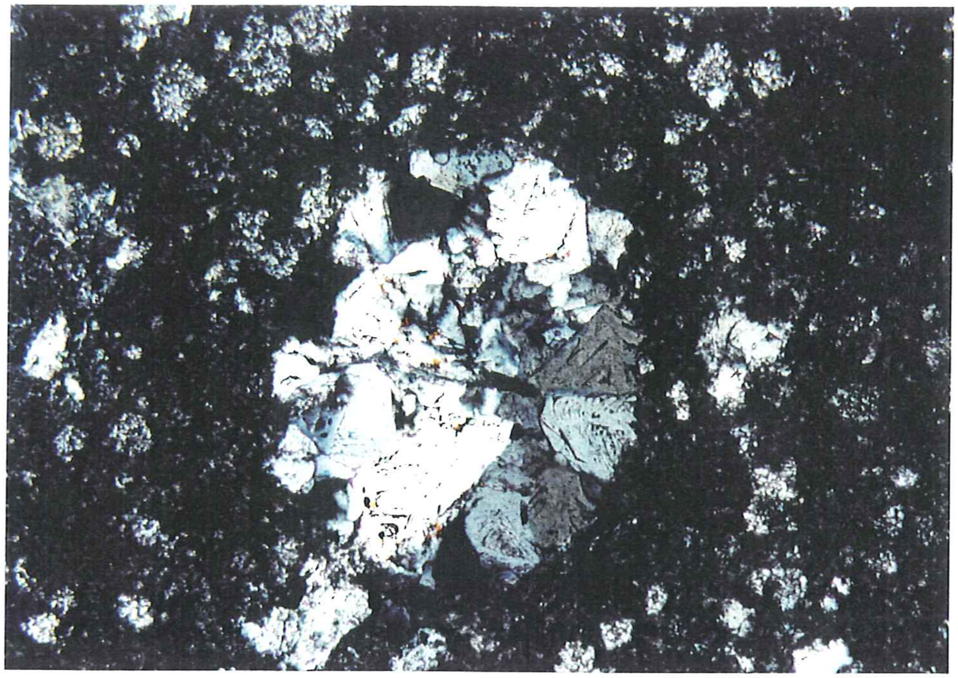

Figure 65a. RB44b/quartz latite porphyry. Quartz with growth zonation fills a miarolytic cavity in the porphyry. TLX; 1cm on the photo= 0.106mm.

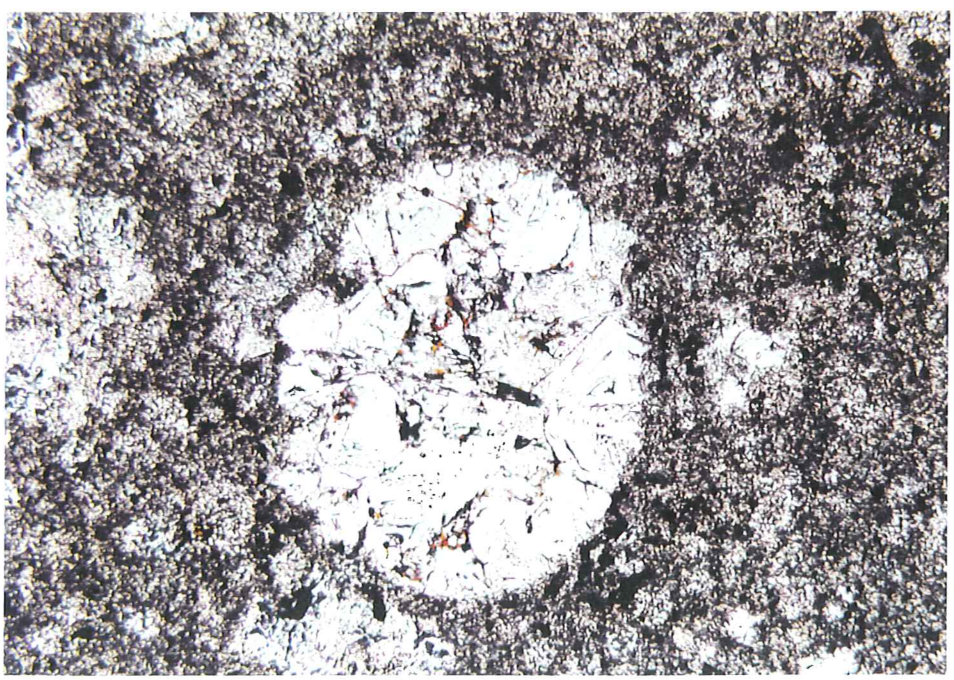

Figure 65b. RB44b/quartz latite porphyry. Same view and scale as Figure 65a. TLP; 1cm on the photo= 0.106mm.

Sample RB-44c (Brecciated and silicified White Alps porphyry)

Sample RB-44c depicts the contact between an altered porphyry and a breccia lithology that may be either an intrusion breccia or perhaps an altered lapilli tuff. The thin section was prepared overly thick, and most of the phenocrysts have been plucked in the porphyry. The porphyry contains < 2% phenocrysts, most of which appear from their tabular, prismatic morphology to have been plagioclase. The plagioclase formed euhedral crystals to 1.5mm in length. Minor biotite microphenocrysts are pseudomorphed by goethite, hematite (goethite >> hematite), calcite, and minor quartz. They tend to be euhedral to subhedral and up to 0.7mm in length. The groundmass has an aplitic texture and is a mosaic of sanidine, quartz, and plagioclase, with abundant fine-grained late calcite. The porphyry is in sharp contact with a fragmental rock that may be either an intrusion breccia or a devitrified lapilli tuff. Lapilli-sized fragments of the same altered porphyry are noted, as well as fragments of finer-grained lithologies (altered tuffs?). The fragments are subangular to subround, and the maximum fragment size exceeds 1cm in diameter. The breccia is matrix-supported, although the fragments constitute more than 50% of the lithology. The groundmass is finer grained than that of the porphyry; average groundmass crystal size is about 0.02mm diameter. The groundmass appears to be a very fine-grained, xenomorphic-granular mosaic of quartz, alkali feldspar, and calcite. It may be fine aplite or devitrified tuffaceous material with later calcite replacement of the feldspar. Field relationships might help resolve alternative petrographic interpretations. An irregular, narrow zone with abundant opaques (goethite) is present along part of the contact between the two lithologies. In this zone opaques have cubic to pyritohedron morphology, and are probably hematite after pyrite. Disseminated opaques in both lithologies away from the contact zone appear to be goethite and lesser hematite after primary Fe-Ti oxide minerals.

CL: There is strong replacement of of both porphyry and breccia by carbonate. Orange red CL of moderate intensity suggests substitional Fe in the calcite lattice. Also present is minor late bright orange CL calcite.

RL: Extremely fine-grained (<0.005mm diameter) hematite dusts some plagioclase phenocrysts. Hematite pseudomorphs fine-grained pyrite with cubic to pyritohedron morphology along the contact zone between the porphyry and the lapilli tuff. Some biotite phenocrysts are partially to completely replaced by goethite and lesser hematite. Disseminated fine-grained hematite and goethite mixtures away from the contact zone are probably replacing primary Fe-Ti oxide phases (magnetite and/or ilmenite?).

Representative photomicrographs from sample RB-44c are given in Figures 25 and 66.

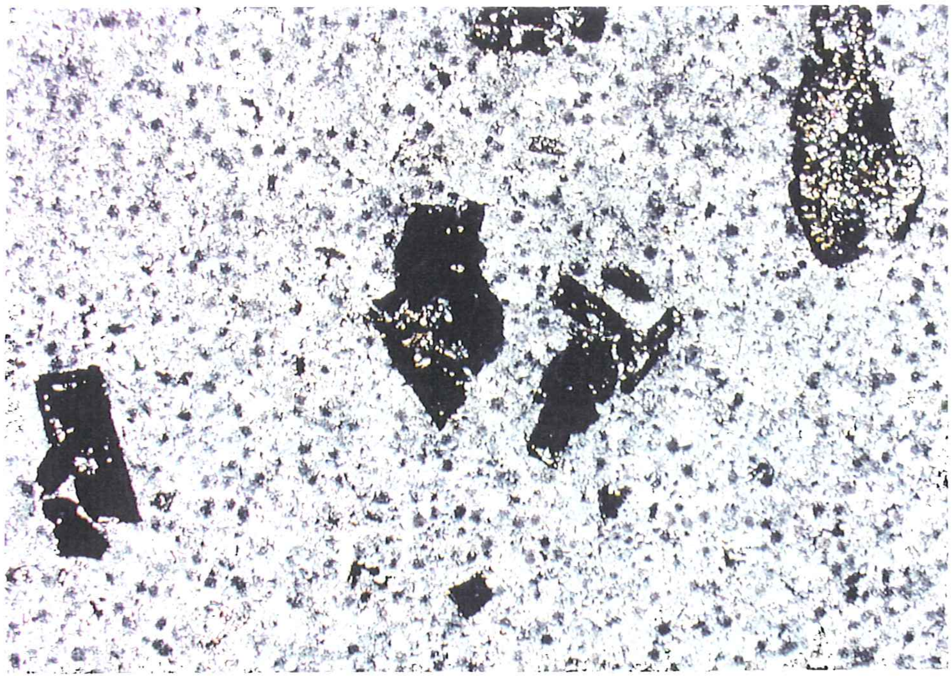

Figure 66a. RB-44c/porphyry. Partly plucked phenocrysts of plagioclase and biotite set in a fine, aplitic groundmass of sanidine, plagioclase, and quartz. TLX; 1cm on the photo= 0.532mm.

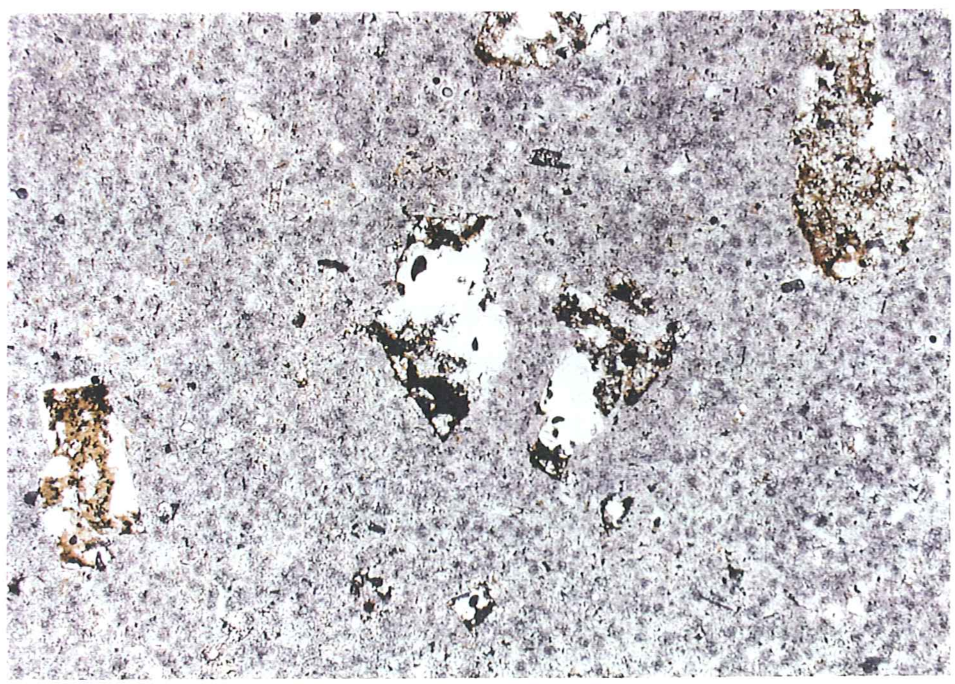

Figure 66b. RB-44c/porphyry. Same view and scale as Figure 66a. TLP; 1cm on the photo= 0.532mm.

Sample RB-45 (Rosebud Qlatite/Bud Marker Porphyry)

Sample RB-45 is a glassy, flow-banded dacite or latite porphyry. It is interpreted to be an extrusive rock. The glassy groundmass is dark to medium brown and weakly devitrified to patchy, microcrystalline quartz and alkali feldspar. The groundmass has irregular, but fine-scale, flow-banding with discontinuous, wispy fine-grained vapor phase (?) quartz. Scattered phenocrysts of feldspar (3-5%) are completely replaced by very fine-grained, nearly cryptocrystalline quartz. The feldspar pseudomorphs are euhedral to subhedral and up to 2.5mm in length. They are mostly dispersed as isolated crystals, but occur also in glomerocrystic aggregates. Locally there is minor replacement by coarser (<0.1mm diameter) polycrystalline vapor phase quartz. Mafic phases constitute less than one percent of the sample. They occur as euhedral to subhedral prismatic crystals to 1.2mm in length. The mafic phenocrysts are pseudomorphed by an assemblage of epidote, carbonate, chlorite, and cryptocrystalline quartz. Chlorite, when present, tends to occur around the margins of the crystals. The primary mafic phase may have been either biotite or hornblende. Patchy zones and discontinuous stringers of very fine-grained, polycrystalline, xenomorphic-granular quartz are probably related to vapor phase deposition during cooling.

CL: Faint indications of carbonate occur throughout the sample. The carbonate appears to b very fine-grained dolomite or high-iron calcite (reddish orange CL). Locally, where the carbonate occurs in tiny, spherical concentrations, it is accompanied by apatite with strong grayish-yellow CL.

RL: Opaque minerals occur as sparsely disseminated, very fine-grained magnetite. The magnetite occurs also within mafic phenocryst pseudomorphs. Some of the magnetite is oxidized to goethite. A trace of very fine-grained pyrite (<0.023mm length/diameter) was noted as well.

Representative photomicrographs from sample RB-45 are given in Figures 26 and 67.

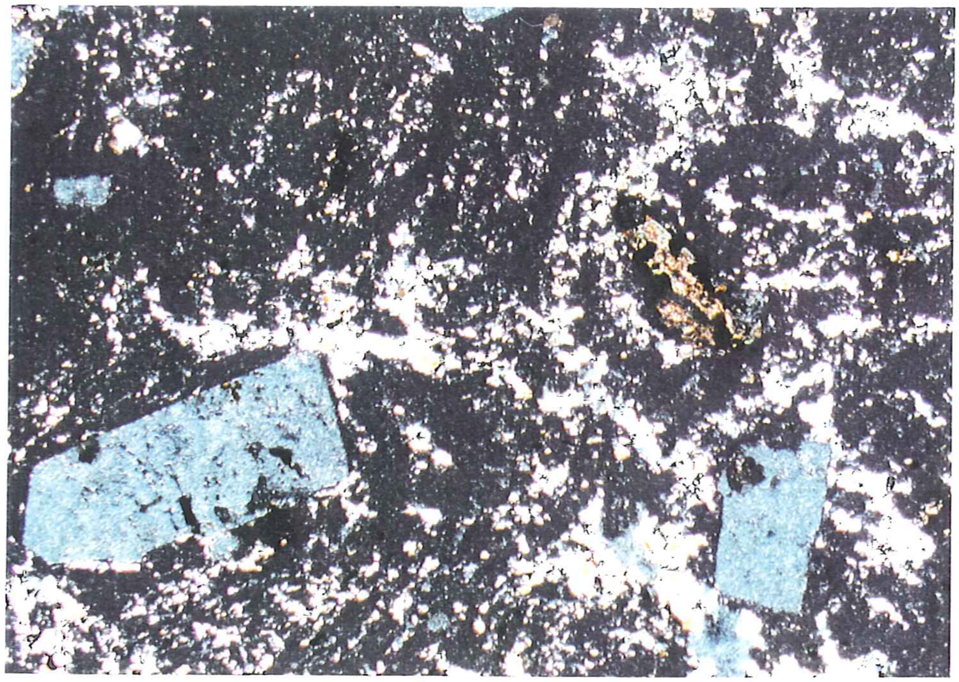

Figure 67a. RB-45/flow-banded porphyry. Feldspar phenocrysts pseudomorphed by microcrystalline quartz set in a partly devitrified, glassy, flow-banded groundmass. TLX; 1cm on the photo= 0.532mm.

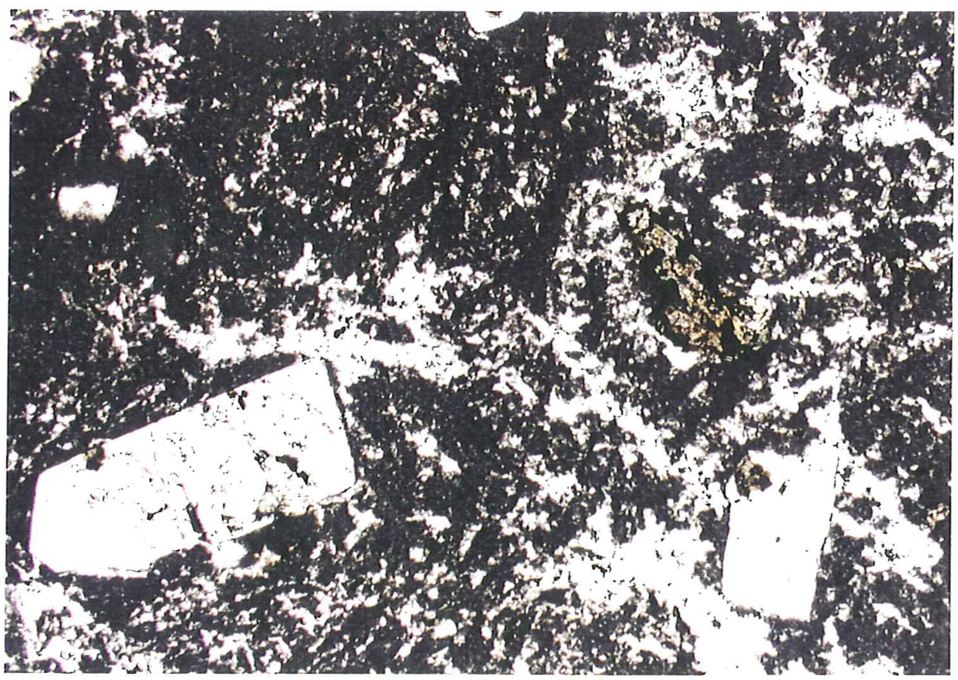

Figure 67b. RB-45/flow-banded porphyry. Same view and scale as Figure 67a. TLP; 1cm on the photo= 0.532mm.

Sample RB-55 (Upper Bud)

Sample RB-55 is a lapilli tuff. It contains abundant sub-round to subangular, green to white felsitic and locally porphyritic lithic fragments to appx 1.3cm diameter, and scattered broken feldspar, biotite, and quartz pyrogenic crystal fragments, dispersed in a green, very fine-grained devitrified groundmass of quartz, alkali feldspar, clay, and calcite. Plagioclase, both as phenocryst or pyrogenic components in the lithic fragments and as pyrogenic fragments in the matrix, is partly to completely replaced by calcite. The original composition appears to be sodic andesine. Maximum plagioclase crystal size is about 1.8mm. Most of the lithic fragments are very fine-grained and sparsely porphyritic with microphenocrysts of plagioclase and sparse biotite. The plagioclase microphenocrysts are commonly dispersed in a fine feldspathic groundmass with crude pilotaxitic texture. Most biotite shows at least partial alteration to chlorite and calcite. One fragment has aplitic texture and phenocrysts of plagioclase and minor hornblende, both partially replaced by calcite. One fragment contains a quartz-sulfide vein. Sulfide forms the margin of the vein and quartz the interior. Calcite forms narrow discontinuous veinlets locally, as well as patchy replacement of groundmass in both fragments and the host tuff. Some fragments contain narrow quartz-clay±sericite veinlets that do not continue into the host tuff groundmass. Some fragments have traces of a bright emerald green phase that may be a high iron leptochlorite (?). The sample contains sparsely disseminated opaques, dominantly pyrite.

CL: Many fragments have a dull blue-gray CL, owing to the presence of quartz and Kspar. Some fragments show partial to complete replacement by calcite (bright orange CL; Mn2+ activation). Calcite also forms narrow, discontinuous stringers

Apatite is present as sparse, fine-grained disseminations. It has strong grayish yellow CL. Apatite is present also associated with sparsely disseminated sulfides.

RL: The sample contains less than 0.5% disseminated sulfides as pyrite and pyrrhotite. The disseminated pyrite occurs as euhedral to subhedral, cubic to rectangular crystals to 0.11mm diameter. A few subhedral marcasite crystals to 0.22mm diameter were noted also as disseminations. The pyrrhotite occurs as a few scattered, elongate bundles of prismatic crystals to 1.6mm in length. It is characterized by a pinkish-tinted yellow-brown color and strong anisotropism. Also observed was a trace of disseminated subhedral sphalerite to 0.1mm diameter.

Representative photomicrographs from sample RB-55 are illustrated in Figures 16, 31, 68, and 69.

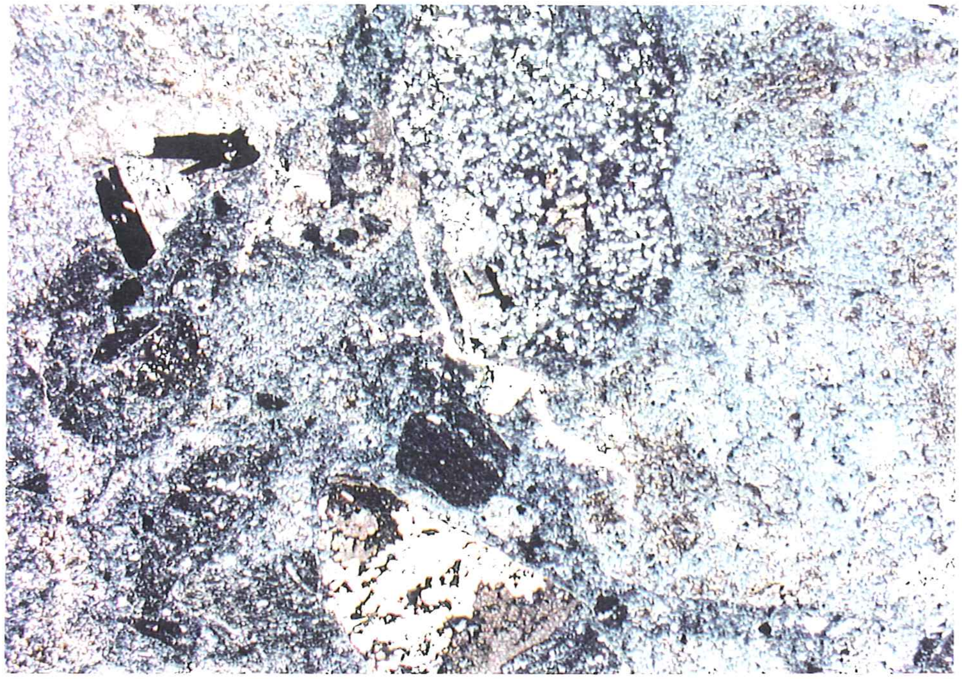

Figure 68a. RB-55/lapilli tuff. Volcanic lapilli are partly replaced by calcite and dispersed in fine devitrified tuffaceous matrix. TLX; 1cm on the photo= 0.532mm.

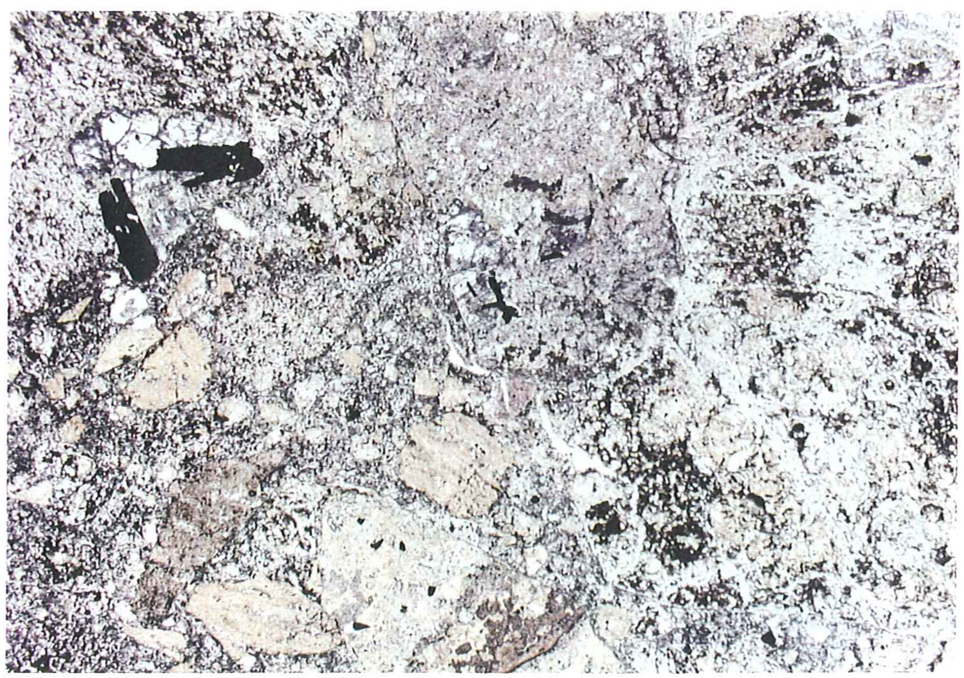

Figure 68b. RB-55/lapilli tuff. Same view and scale as Figure 68a. TLP; 1cm on the photo= 0.532mm.

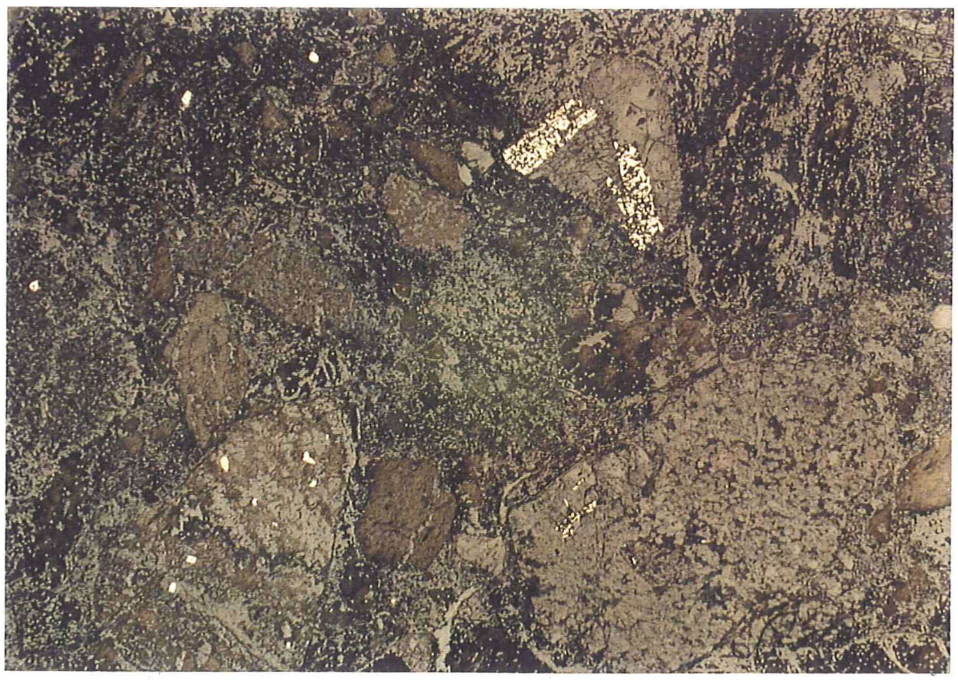

Figure 69. RB-55/lapilli tuff. Disseminated pyrrhotite (larger crystals) and pyrite in lapilli tuff. RL; 1cm on the photo= 0.532mm.

Sample RB-56B (autobx?)

Sample RB-56b is a porphyritic quartz latite in contact with a breccia lithology that may be either a very fine-grained intrusion breccia or, alternatively, a devitrified lithic lapilli tuff. The quartz latite has about 5% euhedral to subhedral feldspar phenocrysts to 3mm in length pseudomorphed by cryptocrystalline quartz and clay. Also present are scattered quartz microphenocrysts (?) that occur generally as aggregates of anhedral crystals to 0.15mm in diameter. The groundmass is a very fine-grained, aplitic or xenomorphic-granular mosaic of quartz and alkali feldspar, with relatively abundant disseminated very fine-grained hematite. Average quartz-feldspar crystal size in the groundmass is approximately 0.05mm diameter. The very fine-grained hematite insinuates itself in a crude network along quartz-feldspar crystal boundaries. Hematite also appears to replace what few mafic phenocrysts there might have been. One hematitic pseudomorph of a former mafic phenocryst appears to have a partial amphibole cross-sectional morphology. A tiny veinlet (± 0.1mm thickness) contains cryptocrystalline quartz and is truncated in a pseudomorphed feldspar phenocryst, composed also of cryptocrystalline quartz.

The breccia lithology has abundant angular to subround lithic fragments to 1cm diameter plus crystals or crystal fragments of feldspar, quartz, and hematized biotite. The groundmass consists of a very fine-grained granular to nearly cryptocrystalline mass of quartz, alkali feldspar, and iron oxide. It is finer-grained than that of the porphyry (average grain size <0.02mm diameter), but is otherwise texturally similar. This matrix may be related to the porphyry, or, alternatively, it could be derived from devitrification of tuffaceous material. Without knowing the field relationships, the former interpretation is preferred. The fragments are similar to the porphyry, although there is some variation in groundmass grain size. The lithic fragments do not have the pervasive iron oxide invasion common to the groundmass. The contact zone is marked by a narrow, irregular zone of FeOx insinuating along quartz-feldspar crystal boundaries in crude network fashion.

Sample RB-56b bears strong similarity to sample RB-44b.

CL: There is weak, but relatively pervasive, replacement by fine-grained calcite with red-orange CL. Several lithic fragments have some relict dull gray CL, possibly a K feldspar CL response.

RL: The sample contains relatively abundant fine disseminated hematite and subordinate goethite. There is a trace of disseminated pyrite, which occurs as subhedral to anhedral crystals to 0.02mm diameter.

Representative photomicrographs from sample RB-56b appear in Figures 70, 71, and 72.

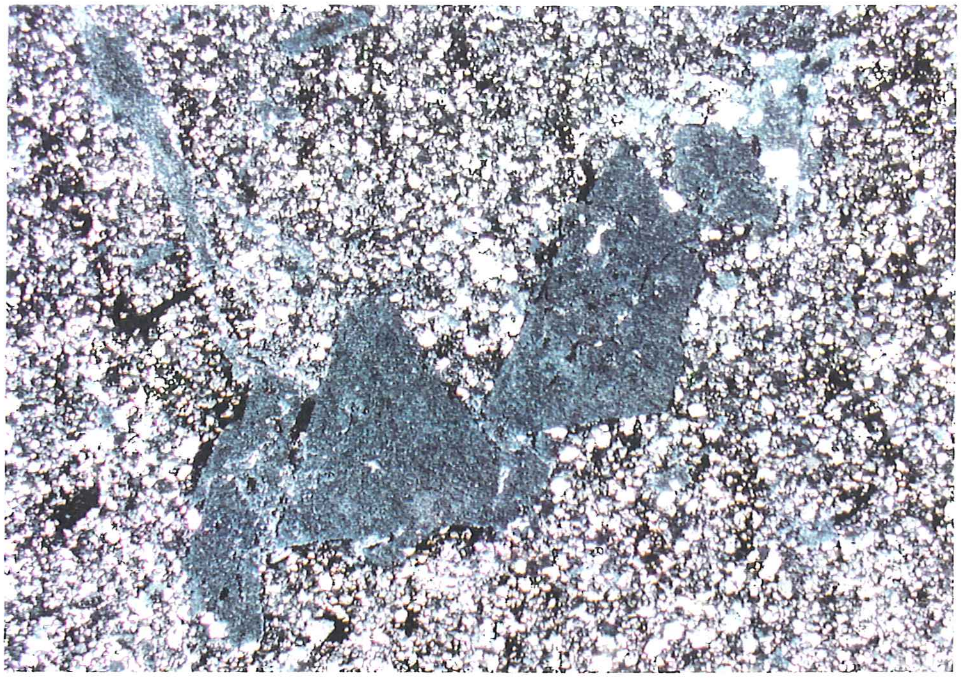

Figure 70a. RB-56b/quartz latite porphyry. Microcrystalline quartz veinlet and feldspar phenocrysts pseudomorphed by similar microcrystalline quartz. The groundmass is a fine, granular mosaic of quartz and alkali feldspar. TLX; 1cm on the photo= 0.532mm.

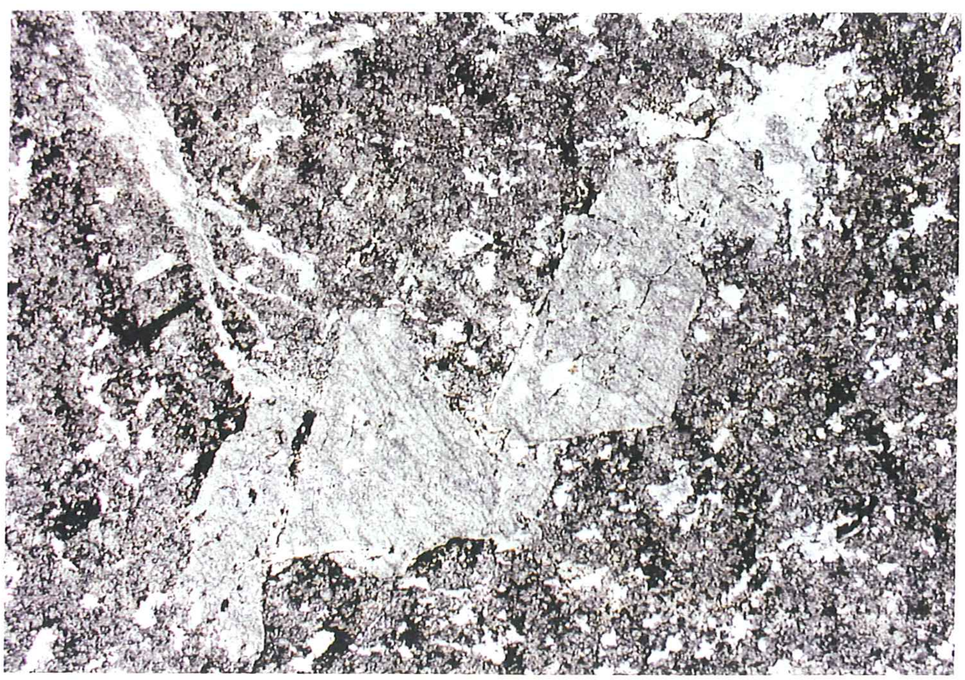

Figure 70b. RB-56b/quartz latite porphyry. Same view and scale as Figure 70a. TLP; 1cm on the photo= 0.532mm.

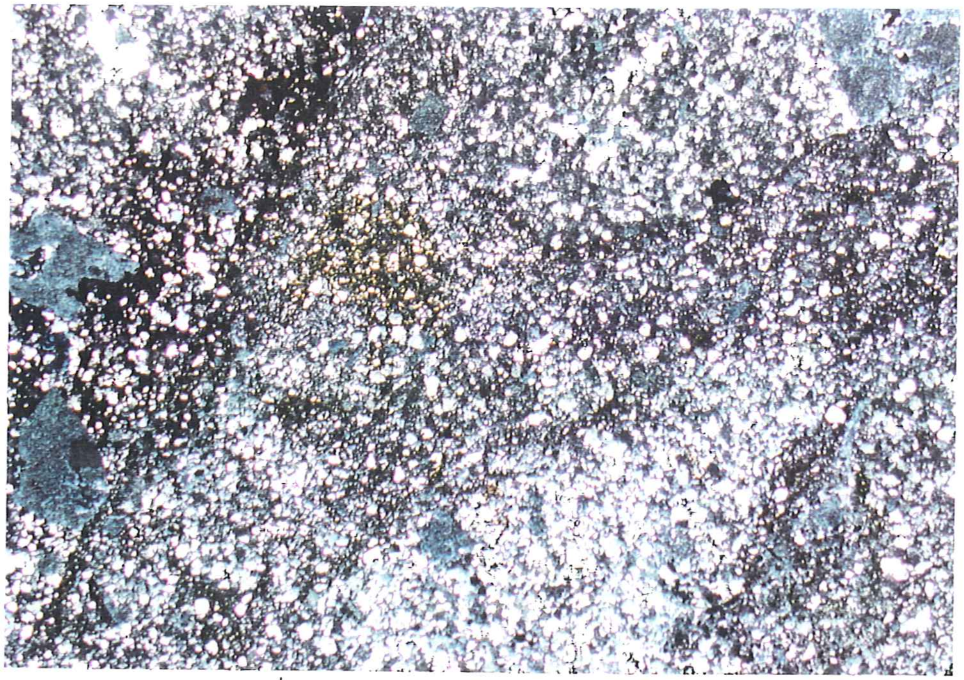

Figure 71a. RB-56b/quartz latite porphyry-intrusion breccia contact. The porphyry is located in the upper left corner of the photo. The breccia contains porphyry fragments in a similar matrix. Hematite is abundant along the contact. TLX; 1cm on the photo= 0.532mm.

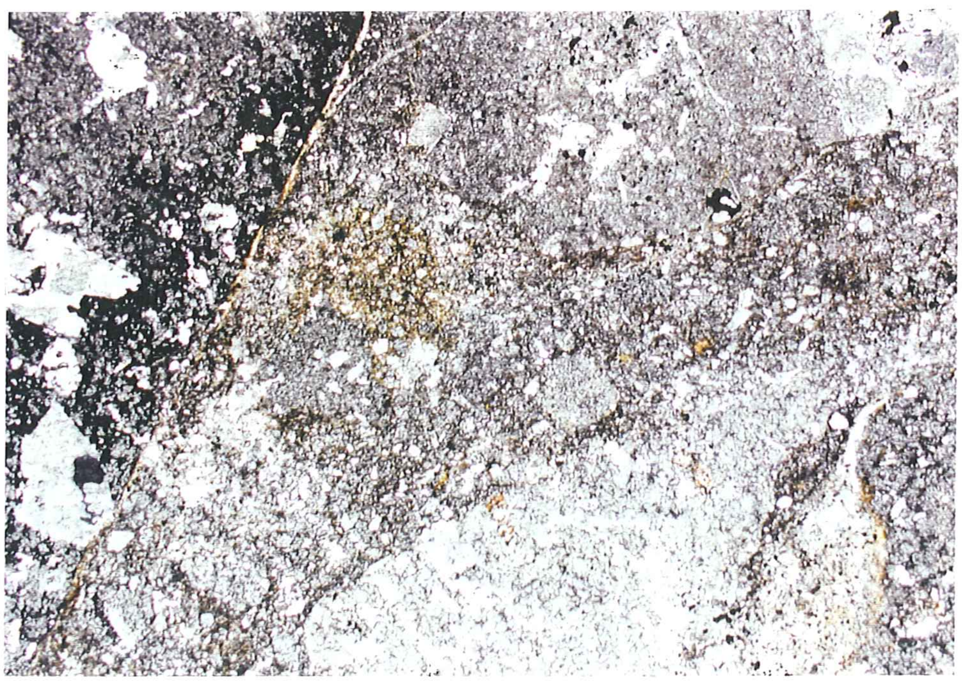

Figure 71b. RB-56b/quartz latite porphyry-intrusion breccia contact. Same view and scale as figure 71a. TLP; 1cm on the photo= 0.532mm.

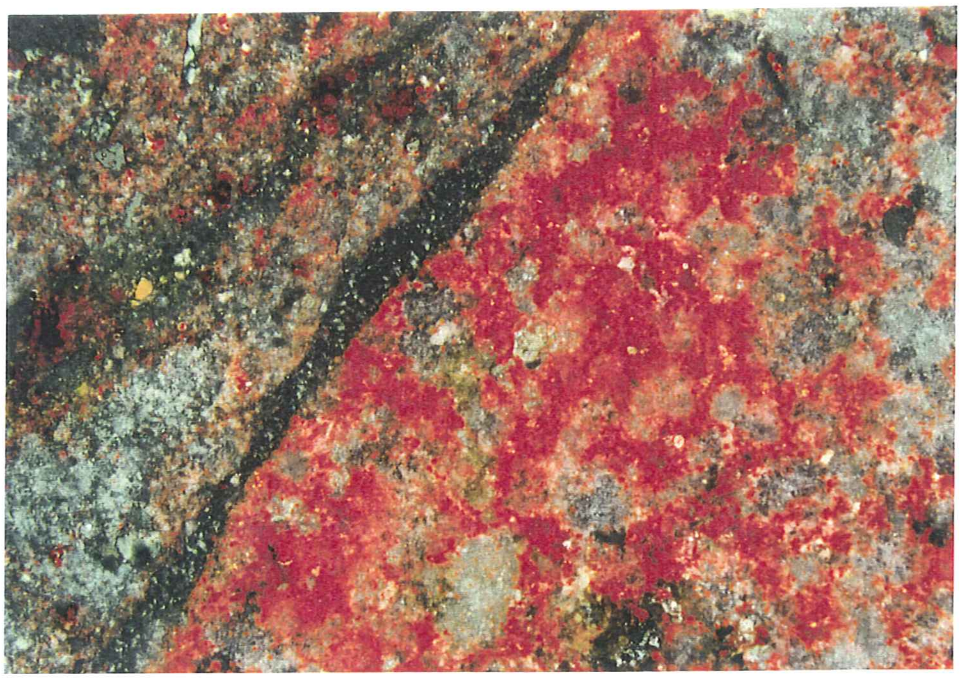

Figure 72. RB-56b/quartz latite porphyry-intrusion breccia contact. Abundant hematite along the contact between the porphyry and the breccia. RL, crossed polars; 1cm on the photo= 0.106mm.

Sample RB-57 (Middle Bud unit; <0.001opt Au, < 0.02 opt Ag)

Sample RB-57 is interpreted to be a lithic lapilli ash flow tuff. Alternatively it may be a flow-banded latitic or dacitic flow breccia. The sample contains approximately 20-25% subangular lithic fragments (devitrified glassy volcanic origin), vein fragments, crystals, and crystal fragments dispersed in a devitrified matrix with well-developed undulatory compaction bedding. Primary phenocryst phases were plagioclase and biotite. Biotite occurs as subhedral crystals to 1mm in length sparsely dispersed in the matrix. The biotites are pseudomorphed by calcite-FeOx-minor sericite, and only a trace of relict biotite remains. Original biotite abundance was less than 0.25 percent. Plagioclase occurs as euhedral to subhedral crystals to 1.2mm in length/diameter. Most of the plagioclase shows strong to complete replacement by calcite. Plagioclase phenocryst (and pseudomorph) abundance is approximately one percent. Lithic and vein fragments reach more than 1cm in diameter. The lithic fragments are very fine-grained and contain minor disseminated opaques and a few crystal fragments. They appear to be of devitrified tuff or glassy volcanic origin, and they are partly replaced by calcite. One fragment appears to contain wispy, discontinuous zones of vapor phase quartz. Several vein fragments contain bladed opaques (pyrrhotite) in a quartz-calcite gangue. The devitrified tuffaceous groundmass is a microcrystalline mass of quartz, alkali feldspar, clay, and calcite. It is likely that the original tuffaceous groundmass devitrified to a microcrystalline mosaic of quartz and alkali feldspar, and that the clay alteration developed later, preferentially along compaction bedding, and at the expense of feldspar and relict glassy ash. Several narrow (<0.25mm), discontinuous veinlets may be late zeolite.

CL: Some fragments and crystals are replaced by calcite with bright orange CL. The sulfide-bearing vein fragment is a calcite-sulfide vein, and there is some calcite replacement of the wall rock, as well.

RL: The sample contains less than 0.25 percent disseminated pyrite as sparse disseminations throughout the matrix. The pyrite forms fine to very fine, generally euhedral cubic, rectangular, or triangular crystals to 0.25mm diameter. Pyrrhotite or, less commonly, pyrrhotite-pentlandite intergrowths occur also as sparse disseminations in the matrix. Locally the pyrrhotite is in edge contact with traces of fine, anhedral sphalerite. It also has local euhedral inclusions of pentlandite (white, isotropic; slightly higher reflectance than the pyrrhotite). Locally pyrite and pyrrhotite occur together in single crystals, with the pyrite forming partial rims on the pyrrhotite. Several lithic fragments contain abundant, relatively coarse bladed pyrrhotite in single crystals to 1.1mm in length and aggregates to 7mm in length. Some of these bladed pyrrhotites contain subhedral, square to prismatic inclusions of pentlandite that reach 0.25mm in length. A trace of fine (0.03mm diameter), anhedral chalcopyrite was observed in one lithic fragment.

Representative photomicrographs from sample RB-57 are shown in Figures 13, 73, and 74.

Figure 73a. RB-57/lithic lapilli ash flow tuff. Welded and devitrified ash flow tuff. Lithic lapilli and pyrogenic plagioclase crystals show partial to complete replacement by calcite. TLX; 1cm on the photo= 0.532mm.

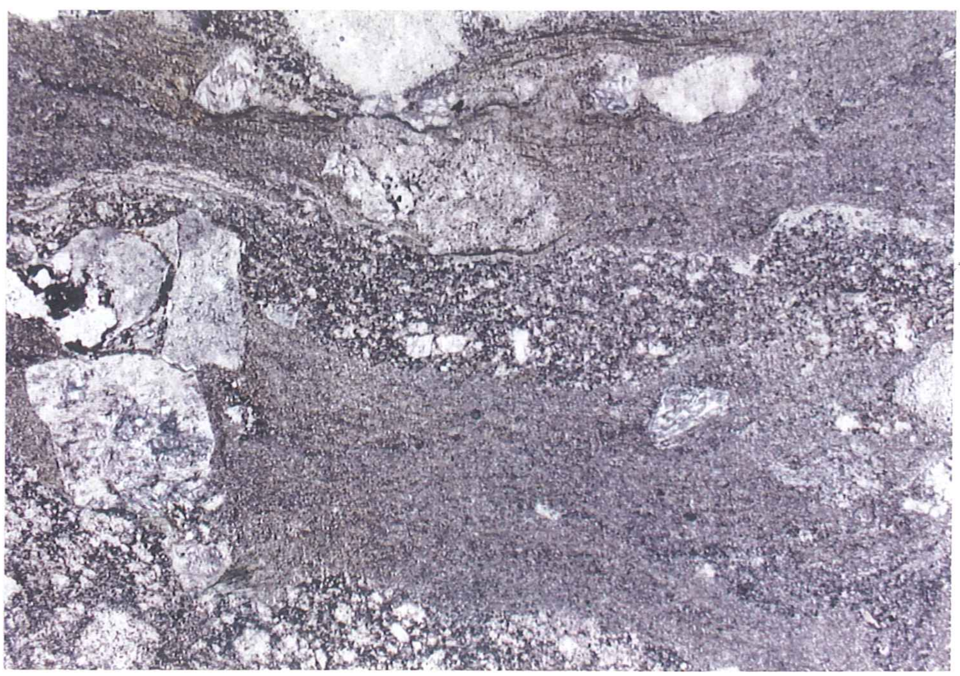

Figure 73b. RB-57/lithic lapilli ash flow tuff. Same view and scale as Figure 73b. TLP; 1 cm on the photo= 0.532mm.

Figure 74a. RB-57/lithic lapilli ash flow tuff. Calcite-sulfide (pyrrhotite-pyrite) vein in lithic lapillus carried by the ash flow tuff. CL; 1cm on the photo= 1.016mm.

Figure 74b. RB-57/lithic lapilli ash flow tuff. Lithic lapillus with calcite-sulfide vein in welded ash flow tuff. Same view and scale as Figure 74a. TLX; 1cm on the photo= 1.016mm.

RB-58 (Bud Marker porphyry; 223ppb Au; 2.7ppm Ag)

Sample RB-58 is a porphyritic quartz latite cut by branching quartz-clay-sulfide veins. The porphyry contains 2-3% phenocrysts of orthoclase, plagioclase, and biotite dispersed in a very fine-grained, granular groundmass of quartz, K feldspar, plagioclase, clay, and minor cloudy grayish brown, partly devitrified glass. Average groundmass crystal size is about 0.06mm diameter. Phenocrysts of orthoclase and plagioclase occur in subequal amounts, and biotite is subordinate. Orthoclase phenocrysts are euhedral to subhedral and reach more than 3.5mm length. Carlsbad twinning is common. The orthoclase shows variable replacement by fine-grained xenomorphic, polycrystalline quartz and minor clay and sericite. Plagioclase phenocrysts are completely pseudomorphed by cryptocrystalline quartz and clay, and locally serve as nucleation sites for bladed sulfides (pyrite-marcasite). Minor coarser polycrystalline quartz is observed also within the plagioclase pseudomorphs. The plagioclase pseudomorphs occur as subhedral crystals to 2.5mm in length. Biotite phenocrysts occur as subhedral crystals to 0.5mm in diameter. They are mostly altered to an assemblage of chlorite, clay, and FeOx. The biotites occur in clusters of 2-3 crystals and are associated with fine-grained primary apatite.

The branching veins contain quartz, clay, and opaque phases. Maximum vein width is approximately 5mm. The vein quartz generally displays a texture in which the long axes of crystals are most often normal to the vein boundary with the wall rock. Maximum crystal size is about 1.3mm length. Clay commonly forms elongate, narrow zones along one or both of the vein margins. The opaque phases form grossly cubic, rectangular, or bladed crystals to 4.5mm length within the veins. Narrow, discontinuous clay stringers are present outside the veins in the wall rock.

CL: The volcanic rock groundmass has generally dull red CL. The former phenocryst phases have dull blue gray CL, possibly from the cryptocrystalline quartz that pseudomorphs them. A few small fragments and some opaque phases associated with the veining have minor, very fine-grained, euhedral apatite. The apatite has a salmon pink to grayish orange CL and is probably of hydrothermal origin. The vein quartz is non-luminescent.

RL: Total vein plus disseminated sulfide in the sample is 2-3%, most of which is concentrated in the veins. The porphyry contains approximately 0.5% disseminated pyrite as fine, euhedral to subhedral cubic, rectangular, and trapezoidal crystals to 0.3mm in length/diameter. The porphyry also hosts minor coarser composite pyrite-marcasite as rectangular crystals to 1.5mm in length that have nucleated within plagioclase pseudomorphs. These coarser crystals commonly contain marcasite as minor irregular to linear intergrowths. Traces of anhedral sphalerite were noted in edge contact with disseminated pyrite locally. Vein sulfides are dominantly composite pyrite-marcasite, most with minor marcasite along crystal margins and as patchy to linear intergrowths. The composite pyrite-marcasite occurs as subhedral cubic to rectangular crystals to 4.5mm in length. One of the less well-formed of these crystals has a porous interior. A trace of sphalerite (± 0.1mm length) was noted in the vein.

Representative photomicrographs from sample RB-58 are given in Figure 75.

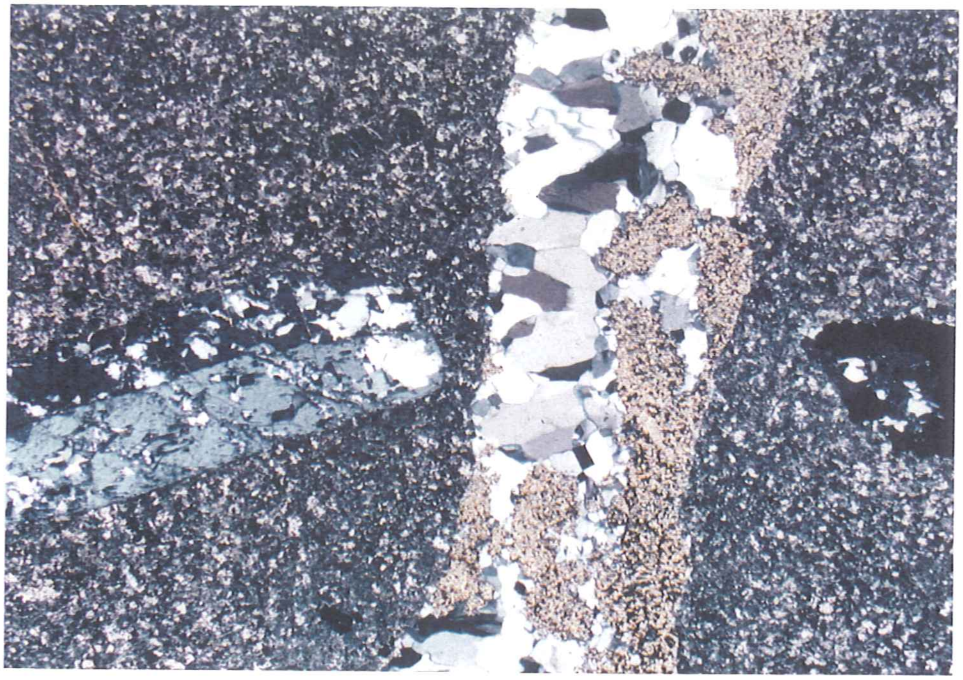

Figure 75a. RB-58/quartz latite porphyry. Phenocryst of orthoclase with Carlsbad twinning in fine, granular matrix of quartz, alkali feldspar, and clay. The porphyry is cut by a quartz-clay-sulfide (pyrite-marcasite) vein. TLX; 1cm on the photo= 0.532mm.

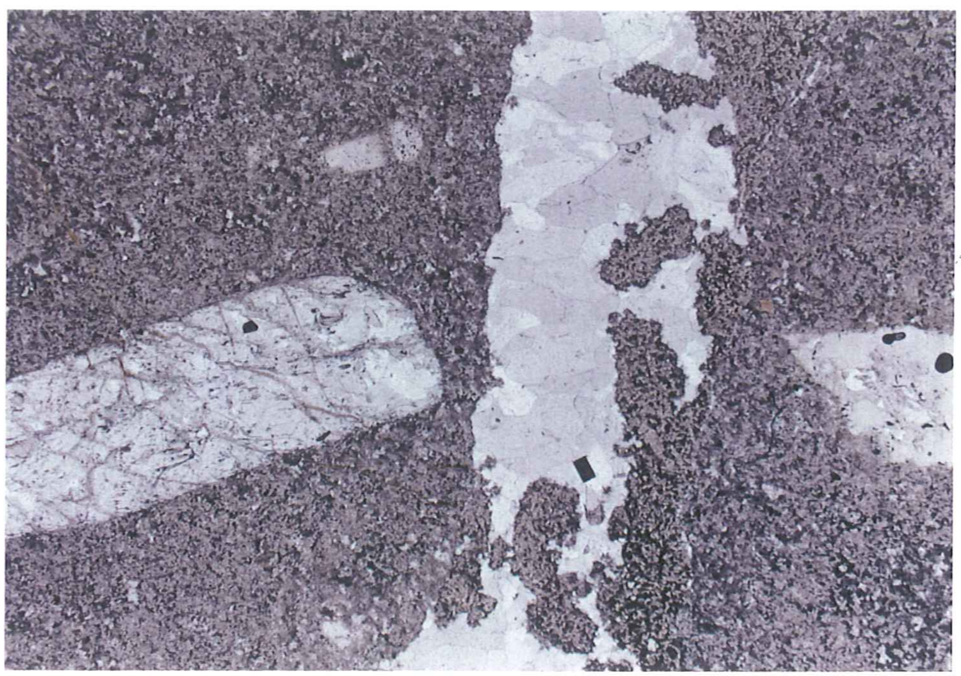

Figure 75b. RB-58/quartz latite porphyry. Same view and scale as Figure 63a. TLP; 1cm on the photo= 0.532mm.

RB-60A (Plat)

Sample RB-60a is a mottled pink to light green felsitic volcanic rock. It is very fine-grained and crudely bedded with scattered tiny crystals and crystal fragments of quartz and plagioclase. The quartz and plagioclase are subhedral to anhedral and reach 0.35mm in length/diameter. The very fine, granular groundmass contains quartz and alkali feldspar and has an average grain size of approximately 0.002mm. This lithology may be an air-fall tuff with a very fine-grained devitrified ash groundmass. Present also are narrow stringers of an optically negative phase with low birefringence (adularia?) and coarse sulfide clots.

CL: The tuff has weak, but pervasive carbonate replacement of groundmass. The carbonate is probably calcite with a significant iron content. The CL response is reddish orange. Fine-grained disseminated apatite (grayish yellow CL; $Mn2+$ activation) is present throughout, including within the area covered by the coarse sulfides.

RL: The sample contains seven to ten percent sulfides, mostly held within two coarse (to >1cm length) clots of intergrown pyrite and marcasite. The clots are composed of densely-packed, irregular anhedral to bladed crystals grown together in aggregate. Minor very fine disseminated pyrite-marcasite is sparsely disseminated outside the clots. Also present are two narrow (to 0.35mm width) pyrite-marcasite stringers with a trace of fine sphalerite (0.1mm diameter) in intracrystalline void space.

Representative photomicrographs from sample RB-60a appear in Figures 76 and 77.

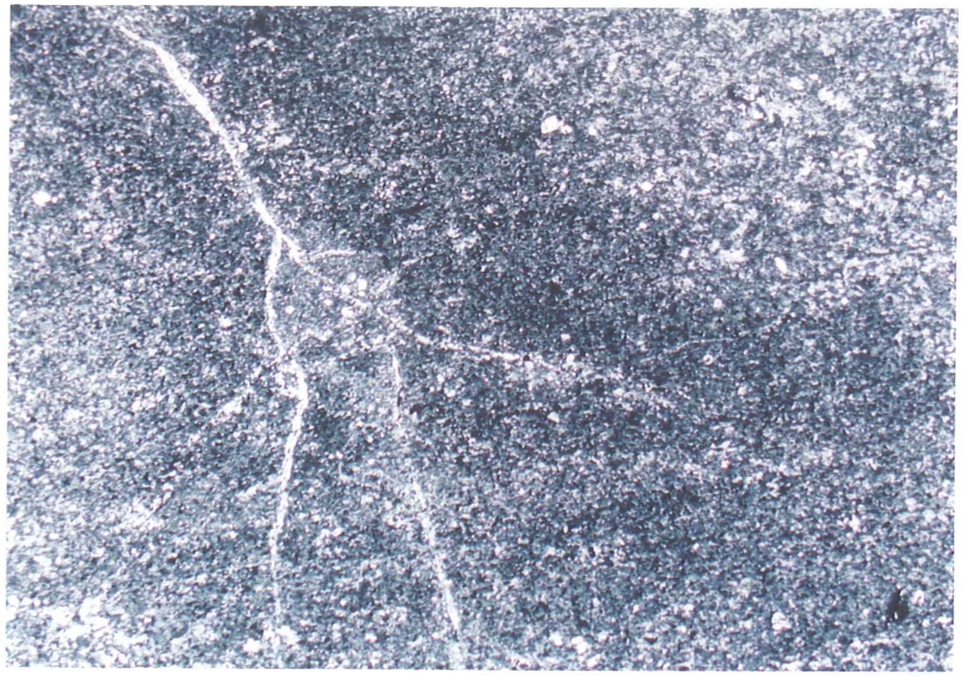

Figure 76. RB-60a/bedded tuff. Pyrogenic crystal fragments of plagioclase and quartz in a crudely bedded groundmass of devitrified ash. The sample also contains stringers of adularia (?) and sparsely disseminated composite pyrite-marcasite crystals. TLX; 1cm on the photo= 0.532mm.

Figure 77. RB-60a/bedded tuff. Sulfide stringer with composite pyrite-marcasite crystals and minor sphalerite locally in intracrystalline void space (upper right quadrant). RL; 1cm on the photo= 0.532mm.

RB-60B (PI at start of ore, WC + pyarg+ sulfides)

The gross lithology of sample RB-60b appears similar to sample RB-60a. It is a mottled pink to white felsitic volcanic rock that shows crude bedding. It is interpreted to be a tuff and is composed of small feldspar, quartz, and biotite crystals and crystal fragments dispersed in a very fine-grained, devitrified tuffaceous groundmass of quartz and alkali feldspar crystallites. Average groundmass grain size is on the order of 0.002 mm. Very fine-grained calcite replaces some of the groundmass feldspar. The tuff contains 1 - 2% disseminated fine-grained opaque phases, most of which have cubic morphology. Average crystal size of the disseminated opaque phases is 0.08mm diameter. The larger feldspar crystals and crystal fragments are plagioclase. The plagioclase has euhedral to subhedral morphology and reaches 0.45mm in length. Most crystals are partly altered to clay and calcite. Biotite occurs as generally euhedral crystals to 1.1mm in length that are completely altered to chlorite. Inclusions of apatite and a brown, high-relief, high-birefringence phase that may be allanite are common. Quartz occurs only as anhedral crystal chips to 0.1mm in length/diameter. Recognizable crystal fragments make up about 3-5% of the slide. The abundance ratio of chloritic biotite pseudomorphs:plagioclase:quartz is approximately 4:2:0.5. The slide contains a single coarser lithic fragment about 3.3mm diameter. The lithic fragment is a fine-grained, hypidiomorphic-granular mosaic of chloritized biotite, plagioclase, and quartz. Average grain size is 0.25mm length/diameter. It is probably intrusive in origin.

The tuff is cut by irregular, generally narrow veins of quartz-sulfide±chclorite±clay. Maximum vein width is approximately 3.3mm. One of the veins is irregular and anastamosing, and contains coarse sulfide clots. Some of the veins have a narrow, dark selvage (chloritic?). Also present are fine, wispy, discontinuous quartz stringers to 0.03mm width.

CL: The vein quartz is non-luminescent. There is weak, but relatively pervasive, replacement of the groundmass by very fine-grained calcite with orange-red CL. There is up to 0.3% apatite as fine, euhedral disseminations throughout. No apatite was observed in the veins. The apatite is either primary or accompanied the calcite replacement episode. The apatite has grayish to orangish yellow CL.

RL: The sample contains one to two percent disseminated pyrite as euhedral to subhedral crystals to 0.25mm diameter, and with cubic, rectangular, and trapezoidal morphology. Also present are scattered prismatic composite pyrite-marcasite crystals to 0.5mm length. The sulfides in the veins are dominantly aggregates and single crystals of pyrite and composite pyrite-marcasite. Crystal aggregates reach 7mm in length, with individual crystals to 0.55mm in length. A trace of pyrargyrite was noted intercrystalline to one of the coarse pyrite-marcasite aggregates.

Representative photomicrographs from sample RB-60b are given in Figures 78 and 79.

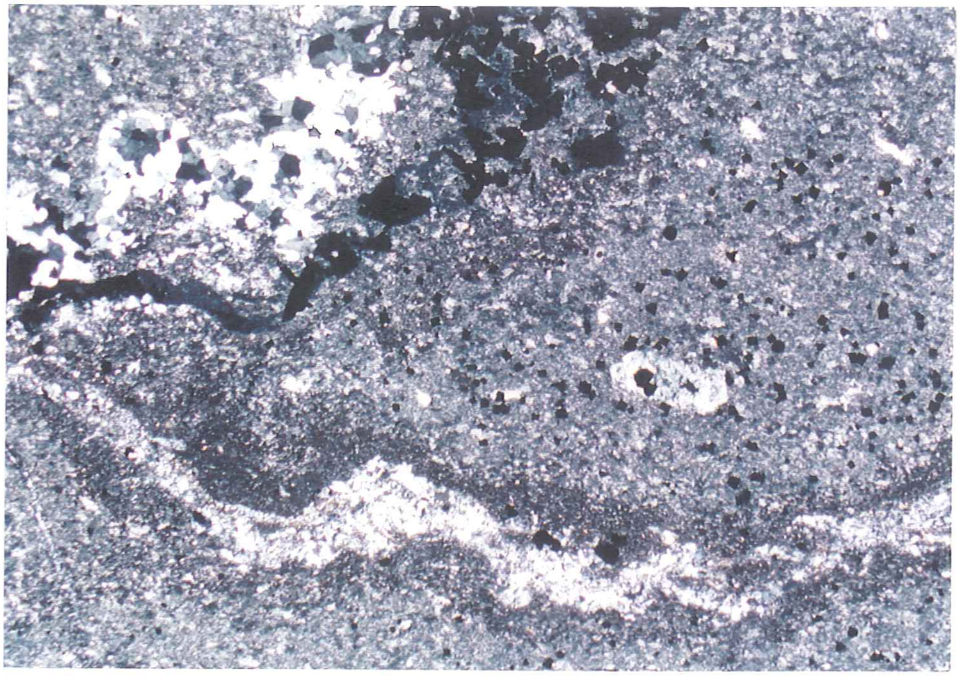

Figure 78a. RB-60b/bedded tuff. The tuff contains quartz-chlorite-sulfide (pyrite-marcasite) veins and abundant disseminated pyrite. There is a crystal of chloritized biotite with included pyrite in the lower right quadrant of the photo. TLX; 1cm on the photo= 0.532mm.

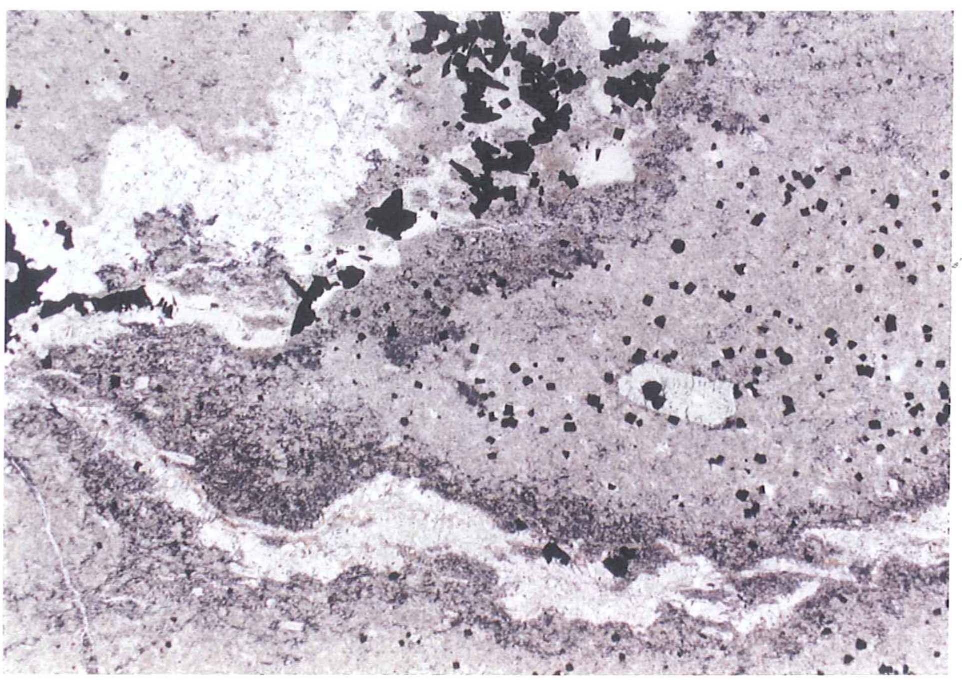

Figure 78b. RB-60b/bedded tuff. Same view and scale as Figure 78a. TLP; 1cm on the photo= 0.532mm.

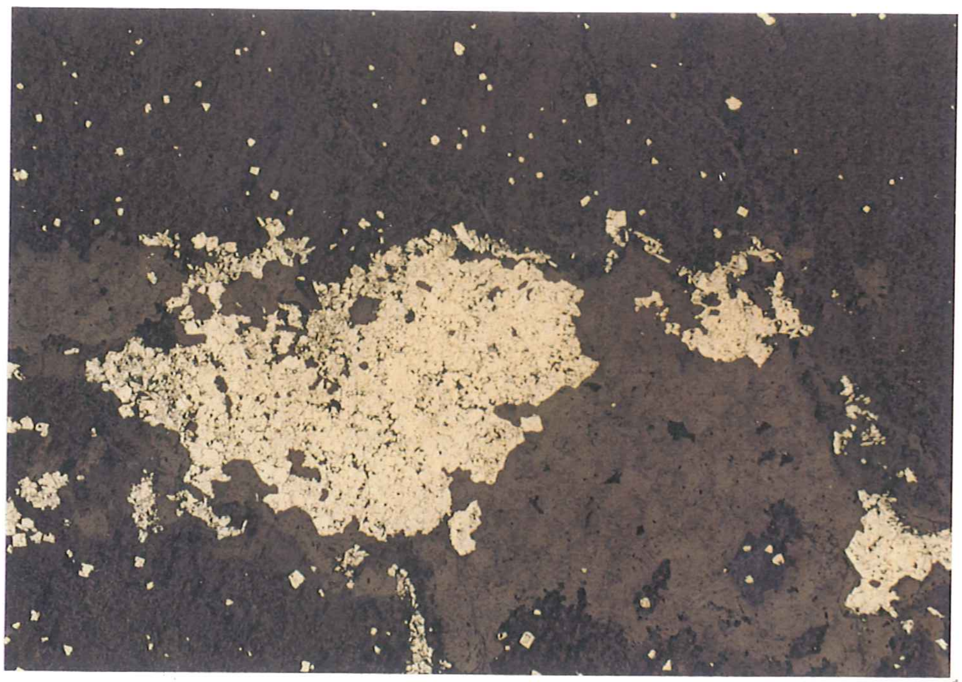

Figure 79. RB-60b/bedded tuff. Quartz vein with coarse py-mc aggregates and a trace of pyrargyrite. The pyrargyrite occupies intracrystalline void space in the coarse py-mc clot at photo center and is barely visible. RL; 1cm on the photo= 0.532mm.

RB-60C (Plat/vitrophyre)

Sample RB-60c is described in the field as a vitrophyre. In the hand specimen from which the thin section was cut the sample appears to be a densely welded lapilli tuff or tuff breccia choked with white, angular, felsitic lithic fragments in a reddish-brown, glassy matrix. In thin section the sample contains abundant monolithic fragments in a microcrystalline matrix of quartz and alkali feldspar. Average matrix crystal size is on the order of 0.004mm diameter. The matrix material represents granophyric devitrification products of the original welded tuffaceous groundmass. Also within the matrix are a few small zones of coarser saccharoidal quartz that may be either of vapor phase or hydrothermal origin. Average crystal size is about 0.03mm diameter. The tuff breccia ranges from fragment-supported to matrix-supported. Approximately 50% of the slide is composed of lithic fragments. The lithic fragments are subangular to subround, poorly-sorted, and reach more than 10mm in diameter. They are of a single lithology and appear as a very fine-grained felted mass of plagioclase, K feldspar, and minor biotite (altered to chlorite) in a finer granular groundmass of quartz and alkali feldspar. The texture has a crude pilotaxitic appearance, imparted by the alignment of the feldspar needles. Average feldspar crystal size is less than 0.6mm, while average groundmass crystal size is on the order of 0.002mm diameter. The lithic fragments probably represent a devitrified tuffaceous lithology. Very narrow (±0.05mm width), discontinuous quartz-chlorite ±pyrite stringers are relatively abundant.

CL: Vein quartz is non-luminescent. Apatite (<0.1%) is present as very fine, euhedral disseminations. The apatite has grayish to orangish yellow CL.

RL: The sample contains one to two percent disseminated pyrite as euhedral to subhedral crystals with mostly cubic to rectangular morphology. Maximum crystal size is 0.8mm length, although most of the disseminations are considerably finer-grained (on the order of ± 0.08mm diameter). The coarser sulfides are composite pyrite-marcasite crystals. Some of the crystals have porous interiors with locally higher marcasite abundance, and dense rims, almost always exclusively of pyrite. One fragment has a margin of fine pyrite crystals. Pyrite occurs also as a component of the narrow quartz-chlorite stringers.

Representative photomicrographs from sample RB-44c are shown in Figures 80 and 81.

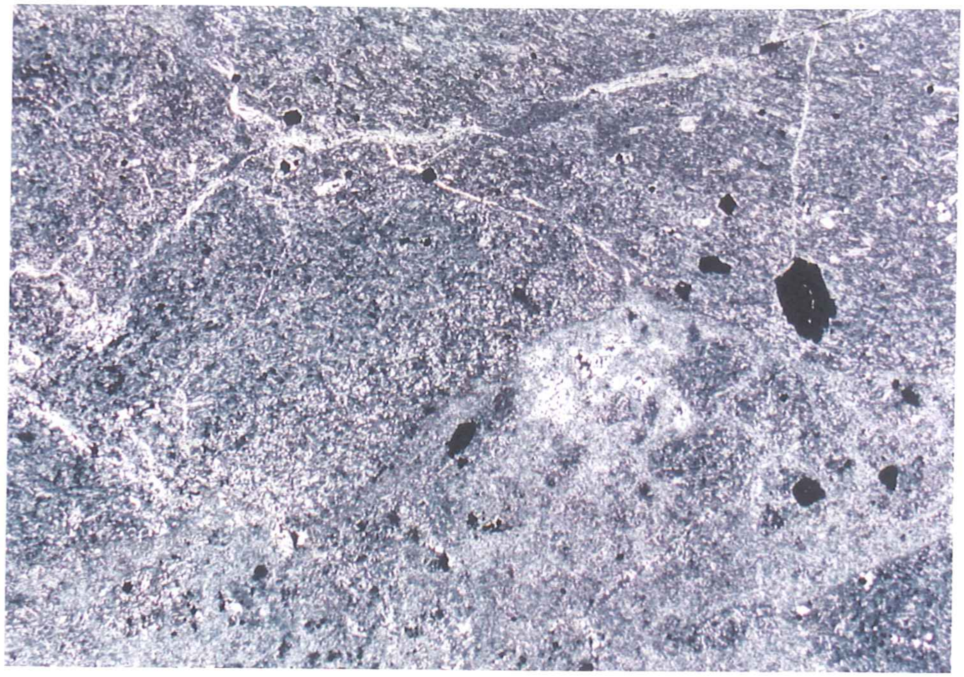

Figure 80a. RB-60c/lapilli tuff. Lithic volcanic lapilli dispersed in a devitrified tuffaceous groundmass. The tuff is cut by quartz-chlorite ± pyrite stringers and contains sparsely disseminated sulfides (pyrite-marcasite). TLX; 1cm on the photo= 0.532mm.

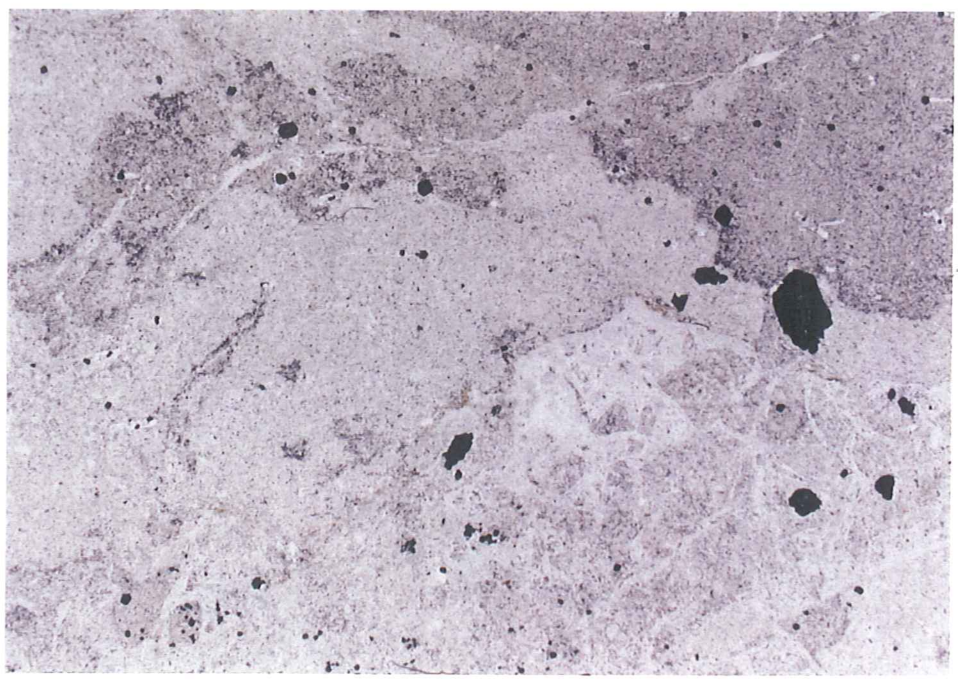

Figure 80b. RB-60c/lapilli tuff. Same view and scale as Figure 80a. TLP; 1cm on the photo= 0.532mm.

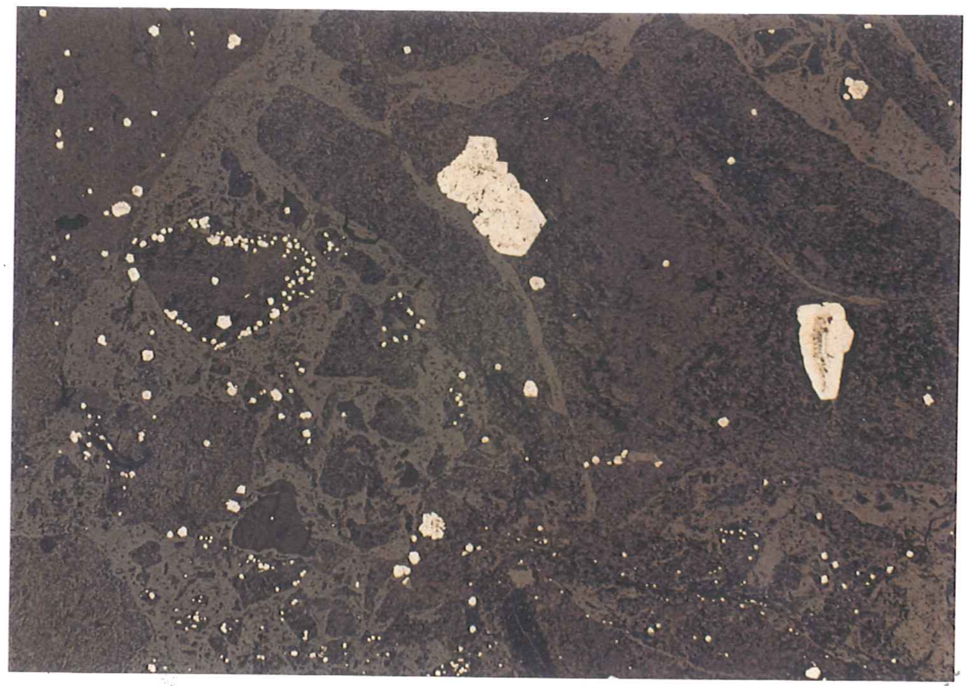

Figure 81. RB-60c/lapilli tuff. Disseminated sulfides in the lapilli tuff are pyrite (finer grained) and composite pyrite-marcasite (coarser crystals). RL; 1cm on the photo= 0.532mm.

RB-61a (LST; 0.128opt Au, 0.3opt Ag)

Sample RB-61a is a well-compacted, devitrified tuff cut by narrow, irregular stringers of quartz and sulfides. The tuff contains 7-10% small pyrogenic crystals and crystal fragments of plagioclase, K feldspar(?), and biotite (chlorite), and a roughly equivalent amount of partly devitrified and replaced coarser glass shards dispersed in a fine ash matrix devitrified to finely granular (<0.006mm) quartz, alkali feldspar, and finely disseminated FeOx. Also present are about 0.5% disseminated cubic and bladed sulfides, probably pyrite and skeletal composite pyrite-marcasite crystals. Narrow (<0.3mm width), discontinuous quartz and quartz-sulfide veins cut the tuff in several areas of the slide.

Pyrogenic crystals of plagioclase are euhedral to subhedral, lath-like, and up to 0.8mm in length. They show weak clay alteration. Euhedral to subhedral, tabular crystals to 0.3mm in length are completely pseudomorphed by clay and polycrystalline quartz, and are interpreted to have originally been K feldspar. No relict primary Kspar crystals of pyrogenic origin appear to have survived. All former biotite crystals are pseudomorphed by chlorite. The biotite pseudomorphs form euhedral crystals to 0.25mm in length. Some of the bladed opaque phases may be nucleated on former pyrogenic feldspar crystals.

Irregularly-shaped bodies to 2mm in length and with a generally brown color under plane-polarized light are interpreted to be partly devitrified volcanic glass shards. The interiors of the shards are brown and amorphous glass, while the outer zone is brown and shows birefringence, perhaps owing to incipient devitrification. Commonly the shards have narrow outer margins of fine disseminated FeOx that gives way to another narrow zone of polycrystalline quartz ± yet another narrow marginal zone of chlorite. Some shards have no remaining glass and have gone to very fine, polycrystalline quartz and/or chlorite.

CL: The vein quartz is non-luminescent. Disseminated apatite is very fine-grained and euhedral. It is present throughout and has grayish to orangish yellow CL. Abundance is estimated at <0.15%. The apatite is interpreted to be primary.

RL: Total opaque mineral abundance is about 0.5 percent. Disseminated pyrite forms generally euhedral to subhedral cubic crystals to 0.15mm in diameter. The bladed disseminated crystals reach 1.8mm in length and are composite pyrite-marcasite. Some of the pyrite shows anisotropism. Vein sulfides are dominantly bladed composite pyrite-marcasite crystals to nearly 2.5mm in length, and with aspect ratios to 25:1. A trace of native gold was identified in the matrix outside, although proximal to, a quartz-pyrite-marcasite stringer. Individual gold crystal size is 0.002mm diameter. Traces of fine-grained (0.03mm diameter) sphalerite are disseminated in the tuff matrix.

Representative photomicrographs from sample RB-61a are given in Figure 82.

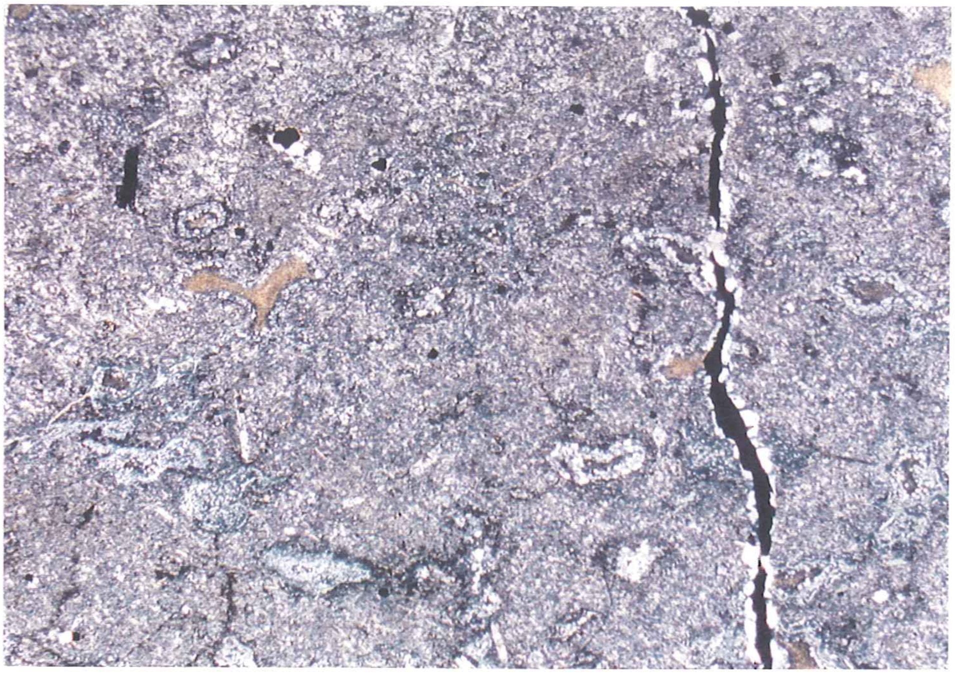

Figure 82a. RB-61a/ash flow tuff. Altered glass shards (?) with narrow quartz rims in devitrified fine ash matrix. The tuff is cut by a quartz-sulfide veinlet. TLX; 1cm on the photo= 0.532mm.

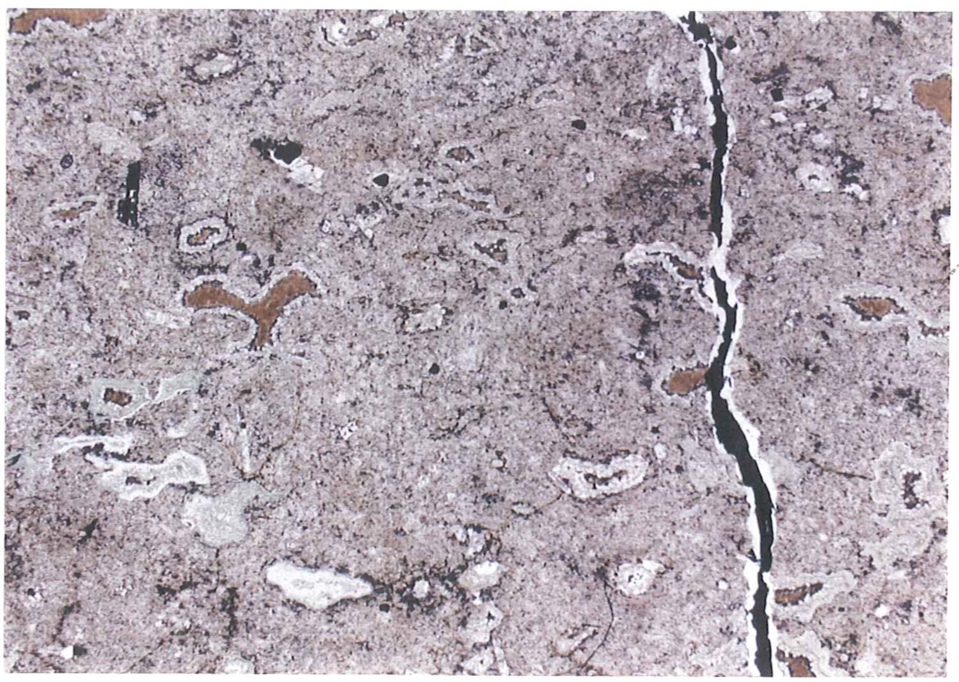

Figure 82b. RB-61a/ash flow tuff. Same view and scale as Figure 82a. TLP; 1cm on the photo= 0.532mm.

RB-61B (LST; 0.014opt Au, 1.06 opt Ag)

Sample RB-61b appears to be a well-compacted, devitrified tuff. In hand specimen it has a dense white porcellaneous character with relatively abundant quartz-sulfide stringers and disseminated sulfides. In thin section the rock has 3-5% altered pyrogenic crystals and crystal fragments of feldspar, hornblende, and possibly biotite, all dispersed in an extremely fine-grained, devitrified tuffaceous groundmass of quartz, alkali feldspar, clay, and cloudy grayish brown relict glass. Average groundmass crystal size is less than 0.002mm. Pyrogenic feldspars are generally euhedral to subhedral and less than 0.4mm in length. They are tabular to nearly needle-like and altered either to clay or clay + polycrystalline quartz. Minor relict plagioclase remains. Pyrogenic hornblendes are euhedral to subhedral and reach 0.15mm in length/diameter. All are altered to chlorite ± sericite. Characteristic amphibole cross sections can be seen locally. Biotite, if present, is also altered to chlorite ± sericite. Its presence is inferred by an equant morphology, more characteristic of biotite cut parallel to the C-axis than of hornblende. Five to seven percent crudely football-shaped lenses that host polycrystalline quartz, sulfides, and/or clay and chlorite are interpreted to represent former fiamme. These lenses show preferred alignment and reach 7mm in length. Long axes of the polycrystalline quartz project inward, roughly perpendicular to the wall of the lens. Several of the lenses have hemispherical bodies of radiating quartz to 0.8mm diameter that may be spherulites. The presence of spherulitic devitrification may indicate that the tuff was strongly welded prior to devitrification. There are abundant anastamosing, narrow, wispy stringers of polycrystalline quartz ± clay ± chlorite ± sulfides, many of which project into the lensoid bodies. The cubic disseminated pyrite is concentrated in one part of the slide in an area about 10mm in diameter.

CL: The groundmass has a dull blue-gray CL, except for a dull reddish brown CL in selvages around the quartz lenses. Present as disseminations are very fine-grained calcite (bright orange CL; Mn^{2+}) and apatite (<0.1%; lemon yellow CL). The hydrothermal quartz does not luminesce.

RL: The slide contains 5-7% total sulfides, primarily as euhedral to subhedral composite pyrite-marcasite crystals with generally bladed morphology. Pyrite is the more abundant of the two phases within the composite crystals. Traces of pyrargyrite occur in intracrystalline voids within some composite pyrite-marcasite crystals. The composite, bladed pyrite-marcasites are generally associated with the discontinuous quartz-sulfide stringers. Present within the tuff matrix are disseminated pyrites to 0.2mm diameter with generally cubic morphology. Many of the pyrite disseminations have porous cores and dense rims. Traces of sphalerite occur within the quartz veins as irregularly-shaped crystals to 0.06mm diameter, and a crystalline aggregate of sphalerite was observed interior to a bladed pyrite-marcasite crystal. Traces of very fine primary disseminated magnetite occur throughout.

Representative photomicrographs from sample RB-61b are illustrated in Figures 83, 84, and 85.

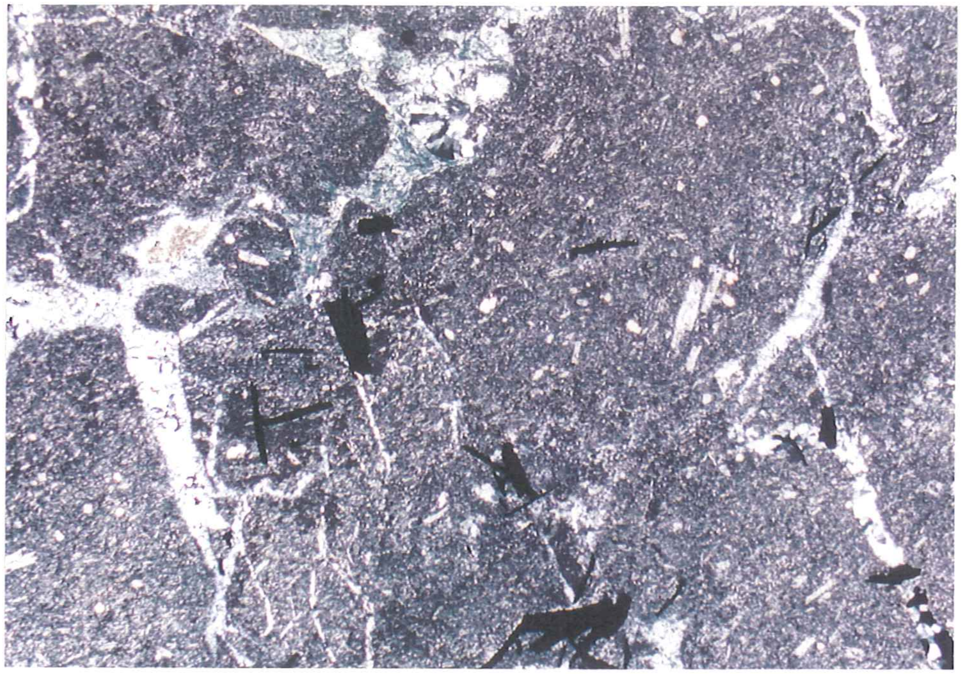

Figure 83a. RB-61b/devitrified tuff. Quartz-clay-chlorite-pyrite/marcasite stringers in microcrystalline groundmass of quartz, alkali feldspar, and clay. The flow banding is not well-represented in this view. Note the spherulitic devitrification with radial quartz crystals near middle upper edge of the photo. TLX; 1cm on the photo= 0.532mm.

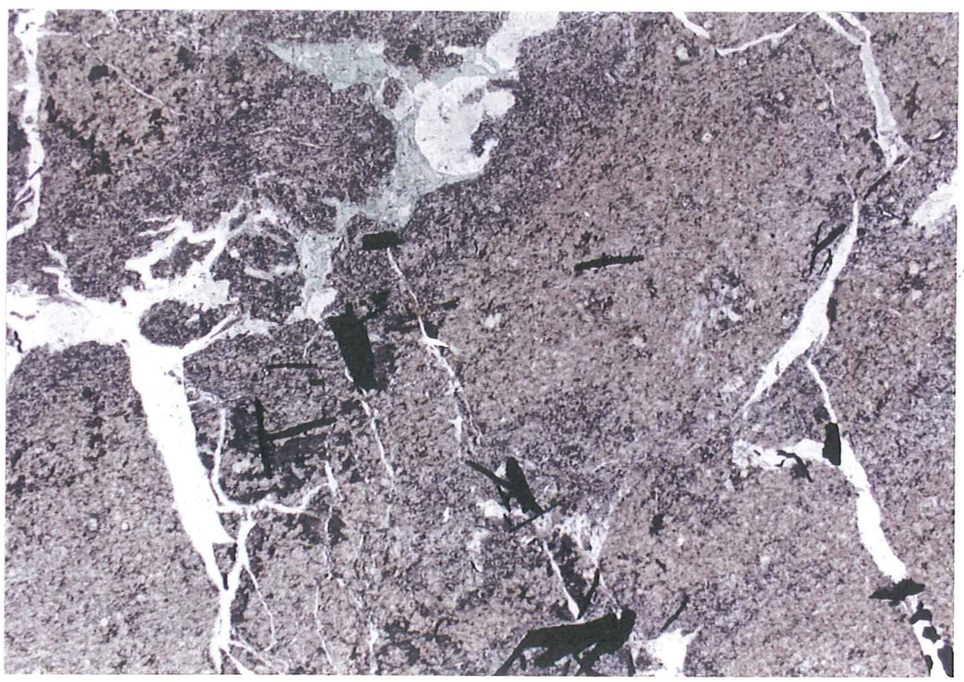

Figure 83b. RB-61b/devitrified tuff. Same view and scale as figure 83a. Disseminated opaques are dominantly composite pyrite-marcasite crystals with lesser pyrite. TLP; 1cm on the photo= 0.532mm.

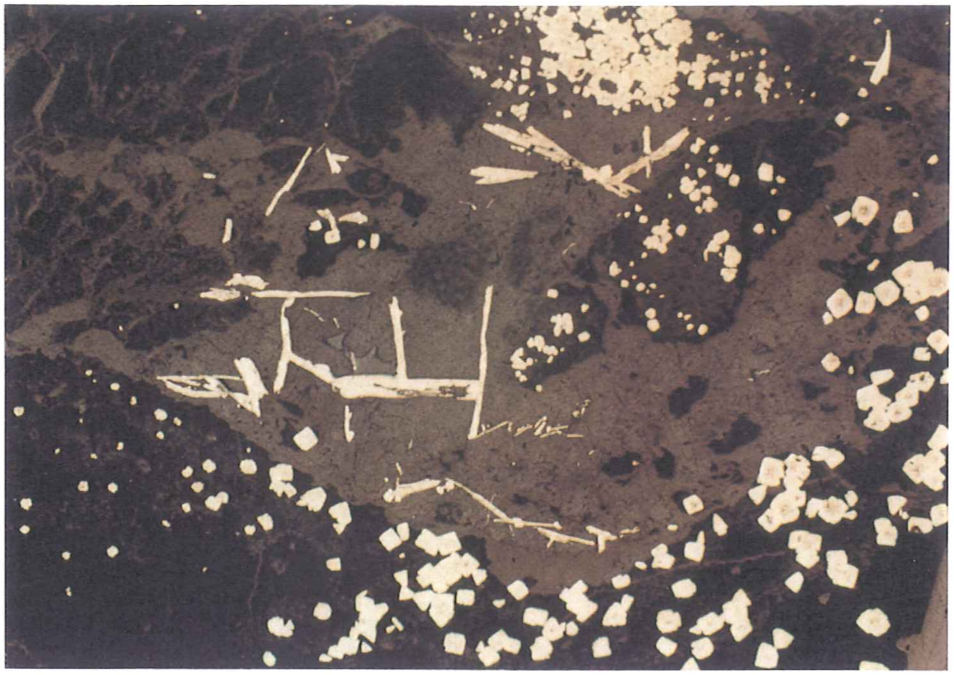

Figure 84. RB-61b/devitrified tuff. Quartz vein with skeletal composite pyrite-marcasite crystals, and disseminated pyrite in bedded tuff. RL; 1cm on the photo= 0.532mm

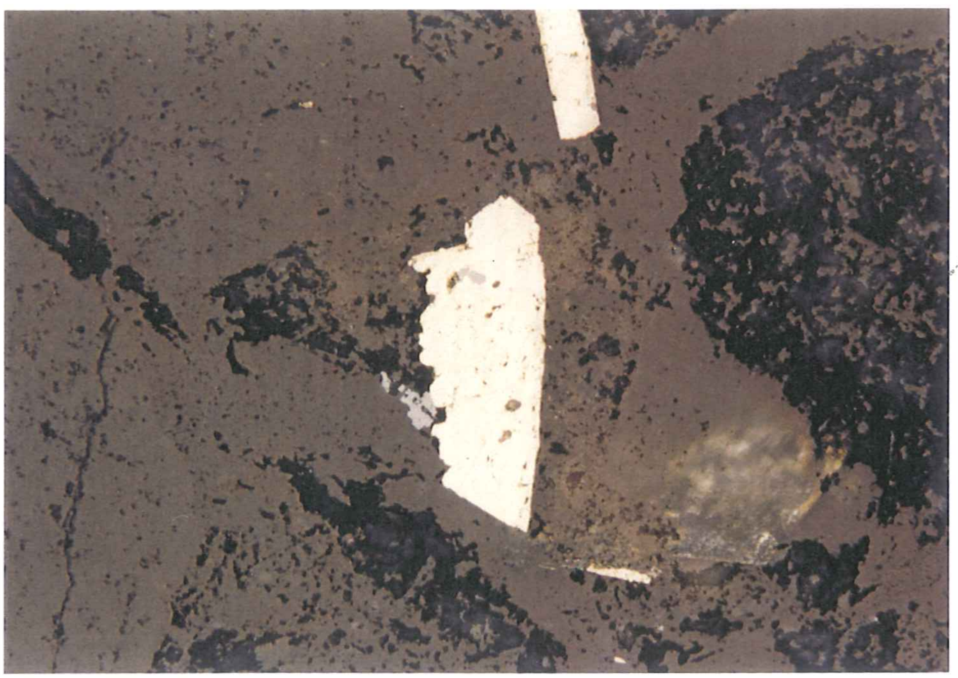

Figure 85. RB-61b/devitrified tuff. Quartz vein with composite pyrite-marcasite. The large py-mc has an inclusion of pyrargyrite (gray; moderate R < py-mc) and a small, anhedral crystal of pyrargyrite in edge contact at the left margin of the py-mc crystal. RL; 1cm on the photo= 0.053mm.

RB-61C (LST)

Sample RB-61c is a well-compacted, devitrified tuff. It contains 3-5% pyrogenic crystals of altered feldspar and subordinate biotite dispersed with crude alignment in a very fine-grained devitrified tuffaceous groundmass composed of alkali feldspar crystallites, microcrystalline quartz and alkali feldspar, clay, and calcite. Alternating, somewhat sinuous, compaction beds are marked by subtle changes in groundmass crystallite size. The pyrogenic crystals tend to be mostly euhedral and up to 0.35mm in length. The plagioclase laths show polysynthetic twinning and partial to complete alteration to clay and polycrystalline quartz. K feldspar forms tabular crystals with common Carlsbad twinning. It shows partial to complete alteration to polycrystalline quartz and minor clay. Locally the Kspar has served as nucleation sites for bladed sulfide crystals. Biotite is also euhedral and pseudomorphed completely by chlorite with very pale green pleochroism. Several percent elongate to lensoid bodies are interpreted to be former fiamme and are now replaced by polycrystalline quartz and clay ± sulfides. Some of the quartz is twinned and has a bladed morphology, and may have originally been trydimite. Several spherulites or partial spherulites with radiating quartz were noted projecting into the fiamme. The spherulites reach 0.35mm diameter. A few narrow(<0.1mm width) stringers of polycrystalline quartz ± clay cut the rock transverse to the compaction bedding. There are 1-2% disseminated sulfides to 0.7mm in length. The sulfides have a bladed morphology and are probably skeletal composite pyrite-marcasite crystals.

CL: The vein quartz is non-luminescent. Very fine-grained calcite (bright orange CL) and apatite (orange yellow CL) occur as sparse disseminations. The apatite is primary.

RL: The sample contains 1-2% disseminated sulfides as euhedral to subhedral, bladed composite pyrite-marcasite crystals to 0.7mm length and finer, generally cubic or pyritohedron pyrite crystals to 0.17mm diameter. The bladed marcasite crystals are found disseminated in the groundmass, within some filled vesicles, and nucleated in former feldspar microphenocryst sites. A trace of native gold was noted adjacent to a composite pyrite-marcasite crystal in vesicle fill. The gold also invades the pyrite-marcasite crystal as a tiny thread.

Representative photomicrographs from sample RB-61c are given in Figures 17, 86, and 87.

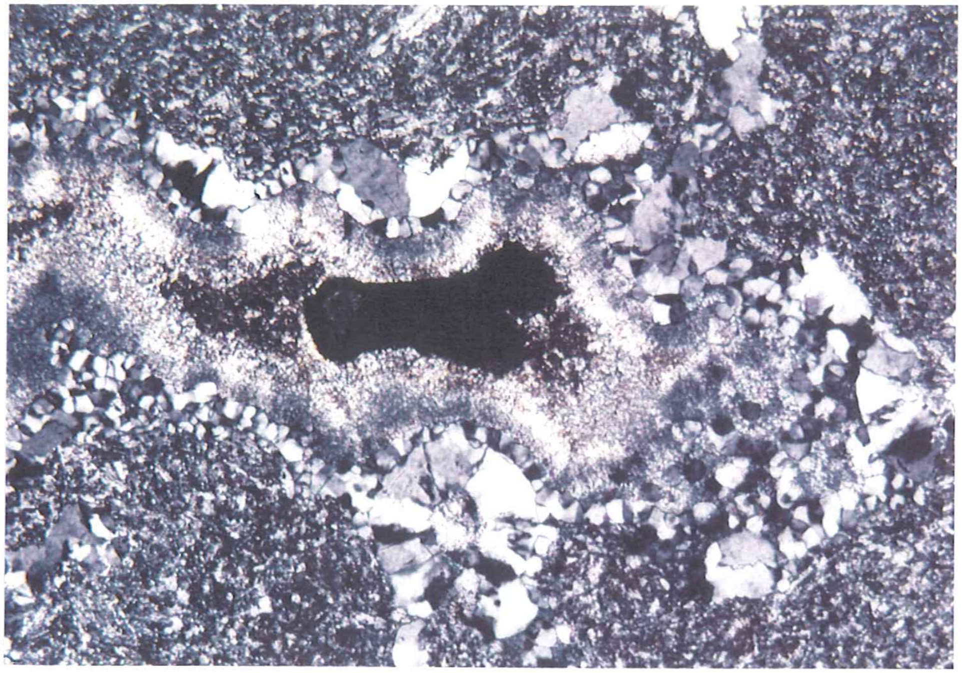

Figure 86a. RB-61c/devitrified tuff. Lensoid former fiamme are filled with quartz and clay ± sulfides. Note spherulites at fiamme margins. Disseminated sulfides are dominantly composite py-mc crystals. TLX; 1cm on the photo= 0.532mm.

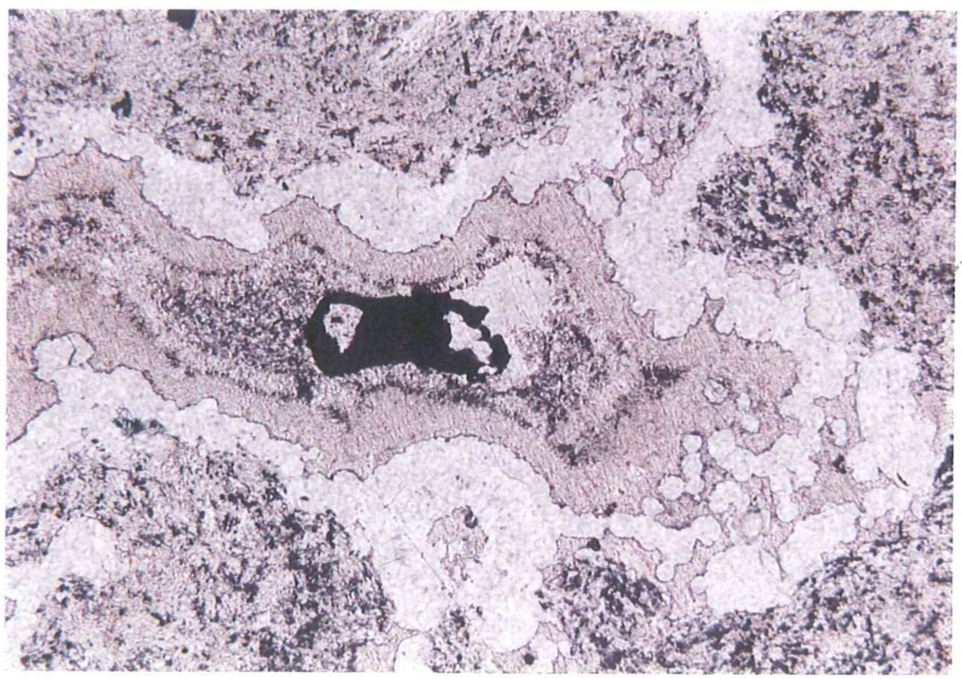

Figure 86b. RB-61c/devitrified tuff. Same view and scale as figure 86a. TLP; 1cm on the photo= 0.532mm.

Figure 87. RB-61c/devitrified tuff. Composite py-mc crystal with fine native gold (pale yellow; high R) filling microfractures and in partial edge contact (lower right quadrant of the photo). This is the same py-mc crystal that occupies the fiamme center in Figures 86 a and b. RL; 1cm on the photo= 0.021mm.

RB-61D (LST)

Sample RB-61d is a well-compacted, devitrified tuff. It has irregular compaction bedding and contains approximately 0.5% pyrogenic crystals of feldspar and subordinate biotite to 0.5mm in length. Pyrogenic feldspars are mostly altered to clay, but what relict feldspar remains suggests that both primary plagioclase and K feldspar (sanidine?) were present originally. Pyrogenic biotites are completely altered to chlorite. Pyrogenic feldspar and biotite both show a crude preferred alignment in accordance with the irregular compaction bedding. Devitrified and replaced fiamme constitute 3-5% of the sample. The fiamme are irregularly-shaped, in part because of the complex spherulitic devitrification along parts of the fiamme margins. They reach a maximum length of nearly 9mm. The replacement fill is complex. The central parts are filled variously by clay, chalcedony, chlorite, or a brown mass of fine alteration minerals that appear nearly amorphous, or some combinations of these phases. The margins have narrow bands of fine, polycrystalline quartz that may originally have been tridymite. Commonly parts of the margins of the fiamme will show partial to complete spherulites derived from devitrification of the former strongly-welded tuffaceous groundmass. The spherulites are formed from radiating quartz blades that may have crystallized initially as cristobalite. The spherulites are up to 0.8mm in diameter. The tuffaceous groundmass is partly devitrified to a mass of quartz and alkali feldspar crystallites in crude alignment with the sinuous compaction beds. The compaction bedding appears to be manifested in the slide by zones of more and less well-developed devitrification. The sinuous nature of the compaction bedding and the development of spherulites may indicate that the tuff was welded densely enough to have flowed rheomorphically following deposition. There are scattered, narrow (to 0.4mm width), irregular stringers of chalcedonic quartz, quartz-pyrite-marcasite, and clay.

CL: All quartz is non-luminescent. Very fine-grained calcite (bright orange CL) and apatite (orange yellow CL) are present as sparse disseminations.

RL: The sample contains 0.5-1.0% disseminated sulfides as very fine-grained pyrite and elongate, skeletal composite pyrite-marcasite crystals. The pyrites have cubic and subordinate pyritohedron morphology and reach 0.15mm diameter, although most are considerably smaller. The larger pyrite disseminations sometimes have a porous marcasite core. The skeletal composite pyrite-marcasite crystals are up to 0.8mm in length and have a maximum aspect ratio of 24:1. They commonly have narrow rims of marcasite and infill of cubic pyrite crystals. Locally there are elongate interior intergrowth zones of marcasite, as well. Present locally within fiamme fill are dense aggregates of pyrite and marcasite crystals to nearly 1mm in diameter. Marcasite crystals usually rim the aggregates and fill interior voids between cubic pyrite crystals. A few narrow (to 0.04mm width) stringers of quartz-pyrite-marcasite were noted also. A single isotropic anhedral crystal (0.02mm diameter) was noted with white color and moderately high reflectance (<pyrite). This phase may be galena.

Representative photomicrographs from sample RB-44c appear in Figure 88.

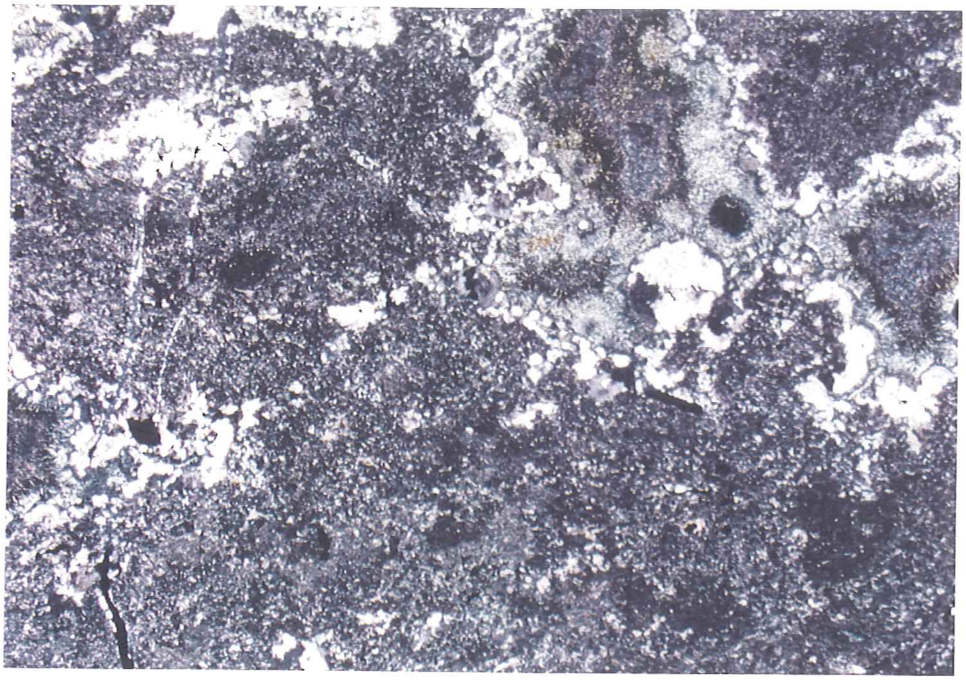

Figure 88a. RB-61d/devitrified tuff. Fine, devitrified tuffaceous groundmass of quartz and alkali feldspar crystallites. Former fiamme are filled with quartz and chlorite. Spherulites with radiating quartz crystals protrude into the replaced fiamme. TLX; 1cm on the photo= 0.532mm.

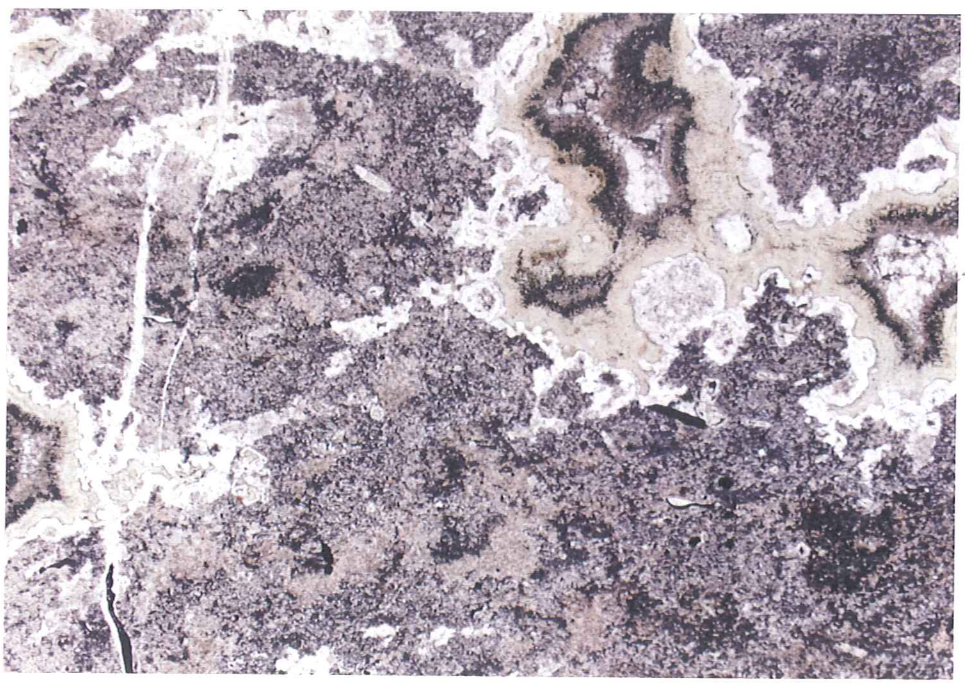

Figure 88b. RB-61d/devitrified tuff. Same view and scale as Figure 88a. 1cm on the photo= 0.532mm.

RB-63A (PMBX w/ sulfide veinlet; 0.967opt Au, 1.44opt Ag)

Sample RB-63a is a volcanic breccia. It contains approximately 25% subangular to subround lithic fragments dispersed in a microcrystalline groundmass of quartz and alkali feldspar. The breccia is traversed by quartz-clay-carbonate-sulfide veinlets, and quartz and calcite stringers. Sulfide phases occur both in veins and as disseminations primarily in the lithic fragments.

Lithic fragments range up to 2cm in length/diameter and appear to be of one lithology. Several of the fragments contain abundant disseminated sulfides with dominantly pyritohedron morphology. The fragments in general contain more disseminated sulfides than does the matrix. The fragments are matrix-supported and only infrequently in point or edge contact. The lithic fragments have a lithology similar to that described for samples RB-61, a-d (tuffs). They contain relatively minor (<<0.5%) pyrogenic crystals of altered feldspar and biotite scattered in a microcrystalline groundmass of feldspar crystallites and microgranular xenomorphic quartz and alkali feldspar. The pyrogenic and groundmass feldspars are partly altered to clay, and the biotite is completely altered to chlorite. There is a crude alignment of pyrogenic feldspar and biotite with the groundmass feldspar crystallites. Some of the lithic fragments are partly replaced by calcite. One of the lithic fragments contains about 15% euhedral disseminated pyrite.

The groundmass matrix is a microcrystalline mosaic of xenomorphic quartz, alkali feldspar, and clay. Average groundmass crystal size is approximately 0.004mm diameter. It is likely that the original groundmass was glassy. The clay is derived from post-devitrification partial alteration of the feldspar. The matrix contains only minor disseminated opaque phases. In addition to the veins the volcanic breccia is cut by narrow (0.1mm), discontinuous, sinuous calcite stringers.

The main vein cutting the volcanic breccia in the slide has a width of approximately 10mm. Coarser polycrystalline quartz (to 0.5mm length) and minor sulfide lines one of the vein-wallrock contacts. This quartz has grown with long axes generally perpendicular to the contact. The narrow margin gives way inward to much finer-grained (± 0.05mm length/diameter) xenomorphic polycrystalline quartz, clay, and sulfides. The clay is distributed along quartz crystal boundaries. A vein branching from the main vein contains significant calcite in addition to fine xenomorphic quartz, skeletal elongate pyrite-marcasite, and clay. Other branching veins contain quartz and clay ± minor calcite and sulfides.

CL: The vein quartz is non-luminescent. Calcite has bright orange CL. It occurs as narrow discontinuous and irregular stringers, as replacement of some lithic fragments, and as a component of some of the quartz-sulfide veins. There are traces of disseminated apatite with lemon yellow CL.

RL: Total sulfide abundance is sample RB-63a is about 10 percent The original abundance may have been higher, because there appears to have been some plucking of sulfides in vein and wallrock during sample preparation. Much of the sulfide is carried in a vein branching from the main vein and as disseminations in the largest lithic fragment. The disseminated sulfides are dominantly euhedral pyrites to 0.5mm diameter and with pyritohedron morphology. Vein sulfides are mostly euhedral to subhedral skeletal composite pyrite-marcasite crystals to

5mm length. Aspect ratios are up to 16:1. Chalcopyrite occurs as fine, anhedral crystals (< 0.07mm diameter) primarily intergranular to xenomorphic quartz and, less commonly, in edge contact with py-mc. Traces of fine acanthite (?) and pyrrhotite were noted intercrystalline to py-mc crystals. Despite significant assays for gold and silver in the sample, only minor silver minerals and no gold minerals were identified in the sample. The presence of chalcopyrite, which commonly accompanies high-grade gold-silver mineralization in the Rosebud epithermal system, suggests that there may have initially been gold and silver minerals in the sample, but they may have been plucked during sample preparation.

Representative photomicrographs from sample RB-63a are found in Figures 6, 89, 90, and 91.

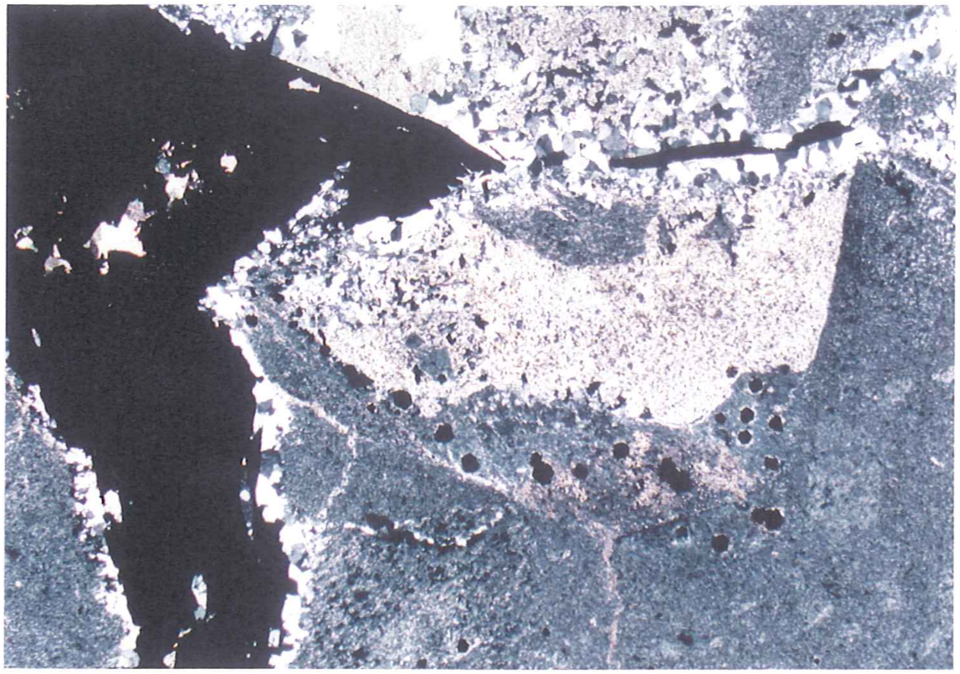

Figure 89a. RB-63a/volcanic breccia. Quartz-calcite-clay-sulfide vein cuts volcanic breccia. TLX; 1cm on the photo= 0.532mm.

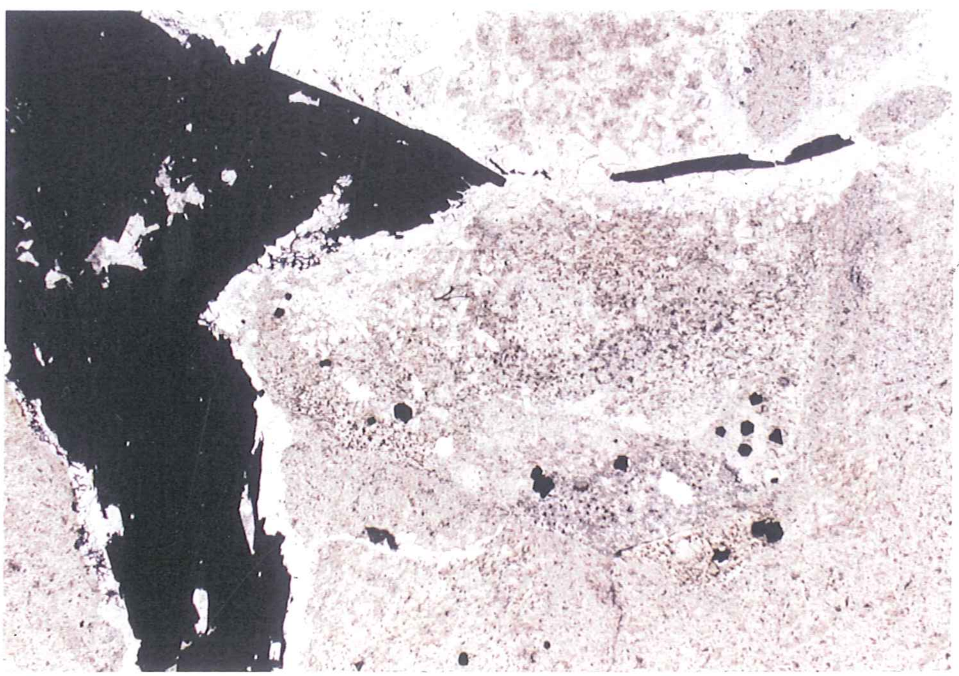

Figure 89b. RB-63a/volcanic breccia. Same view and scale as figure 89a. TLP; 1cm on the photo= 0.532mm.

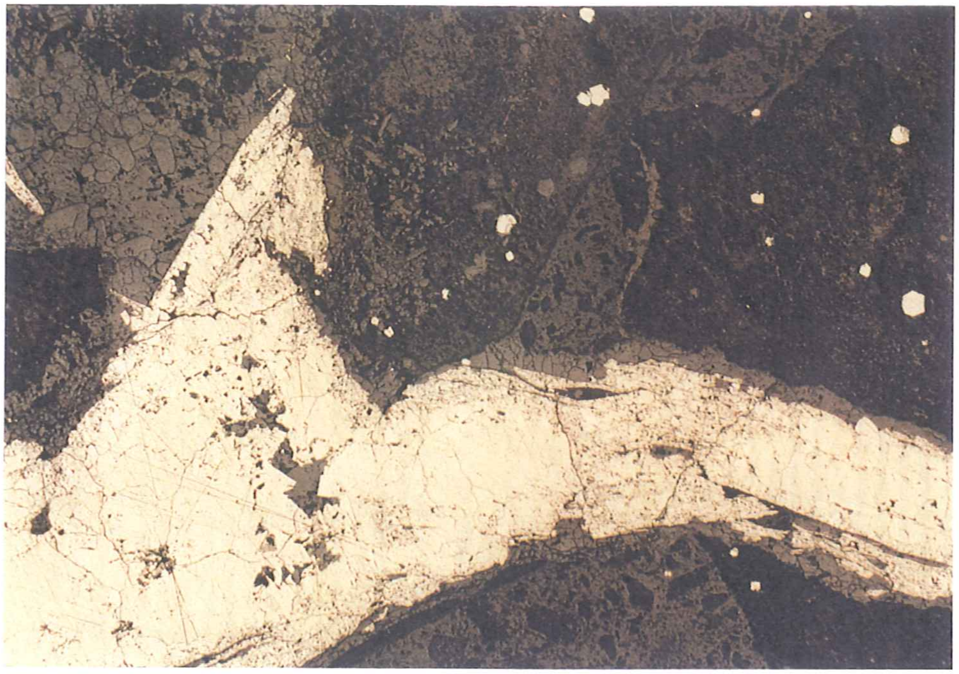

Figure 90. RB-63a/volcanic breccia. Quartz-sulfide vein cuts volcanic breccia. The dominant sulfide is composite pyrite-marcasite. RL; 1cm on the photo= 0.106mm.

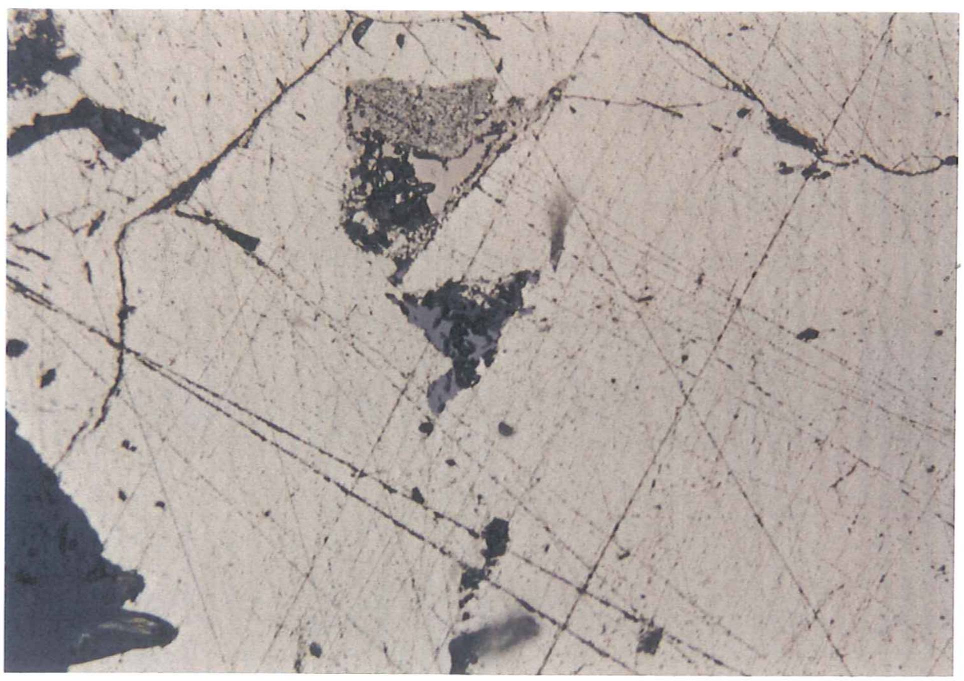

Figure 91. RB-63a/volcanic breccia. Sphalerite and pyrrhotite in intracrystalline voids in a composite pyrite-marcasite crystal. RL; 1cm on the photo= 0.053mm.

RB-63B (PMBX)

In hand specimen sample RB-63b is a mottled pink to white felsitic rock with an anastamosing network of stockwork quartz veinlets. In thin section the stockwork quartz-clay-sericite veins reside in a relatively featureless microcrystalline mosaic of quartz, alkali feldspar, and minor clay derived from alteration of the feldspar. Average groundmass crystal size is on the order of 0.01-0.02mm diameter. Traces of accessory zircon were noted in the groundmass. The lithology may be of glassy volcanic origin. Quartz-clay-sericite-sulfide veins in the network are up to 1.7mm in width. Many are wispy and discontinuous. Some of the veins incorporate small wall rock fragments. Very little sulfide occurs outside of the veinlets. Some of the sulfide may have been plucked from the veinlets during thin section preparation.

CL: The vein quartz is non-luminescent. Traces of very fine-grained hydrothermal apatite with yellow-orange to salmon pink CL were noted adjacent to some veins.

RL: Total sulfide abundance is about 0.3%. Sulfides occur as very fine-grained, subhedral to euhedral pyrite to 0.1mm diameter. The pyrite disseminations have cubic to pyritohedron morphology. Remaining sulfides are composite pyrite-marcasite crystals associated with an anastamosing to stockwork vein network. Some of these composite crystals have skeletal form and reach 1.6mm length with aspect ratios to 16:1. Some of the composite pyrite-marcasite crystals associated with the vein network form coarser subhedral aggregates to 1.6mm in diameter.

Representative photomicrographs from sample RB-63b are found in Figure 92.

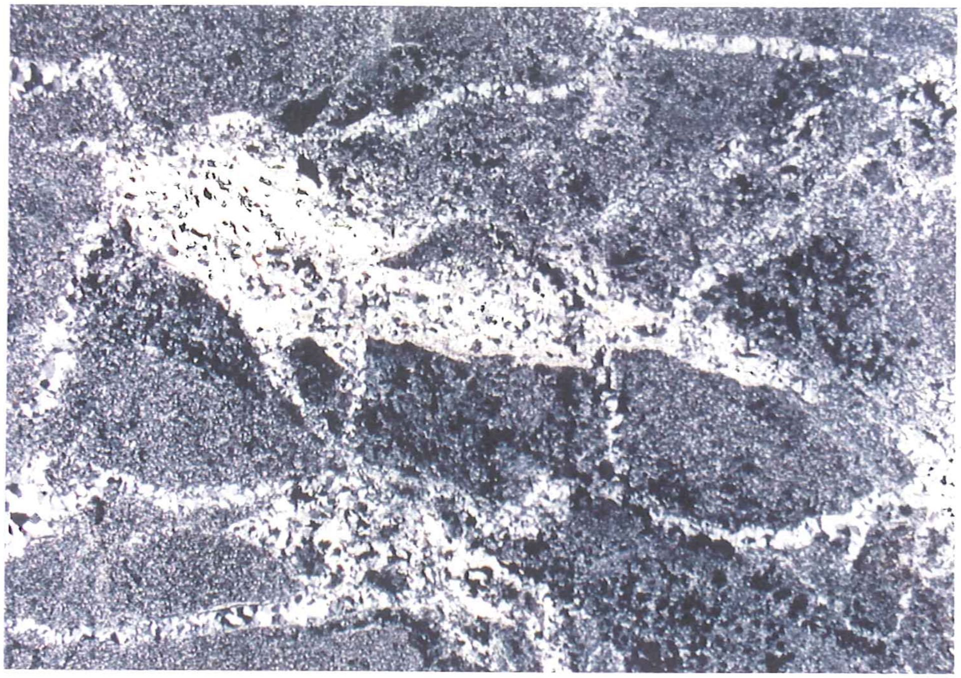

Figure 92a. RB-63b/felsitic crackle breccia. Stockwork quartz-clay/sericite-py/mc veins in a relatively featureless microcrystalline groundmass of quartz, alkali feldspar, and minor clay derived from alteration of the feldspar. TLX; 1cm on the photo= 0.532mm.

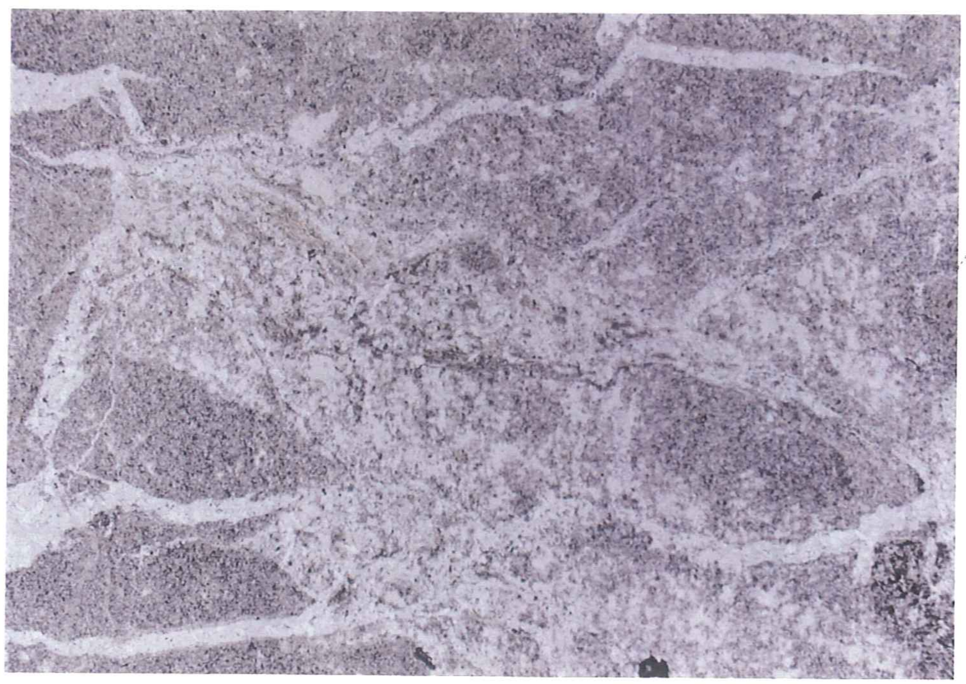

Figure 92b. RB-63b/felsitic crackle breccia. Same view and scale as figure 92a. TLP; 1cm on the photo= 0.532mm.

RB-64 (Lower Plam)

Sample RB-64 is a very fine-grained, pink to grayish white felsite carrying about 5% sulfides in quartz veins and disseminations. It shows crude lamination or compaction bedding, and is traversed by quartz-sulfide veins that cross the faint bedding at high angle, and narrower vein offshoots that cross the banding at a lower angle. In thin section the wallrock contains abundant fine (0.1-0.15mm length) laths and needles of alkali feldspar aligned so as to impart the compaction bedding. These alkali feldspars may include both sanidine and oligoclase, and are distributed in a fine microcrystalline matrix of quartz and alkali feldspar. The groundmass was probably original fine glassy ash that is now devitrified. All the feldspars show minor to moderate clay alteration. Minor biotite is present also as subhedral books to 0.04mm length that have been pseudomorphed by chlorite and/or sericite. One subhedral pyrogenic biotite about 0.45mm in length was noted. The core of the biotite is corroded, but the crystal is otherwise little-altered. The groundmass contains roughly 2% disseminated pyrite as subhedral to euhedral crystals and crystal aggregates to 0.3mm diameter. The disseminated sulfides are aligned crudely with the compaction bedding. The original lithology was probably a fine-grained, laminated tuff.

The main vein crosses the compaction bedding at a high angle. It has a maximum width of 1.6mm and contains quartz, clay, sulfides, and calcite. The xenomorphic, polycrystalline quartz has a maximum crystal size of 0.25mm. The stringers of calcite may be later than the quartz and sulfide. Some of the calcite occurs as narrow insinuations along the vein margin. Clay pods occur intergranular to the quartz and along crystal boundaries. Several branching veins emanating from the main veins extend into the wall rock at lower angles than do the main veins and form a weak to moderate stockwork. Sulfides occupy the centerline of some veins. A few narrow clay stringers cross the faint compaction bedding at low angle. Several narrow, discontinuous stringers contain quartz and sericite, although the main veins do not have sericite.

CL: There is moderate, but pervasive, carbonate (calcite with slightly elevated iron content) flooding of the tuffaceous matrix. The calcite has moderate reddish-orange CL (Mn^{2+} activation). Calcite with bright orange CL (Mn^{2+} activation) invades the primary quartz-sulfide vein.

RL: Veinlet sulfides are primarily skeletal, composite pyrite-marcasite crystals. They are euhedral to subhedral and reach more than 5mm in length. Some show sinuous growth along the centerline of the veinlets. The disseminated phases are dominantly pyrite, although some of the pyrite disseminations have minor intergrown marcasite.

Representative photomicrographs from sample RB-64 appear in Figures 18 and 30.

RB-65A (Lower PMBX)

Sample RB-65a appears to have been collected along the contact between two glassy volcanic lithologies. One of the postulated units is a light mottled pink to white felsite in the hand sample, while the other is a white felsitic rock invaded by a coarse, irregular mass of radiating sulfides, quartz, and calcite. Owing to the scale of the thin section, it may be that the sulfide mass with quartz and calcite represents a vein or breccia matrix.

The pink and white felsite is crackle brecciated and has 2-3% disseminated sulfides. In thin section it appears to be composed of a brown, partly devitrified glassy matrix. Devitrification is manifested as microcrystalline xenomorphic patches of alkali feldspar and quartz intermingled with cloudy brown relict glass. At least some of the feldspar shows polysynthetic twinning on the albite law and is probably in the oligoclase compositional range. Devitrification crystal size is on the order of 0.01mm. Also noted are slightly coarser (± 0.04mm length) feldspars that are optically continuous, but have relatively indistinct margins (microphenocrysts?). The unit shows local micro-brecciation with a microcrystalline granular quartz matrix. The quartz breccia matrix has an average crystal size of about 0.01mm diameter. The microcrystalline quartz is sometimes accompanied by mats of very fine sericite or clay. Although there is some local fragment rotation, most of the brecciation is fragment-supported and more of a crackle breccia. Fragments of host rock are dominantly angular. Breccia matrix and fragments are invaded by narrow anastamosing microveinlets of quartz and sericite ± calcite. Microveinlet widths are no more than 0.1mm. Also present in this lithology is an aggregate of fine-grained quartz and a coarser phase (to 0.35mm length) with moderate relief and birefringence (alunite?). Near the contact with the second glassy unit is an irregular quartz-calcite-sulfide vein similar to those that cut the second unit. Locally within this vein drusy quartz to 0.45mm length has grown into void space. This vein cuts the microbreccia. The disseminated sulfides are generally euhedral to subhedral, elongate skeletal pyrite-marcasite crystals to 0.45mm in length. Except for the one quartz-calcite-sulfide vein, little of the sulfide resides in the veinlets and breccia matrix.

The postulated second glassy volcanic unit is a white felsite in the hand specimen. It contains abundant coarse sulfides, primarily as aggregates of bladed composite pyrite-marcasite crystals in an irregular, coarse vein with calcite and quartz. This part of the section is thick, and the quartz appears to have higher than expected birefringence. Individual pyrite-marcasite crystals reach more than 5mm in length. Some pods of pyrite-marcasite crystals occur as radiating aggregates.The matrix of dark brown glass shows little devitrification, but is extensively flooded with calcite. Protolith may have been a vitrophyre of initial pyroclastic origin.

A calcite vein marks part of the contact zone between the two units.

CL: There is intense calcite flooding of the brown, densely welded tuff (white felsite unit with the coarse sulfide-calcite-quartz vein). The calcite has bright orange CL and accompanies coarse, skeletal py-mc crystals.

RL: As a whole the slide contains 20-25% total sulfide minerals, predominantly subhedral, bladed, composite skeletal pyrite-marcasite crystals. The pink to white mottled felsite unit contains 2-3% disseminated sulfides, again primarily skeletal pyrite-marcasite crystals to 0.45mm in length. Subordinate pyrite with subhedral cubic morphology occurs also as disseminations. Traces of chalcopyrite and sphalerite were noted as well in the disseminated assemblage. The chalcopyrite is generally very fine-grained, anhedral crystals to 0.03mm diameter. The rare sphalerite was observed in edge contact and partly intergrown along one edge with pyrite.

Sulfides in the calcite-sulfide-quartz veins make up more than 50% of the veins and are predominantly bladed composite pyrite-marcasite crystals to 5mm length. Maximum aspect ratio is approximately 15:1. Pyrite occurs in subordinate amounts as aggregates or single crystals of somewhat equant morphology. Maximum pyrite crystal size is about 0.5mm diameter. Pyrite is present also in cores of some composite pyrite-marcasite crystals. Chalcopyrite is common in the veins and occurs generally as subhedral to anhedral crystals in edge contact with the pyrite-marcasite or pyrite crystals. It occurs also as discrete subhedral to anhedral crystals in the calcite vein matrix. Maximum chalcopyrite crystal size is about 0.35mm diameter.

Gold and silver mineralization occur primarily as electrum (white color, high reflectance, isotropic). The electrum is present as fine-grained, irregular crystals that are dispersed in the calcite-quartz matrix, in intracrystalline voids within pyrite or composite pyrite-marcasite crystals, or in edge intergrowth with pyrite and pyrite-marcasite crystals. Maximum electrum crystal size is 0.16mm length/diameter. Silver resides also in minor acanthite. The acanthite occurs as subhedral to anhedral crystals to 0.12mm length in edge contact with pyrite or pyrite-marcasite crystals, or intergrown with chalcopyrite. Traces of a silver sulphosalt mineral (gray, low reflectance, anisotropic, deep red internal reflections; pearceite?) are observed in intracrystalline void spaces in composite pyrite-marcasite crystals locally.

Representative photomicrographs from sample RB-65a are illustrated in Figures 8, 19, 93, 94, and 95.

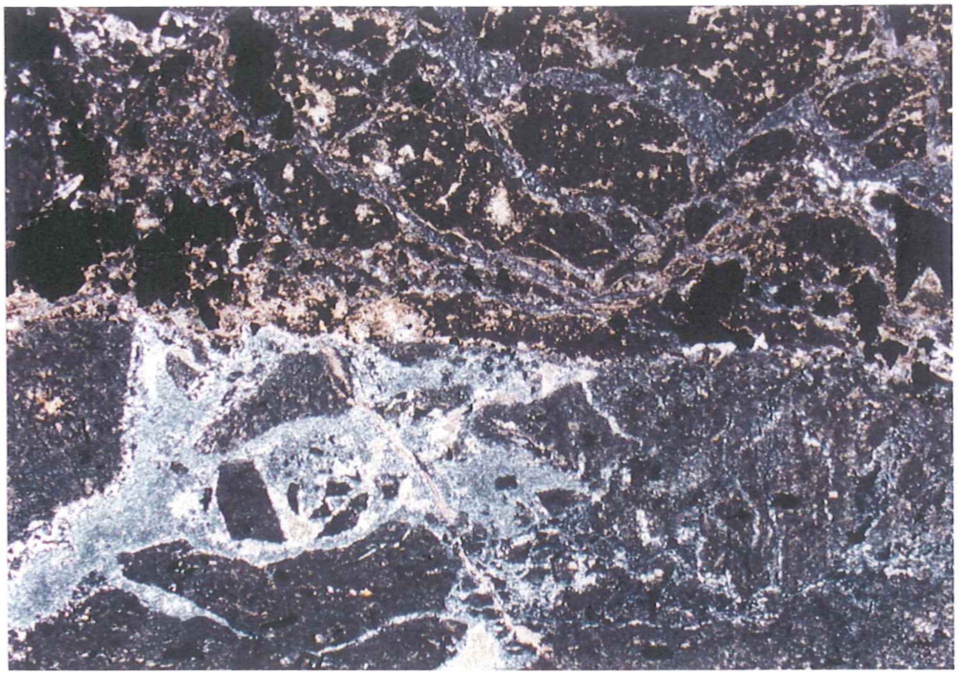

Figure 93a. RB-65a/Lower PMBX. Contact zone between two glassy volcanic lithologies of probable pyroclastic origin. The lithology in the lower half of the photo shows partial to complete devitrification. Both lithologies are invaded by anastamosing veinlets of microcrystalline quartz-clay/sericite ± calcite. TLX; 1cm on the photo= 0.532mm.

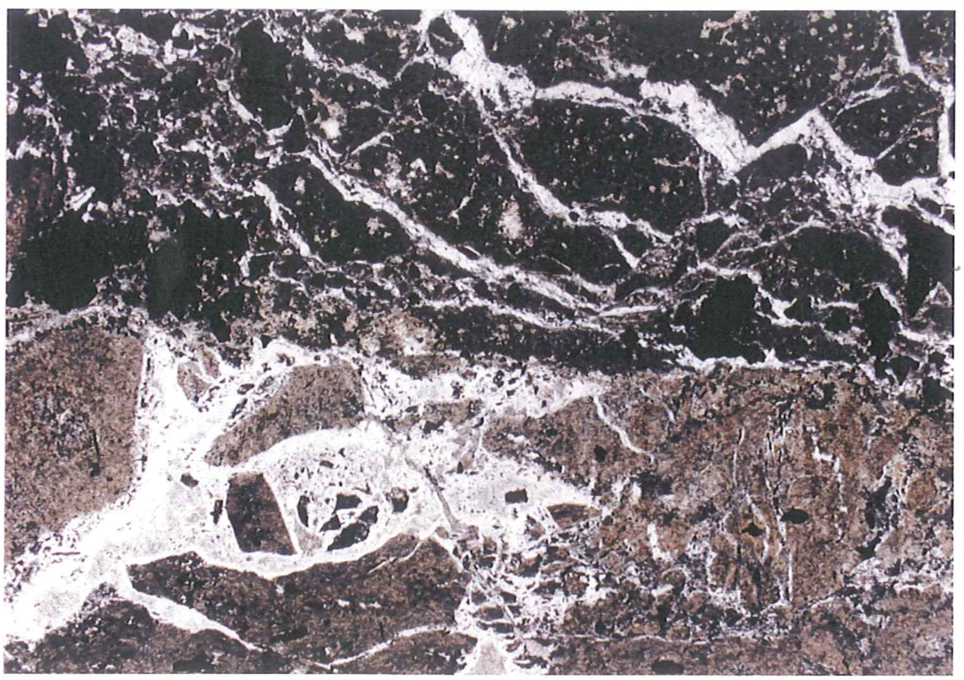

Figure 93b. RB-65a/Lower PMBX. Same view and scale as Figure 93a. TLP; 1cm on the photo= 0.532mm.

Figure 94. RB-65a/Lower PMBX. Quartz-calcite-sulfide vein. The sulfides are dominantly composite pyrite-marcasite crystals with minor chalcopyrite and electrum. The chalcopyrite (mustard yellow) is in edge contact with the py-mc near photo center. Electrum (white; high R) occurs in intracrystalline voids, also at photo center. RL; 1cm on the photo= 0.532mm.

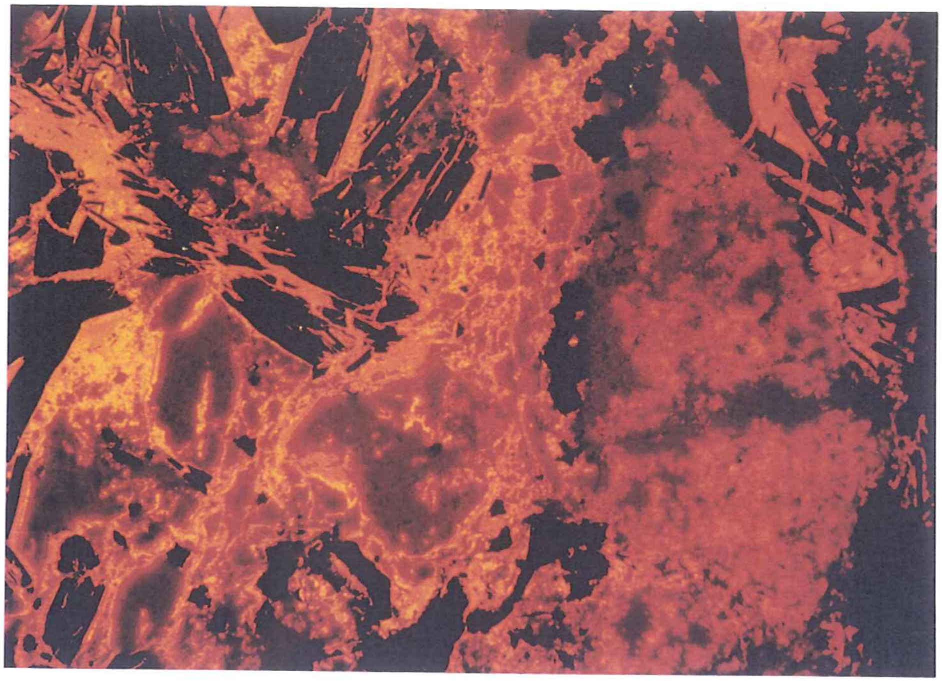

Figure 95a. RB-65a/Lower PMBX. Calcite-flooded welded tuff with abundant coarse skeletal composite pyrite-marcasite crystals. Calcite has bright orange CL (Mn^{2+} activation). CL; 1cm on the photo= 1.016mm.

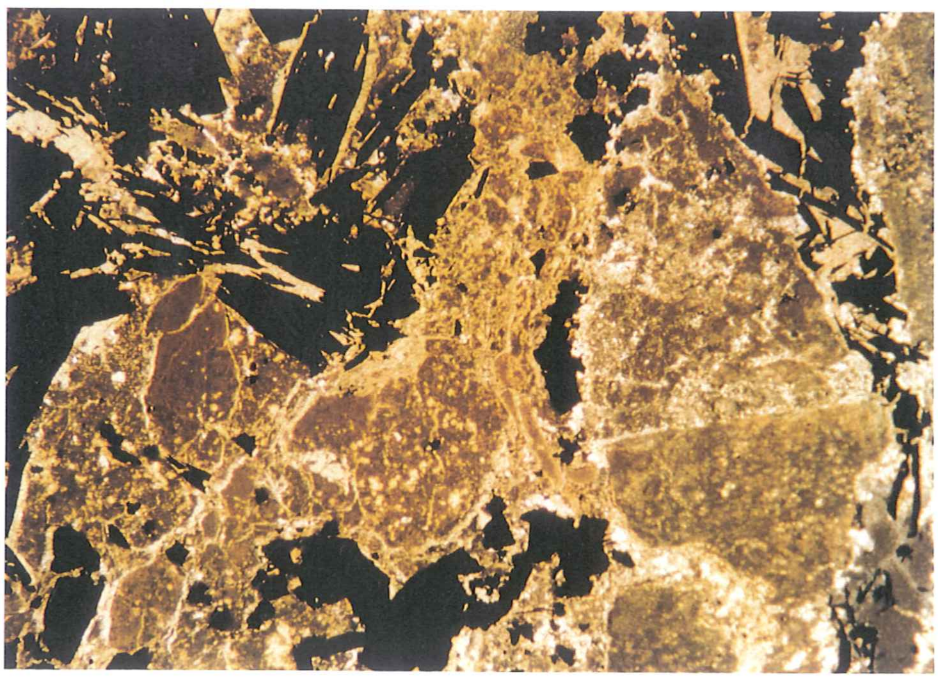

Figure 95b. RB-65a/Lower PMBX. Same view and scale as figure 95a. CL; 1cm on the photo= 1.016mm.

RB-69A (TOS; < 0.001opt Au, < 0.02 opt Ag)

Sample RB-69a may be either a volcaniclastic lithic breccia or possibly a lithic-crystal lapilli tuff. It contains 35-40% angular to subround, lapilli-sized lithic fragments and scattered pyrogenic (?) crystals of quartz, chloritized biotite, and perhaps feldspar pseudomorphed by quartz and clay. Lithic fragments range up to about 2cm in length or 1cm in diameter and consist of several lithology types. The most abundant have a microcrystalline, xenomorphic quartz-alkali feldspar groundmass with microphenocrysts of plagioclase and chloritized biotite. This lithology may be a devitrified glassy rock of volcanic origin. Also present are fragments of what may be epiclastic volcanic siltstone. These fragments show moderate sorting of angular to subround grains of quartz and minor plagioclase and biotite to 0.1mm diameter in a much finer matrix cement of microcrystalline quartz and clay. A crude bedding is observed in some fragments. The feldspars show minor clay alteration. Several fragments of polycrystalline, xenomorphic quartz may be vein fragments. A rectangular fragment of xenomorphic, polycrystalline quartz about 0.5mm in diameter may be a fragment of older metamorphic quartz vein. Some of the lapilli are partially replaced by calcite.The devitrified tuffaceous matrix is an extremely fine-grained microcrystalline mosaic of quartz, alkali feldspar, clay, and minor fine, disseminated calcite. The sample is laced by feathery, discontinuous, wispy veinlets of clay-carbonate-minor quartz, all very fine-grained. The sample contains approximately 2-3% disseminated fine-grained pyrite, most with cubic morphology. The pyrite disseminations occur both in the matrix and in the lapilli. Some lapilli concentrate the pyrite disseminations.

CL: There is partial flooding of some lapilli fragments by calcite (elevated iron content; reddish orange CL), as well as minor disseminated calcite. Scattered lapilli fragments have weak blue-gray CL from alkali feldspar-quartz (devitrification products).

RL: Sample RB-69a contains 2-3% very fine-grained disseminated pyrite as cubic to triangular crystals up to 0.16mm in diameter. Many of the larger crystals have porous interiors and dense rims.Locally crystal aggregates of pyrite to 1.1mm diameter are present. Several coarser composite pyrite-marcasite crystals were observed. The crystals are up to 2.2mm length. Traces of disseminated sphalerite were noted, as well. The sphalerite is very fine-grained (<0.025mm length/diameter) and anhedral.

Representative photomicrographs from sample RB-69a are found in Figures 20, 96, and 97.

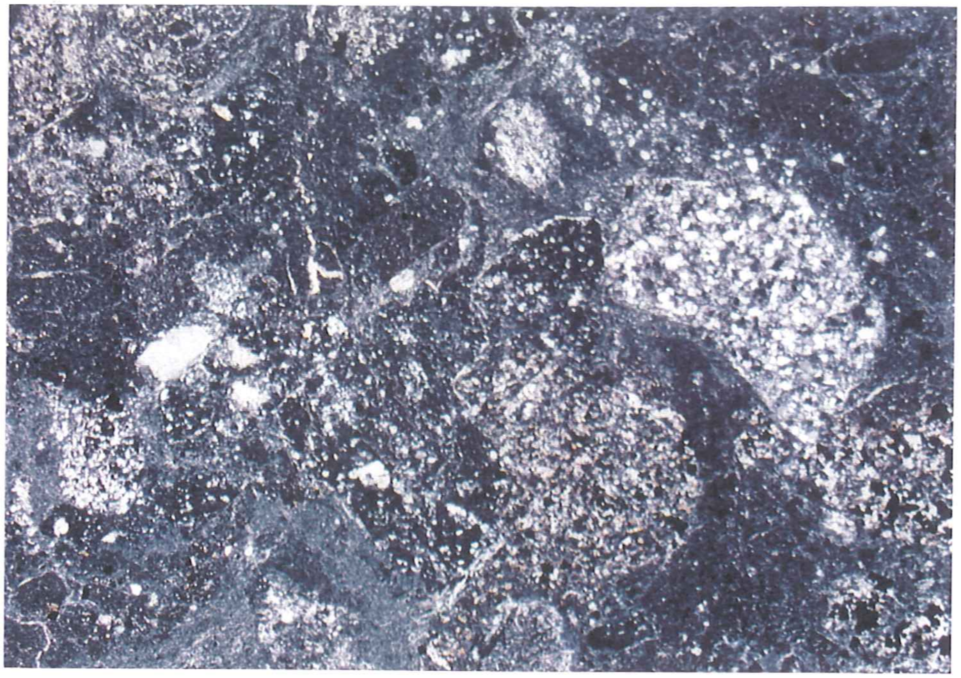

Figure 96a. RB-69a/TOS. Volcanoclastic lithic breccia or crystal-lithic lapilli tuff. Lithic fragments dispersed in a devitrified tuffaceous matrix. A fragment of epiclastic volcanic siltstone (?) is present in the right third of the photo. TLX; 1cm on the photo= 1.532mm.

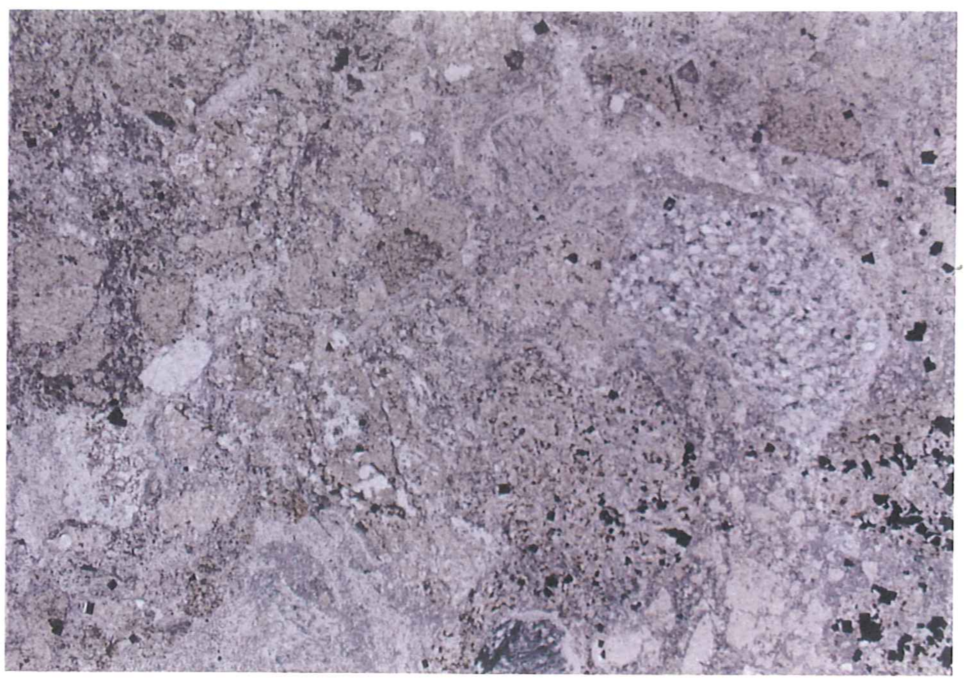

Figure 96b. RB-69a/TOS. Same view and scale as Figure 96a. TLP; 1cm on the photo= 0.532mm.

Figure 97. RB-69a/TOS. Disseminated pyrite in TOS. RL; 1cm on the photo= 0.532mm.

RB-69B (TOS; 0.006 opt Au, < 0.02 opt Ag)

Sample RB-69b is a volcaniclastic lithic breccia. It is essentially fragment-supported and choked with angular to subround, lapilli-sized lithic fragments to 6mm in diameter. The lithic fragments all appear to be of pyroclastic origin and include partly devitrified vitrophyre and densely welded tuff. Some of the fragments have traces of pyrogenic biotite and feldspar altered to chlorite and clay, respectively, but the lithic fragments commonly lack pyrogenic crystal phases. The devitrified fragments contain relict brown glass and very fine crystallites of quartz and alkali feldspar, some of which has altered to clay. The fragments are locally flooded by calcite. There is a crude stratification of the fragments in the very fine-grained devitrified ash matrix. The matrix is composed of a microcrystalline mosaic of quartz, clay, possibly alkali feldspar, and late disseminated calcite. Average matrix crystal size is on the order of 0.01mm diameter.There are scattered thread-like, discontinuous microveinlets of quartz, clay, and calcite, some of which transgress both lapilli and matrix. Areas with slightly coarser (± 0.1mm) polycrystalline xenomorphic quartz are present in some lithic fragments and, less frequently, in the matrix. In the fragments rectangular areas of polycrystalline quartz may be ascribed to pseudomorphs after primary pyrogenic feldspar. Less regular areas of polycrystalline quartz either fill voids or may be due to recrystallization of the devitrified groundmass by fluids accompanying sulfide introduction. The sample contains approximately 0.25% disseminated fine-grained sulfides, primarily as euhedral to subhedral pyrite with cubic morphology.

CL: Some fragments are partly flooded by calcite with elevated iron content (reddish-orange CL). Calcite is present also as minor disseminations (bright orange CL). Some fragments have a weak yellowish-brown CL that may derive from very fine-grained plagioclase relict in the fragments (Fe^{2+} activation). (No CL photo taken).

RL: Sample RB-69b contains approximately 0.25% disseminated sulfides, nearly all of which are pyrite. The pyrite disseminations reach 0.25mm in diameter. Cubic morphology is dominant, triangular and trapezoidal morphology subordinate. Locally pyrite cubes nucleate with quartz as pseudomorphs after pyrogenic feldspar in some lithic fragments. Traces of fine sphalerite were noted, as well. The sphalerite occurs as anhedral crystals to 0.025mm diameter.

Representative photomicrographs from sample RB-69 appear in Figure 98.

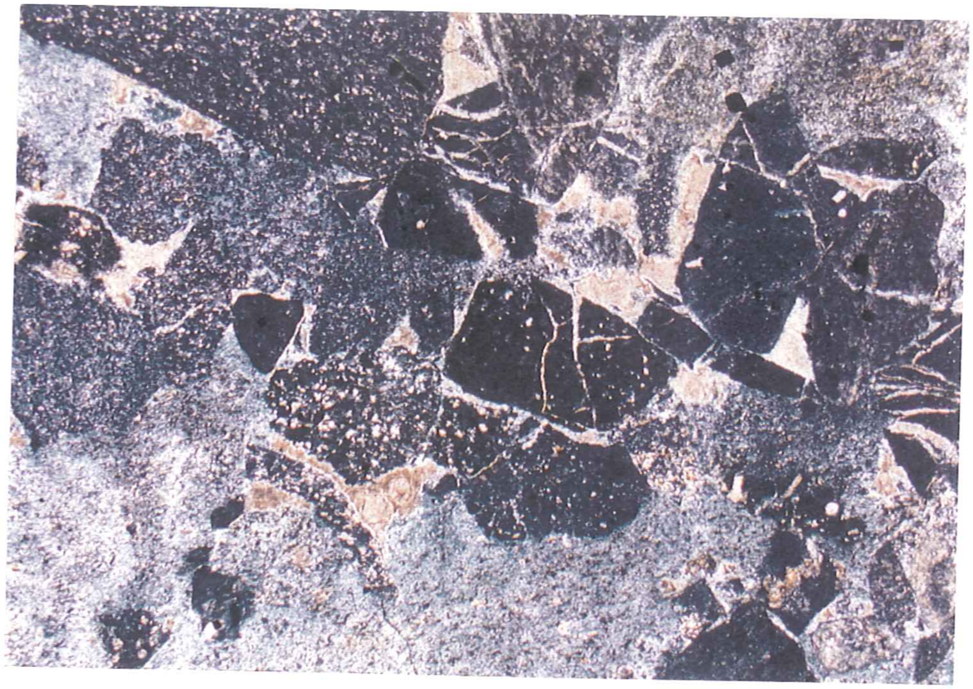

Figure 98a. RB-69b/TOS. Volcaniclastic lithic breccia. The lithic fragments are all of pyroclastic origin. The breccia is laced with discontinuous, thread-like microveinlets of quartz, clay, and calcite. TLX; 1cm on the photo= 0.532mm.

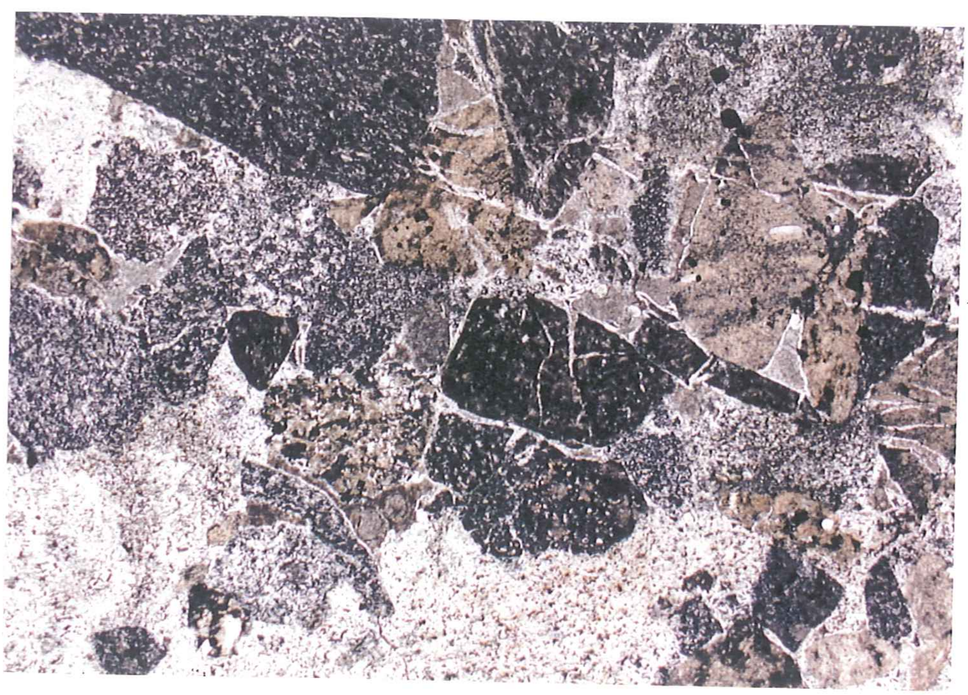

Figure 98b. RB-69b/TOS. Volcaniclastic lithic breccia. Same view and scale as Figure 98a. TLP; 1cm on the photo= 0.532mm.

RB-70A (Dozer formation)

In hand specimen sample RB-70a is a white felsite with fine, disseminated pyrite and a fine quartz veinlet stockwork. In thin section it appears to be a devitrified tuff that contains fine, irregular bits of cloudy brown glass, and quartz, clay, and alkali feldspar devitrification products. No pyrogenic crystal phases or alteration pseudomorphs are in evidence. The tuff is laced by a stockwork of very fine, wispy quartz and quartz-clay veinlets. Some of the quartz-clay veinlets may also contain fine carbonate. If present the carbonate must have a high Fe content, because characteristic calcite CL was not observed under the Luminoscope. The veinlets in the stockwork are less than 0.3mm in width. Locally the veinlet stockwork disrupts the host tuff in small areas of microbreccia. Polycrystalline xenomorphic quartz also accompanies the narrow, discontinuous stringers of composite skeletal pyrite-marcasite. Scattered throughout the tuff are patches of very fine-grained polycrystalline quartz that result from the partial silicification of the tuff. This quartz probably formed during the same episode of rock-fluid interaction that produced the stockwork veinlets. Sulfides occur as disseminations and in quartz-sulfide stringers. Total sulfide abundance is approximately one percent.

CL: Quartz has no luminescence. No calcite was visible under CL.

RL: Sample RB-70a contains approximately one percent total sulfides, primarily as disseminations of very fine-grained, generally cubic pyrite, and elongate rectangular skeletal composite pyrite-marcasite crystals. The cubic pyrites reach 0.1mm in diameter, while the skeletal composite pyrite-marcasite crystals are up to 0.16mm in length and have aspect ratios to 15:1. The skeletal pyrite-marcasite crystals generally have a thin irregular margin of marcasite, with interiors filled by aggregates of cubic pyrite crystals. Marcasite partially fills intercrystalline voids between the cubic pyrite crystals. Composite, skeletal pyrite-marcasite crystals also form several thin (± 0.25mm), discontinuous stringers to 7mm length.

Representative photomicrographs from sample RB-70a are found in Figures 21 and 99.

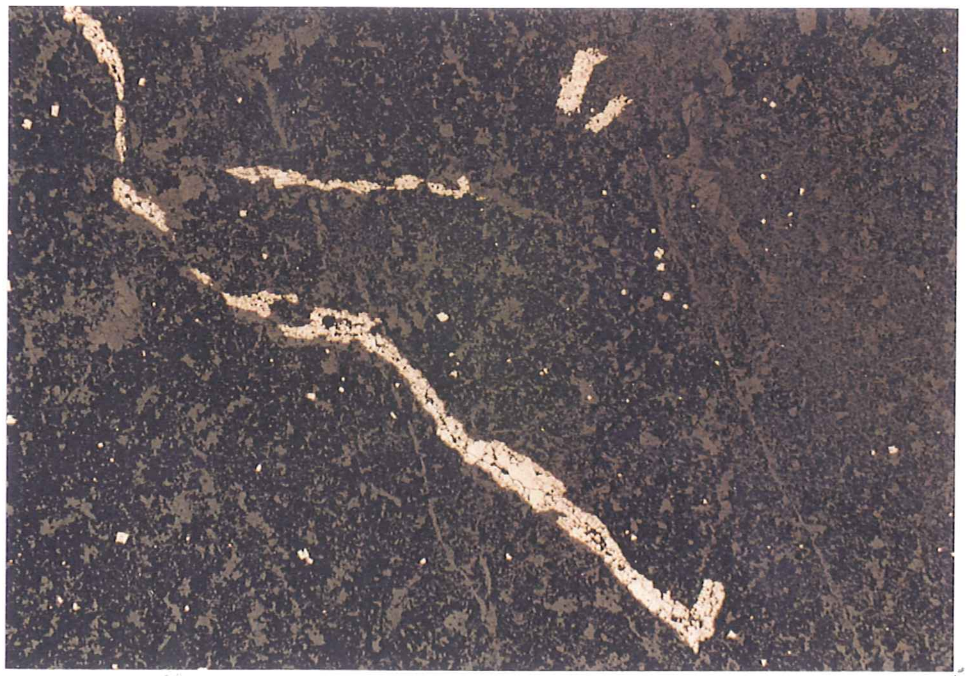

Figure 99. RB-70a/Dozer formation. Stringers of composite pyrite-marcasite crystals and disseminated pyrite in devitrified tuff. RL; 1cm on the photo= 0.532mm.

RB-70B (Dozer formation)

Sample RB-70b is a very fine-grained bedded tuff cut by a quartz-sulfide vein. The faint bedding is ± centimeter-scale, and the bedding has a dilational offset of about 3mm along the vein. The tuff has a very fine-grained, devitrified matrix that appears to be predominantly a microcrystalline mosaic of quartz, alkali feldspar, and clay, plus remnant bits of cloudy brown glass Average crystal size is about 0.015mm diameter. Clay occurs also in irregular elongate patches to 1mm in length. Patchy, irregularly-shaped areas of even finer-grained microcrystalline quartz and clay (average crystal size ± 0.004mm) to 0.35mm in length/diameter may be devitrified fragments of coarser ash. Sparsely dispersed throughout are pyrogenic crystal fragments of quartz and clay-quartz-altered feldspar. Traces of relict pyrogenic feldspar indicate that it is plagioclase of probable sodic oligoclase composition. The main quartz-sulfide vein has a maximum width of 1.7mm. It contains saccharoidal polycrystalline quartz with a maximum crystal size of 0.25mm, minor clay, and elongate, skeletal composite pyrite-marcasite crystals to 4mm in length. The main vein incorporates minor fragments of tuff within its boundaries. There are a few other very thin, discontinuous quartz-sulfide veins, some of which branch off from the main vein. The bedded tuff also contains minor fine disseminated pyrite (<0.3%) to <0.25mm diameter.

CL: The vein quartz does not luminesce. Traces of disseminated apatite needles with bright lemon CL are probably primary. There are faint traces of disseminated calcite with bright orange CL. (No CL photos taken).

RL: The primary sulfide components in the veins are elongate, skeletal composite pyrite-marcasite crystals. They are generally euhedral and reach a length of 4.4mm. The tuff contains about 0.3% disseminated pyrite with dominantly cubic morphology. The pyrite disseminations are euhedral to subhedral and reach 0.25mm diameter. A trace of very fine, anhedral sphalerite was also noted.

Representative photomicrographs from sample RB-70b are found in Figures 100 and 101.

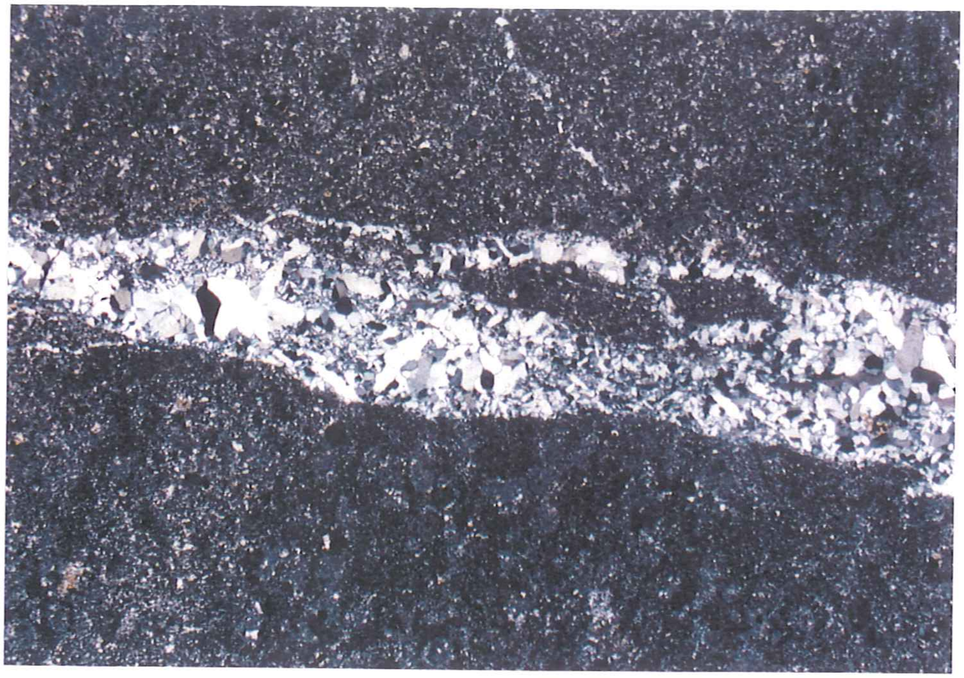

Figure 100a. RB-70b/Dozer formation. Devitrified bedded tuff with dilational offset of the bedding along a quartz vein. The bedding runs nearly parallel to the short edge of the photo. TLX; 1cm on the photo= 0.532mm.

Figure 100b. RB-70b/Dozer formation. Same view and scale as Figure 100a. The bedding offset is more easily visible under TLP. TLP; 1cm on the photo= 0.532mm.

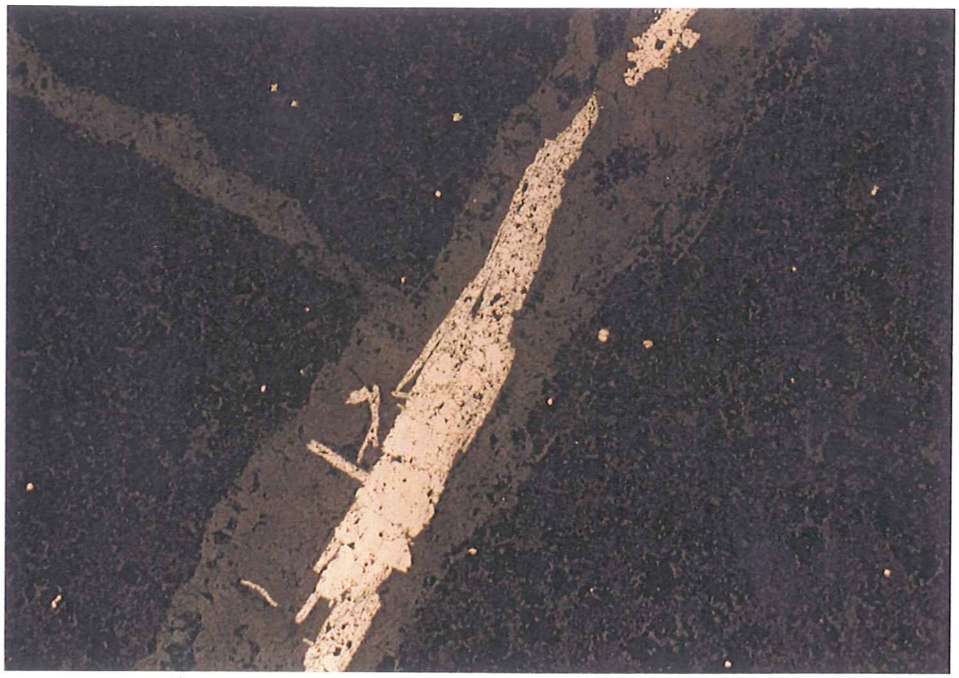

Figure 101. RB-70b/Dozer formation. Bedded tuff with minor disseminated pyrite and a quartz-pyrite/marcasite vein. RL; 1cm on the photo= 0.532mm.

RB-71 (Volcaniclastic sediments)

Sample RB-71 is a finely laminated, bedded crystal-lithic tuffaceous sandstone with significant organic material content. The sandstone is very fine-grained and moderately well-sorted. It contains abundant crystal fragments of quartz, biotite, and feldspar, plus microcrystalline lithic fragments, most of which are of probable volcanic origin, in a very fine-grained, microcrystalline groundmass of quartz, alkali feldspar, and clay that probably represents devitrified fine, ashy material. Relative abundance of the crystal fragments is quartz > biotite > feldspar. Biotite commonly shows partial to complete alteration to chlorite ± sericite, and the feldspar is partly altered to clay. The crystal fragments are generally anhedral and reach 0.25mm in length/diameter, although most are less than 0.1mm in diameter. The lithic volcanic fragments are subangular to subround and up to 0.5mm in length/diameter. Also noted are scattered, subround fragments of a coarser-grained intrusive rock that contains quartz, K feldspar, plagioclase, and sericitized biotite. Average crystal size is about 0.12mm diameter, and the fragments are up to 0.5mm diameter. Fine, crenulated wisps of organic material impart a finely-laminated texture to the tuffaceous sediment. There are a few concordant, very narrow (to 0.15mm width), discontinuous quartz veins that appear to occlude bits of organic matter. The laminations show millimeter-scale offsets in several places along very narrow, discordant clay or clay-quartz (± py) veinlets.

CL: The vein quartz is non-luminescent. There is a trace of very fine-grained disseminated iron-rich calcite with reddish-orange CL.

RL: Total sulfides in this sample are less than 0.1 percent. There is a trace of anhedral, angular pyrite crystals to 0.01mm diameter in the vein that offsets bedding, and a trace of circular granular (framboidal?) pyrite approximately 0.02mm diameter. Also present are traces of fine disseminated sphalerite and anatase after rutile.

Representative photomicrographs from sample RB-71 appear in Figures 22and 102.

Figure 102. RB-71/laminated tuffaceous sandstone. Framboidal pyrite in carbonaceous, tuffaceous sandstone. RL; 1cm on the photo= 0.021mm.

RB-72 (ALS; < 0.001 opt Au, < 0.02 opt Ag)

Sample RB-72 is a carbonaceous shale. Its finely-laminated structure is imparted by fine streaks and lenticles of black to very dark green organic material. The spaces between the organic lenticles consist dominantly of microcrystalline quartz, white mica, and, locally, lensoid zones of slightly coarser (± 0 0.05mm diameter) polycrystalline quartz. Some micro-scale bedding is visible based on abundance of organic material. The carbonaceous shale is cut by narrow, anastomosing quartz veinlets (± pyrite and marcasite). There is a 1.5-2.0mm bedding offset along one quartz vein. The bed that is noticeably offset is about 2mm thick and contains more quartz and disseminated pyrite than elsewhere in the sample. The enhanced quartz and pyrite abundances were probably introduced during veinlet deposition and were fed by the veins. Maximum veinlet thickness is 1.1mm. The thickest vein has fine cockscomb quartz projecting into void space from the vein wall. Maximum crystal size for the cockscomb quartz is 0.4mm length. A lensoid zone of coarser polycrystalline quartz at edge of the slide is probably related to another vein.

CL: There is abundant, very fine-grained, disseminated apatite with salmon pink CL (hydrothermal?), and trace of very fine-grained high-iron calcite with reddish orange CL.

RL: Total sulfides are approximately 2-3%, primarily as fine-grained disseminated pyrite. The disseminated pyrite occurs as subhedral to anhedral crystals with variable cubic, rectangular, prismatic, and framboidal morphologies. Maximum pyrite crystal size is 0.4mm diameter for a subhedral cubic crystal. Most of the pyrites are considerably smaller than the maximum size, on the order of 0.06mm or less in diameter. Some of the coarser pyrite has minor intergrown marcasite. Where they are elongate, the pyrites have their long crystal axes oriented parallel to the bedding. Spherical blebs of framboidal pyrite are generally very fine-grained (<0.01mm diameter). One thin bed (appx. 2mm in thickness) preferentially concentrates pyrite. Within this bed pyrite constitutes approximately 10-15% by volume. The pyrite-rich bed is offset approximately 1.5-2mm along a quartz-pyrite vein. Some of the quartz veins contain minor elongate, subhedral, composite pyrite-marcasite crystals to 1.1mm in length.

Locally the coarser pyrite disseminations display simple intergrowths with a gray, low reflectance, weakly anisotropic to isotropic phase that may be magnetite.

Representative photomicrographs from sample RB-72 are found in Figures 27 and 103.